UNIVERSITÀ
DEGLI STUDI
DI PADOVA

Università degli Studi di Padova

Dipartimento di Biologia

SCUOLA DI DOTTORATO DI RICERCA IN BIOSCIENZE E BIOTECNOLOGIE

INDIRIZZO: GENETICA E BIOLOGIA MOLECOLARE DELLO SVILUPPO

CICLO: XXIV

Molecular and functional characterization of *2mit*, an intronic gene of *Drosophila melanogaster timeless2* locus

Direttore della Scuola: Prof. Giuseppe Zanotti

Coordinatore d'indirizzo: Prof. Paolo Bonaldo

Supervisore: Prof. Federica Sandrelli

Dottorando: Francesca Baggio

INDEX

Molecular and functional characterization of *2mit*, an intronic gene of *Drosophila melanogaster timeless2* locus

Abstract

Drosophila melanogaster 2mit is a nested gene of *timeless2* (*tim2*), a locus which controls both chromosome stability and circadian photoreception. *2mit* is localized in *tim2* intron 11 and is transcribed in opposite direction with respect to its host gene. *In silico* analyses suggest that it codes for a putative 1141 aa transmembrane protein characterized by a conserved extracellular leucine-rich repeat (LRR) domain, known to be important for protein-protein interactions.

2mit mRNA is expressed from early embryonic stages, prevalently in the developing central nervous system. In adult brains, *2mit* mRNA is mainly localized in mushroom bodies and ellipsoid-body, structures involved in the control of locomotor activity and memory, and at minor level in optic lobes.

The aim of this project is to determine *2mit* role in *Drosophila* nervous system, mainly focusing on the adult stage, paying also attention on a possible *2mit* functional correlation with *tim2*.

2mit mRNA levels have been determined in six independent strains, each carrying a transposon insertion in proximity or within *2mit* locus. Only one strain, $PB2mit^{c03963}$, showed a significant *2mit* mRNA decrement compared to the wild-type (~50% in larvae, ~85% in adult heads).

This $PB2mit^{c03963}$ strain and lines presenting double strand RNA interference-mediated *2mit* knock down (KD), either pan-neuronal or in specific brain tissues, were used for *2mit* functional characterization.

Given *2mit* mRNA expression in optic lobes of wild-type brains, we evaluated visual system integrity in $2mit^{-}$ lines at both larval and adult stage. We found that $PB2mit^{c03963}$ mutants displayed defects in optic-motor coordination at adult stage.

Since *tim2* is involved in circadian photoreception, we investigated a possible *2mit* role in the circadian system. $PB2mit^{c03963}$ flies displayed a circadian photoreception similar to that of wild-type, suggesting that *2mit* has a different role with respect to *tim2*. However, both $PB2mit^{c03963}$ strain and lines with pan-neuronal *2mit* KD exhibited a slight but significant lengthening of circadian periodicity in constant conditions. Moreover, $PB2mit^{c03963}$ mutants showed a mild modification in the 24 h kinetics of the clock protein PERIOD in brain neurons important for the control of circadian periodicity.

As *2mit* expression pattern in wild-type brains includes mushroom bodies and ellipsoid-body, we analysed general locomotor activity parameters (such as distance moved and immobility time) at both larval and adult stage, but no significant effects were detected in $2mit^{-}$ flies. In addition, we tested $PB2mit^{c03963}$ flies short-term associative memory phenotype, obtaining that $PB2mit^{c03963}$ mutants showed memory impairments compared to controls.

In order to confirm *2mit* involvement in visual response, memory and circadian periodicity, we produced and tested several transgenic lines carrying a construct for *2mit* overexpression, in $PB2mit^{c03963}$ mutant background. Rescue experiments

confirmed a *2mit* role in motion vision and in short-term associative memory, but not its putative function in the control of *free running* periodicity.
To better understand 2MIT molecular functions, we searched for 2MIT possible interactors screening a *Drosophila* cDNA library in yeast two-hybrid system. As possible candidate we found NCKX30C, a transmembrane protein involved in signaling events, expressed both during development and in adult nervous system.
Taken together, the achieved results suggest that 2MIT protein might represent a brain membrane receptor with different roles in signaling circuits of *Drosophila* adult brain.

Riassunto

Drosophila melanogaster 2mit è un gene intronico di *timeless2* (*tim2*), un locus genico coinvolto sia nella stabilità cromosomica che nella fotorecezione circadiana (Benna et al., 2010). *2mit* è localizzato nell'undicesimo introne di *tim2* ed è trascritto nella direzione opposta rispetto al suo gene ospite. Analisi *in silico* suggeriscono che *2mit* codifica per una proteina transmembrana putativa di 1141 aa, che presenta, nella sua porzione extracellulare, un dominio conservato formato da ripetizioni ricche in leucine (*leucine-rich repeats*; LRR), importante per interazioni proteina-proteina.

L'mRNA di *2mit* è espresso fin dallo stadio embrionale, prevalentemente nel sistema nervoso in via di sviluppo. In cervelli allo stadio adulto, l'mRNA di *2mit* è principalmente localizzato a livello dei corpi fungiformi e del corpo ellissoidale, strutture coinvolte nel controllo dell'attività locomotoria e della memoria, ed una debole espressione è rilevata anche in corrispondenza del lobo ottico.

Lo scopo di questo progetto è determinare il ruolo di *2mit* nel sistema nervoso di *Drosophila*, con particolare attenzione allo stadio adulto, con l'intenzione anche di valutare se *2mit* presenta una possibile correlazione funzionale con il suo gene ospite *tim2*.

I livelli di espressione dell'mRNA di *2mit* sono stati determinati in sei ceppi indipendenti, ognuno dei quali caratterizzato dall'avere un transposone inserito in prossimità o all'interno del locus di *2mit*. Solo uno di questi ceppi, $PB2mit^{c03963}$, ha mostrato una significativa riduzione dei livelli di mRNA di *2mit* rispetto a quelli del controllo (50% nelle larve, ~85% nelle teste di adulto).

Il ceppo $PB2mit^{c03963}$ e linee caratterizzate dall'avere un *knock-down* (KD) di *2mit*, sia a livello pan-neuronale che in specifiche regioni del cervello, dovuto all'attivazione del meccanismo dell'RNA *interference*, sono state utilizzate per la caratterizzazione funzionale di *2mit*.

Data l'espressione dell'mRNA di *2mit* nei lobi ottici di cervelli *wild-type*, abbiamo valutato l'integrità del sistema visivo nelle diverse linee $2mit^{-}$, sia allo stadio larvale che adulto. Abbiamo trovato che mutanti $PB2mit^{c03963}$ hanno esibito difetti nella coordinazione ottico-motoria allo stadio adulto.

Poiché *tim2* è coinvolto nella fotorecezione circadiana, abbiamo investigato un possibile ruolo di *2mit* nel sistema circadiano. Individui $PB2mit^{c03963}$ hanno mostrato un comportamento legato alla fotorecezione circadiana simile a quello dei controlli, indicando che *2mit* ha un ruolo diverso rispetto a *tim2*. Comunque, sia il ceppo $PB2mit^{c03963}$ che le linee con KD di *2mit* guidato in tutto il sistema nervoso hanno esibito un leggero ma significativo allungamento della periodicità circadiana in condizioni costanti. Inoltre, mutanti $PB2mit^{c03963}$ hanno presentato una leggera alterazione nella cinetica di accumulo nucleare durante le 24 ore della proteina orologio PERIOD in neuroni del cervello importanti per il controllo della periodicità circadiana.

Poiché l'espressione di *2mit* in cervelli *wild-type* comprende i corpi fungiformi ed il corpo ellissoidale, abbiamo analizzato parametri dell'attività locomotoria generale (come la distanza percorsa e il tempo di immobilità) in mutanti *2mit*$^{-}$, sia allo stadio larvale che adulto, ma non sono stati rilevati effetti significativi. In aggiunta, abbiamo testato il fenotipo della memoria associativa a breve termine in individui *PB2mit*^{c03963}, ottenendo che i mutanti hanno mostrato un danneggiamento associato alla memoria in confronto ai controlli.
Per confermare il coinvolgimento di *2mit* nella risposta visiva, nella memoria e nella periodicità circadiana, abbiamo prodotto e testato diverse linee transgeniche contenenti un costrutto per la sovraespressione di *2mit* nel background genetico mutante *PB2mit*^{c03963}. Esperimenti di rescue del fenotipo hanno confermato un ruolo di *2mit* nella percezione visiva del movimento e nella memoria associativa a breve termine, ma non hanno confermato il suo coinvolgimento nella modulazione della ritmicità circadiana in condizioni costanti.
Per meglio comprendere le funzioni molecolari di 2MIT, abbiamo cercato dei suoi possibili interattori attraverso lo screening di una libreria di cDNA di *Drosophila* nel sistema del doppio ibrido di lievito. Come possibile candidato abbiamo individuato NCKX30C, una proteina transmembrana coinvolta in eventi di *signaling* ad espressa sia durante lo sviluppo che nel sistema nervoso adulto.
In conclusione, considerati nell'insieme, i risultati ottenuti indicano che la proteina 2MIT potrebbe rappresentare un recettore di membrana con diversi ruoli nei circuiti cerebrali nel cervello adulto di *Drosophila*.

CHAPTER 1:

Introduction

1.1 Nested genes

1.1.1 Defining nested genes

A nested gene is defined as a gene whose entire coding sequence is localized within the boundaries of the start and stop codons of a larger external gene. In other words, a nested gene is entirely contained within the chromosomal region occupied by the host gene (Henikoff et al., 1986). In general the position of the transcriptional start sites and the coding sequences of nested genes vary considerably from those of their external host sequences.
Nested genes are classified in two principal subtypes: intronic and non-intronic genes. Intronic genes are contained within an intron of an external host gene and they represent the most common type, particularly in higher eukaryotic genomes (Fig.1.1a). They are generally oriented opposite their host genes and located in large introns (Henikoff et al., 1986; Yu et al., 2005). On the other hand, non-intronic genes are fully inserted in an exon of the host gene, but in antisense direction (Fig.1.1b). They are less frequent than intronic genes, being uncommon in higher eukaryotic genomes, where in the most of the cases only partially overlap their hosts (Sanna et al., 2008). They have revealed to be much more common in Prokaryotes (Rak et al., 1982; Sawers et al., 2005), and in lower Eukaryotes such as yeast (Coelho et al., 2002; Ma et al., 2008) and *Tetrahymena* (Zweifel et al., 2009; Kumar, 2009).

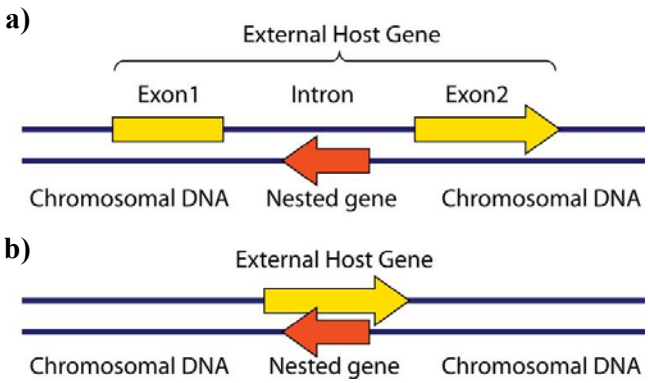

Fig.1.1 Schematic representation of **a)** an intronic nested gene **b)** a non-intronic nested gene (Kumar, 2009). The nested gene is represented by a red arrow and the external host gene is represented by a yellow arrow.

In *D. melanogaster* 792 embedded intronic genes have been identified. They represent ~6% of the total gene complement and the majority of them (85%) are predicted to encode proteins, while the remaining are predicted to generate non-coding RNAs (Assis et al., 2008; Misra et al., 2002). In other species, such as *Caenorhabditis elegans* and *Homo sapiens,* the number of putative nested genes are estimated to be 429 and 158 (protein-coding), respectively (Assis et al., 2008; Yu et al., 2005; Kumar, 2009).

1.1.2 Evolution and biological meaning of nested intronic genes

A study performed by Assis and colleagues (2008) suggested that most of intronic genes have been originated through insertion of a DNA sequence into an intron of a pre-existing locus, following either gene duplication or retrotransposition. However, less frequently a nested gene might have been generated *de novo* in an intron of a host gene. An example of this last possibility is provided by eleven *D. melanogaster* intronic nested genes, which exhibit no sequence similarity to any genes of the closely related *D. yakuba* species, meaning that they originated *de novo* (Assis et al., 2008).

Interestingly, in eukaryotic genomes the number of novel appearing intronic nested genes is higher with respect to that of disappearing ones, meaning that they are associated to higher rates of evolutionary gains than losses. Also *Drosophila* confirms this statement of preferential evolutionary gain with 52 nested genes emergences against 17 losses (Assis et al., 2008; Kumar, 2009).

Even if the presence of non-intronic nested genes in compact prokaryotic genomes is selectively advantageous, because it optimizes the time required for DNA replication, it is not apparently clear why in eukaryotic genomes, that do not have the same size constraints, nested genes are present (Kumar, 2009). Generally, the acquisition of nested gene structures in eukaryotic genomes is considered an evolutionarily neutral process in which long intronic sequences provide a niche for gene insertion (Assis et al., 2008; Lynch et al., 2002; Lynch et al., 2003; Kumar, 2009). Nevertheless, despite many nested genes exhibit expression patterns and roles that are different from those of their hosts, there are also example showing that nesting is correlated to co-regulated expression and/or functional correlation between nested intronic and host genes. In fact, since intronic gene promoter is localized in a different position with respect to that of its host gene, the regulation of expression of both genes may depend on the interaction between their transcriptional elements (Uptain et al., 1997; Gibson et al., 2005). Moreover, in some cases natural selection may favor functional benefits associated to nesting, with nested genes encoding proteins characterized by complementary or similar functions with respect to those of their hosts.

Regarding the possible relation between nested coding sequence and host gene, nowadays it is not possible to postulate *a priori* a general rule. One of the cases supporting the assumption of regulative and functional correlation between nested and host genes is represented by the human tumor suppressor *neurofibromin1* (*NF1*) gene (Habib et al., 1998a), which houses the three intronic genes *EV12A*, *EV12B* and *oligodendrocyte-myelin glycoprotein* (*OMG*; Viskochil et al., 1993; Cawthon et al., 1990). *OMG* codes for a protein that, despite it does not share any structural similarity with NF1 protein, presents both common expression pattern and functional similarity, acting as a growth suppressor (Habib et al., 1998b). Moreover, *EV12B*, belonging to the same locus, encodes a protein that, as NF1, is

involved in both melanocytes and keratinocytes differentiation (Kaufmann et al., 1999).
On the other hand, there are cases which support the idea of a non-correlation among intronic and host genes. In *Drosophila* for example *dunce* (*dnc*) locus carries six nested genes *ng1-4, Sgs-4* and *Pig-1* (Chen et al., 1987; Furia et al., 1993). While *dunce* gene codes for a cAMP phosphodiesterase implicated in adult learning and memory, circadian rhythmicity and female fertility (Levine et al., 1994; Qiu and Davis, 1993), five out of the six intronic genes have a completely different function, being salivary gland specific. Moreover, they are not coordinately regulated with *dunce* and are expressed exclusively during larval instars (except *ng-4*; Furia et al., 1993).
There are also cases in which coordinated regulation in nested-host genes expression is associated to a lack of functional correlation. An example is given by *Drosophila adenosine3* (*Gart*) gene, encoding three enzyme activities involved in purine pathway biosynthesis (Johnstonen et al., 1985; Tiong et al., 1990). *Gart* contains an intronic gene, called *Pupal cuticle protein* (*Pcp*), encoding a structural constituent of the pupal chitin-based cuticle (Henikoff et al., 1986). Although the apparent lack of functional correlation, *Gart* and *Pcp* genes display coordination in the regulation of their expression (Henikoff and Eghtedarzadeh, 1987).

1.2 *Drosophila melanogaster* as a model organism

Drosophila melanogaster is one of the most important and studied organisms in biological research, particularly in the fields of classical and molecular genetics, as well as developmental biology. It was introduced as model organism for studies in Genetics by Thomas Morgan in 1909. There are several reasons why fruit fly is considered a good model for biological studies. It is small and easy to grow in laboratory, it has a short life cycle and generation time (about 10 days at room temperature), it is easily available and manipulable, it has high fecundity (females can lay >800 eggs in their life time) and a high number of offspring, mutants are readily obtainable, males do not show meiotic recombination (facilitating genetic studies). In addition, its genome has been completely sequenced (Adams et al., 2000), showing a large number of orthologues to human genes. In fact, ~75% of known human disease genes have a recognizable match in the *Drosophila* genome (Reiter et al., 2001) and 50% of fly protein sequences present mammalian orthologues.
Drosophila is a holometabolous insect, which undergoes a complete metamorphosis during its development. The fruit fly life cycle is distinct in four successive stages: embryo, larva (the larval stage consists of three instars), pupa (the pupal stage consists of two instars) and adult (Fig.1.2). *Drosophila* has been used as a genetic model for studies on different general biological phenomena as well as for analyses of several human diseases. The fly has been used to explore mechanisms underlying for example vision, olfaction, audition, learning/memory,

courtship, sleep/wake cycles, circadian behaviour and ageing as well as oxidative stress, diabetes, immunity, cancer and drug abuse.

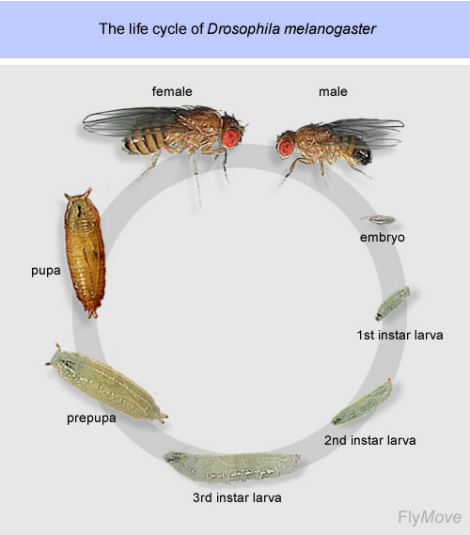

Fig.1.2 *Drosophila melanogaster* life cycle. The fruit fly life cycle comprises four successive stages: embryo, larva (the larval stage consists of three instars), pupa (the pupal stage consists of two instars) and adult (from http://flymove.uni-muenster.de/).

1.3 The *Drosophila* genome

Drosophila melanogaster genome is organized in four pairs of chromosomes: an X/Y pair, and three autosomes named 2, 3, and 4. The X chromosome is telocentric, 2 and 3 chromosomes are metacentric and appear with a left (2L and 3L) and a right (2R and 3R) arm, and the 4 chromosome is telocentric. The *Drosophila* sequenced genome of ~165 Mb pairs has been annotated (Halligan and Keightley, 2006) and contains 13,767 protein-coding genes which comprise ~20% of the genome.

1.4 The *Drosophila* brain

1.4.1 The *Drosophila* nervous system: focusing on the brain structures

In Insects, the nervous system consists of a head ganglion, three thoracic ganglia and different abdominal ganglia. In *Drosophila*, the three thoracic and the abdominal ganglia are fused into one thoracic ganglion, connected to the head ganglion by the cervical connective harboring the axons of ~3600 descending and ascending neurons (Coggshall et al., 1973). The head ganglion is constituted by six pairs of ganglia fused in two distinct cerebral structures. The first three pairs of ganglia are fused to form the brain (also defined as *cerebrum* or supraesophageal ganglion) while the three following pairs are fused to form the *gnatocerebrum* (also defined as subesophageal ganglion), a structure localized under the esophagus. The brain and the *gnatocerebrum* are connected by two

commissures forming a ring structure, called periesophageal track, surrounding the esophagus.

The *Drosophila* adult brain consists of neuropiles, fiber tracts and a surrounding cell body layer (http://flybrain.neurobio.arizona.edu/; Fig.1.3). It is composed by about 200 000 neurons: 120 000 neurons are in optic lobes whereas 80 000 are shared between antennal lobes and central brain. It is anteroposteriorly subdivided into three components: *i*) *proto-*, *ii*) *deuto-* and *iii*) *tritocerebrum*. *i*) The *protocerebrum* consists of discrete interlinked neuropiles and comprises optic lobes, *ocelli* and central brain. The central brain is subdivided in two great structures: the mushroom bodies (*corpora peduncolata*) and the central complex. The central complex consists of four substructures: the ellipsoid-body, the protocerebral bridge, the fan-shaped body and the noduli (Hanesch et al., 1989). *ii*) The *deutocerebrum* includes the antennal lobes, which are first order neuropiles for olfactory perception and chemosensory pathway. Each consists of 40 identified *glomeruli* (Laissue et al., 1999), which receive olfactory receptor fibers of the third antennal segment and the maxillary palp, collect fibers of the same chemosensitivity and transmit their activity to intrinsic fibers and projection neurons. *iii*) The *tritocerebrum* innervates the esophagous and houses neurons of the visceral nervous system projecting to the anterior gut.

Fig.1.3 *Drosophila* adult brain shown in the head capsule. Red: antennal lobes; Blue: mushroom bodies; Green: optic lobes; Orange: central complex; Yellow: supraoesophageal ganglion (Heisenberg, 2003).

1.4.2 The retina and optic lobes

The *Drosophila* visual system is constituted by the retina of compound eyes, and optic lobes. Each optic lobe is formed by three successive neuropiles (or ganglia): lamina, medulla and lobula complex, subdivided into an anterior "lobula" and a

posterior “lobula plate”. Each of these three regions is characterized by a retinotopic organization, forming a sort of neuronal map composed by repetitive columnar elements. The retina of each compound eye is formed by ~800-1000 units, called ommatidia or facets. Each ommatidium is arranged in a hexagonal structure and is equipped with eight photoreceptor cells termed rhabdomeres (or R cells) housing photopigments. The six external R1-6 rhabdomeres surround the two central ones, R7 and R8, that are positioned one on top of the other. R1-6 cells mostly express the photopigment Rhodopsin 1 (Rh1), the opsin with the wider absorption spectrum, and are necessary for motion detection, while R7 and R8 inner cells express different Rhodopsins and have a role in color vision (Pichaud et al., 1999; Wang and Montell, 2007). From a functional point of view, R1-R6 photoreceptors resemble the vertebrate rods, whereas R7 and R8 photoreceptors are similar to the vertebrate cones. R1-6 cells project to the lamina, whereas R7 and R8 cross the lamina layers without forming any synapse and send their projections to specific layers of the medulla (Borst, 2009; Morante and Desplan, 2004; Ting and Lee, 2007). The first optic ganglion is the lamina characterized by columns, termed “cartridges”. Each cartridge houses, in addition to amacrine cells, eight different cell types connecting the lamina to the medulla (Takemura et al., 2008): the two centrifugal cells C1 and C2, the five lamina monopolar cells L1-5 and the T1 cell. The R1-6 axons form synapses with amacrine and L1-3 cells (Meinertzhagen and O’Neil, 1991) provided by chloride channels that respond to histamine, the photoreceptor neurotransmitter (Hardie, 1989). The second optic neuropile, the medulla, is subdivided into layers and columns. Each column is organized into 10 layers (Fischbach and Dittrich, 1989), defined as M1-M10, and harbors ~60 distinct columnar neurons in addition to the lamina pre-synaptic terminals. R7 and R8 cells directly project to medulla columnar elements (in M3 and M6 layers) while R1-R6 send indirect inputs to the medulla through lamina neurons (in M1-M5 layers; Ting and Lee, 2007). Albeit some columnar neurons maintain the retinotopic map (Franceschini et al., 1989), many medulla cells have been described to make synapses over different columns (Strausfeld, 1976; Fischbach and Dittrich, 1989).

The higher optic ganglion is the lobula complex, constituted by the lobula and the lobula plate (Fischbach and Dittrich, 1989; Scott et al., 2002; Morante and Desplan, 2004). Also the lobula complex is organized in layers and columns and various subtypes of medulla neuron establish connections to lobula complex in a stereotyped manner. In particular, the lobula plate houses ~15 000 neurons (Hofbauer and Campos-Ortega, 1990) and among them there are the best characterized neurons of the lobula complex, which are the giant lobula plate tangential neurons. They are classified in two classes: the horizontal system (HS-cells) and the vertical system (VS-cells) (Fischbach and Dittrich, 1989; Scott et al., 2002; Joesch et al., 2008; Raghu et al., 2007). These neurons are very important for *Drosophila* vision because, being motion-sensitive, they are responsible for motion detection (Hausen, 1984; Hengstenberg et al., 1982;

Douglass and Strausfeld, 1996). In these neurons both excitatory acetylcholine receptors and inhibitory GABA receptors have been identified (Brotz and Borst, 1996; Raghu et al., 2007; 2009). Very few is known about the input and output neurons contacted by tangential cells. Anyway, post-synaptic neurons do not seem to maintain the retinotopic organization (Strausfeld, 1976).
A schematic representation of cell types in the fly visual system is provided in Fig.1.4.

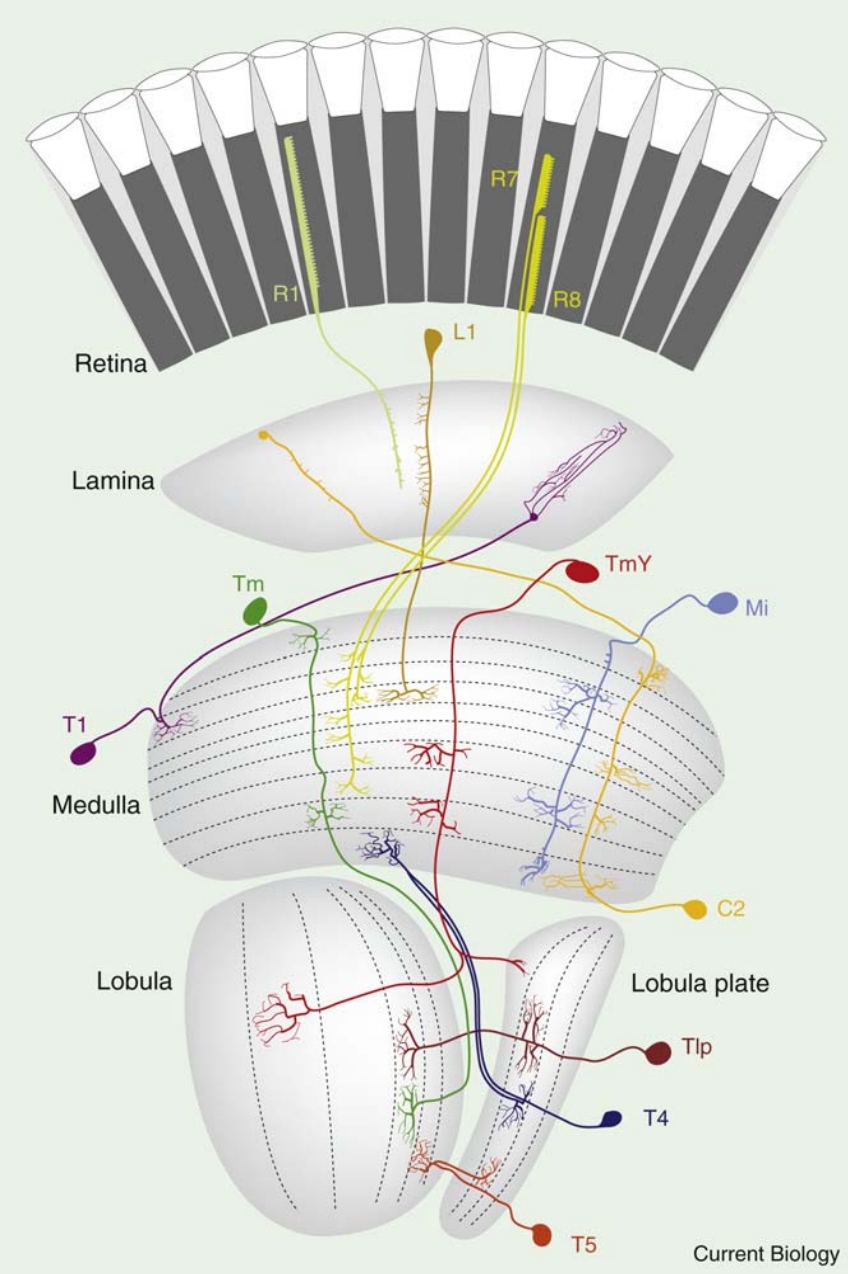

Fig.1.4 Retinotopic map of columnar cell types in *Drosophila* visual neuropiles (Borst, 2009).

1.4.3 *Drosophila* vision: a focus on motion detection

Vision is classified into different categories such as polarization vision, depth perception, color vision and motion vision (Borst, 2009). We will focus on motion vision, that represents an important source to detect information about the surrounding environment, but it is also necessary to perceive self-motion information. *Drosophila* is characterized by a clear motion vision phenotype (Blondeau and Heisenberg, 1982), which can be measured by the analysis of its "optomotor response". The "optomotor response" is a rection correlated with motion detection and is due to the tendency of a fly, placed in a rotational environment around its body axis, to move in a syndirectional manner with respect to the motion of the surround (Burnet and Beck, 1968). In the neural circuits involved in the optomotor response, a primary role is played by R1-6 retinal cells and by their synapses formed into the lamina (Heisenberg and Buchner, 1977). In fact, as already mentioned, these photoreceptors are involved in motion detection and image formation. At level of lamina there are four different channels involved in the transfer of motion detection signal from the retina to following components of the circuit underlying optomotor response. These input pathways are provided by L1-L3 monopolar cells, directly connected to retina, and by T1 neurons, indirectly connected to R1-R6 photoreceptors via amacrine cells. In particular, both L1 and L2 monopolar neurons are presented as necessary and sufficient inputs (Rister et al., 2007; Borst, 2009). Therefore, it appears that there is not only a single network for the detection of movement. Concerning the medulla, there are evidences that bushy T cells, T4 and T5 cells seem to be potentially involved in the motion vision network (Douglass and Strausfeld 1995, 1996; Strausfeld and Lee 1991). At level of the lobula plate, giant tangential cells are a cardinal component for optomotor response (Heisenberg et al., 1978). Indeed, these cells play a key role because they integrate the motion information, establish extensive interactions with each other and transmit their elaborated information to postsynaptic descending neurons. These latter neurons instruct the thoracic ganglion motor centers for locomotion and flight (Borst et al., 2010).

1.4.4 The mushroom bodies

In the insect brain, mushroom bodies (*corpora peduncolata*) are a pair of lobate neuropiles with a symmetric structure. They are globally composed by ~5000 thin and parallel neurons called Kenyon cells. In each brain hemisphere, mushroom bodies (MBs) consist of a densely packed bundle of 2500 thin parallel Kenyon fibers running on either side of the central complex. The Kenyon cells axons form a massive stalk called "peduncle" while their somas are clustered at the dorsal posterior surface of the central brain forming a large cup-shaped protrusion called "calix" (Heisenberg, 2003). The peduncle branches into five terminal lobes

projecting in roughly orthogonal directions (Crittenden et al., 1998). It bifurcates into two major branches, one pointing vertically and the other one horizontally. The vertical branch is subdivided in α and α′ lobes; the horizontal one is composed by three lobes named β, β′ and γ lobes (Fig.1.5). There are at least three Kenyon cell types constituting the MBs: one type projects its axons only to the α and β lobes, a second type projects its axons to α′ and β′ lobes and a third type projects only to the γ lobe (Lee et al., 1999a; Crittenden et al., 1998; Margulies, 2005; Fahrbach, 2006).

In *Drosophila*, MBs have a role in olfactory learning and memory (de Belle and Heisenberg, 1994; Heisenberg, 2003; Davis, 2005; Fahrbach, 2006). In addition, MBs have been shown to influence locomotor activity, being involved in the suppression of walking activity (Martin et al., 1998; 1999b).

The anatomical/structural subdivision of MBs lobes corresponds to a functional specialization. In particular, concerning olfactory learning and memory, γ lobes are important for short-term memory (Zars et al., 2000), while α/β lobes are fundamental for long-term memory formation (Pascual and Preat, 2001; Blum et al., 2009). Regarding locomotor activity, it has been demonstrated that γ lobes are important for centrophobism/thigmotaxis behaviour, which is the tendency to remain close to boundaries of a defined locomotor activity area, avoiding the center of it (Besson and Martin, 2005).

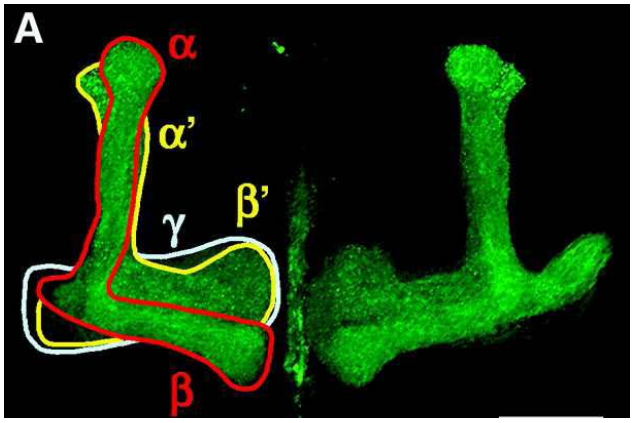

Fig.1.5 Confocal images of an adult wild-type mushroom body. Three sets of neurons generate five axonal lobes. The γ lobe is outlined in white, the α and β lobes are outlined in red, and the α' and β' lobes are outlined in yellow (Pascual and Preat, 2001).

In *Drosophila*, the main MBs neuronal input is provided by neurons of antennal lobes, important components of primary olfactory pathway. These neurons connect single antennal lobe glomeruli to the antennal horn but a subset of them sends also side branches to the calix of MBs (Fig.1.6; Marin et al., 2002; Wong et al., 2002; Heisenberg, 2003). Different neurotransmitters are implied in the olfactory inputs to the MBs: mainly acetylcholine (Gorczyca et al., 2003; Yasuyama et al., 2003) and at minor levels GABA (Yasuyama et al., 2002), octopamine and dopamine (Schwaerzel et al., 2003).

It is important to underline that albeit the anatomical connection of the MBs with brain component subtends the olfactory pathway, MBs are not only involved in

olfactory processing but they also have functions in the regulation of other behaviours, such as transition from walking to rest and visual learning (Zars, 2000).

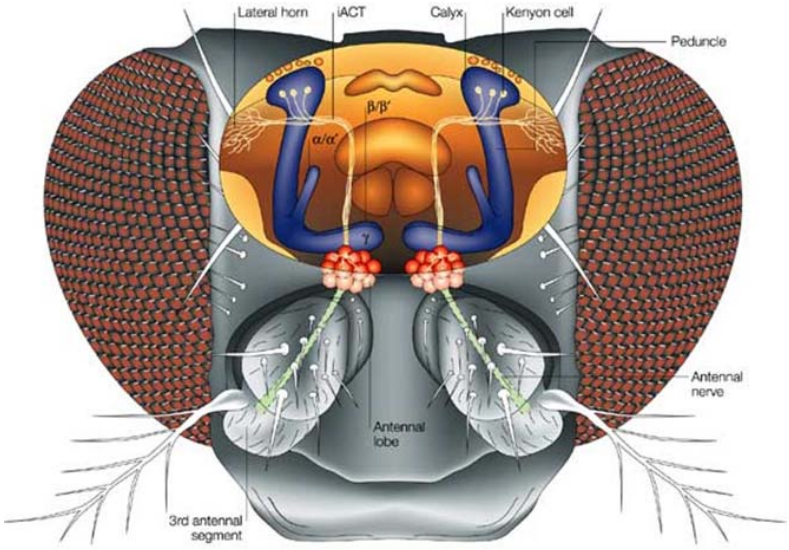

Fig.1.6 *Drosophila* olfactory pathway. Olfactory information is transmitted from the third antennal segments and maxillary palps (not shown) to ~40 glomeruli of antennal lobes. Single glomeruli are connected to both mushroom body calyx and lateral horn of dorsolateral protocerebrum through the inner antennocerebral tract (iACT). The mushroom body lobes subsets are indicated with α/α′, β/β′ and γ (Heisenberg, 2003).

1.4.5 Neuronal bases of *Drosophila* memory

Drosophila is a considered as a good model for the study of learning and memory as behavioural manifestations of neuronal plasticity. In this organism the most examined memory phenotypes are those associated to olfactory pathways (Margulies et al., 2005). Four distinct phases underlying olfactory memory retention have been identified (Fig.1.7): short-term memory (STM), middle-term memory (MTM), anesthesia-resistant memory (ARM) and long-term memory (LTM; Tully et al., 1994).

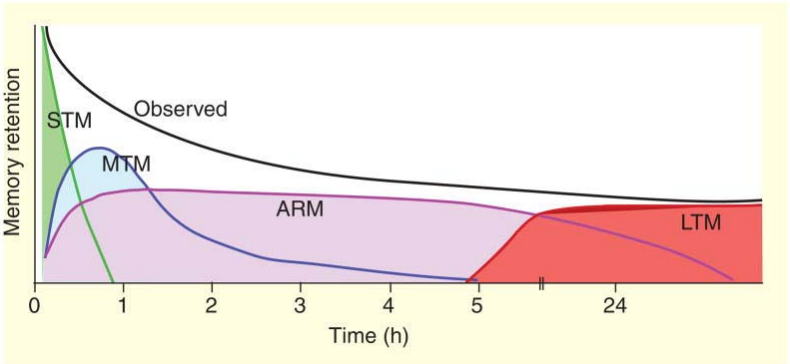

Fig.1.7 *Drosophila* memory phases. In *Drosophila*, memory retention is organized in four distinct phases: short-term memory (STM; green), middle-term memory (MTM; blue) anesthesia-resistant memory (ARM;

purple) and long-term memory (LTM; red). The black line represents the observed decay of memory at behavioural level (Margulies et al., 2005).

A transduction pathway particularly important for olfactory learning and memory is based on cAMP signaling. In fact the most known and characterized memory mutants have impairments in genes coding for components of this signaling pathway. For example, *rutabaga* (*rut*) gene, which is mainly expressed in MBs, encodes a calcium/calmodulin-dependent adenylyl cyclase (Rut-AC; Levin et al., 1992; Zars et al., 2000). *dunce* (*dnc*) gene, another gene mostly expressed in MBs, codes for a cAMP-specific phosphodiesterase (Byers et al., 1981). *amnesiac* (*amn*) gene, which is expressed in two neurons projecting to MBs, encodes a putative neuropeptide similar to pituitary adenylyl cyclase-activating peptide (PACAP; Feany and Quinn, 1995). In a model on the role of MBs in memory formation, Dopamine (DA), Octopamine (OA) and Amnesiac inputs activate through G protein-coupled receptors the Rut-AC. The *neurofibromin* gene (*nf1*) encodes a protein that seems to have a function in sustaining Rut-AC activity. The DNC phosphodiesterase is needed for cAMP degradation in order to prevent excessive cAMP concentration. The cAMP signaling pathway leads to the establishment of either short-term memory, though the phosphorylation of specific substrates, or long-term memory, through the phosphorylation of cAMP response binding element (CREB; Davis, 2005; Margulies et al., 2005)
Both genetic dissection and temporal organization of circuits underlying memory formation and consolidation have been elucidated though a wide range analyses of memory mutants (Fig.1.8; Margulies et al., 2005).

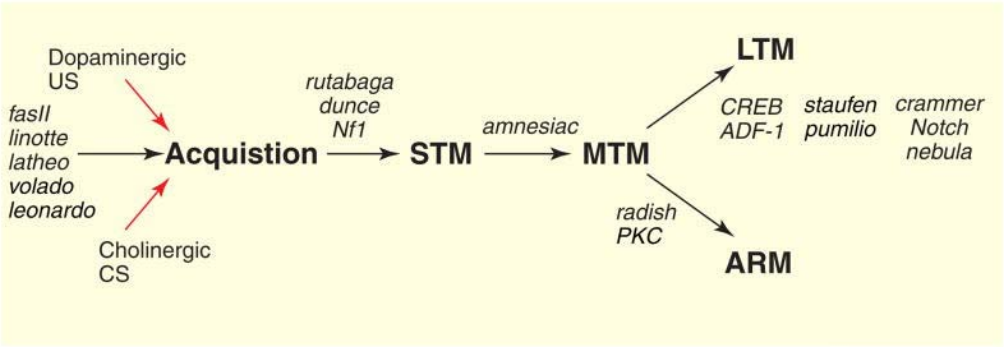

Fig.1.8 Dissection of pathways involved in memory formation. There are mutants preferentially impairing learning/acquisition (*fasII, linotte, latheo, volado* and *leonardo)*, STM (*rutabaga, dunce, Nf1*), MTM (*amnesiac*), ARM (*radish*) and LTM (*CREB, ADF-1, staufen, pumilio, crammer, Notch, nebula*). Every gene may participate at more than one single neural circuit and memory phase (Margulies et al., 2005).

1.4.6 The central complex

The central complex (CC) is a typical structure of the adult insect brain and consists in a system of interlocked neuropiles. It lies in the middle of the brain above the esophagus, between the MBs peduncles and it is laterally bounded by

the two antennal-glomerular tracts (Hanesch et al., 1989; Homberg, 1987). In *Drosophila,* the CC is essentially an adult-specific brain structure, with only a rudimentary counterpart in the larval brain (Renn et al., 1999).
The CC is composed by four interconnected substructures which are schematic represented in Fig.1.9. These substructures are:
a) the ellipsoid-body (eb), a doughnut-shaped neuropile. It is characterized by a concentric pattern of 12-16 glomeruli around its circumference. The principar eb neuronal projections are GABA-ergic ring-like arborizations of large-field neurons, defined as Ring neurons (R neurons). The R cells (R1-4) are classified on the basis of the position of axon entrance within the eb and on the radius of their concentric arborization (Hanesch et al., 1989). The eb is implicated in the fine regulation of locomotor activity, in particular it has a role in the control of the temporal pattern of walking activity (Martin et al., 2001).
b) the protocerebral bridge (pb), that resembles a pair of outstretched wings. It is located between the two MBs calyces and it is constituted by a system of commissural fibers, connecting the two dorsal lobes of the protocerebrum. Its structure is built by 16 glomeruli disposed in a row (8 on each side of the midline).
c) the fan-shaped body (fb), which is saucer-shaped neuropile with a convex side, forming a regular range of strata and columns. Its structure is equipped with eight vertical segments and six parallel horizontal layers.
d) the noduli (no), that are two paired mirror-symmetrically arranged structures with a ball-like shape. Each of them is formed by concentric layers generating a small compact lobe underlying the fb.
Two accessory areas are associated with the CC substructures: the paired ventral bodies (vb) and the paired lateral triangles (ltr; Hanesch et al., 1989).

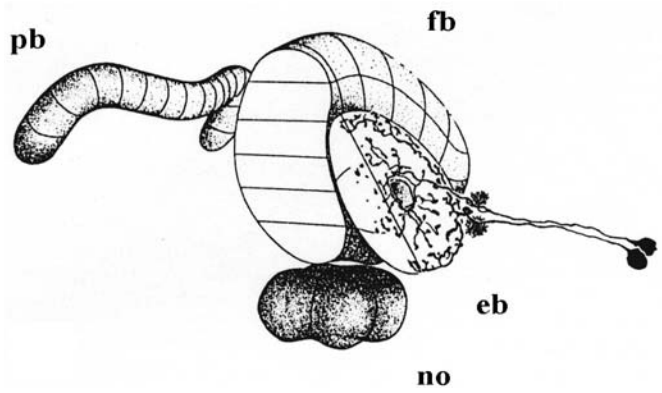

Fig.1.9 Schematic drawing of the central complex. pb: protocerebral bridge; fb: fan-shaped body; eb: ellipsoid-body; no: noduli (Strauss and Heisenberg, 1993).

The CC components are characterized by a repetitive structural organization based on a pattern of vertical segments intercrossed by horizontal strata (Homberg,

1987). In the CC, neurons connecting all the four substructures are not present because the CC cells have at maximum three ramifying regions. The majority of CC neurons are classified into one of these two categories: small-field neurons, constituting the columns or matrix elements, and large-field (tangential) neurons, representing layers perpendicular to the columns. Most small-field neurons are intrinsic to the CC and connect small substructural domains; large-field neurons branch in one or more strata of a single substructure and connect it to one or two central brain regions outside the CC, such as the accessory areas (Hanesch et al., 1989). In the CC it seems that acetylcholine excitatory and GABA inhibitory inputs are separately located (Hanesch et al., 1989), while immuhystochemical experiments indicate also the presence of serotonin, neuropeptides and monoamines transmitters (Homberg, 1987).
The CC is considered to be the higher pre-motor center in the brain, implied in the control and fine regulation of locomotor activity (Strauss et al., 1992; Strauss and Heisenberg, 1993; Strauss, 2002). The CC receives sensory informations and elaborates locomotor activity response, in interplay with the MBs. Thus, CC regulates locomotor activity, optimises walking speed by controlling step length, establishes the across-body symmetry of strides through right-left bargaining and facilitates orientation behaviour (Strauss, 2002). Moreover, the CC has been found to be involved in some forms of memory, such as orientation memory (Neuser et al., 2008), visual pattern recognition memory (Liu et al., 2006; Zars, 2010) and also memory associated to courthship conditioning (Sitnik et al., 2003; Joiner and Griffith, 1999).

1.5 The *Drosophila* circadian clock

1.5.1 General properties of circadian rhythms

The cyclic variation of light, temperature, humidity and other parameters during a 24 h period is a consequence of Earth rotation. Organisms, from *Cyanobacteria* to humans, have evolved an endogenous circadian clock (from latin “circa dies”, which means “about a day”) that permits them to anticipate daily environmental changes and as consequence, to optimize their physiological, metabolic and behavioural processes accordingly.
In *Drosophila* pupal eclosion and adult locomotor activity are phenotypes under the influence of the circadian system (Hall, 2003).
Biological circadian clocks are characterized by basic properties:
- they are able to persist under constant environmental conditions (such as constant darkness) with a period of about 24 h, defined as *free running* period;
- they can be synchronized (or entrained) by external environmental stimuli defined as *Zeitgebers* (time givers), such as light (the most important one), temperature, food and social cues;

- they are temperature compensated meaning that they present almost the same characteristics even in conditions of temperature variation.
In the circadian clocks organization, three main components can be distinguished:
- an input pathway, which perceives environmental stimuli and transmits them to the central oscillator, thus synchronizing the clock accordingly;
- the central pacemaker, which represents the core endogenous mechanism that generates rhythmicity;
- an output pathway which relays the time information established by the central pacemaker to peripheral oscillators and to behavioural, metabolic and physiologic processes.

1.5.2 *Zeitgeber* time and Circadian time

In Chronobiology, there are two distinct ways to measure the time: the *Zeitgeber* time (ZT) and the Circadian time (CT). ZT refers to the presence of an external stimulus that leads to the synchronization of the core circadian clock with environmental changes. CT represents the time measured in constant regimes (or *free running* conditions), when environmental parameters, such as light or temperature, do not vary during the 24 h day.
In ZT conditions, individuals can be entrained in 12 hours of light and 12 hours of darkness (12:12 LD) conditions at constant temperature, with light representing the *Zeitgeber*. In this cycle, ZT0 corresponds to the lights-on, while ZT12 corresponds to the lights-off. In CT regimes, individuals can be maintained in constant darkness (DD) and constant temperature conditions. In this cycle, CT0 corresponds to the beginning of subjective day, while ZT12 corresponds to the beginning of subjective night.

1.5.3 *Drosophila* locomotor activity

Drosophila circadian rhythms are usually studied by recording locomotor activity. In fact *Drosophila* locomotor activity represents one of the most robust, reliable and easily detectable circadian clock-controlled behaviours and is then considered a good system for chronobiological studies. In 12:12 LD conditions, *Drosophila* locomotor activity shows a bimodal distribution along the 24 h day, with two activity peaks, one in the morning and one in the evening, in correspondence to lights-on (ZT0) and lights-off (ZT12) transitions, respectively. Moreover, just before both lights-on and lights-off transitions, wild-type activity gradually raises and this phenomenon is called "anticipation" (Fig.1.10). There is also a burst of activity right after light transitions and this response is called "masking" because it is only due to environmental changes and not to the endogenous circadian function. In wild-type individuals, having an intact endogenous clock, the rhythmicity in the locomotor activity profile persists under constant conditions. In constant darkness conditions the bimodal profile becomes less pronounced with a

tendency to unimodal profile with activity bouts concentrated in correspondence of the subjective evening peak.

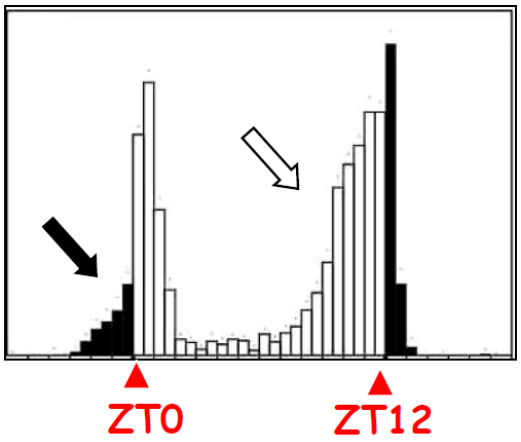

Fig.1.10 Locomotor activity profile of a wild-type fly during ZT time. Single day recording at 12:12 LD condition. ZT0: lights-on; ZT12: lights-off. Bin: 30 min recording. White bins: light; dark bins: dark. Black and white arrows indicate anticipation before lights-on and lights-off transition respectively.

1.5.4 Molecular mechanisms underlying the *Drosophila* circadian clock

At molecular level, in the vast majority of organisms, the regulation of the circadian clock is based on transcriptional feedback loops, in which specific proteins favor the expression of their own repressors (Fig.1.11).
In the main feedback circuit of *Drosophila* the helix-loop-helix transcription factors CLOCK (CLK) and CYCLE (CYC) form heterodimers, activating the expression of different circadian regulated genes by binding to E-Box sequences (CACGTG) in their target promoters (Allada et al., 1998; Darlington et al., 1998; Rutila et al., 1998). The key of this principal feedback loop is represented by the activation of *period* (*per*) and *timeless1* (*tim1*) genes, whose mRNA levels increase in the early night. PER and TIM1 proteins accumulate and dimerize in the cytoplasm, where TIM1 is important for PER stabilization (Lee et al., 1996; Meyer et al., 2006). Then, TIM1 and PER transfer to the nucleus (midnight) alone or forming a heterodimer (Curtin et al., 1995; Shafer et al., 2002) and bind to CLK/CYC heterodimers, leading CLK hyperphosphorylation and to the removal of CLK/CYC complex from binding to the DNA. The final effect is the repression of *tim1* and *per* transcription (late night; Lee et al., 1999b; Yu et al., 2006).
A fundamental characteristic of the circadian clock is its ability to be synchronized by the environment. One of the most important environmental cues in circadian synchronization is represented by light. In *Drosophila*, at molecular level, light activates the blue-light photopigment CRYPTOCROME (CRY) promoting its association with TIM1. This interaction stimulates TIM1 ubiquitinization and degradation, via proteasome pathway (Koh et al., 2006; Peschel et al., 2006). In absence of TIM1, PER is phosphorylated by the DOUBLE-TIME (DBT) kinase (Price et al., 1998), ubiquitinated and then

degraded in the proteasome (Grima et al., 2002). On the consequence, the clock resets.

A second feedback loop, interlocking the first one, provides an additional regulation step on the activity of the CLK/CYC heterodimer by regulating *Clk* transcription. In this second circuit CLK/CYC complex activates the transcription of other circadian genes: *Vrille* and *Pdp1e* (Cyran et al., 2003). PDP1e promotes *Clk* transcription whereas VRI exerts an inhibitory effect (Peschel and Helfrich-Forster, 2011; Allada and Chung, 2010).

Although virtually all *Drosophila* body cells have a running molecular clock, the central pacemaker resides in the brain (Nitabach and Taghert, 2008; Helfrich-Forster et al., 2007).

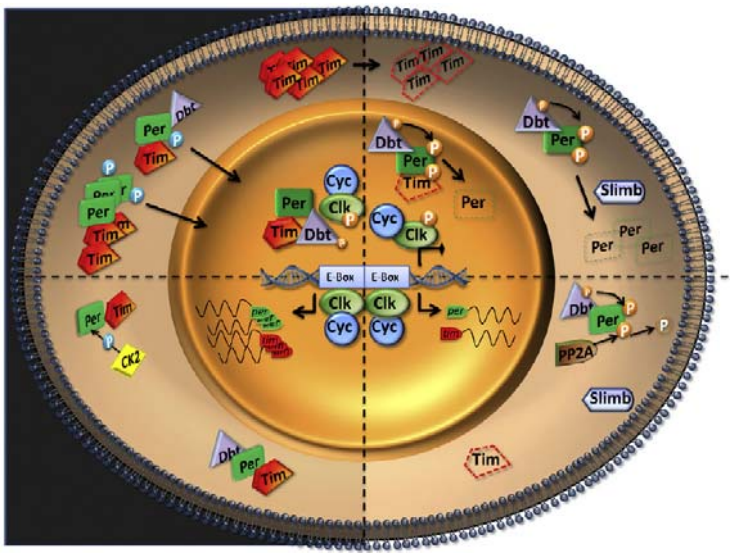

Fig.1.11 Molecular mechanisms of the interlocked feedback loops in the *Drosophila* circadian clock. Dashed arrows on proteins indicate proteasomal degradation, normal arrows indicate movement (Peschel and Helfrich-Forster, 2011).

1.5.5 Anatomical organization of the central clock

The master circadian clock of *Drosophila melanogaster* is localized in the brain and is composed by ~70 clock neurons for each brain hemisphere (Fig.1.12). These clock neurons are clustered in two main groups per hemisphere named according to their anatomical position: the Dorsal Neurons (DNs), laying in the dorsal *protocerebrum* and the Lateral neurons (LNs), located between the optic lobe and the central brain. Neurons belonging to these two clusters can be further subdivided according to their size, protein content and/or function. Three different groups can be distinguished for DNs: DN1s, DN2s and DN3s. The LNs are classified in: small Ventral Lateral neurons (four s-LNvs and the 5th s-LNv), large ventral Lateral Neurons (l-LNvs), dorsal Lateral neurons (LNds) and the recently identified lateral Posterior Neurons (LPN) (Kaneko and Hall, 2000; Shafer et al., 2006; Helfrich-Forster et al., 2007; Peschel and Helfrich-Forster, 2011).

Four out of five s-LNvs are the main pacemaker neurons with a role in driving the morning anticipation of lights-on transition and are sufficient for oscillatory behaviour maintenance in constant darkness conditions (Grima et al., 2004; Stoleru et al., 2004). LNds are involved in the evening anticipation of lights-off transition (Grima et al., 2004; Stoleru et al., 2004). The 5th s-LNv seems to be also implicated in the control of the evening anticipation (Grima et al., 2004), but its function remains to be further elucidated. l-LNvs are supposed to modulate arousal and wakefulness as well as sleep stability (Sheeba et al., 2008). DN1s are involved in light sensitivity and in sustaining rhythmic behaviour in constant light regime (Klarsfeld et al., 2004; Murad et al., 2007; Stoleru et al., 2007). DN2s and LPNs have a role in temperature sensitivity (Yoshii et al., 2005; Miyasako et al., 2007). DN3s contribute to the evening peak of activity in LD conditions (Veleri et al., 2003).

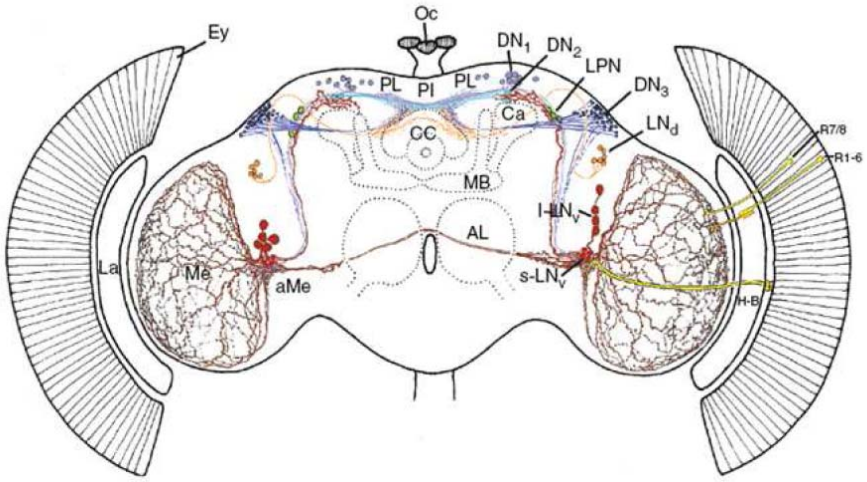

Fig.1.12 Schematic representation of *Drosophila* brain (Helfrich-Forster et al., 2007).

1.6 The *Drosophila timeless2* locus

timeless2 (*tim2* or *timeout*) is a large *Drosophila melanogaster* gene localized in the right arm of the third chromosome (chr 3R). It spans ~75 kb and it is composed by 18 exons and 17 introns (Benna et al., 2000; Gotter et al., 2000).
It represents the paralogous of the widely characterized *timeless1* (*tim1*) gene (Sehgal et al., 1994), that plays a key role in the central pacemaker of the endogenous *Drosophila* circadian clock (Perschel and Helfrich-Forster, 2011).
tim2 transcription gives rise to a main mRNA which codes for a putative 1384 aa TIM2 protein and three smaller transcripts expressed at very low levels during *Drosophila* development.
mRNA *in situ* hybridization experiments showed that *tim2* is expressed in ovaries, in particular in nurse cells, and during all the developmental stages. In embryos it starts to be detected from the earliest stages (blastoderm) where its expression pattern appears quite diffuse. In adult stage, mRNA *in situ* hybridization

experiments performed on adult brains showed that *tim2* is mainly expressed in a subregion belonging to the optic lobes, specifically in T1-basket neurons of the medulla, which is the second optic neuropile. T1-basket neurons project to both an outer medulla region and to the lamina where they form a basket-shaped arborization pattern (Meinertzhagen and O'Neil, 1991; Takemura et al., 2008). Moreover, a weak *tim2* expression is present at level of the ellipsoid-body of the central complex and in mushroom bodies, whereas, unlike its paralogous *tim1*, *tim2* mRNA is not localized in circadian clock neurons (Benna et al., 2010).

Drosophila tim2 exerts an essential role during development, being involved in the maintenance of chromosome integrity under both physiological and genotoxic stress conditions. In fact $tim2^{-}$ mutations are lethal at pupal stage in homozygousity and $tim2^{-}/tim2^{-}$ mutants exhibit a phenotype characterized by chromosomal aberrations in larval neuroblasts (Benna et al., 2010). Furthermore, *tim2* exerts a second role peculiar of the adult stage. In fact it is involved in the synchronization of the endogenous circadian clock to external environmental light cues (Benna et al., 2010).

Drosophila tim2 locus harbors at least four transcribed intronic sequences, two localized in intron 2 (*CG34308* and BK002510) and two in intron 11 (*2mit* and *AY118619*; Fig.1.13).

On the basis of bioinformatic analyses, *CG34308*, *BK002510* and *AY118619* intronic sequences do not seem to represent protein-coding nested gene. It has been hypothesized that they might be primary miRNA precursors, transcribed pseudogenes or, alternatively, long non-protein-coding RNAs (Benna et al., 2010). On the other hand, *in silico* predictions have indicated that *2mit* might represent a protein-coding intronic gene.

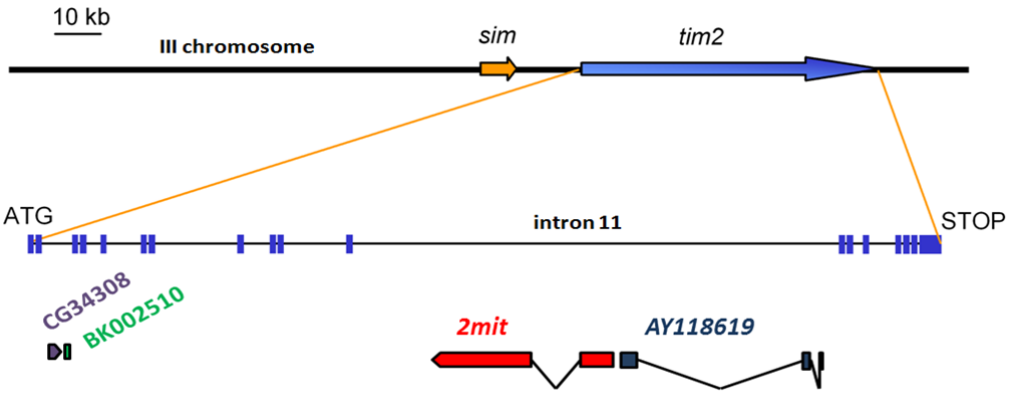

Fig.1.13 Schematic representation of the *timeless2* locus. *timeless2* locus spans 75 kb, is organized in 18 exons and 17 introns and harbors actively transcribed sequences in its 2nd intron (*CG34308* and *BK002510*) and 11th intron (*2mit* and *AY118619*).

1.7 The *Drosophila 2mit* locus

1.7.1 *2mit* gene

2mit gene is localized within the 11th intron of *tim2* locus and is oriented in the opposite transcriptional direction with respect to its host gene (Fig 1.13). Indeed, the name *2mit* is reminiscent of that. *2mit* gene is composed by 2 exons and one intron. *2mit* is transcribed in two mRNA isoforms: a 5399 and a 3860 nt transcripts which differ in the length of their 3' UTR sequences. *In silico* translation suggests that *2mit* gene codes for a 1141 aa transmembrane protein (Fig.1.14; Benna et al., 2010).

1.7.2 2MIT putative protein

2MIT putative protein is classified as type I transmembrane protein because its N-terminal portion (till the 930 aa) is extracellular and its C-terminal portion (954-1141 aa) is localized in the cytoplasm (Fig.1.14). Sequence analyses identified the presence of a signal peptide (1-28 aa), a transmembrane domain (TM; 931-953 aa) and different putative domains such as an extracellular Leucine-Rich Repeat (LRR) motif (100-500 aa), and an intracellular Ser-rich region (1037-1076 aa) in proximity to the C-terminal, which might present putative phosphorylation sites (Fig.1.14).

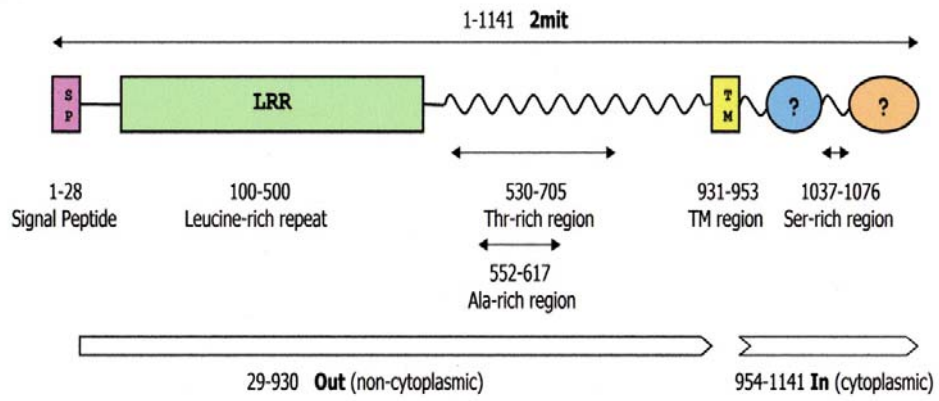

Fig.1.14 2MIT protein putative structure.

1.8 The Leucine-Rich Repeat domain

The leucine-rich repeat (LRR) is a widespread and very conserved structural motif characterized by an arrangement in tandems of internal repetitive stretches. It has been identified in protein sequences belonging to all life forms, from viruses to Eukaryotes, including bacteria, fungi, plants and animals. The ribonuclease

inhibitor (RI) was the first structure to have been identified as containing LRR repeats (Kobe and Deisenhofer, 1993). Although LRR domains are found in proteins presenting heterogeneous and unrelated structure, localization and function (Kajava, 1998; Kobe and Kajava, 2001), these LRR regions have a primary common function. In fact LRR motifs are involved in the formation of protein-protein interactions generated by exploiting their versatile and highly evolvable structural framework (Dolan et al., 2007).
Seven classes (Kobe and Kajava, 2001) of LRR have been defined and all of them share a typical structure characterized by motifs that are 20-29 aa long and rich in the hydrophobic leucine amino acid. Each repeat is characterized by a conserved N-terminal sequence of 9-12 aa and by a C-terminal stretch of 10-19 aa which is more variable in sequence, length and structure with respect to the N-terminal one. Specifically, the N-terminal stretch presents hydrophobic residues (usually leucines) in precise positions and forms a β-strand. The global arrangement of multiple repeats in tandem produces a horseshoe-shaped solenoidal structure, whose concave surface is formed by β-strands and the convex one is composed by variable stretches (Kajava, 1998; Kobe and Kajava, 2001; Bell et al., 2005; Mosyak et al., 2006; He et al., 2003). The majority of LRR domains, in particular the ones of extracellular proteins, present typical N-terminal and C-terminal cap regions carrying precisely positioned cysteine residues (Kajava et al., 1998) that form disulfide bonds and, on the consequence, confer stability to the LRR structure (Leonardi et al., 2011). Many LRR proteins have known functions in the immune response, embryonic development, neuronal development and connectivity, cell adhesion and signalling (for example growth factor pathways), platelet aggregation, extracellular matrix assembly, RNA processing, adhesion and invasion of pathogenic bacteria to host cells, pathogen recognition and disease resistance in plants (Bella et al., 2008).
LRR domain of 2MIT putative protein is composed by four predicted 24 aa motifs characterized by the classic consensus sequence, repeated in tandem. Moreover, cystein residues at the extremities of the LRR domain provide the typical N-terminal and C-terminal boundaries.

1.9 State of the art

At the beginning of my project, in the laboratory where I have attended my PhD, some results about *2mit* characterization were already available. Here I provide a brief description of them, as they represented the starting point for my research.

1.9.1 *2mit* expression pattern in ovaries and during embryonic development

mRNA *in situ* hybridization experiments on wild-type ovaries and embryos were performed. In ovaries, *2mit* mRNA is detected in follicolar cells from stadium 10 of the ovary chamber development (Fig.1.15a-c). In embryos, *2mit* mRNA is

expressed from blastoderm stage, 2 h after egg-laying, with a diffuse expression pattern (Fig.1.16a). During gastrulation, at ~4 h after egg-laying, its expression mainly localizes in the medium gut and in tissues that will generate the nervous system (Fig.1.16b). Subsequently, during segmentation, at ~12 h after egg-laying, *2mit* mRNA expression profile is prevalent at level of the central and pheripheral developing nervous system (Fig1.16.c-d).

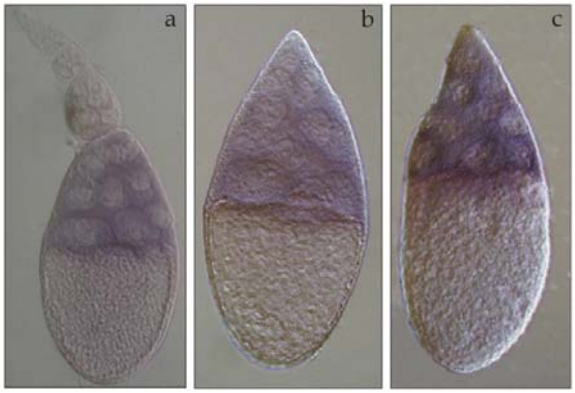

Fig.1.15 mRNA *in situ* hybridization of *Drosophila* wild-type ovaries treated with *2mit*-fluorescein antisense probe and anti-fluorescein antibody. **a)** ovary chamber at 10 stadium of development with a typical elongated shape: *2mit* expression at previous stages is not detectable. **b-c)** ovary chamber at 10 and 11 stadium, where the oocyte grows taking gradually more space: *2mit* mRNA expression is visible in the follicular cells, even if it is not very intense.

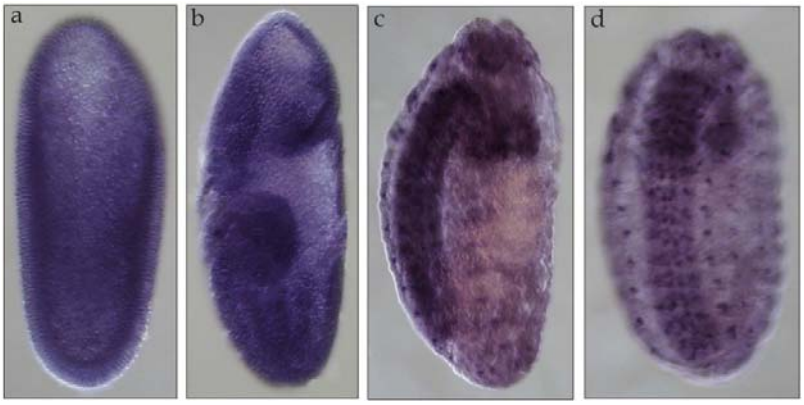

Fig.1.16 mRNA *in situ* hybridization of wild-type *Oregon-R* embryos treated with *2mit*-fluorescein antisense probe and anti-fluorescein antibody. **a)** 2 h after egg-laying: *2mit* mRNA expression is diffuse. **b)** 3-4 h after egg-laying: *2mit* mRNA is mainly localized in developing Central Nervous System (CNS) and medium gut. **c)** lateral and **d)** frontal vision 12 h after egg-laying: *2mit* mRNA is localized in both CNS and peripheral ganglia corresponding to parasegments.

1.9.2 Generation and first characterization of *2mit* double strand RNA interference strains

Double strand RNA interference (RNAi) is a powerful technique used to induce knock-down (KD) of a target gene. In *Drosophila* it is possible to induce a stable KD via RNAi using a strategy based on transgenic generation and on the use of

the UAS-GAL4 binary system (Brand and Perrimon, 1993), as described in Chapter 3 (Materials and Methods section).
In the laboratory where I performed my PhD thesis, three independent lines, transgenic for *2mit* RNAi construct, have been generated: *6.1-2miti*, *16.2-2miti* and *61.1-2miti*. For all of them, an early and general induction of *2mit* KD (using *ActGal4* driver) caused lethality at pupal stage, with defects characterized by partial hystolitic tissue, necrotic zones and disorganized thoracic bristles in correspondence to the abdominal region (Fig.1.17). This suggested that *2mit* is an essential gene, with a fundamental role during metamorphosis.

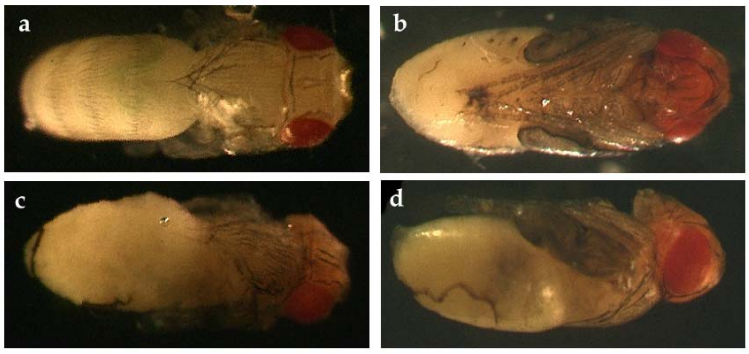

Fig.1.17 Frontal vision of *ActGal4/2miti* individuals. **a)** wild-type control (*Oregon-R* genotype). **b)** *ActGal4/2miti* individual characterized by developmental arrest at level of the abdomen (the most observed phenotype). **c)** *ActGal4/2miti* individual characterized by disorganization of thoracic bristles. **d)** *ActGal4/2miti* individual showing hystolitic and necrotic zones at level of the abdomen.

The strongest *2mit* KD effect was detected using *6.1-2miti* line, in which only 0.5% of pupae reached the adult stage. Anyway, employing *16.2-2miti* and *61.1-2miti* lines to drive *2mit* KD, ~15% of escapers, mostly females, overcame the pupal stage and eclosed as adult individuals.
Via Northern blot assays, a specific *2mit* mRNA decrement was demonstrated in *2mit* KD pupal samples, suggesting a relation between *2mit* depletion and pupal lethality (Fig.1.18).

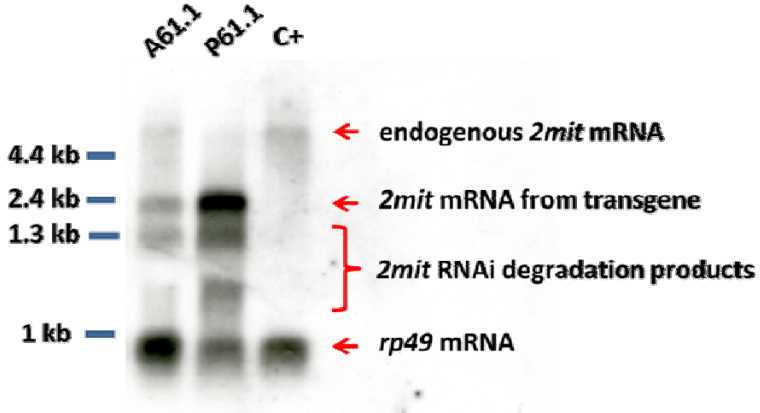

Fig.1.18 Northern blot experiments performed on *2mit* mRNA extracted from *ActGal4/61.1-2miti* adult escapers (A61.1), *ActGal4/61.1-2miti* pupal samples (P61.1) and *Oregon-R* adults (positive control, C+). In

Oregon-R positive control and escapers samples the band >4.4 kb corresponds to ~ 5 kb most abundant *2mit* mRNA isoform. In addition, in both escapers and pupal samples a band at ~2.5 kb, corresponds to *2mit* mRNA transgene. In both samples, a series of bands at lower molecular weights represents *2mit* degradation products generated by activation of RNAi machinery.

1.9.3 *Drosophila melanogaster 2mit* orthologues and phylogenesis

An *in silico* analysis using *Drosophila melanogaster* (*Dm*) 2MIT sequence as query was performed in order to identify hypothetical orthologues.
This analysis led to the identification of *2mit* putative orthologues in 10 Drosophilid species and in the following Insects: *Culex quinquefasciatus*, *Apis mellifera*, *Pediculus humanus* and *Acyrthosiphon pisum*. All genes appear to be transcribed, as demonstrated by the presence of EST sequences in dbEST database (http://www.ncbi.nlm.nih.gov/dbEST/).
A phylogenetic analysis, performed including all identified 2MIT putative proteins (Fig.1.19a) contributed to indicate that 2MIT is conserved among all Drosophilid species, whose homologues are closer to *Dm* 2MIT sequence with respect to those identified in other Insects. A comparison with TIM2 protein homologues phylogenetic tree (Fig.1.19b) suggests that TIM2 and 2MIT phylogenetic distances with their orthologues are similar.

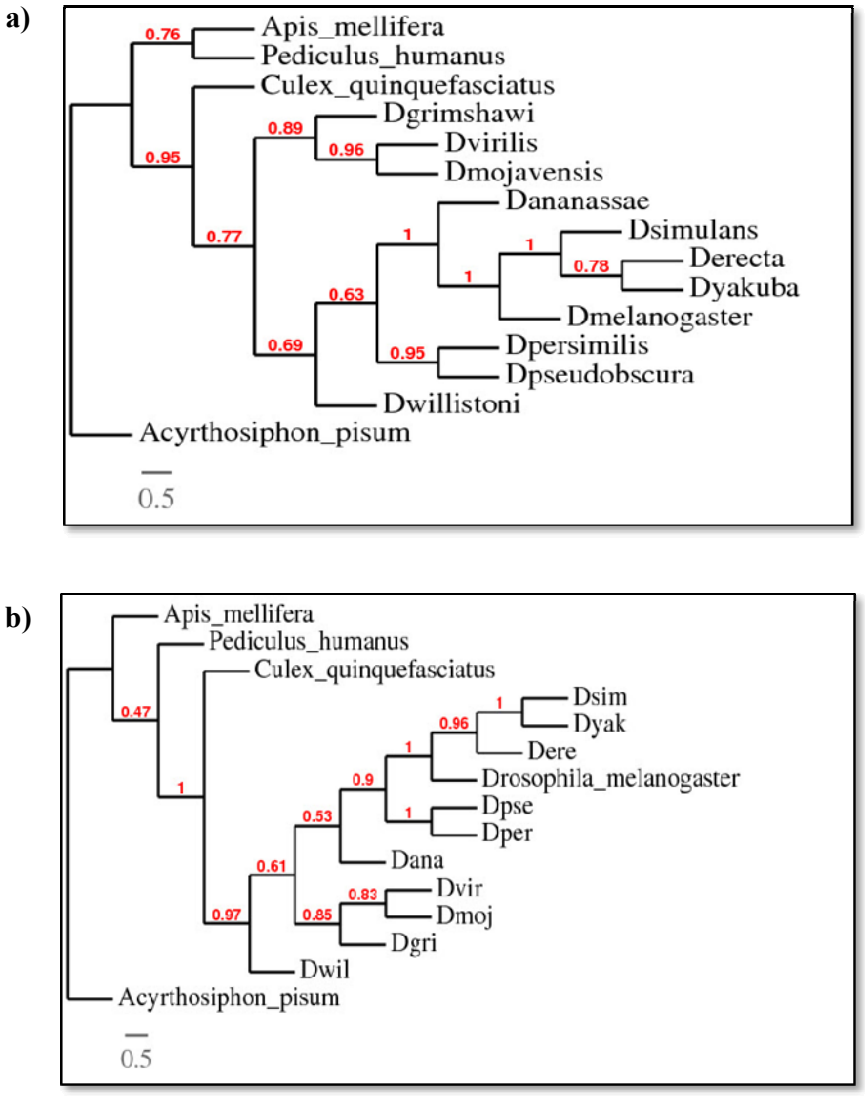

Fig.1.19 Phylogenetic tree of **a)** 2MIT and **b)** TIM2 protein similarity distances and conservation in Drosophilids and other Insects. Statistical support for nodes on the trees was evaluated by the bootstrapping values (×1000) shown in each branch point obtained by the Maximum-Likelihood method included in the PHYLIP software package program (Guindon and Gascuel, 2003). *Acyrthosiphon pisum* was considered as outgroup. The scale bar corresponds to the amino acid substitution per site.

A multiple sequence alignment among eleven Drosophilids 2MIT polypeptides, using PRALINE software (http://www.ibi.vu.nl/), showed a high conservation degree during *Drosophila* speciation. Effectively, the typical 2MIT Leucine-Rich Repeats (LRR) domains and the C-terminus trans-membrane domain appeared conserved. A multiple alignment including also 2MIT predicted protein sequences found in other Insects, showed that all these 2MIT orthologues share the same global features of *Dm* 2MIT.

The analysis of the chromosomal regions harboring *Dm 2mit* and the other Drosophilds *2mit* genes permitted to identify conserved synteny in all Drosophilid

species when using a 200kb-gene sliding window. Fig.1.20 illustrates an example of synteny maintenance, between *Dm 2mit* and *D grimshawi 2mit* orthologue.

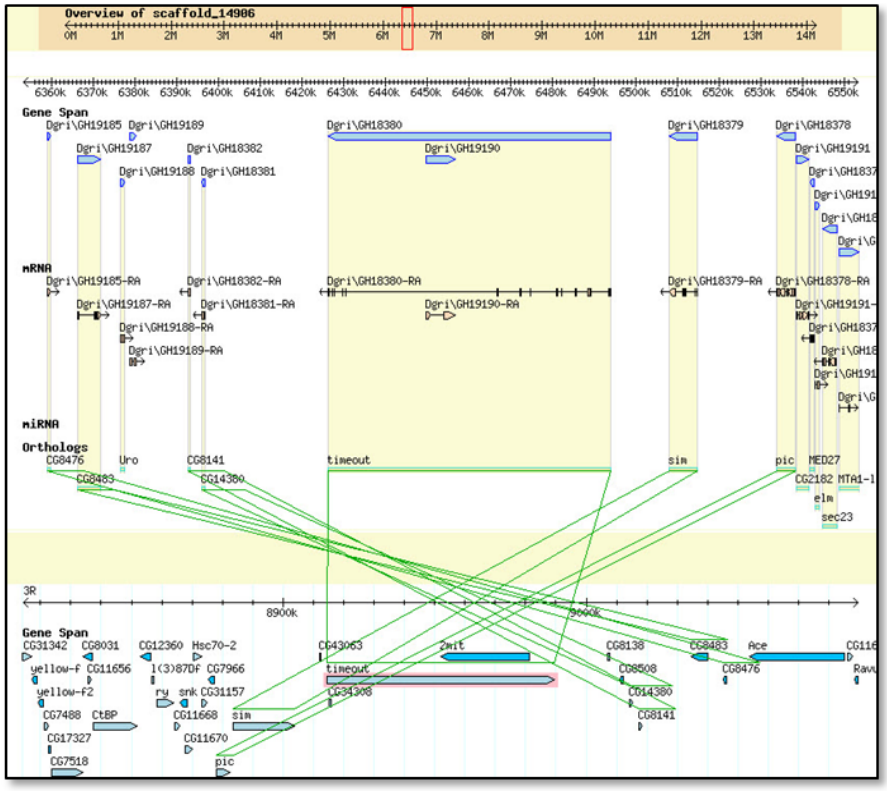

Fig.1.20 *2mit* synteny maintenance between *Dm* and *Dgrimshawi* species. The genome organization in regions flanking *Dm 2mit* and *Dgrim 2mit* orthologue (taken as an example) is conserved; also the *Dm 2mit* and *Dgrim 2mit* orthologue genomic localization and orientation correspond (http://flybase.org/).

1.10 Aim of the work

The aim of the project is to determine the role of *Drosophila 2mit*, the unique *tim2* intronic gene predicted coding for protein. This project was developed performing analyses both at molecular and behavioural levels. The elucidation of *2mit* function has been made also with the intention to evaluate the possible relationship with its host gene *tim2*.

As illustrated in the following chapters, the evaluation of the *2mit* role has been studied analysing *2mit* expression pattern in the adult brain, exploring the effects of *2mit* mRNA depleted levels, characterizing *2mit* overexpression in the *2mit*$^{-}$ mutant genetic background and finally searching 2MIT protein putative interactors in Yeast Two Hybrid System.

CHAPTER 2:

Characterization of *2mit* expression in wild-type and insertional mutant strains

2. Introduction

This chapter reports the molecular characterization of *Drosophila melanogaster* *2mit* gene in wild-type and mutant strains.
In the first part, we describe our investigations on *2mit* mRNA expression in wild-type adults based on *2mit* mRNA levels determination in heads during the 24 h day and on *2mit* mRNA localization in brains. Then, we describe the characterization of several transgenic strains, carrying a transposon insertion nearby or inside *2mit* locus, performed in order to identify in which strains *2mit* mRNA expression levels are perturbed. Finally, we characterize *2mit* mRNA expression pattern in *2mit* mutant brain.

2. Results

2.1 Characterization of *2mit* mRNA expression levels during the 24 h day in *Drosophila* wild-type adult heads

Real-time PCR experiments were performed in order to evaluate *2mit* mRNA levels during the 24 h in wild-type adult heads. Each sample was composed by ~50 adult heads of 3-7 days old wild-type individuals (*white*^{1118} genotype), collected at different ZTs (ZTs: 0; 4; 8; 12; 16; 20) in 12:12 LD conditions and different CTs (CTs: 48; 52; 56; 60; 64; 68; 72) in DD conditions at 23°C . Before sampling, all individuals were entrained in 12:12 LD conditions for three days. For the analysis in *free running* conditions, individuals were transferred in DD regime for further three days before sampling. Three replicates per time point were performed.
2mit mRNA levels in heads from individuals entrained in 12:12 LD conditions showed an oscillating profile with a slight but significant variation along the 24 h (Fig.2.1a). The peak of expression was around the end of the night, between ZT20 and ZT0, while the minimum *2mit* mRNA expression level was at ZTs 8-12, around the end of the day (Fig.2.1a). *2mit* mRNA levels from individuals entrained in DD did not display any significant variation among the different time points meaning, that *2mit* mRNA expression became constitutive in constant conditions (Fig.2.1b).

a)

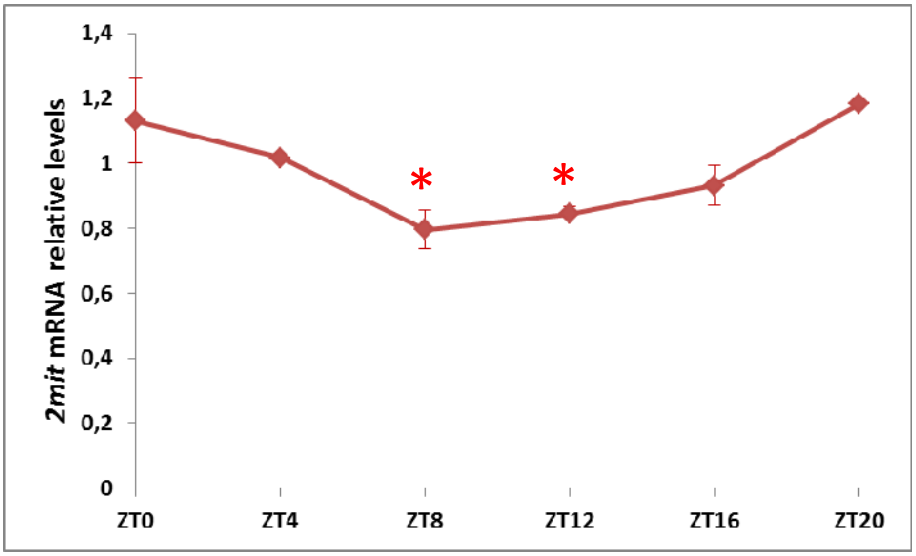

b)

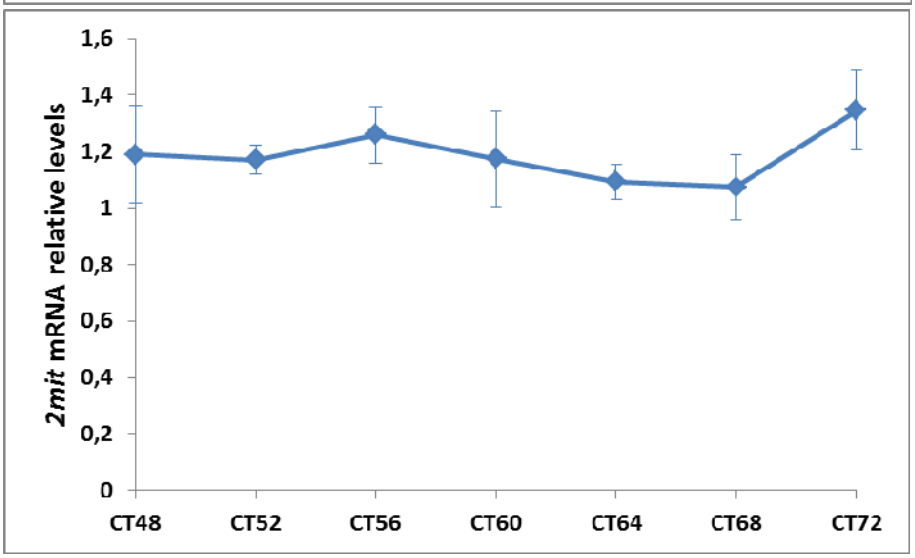

Fig.2.1 Real-time PCR values of *2mit* mRNA expression levels in *Drosophila* wild-type heads during the 24 h day, normalized with respect a control sample considered as having *2mit* mRNA levels equal to 1. **a)** 12:12 LD conditions: ANOVA: *$F_{(5,10)}$=7.885 p=0.003. *2mit* expression levels show a slight but significant 24 h variation. **b)** DD conditions: ANOVA: $F_{(6,14)}$=0.559 p=0.756 n.s. *2mit* expression levels do not show a significant circadian oscillation. *:statistically significant. n.s.:not significant.

2.2 Characterization of *2mit* mRNA expression pattern in *Drosophila* wild-type adult brains

In order to precisely evaluate *2mit* expression pattern in *Drosophila* wild-type adult brains, mRNA *in situ* hybridization experiments were performed using two specific antisense probes: a Biotin-labeled probe specific for *2mit* mRNA detection and a Digoxigenin-labeled probe recognizing *cryptochrome* (*cry*) mRNA. In *Drosophila*, *cry* is a fundamental component of the central circadian clock and in these experiments *cry* probe was used to mark the brain circadian neurons.

Initially, mRNA *in situ* hybridization experiments were performed on whole-mount wild-type adult brains, dissected at ZT1 (one hour after lights-on). We chose ZT1 time point because it is comprised in the time window in which we found higher *2mit* mRNA levels in real-time PCR experiments. For these experiments four replicates were performed and, for each of them, at least five brains were analysed.

In Fig.2.2a the *2mit* mRNA localization signal is reported for a single confocal brain section. The analysis of *2mit* mRNA staining pattern revealed a strong hybridization signal mainly at level of ellipsoid-body, the doughnut-shaped structure lying in the middle of the brain that is a component of the *Drosophila* central complex. In addition, *2mit* mRNA was also strongly expressed in correspondence to mushroom bodies lobes (Fig.2.2a), a pair of symmetrical structures flanking the ellipsoid-body. A further weak *2mit* mRNA signal was identified in optic lobes (Fig.2.2a). In fact, despite a mild background staining was detected in optic lobes of negative controls using the *2mit* sense probe (Fig.2.2d), the *2mit* mRNA signal revealed with the antisense probe seemed to be slightly more intense.

Fig.2.2c shows that the merge between *2mit* (in green, Fig.2.2a) and *cry* (in red, Fig.2.2b) hybridization signals did not overlap, suggesting that *2mit* mRNA expression was not localized at level of the circadian neurons where *cry* signal was detected.

Subsequently, *2mit* mRNA *in situ* hybridization experiments were performed on whole-mount wild-type brains dissected from individuals collected at different ZTs (ZTs: 1; 5; 9; 13; 17; 21) in 12:12 LD condition, or at different CTs (CTs: 49; 53; 57; 61; 65; 69) in DD regime. These series of experiments were performed in order to determine whether *2mit* mRNA localization profiles varied in the brain during the 24 h. In both LD and DD conditions, *2mit* mRNA localized mainly at level of ellipsoid-body and mushroom bodies, with a faint expression in optic lobes, as revealed for brains collected at ZT1, while no other brain regions seemed to express *2mit* gene (data not shown).

In addition, in order to determine whether there was a co-localization between *2mit* and *tim2* mRNAs in correspondence to optic lobes, given the *tim2* expression in T1-basket neurons of the second optic neuropile (Benna et al., 2010), mRNA *in situ* hybridization experiments with specific *2mit* and *tim2* antisense probes were performed. Unfortunately, the obtained results failed to be clear and this was probably due to inefficiency of the *2mit* probe used, that was the one Digoxigenin-labeled. In fact both *tim2* and *2mit* Biotin-labeled antisense probes were much more efficient with respect to the Digoxigenin-labeled ones. On the consequence the mRNA *in situ* hybridization experiments regarding *2mit-tim2* co-localization were shelved.

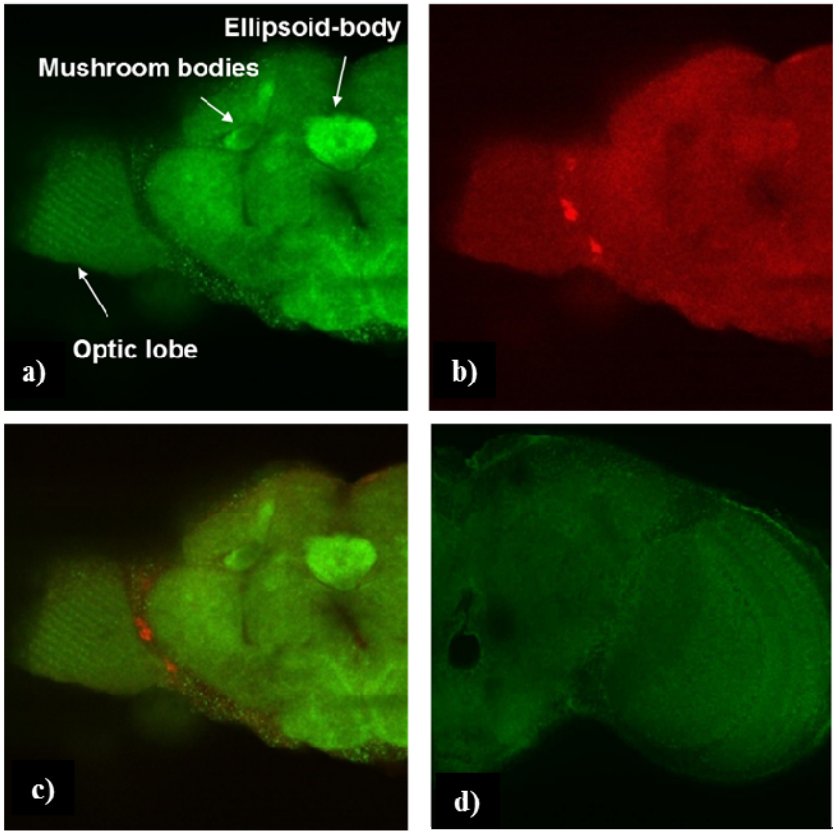

Fig.2.2 mRNA *in situ* hybridization experiments showing *2mit* mRNA expression pattern in a confocal section of an adult *Drosophila* wild-type brain at ZT1. GREEN: *2mit* mRNA; RED: *cry* mRNA (clock neurons marker) **a)** *2mit* mRNA is expressed in the ellipsoid-body of the central complex and in mushroom bodies; a mild expression is also detected in the optic lobe (arrows). **b)** expression pattern of *cry* in clock neurons. **c)** merge of both expression patterns. *2mit* mRNA does not localize at level of *cry* mRNA-positive clock neurons. **d)** negative control obtained using the *2mit* mRNA sense probe.

2.3 Characterization of *2mit* mRNA levels in strains carrying a transposon insertion in intron 11 of *tim2* locus

Six different strains, each generated by an independent insertion of either a *PiggyBac* (*PB*, also marked with *c* or *f*) or a *Minos* (*Mi*, marked with *MB*) transposon produced by Exelixis Gene Disruption Project (Bellen et al., 2004), were characterized. Transposon insertion sites in all these strains localize within the *tim2*'s 11th intron, in proximity or inside *2mit* locus (Fig.2.3).
Real-time PCR experiments were performed in order to determine whether the transposon insertions affected *2mit* mRNA expression.

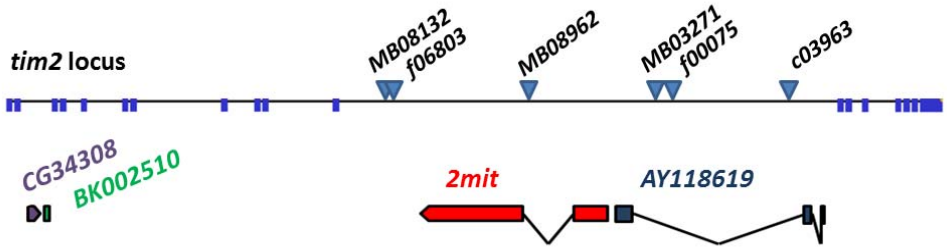

Fig.2.3 *tim2* locus showing the localization of transposon insertions, in its intron 11, of six different insertional strains.

Initially, levels of *2mit* mRNA were determined at third larval stage (L3). Each sample was composed by 10 L3 larvae and at least two replicates per genotype were analysed.

Only the *c03963* strain (also named *PB2mit*^{c03963}), carrying a *PiggyBac* transposon inserted at ~20 kb upstream *2mit* locus with respect to *2mit* gene orientation (Fig.2.3), at L3 stage showed a significant *2mit* mRNA levels decrement of ~50 % in comparison to the *white*^{1118}control (Table 2.1; Fig.2.4). On the contrary, in *f06803*, *f00075*, *MB08132*, *MB08962* and *MB03271* insertional strains, *2mit* mRNAs levels remained comparable to those of *white*^{1118} genotype (Table 2.1; Fig.2.4).

Subsequently, to determine that *2mit* mRNA depletion in *PB2mit*^{c03963} strain was specifically due to *PB* transposon insertion, we changed its genetic background by outcrossing it for eight generations with the *white*^{1118} strain. *white*^{1118} is a well characterized strain that could be considered as wild-type for many behavioural phenotypes such as locomotor activity, circadian rhythmicity and memory. In addition, it represented the starting strain through which the *PB2mit*^{c03963} strain has been generated by transposon insertion. Outcrossing is a common strategy in *Drosophila* and it is necessary to counteract the genetic drift effect on the analysed genotypes.

Subsequently, real-time PCR experiments on L3 larval samples were repeated for the outcrossed *PB2mit*^{c03963} strain, showing *2mit* mRNA decreased levels comparable to those detected for the same strain before outcrossing (Table 2.1; Fig.2.4). This result confirmed that in the *PB2mit*^{c03963} strain *2mit* mRNA expression was specifically affected by *c03963* transposon insertion.

genotype	*2mit* (N) mean± s.e.m.	*tim2* (N) mean± s.e.m.	*GC34308* (N) mean± s.e.m.	*BK002510* (N) mean± s.e.m.	*AY118619* (N) mean± s.e.m.
PB2mit^{c03963}	(8) 0.542±0.052*	(3) 1.259±0.252	(4) 1.129±0.334	(4) 1.274±0.572	(4) 0.884±0.120
f06803	(2) 1.301±0.004	(4) 0.246±0.149*	(1) 3.477	(1) 3.687	(1) 1.457
f00075	(2) 0.948±0.126	(2) 0.745±0.136	(1) 1.593	n.d.	(1) 0.967
MB08132	(3) 1.349±0.187	(3) 0.929±0.027	n.d.	n.d.	n.d.
MB08962	(3) 1.039±0.234	(2) 0.947±0.009	n.d.	n.d.	n.d.
MB03271	(4) 1.285±0.132	n.d.	n.d.	n.d.	n.d.
white^{1118}	(6) 1.290±0.171	1	1	1	1

Table 2.1 Mean and standard error of the mean (s.e.m.) of L3 larval mRNA levels of *2mit*, *tim2* and *CG34308*, *BK002510* and *AY118619* intronic sequences in *PB2mit^{c03963}*, *f06803*, *f00075*, *MB08132*, *MB08962* and *MB03271* strains compared to the *white^{1118}* control. N indicates the number of tested samples. ANOVA regarding *2mit* mRNA levels is reported in Fig.2.4; ANOVA was perfomed for *tim2* and its intronic trancripts in *PB2mit^{c03963}* strain whereas only for *tim2* in the other insertional strains. For all strains ANOVA was made with respect to *white^{1118}*. *PB2mit^{c03963}*: $F_{(4,14)}$=0.257 p=0.901 n.s.; *f06803*: *$F_{(1,3)}$=22.246 p=0.018, *tim2* mRNA levels significantly differ from those of the control; *f00075*: $F_{(1,1)}$=1.168 p=0.475 n.s.; *MB08132*: $F_{(1,2)}$=1.777 p=0.314 n.s.; *MB08962*: $F_{(1,1)}$=12.996 p=0.172 n.s.. Data were normalized with respect to a *white^{1118}* control sample whose *2mit* mRNA levels were considered equal to 1. n.d.=not determined. * indicates a statistically significant difference. n.s.=not significant.

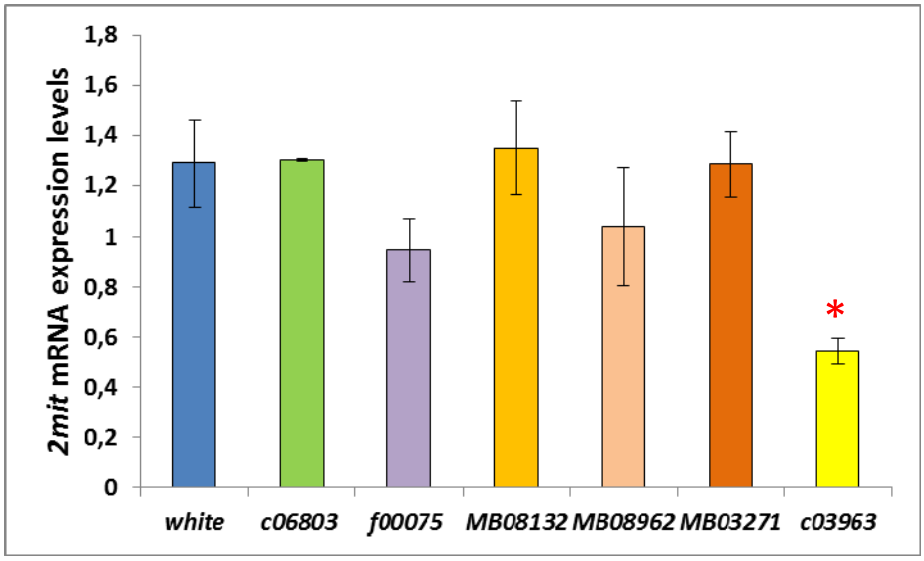

Fig.2.4 Real-time PCR values of *2mit* mRNA expression levels in **t**hird instar larval samples from 6 different strains carrying a transposon insertion in intron 11 of *tim2* locus, compared to the *white^{1118}* control. ANOVA: *$F_{(6,21)}$=5.878 p=0.001; test *post hoc* Newman-Keuls between *white^{1118}* and: *f06803* p=0.962 n.s.; *f00075* p=0.474 n.s.; *MB08132* p=0.966 n.s.; *MB08962* p=0.539 n.s.; *MB03271* p=0.983 n.s.; *c03963* *p=0.031. Data were normalized with respect to a *white^{1118}* control sample whose *2mit* mRNA levels were considered equal to 1. * indicates a statistically significant difference. n.s.=not significant.

In parallel, real-time PCR experiments were carried out to determine mRNA levels of *tim2* host gene and of the other intronic transcripts of *tim2* locus (*GC34308*, *BK002510* and *AY118619*) for *PB2mit^{c03963}*, *f06803*, *f00075*, *MB08132* and *MB08962* insertional strains (Table 2.1). Again, each sample was composed by 10 L3 larvae and at least two replicates per genotype were analysed.

The *PB2mit*^{c03963} strain did not show any significant depletion in mRNAs levels of *tim2* and of the other intronic sequences (Table 2.1). In addition, the values obtained for *f06803*, *f00075*, *MB08132* and *MB08962* strains are also reported, showing a significant *tim2* mRNA decrement only in the *f06803* strain (Table 2.1).

Furthermore, real-time PCR experiments were fulfilled to establish the degree of *2mit* mRNA depletion in the outcrossed *PB2mit*^{c03963} strain at the adult stage, in head samples. Each sample was formed by ~50 adult heads and at least five replicates were analysed for both the *PB2mit*^{c03963} strain and *white*^{1118} control. Given the slight but significant variation in *2mit* mRNA expression levels in wild-type adult heads during the 24 h in 12:12 LD regime (paragraph 2.1), adult heads were collected at the same time points (ZT0/ZT1) from 3-5 days old individuals entrained for at least three days in 12:12 LD conditions at 23°C. The achieved results displayed a very significant decrement of ~85% of *2mit* mRNA expression levels in the *PB2mit*^{c03963} strain with respect to those of the *white*^{1118} strain (Fig.2.5).

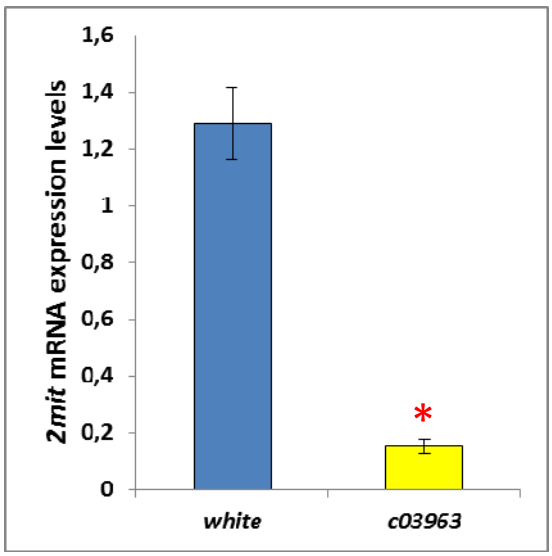

Fig.2.5 Real-time PCR values of *2mit* mRNA expression levels in adult head samples of outcrossed *PB2mit*^{c03963} insertional strain (N=9) compared to the *white*^{1118} control (N=5). ANOVA: *$F_{(1,12)}$=130.944 p<0.0001. Data were normalized with respect to a *white*^{1118} control sample whose *2mit* mRNA levels were considered equal to 1. * indicates a statistically significant difference.

On the basis of these results, the *PB2mit*^{c03963} strain was considered a *2mit* mutant insertional strain, suitable to perform behavioural analyses, described in the next chapter, in order to determine which phenotypes are affected by *2mit* decremented levels and, on the consequence, in order to identify *2mit* functions.

2.4 Characterization of *2mit* mRNA expression pattern in *PB2mit*^{c03963} adult brains

mRNA *in situ* hybridization experiments were performed on *PB2mit*^{c03963} mutant dissected brains. The aim of this experiment was to investigate whether *2mit* mRNA distribution was modified in *PB2mit*^{c03963} adult brains in comparison to

that of *white*^{1118} control. For this analysis, 3-5 days old *PB2mit*^{c03963} and *white*^{1118} individuals were dissected at ZT1, after entrainment for at least three days in 12:12 LD conditions at 23°C. Brains were then treated following the mRNA *in situ* hybridization protocol, using the Biotin-labeled probe specific for *2mit* mRNA detection and the Digoxigenin-labeled probe against *cry* mRNA.
Images in Fig.2.6 show that in *PB2mit*^{c03963} adult brains *2mit* expression pattern appeared to be generally weaker with respect to that of *white*^{1118} genotype. In *PB2mit*^{c03963} brains, a robust *2mit* mRNA signal depletion was evident in correspondence of mushroom bodies and ellipsoid-body, brain regions showing the strongest *2mit* mRNA staining in *white*^{1118} control.

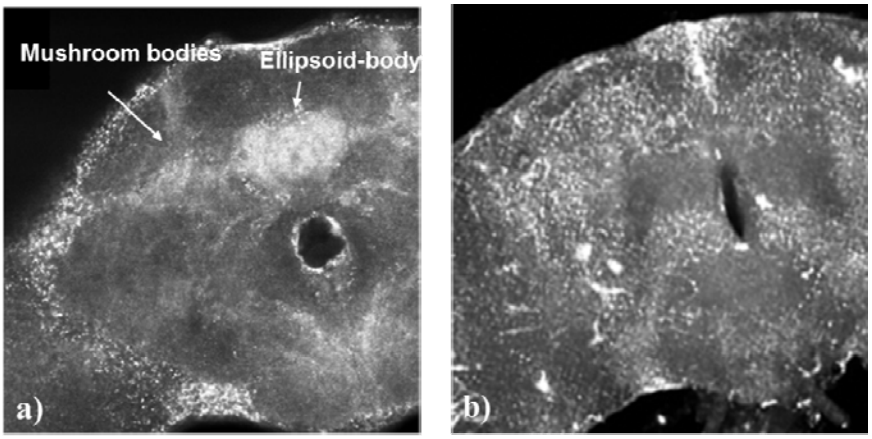

Fig.2.6 mRNA *in situ* hybridization experiments showing *2mit* mRNA expression pattern at ZT1 in a *PB2mit*^{c03963} adult brain compared to the *white*^{1118} control. **a)** *2mit* mRNA expression pattern in a *white*^{1118} wild-type brain: as previously described, *2mit* mRNA mainly localizes in mushroom bodies and in the ellipsoid-body. The optic lobes are not shown. **b)** *2mit* mRNA expression pattern in a *PB2mit*^{c03963} brain (image obtained through the assembly of all z-stacks): *2mit* mRNA is missing in mushroom bodies and its expression in ellipsoid-body is impaired.

2. Discussion

In the first part of this chapter, we describe the *2mit* mRNA characterization at level of adult heads, carried out via real-time PCR experiments, and at level of adult brains, with mRNA *in situ* hybridization assays.
Real-time PCR experiments were performed to evaluate whether *2mit* mRNA expression levels change in wild-type adult heads during the 24 h, in both 12:12 LD and DD conditions at 23°C. In 12:12 LD conditions, *2mit* mRNA expression levels showed a slight but significant 24 h variation in wild-type heads, with higher expression at the end of the night (ZTs 21-0) and lower expression at the end of the day (ZTs 8-12). In same conditions, the 24 h mRNA expression profile of the host gene *tim2* showed mRNA levels characterized by a significant oscillating profile with a peak of expression just after lights-off, between ZT12 and ZT15 (Benna et al., 2010). Therefore, at level of heads, which includes both brains and compound eyes, *2mit* and *tim2* mRNA expressions seemed to be not

co-regulated. In fact, although both *2mit* and *tim2* showed a cyclic variation in LD, *2mit* mRNA reached higher expression levels ~8 h later of those of *tim2* mRNA, a time window which indicates that *2mit* and *tim2* genes do cycle neither in phase nor in anti-phase. However, as previously shown for *tim2* host gene, in DD no cyclic variations in *2mit* mRNA expression profiles were revealed. These data suggest that both *tim2* and *2mit* expressions are influenced by light, rather than to be under a circadian control.

In order to localize *2mit* mRNA in adult brain and to establish whether *2mit* mRNA expression pattern was related to that of *tim2* mRNA in this organ, *2mit* mRNA *in situ* hybridization experiments were performed in $white^{1118}$ adult brains.

In brain, *2mit* mRNA resulted mainly expressed in the ellipsoid-body and in mushroom bodies, while a faint expression was revealed at level of optic lobes. Ellipsoid-body is a component of the central complex, which in *Drosophila* represents the higher pre-motor center for the control of locomotor activity at adult stage (Strauss et al., 1992; Strauss and Heisenberg, 1993; Strauss, 2002). In addition, the central complex has a minor role in memory formation (Joiner and Griffith, 1999; Sitnik et al., 2003; Neuser et al., 2008; Liu et al., 2006). The mushroom bodies are important in olfactory learning and memory (de Belle and Heisenberg, 1994; Heisenberg, 1998; Zars et al., 2000; Pascual and Preat, 2001) and in balancing locomotor activity (Martin et al., 1998). Data obtained on *2mit* mRNA hybridization on adult brains therefore suggest that *2mit* gene might be implicated in the control of phenotypes regulated by these regions, such as locomotor activity and/or memory formation.

In brain, mRNA of *tim2* host gene mainly mapped at level of optic lobes, specifically in medulla T1-basket neurons (Benna et al., 2010). In addition, a weak *tim2* mRNA presence was noticed at level of mushroom bodies. Given the trace of *2mit* mRNA expression in optic lobes, we investigated whether *2mit* mRNA co-localizes with *tim2* mRNA at level of T1-basket cells. Anyway, problems arisen by performing the mRNA *in situ* hybridization procedure did not allowed us to clarify this point and, until now, we have not been able to establish a more precise *2mit* localization pattern in this brain component. However, the comparison between *tim2* and *2mit* mRNA hybridization patterns on whole adult brains indicates that the two expression profiles seem to be complementary. In fact, in brain regions where *tim2* was weakly expressed, *2mit* showed the strongest hybridization signals, as shown for ellipsoid-body and mushroom bodies. On the contrary, in optic lobes, where *tim2* mRNA resulted more expressed (Benna et al., 2010), *2mit* mRNA signal was weak.

In the second part of the chapter we describe the *2mit* mRNA characterization, performed via real-time PCR, on six strains presenting a transposon insertion beside or within *2mit* locus, in order to identify in which ones *2mit* mRNA expression was disturbed by the presence of the transposon. We identified only one strain, the $PB2mit^{c03963}$, presenting a *2mit* mRNA depletion of ~50% in L3 samples with respect to wild-type. This strain was outcrossed and the ~50% *2mit*

mRNA reduced levels in L3 samples were maintained. Moreover, we found that in *PB2mit*^{c03963} adult flies heads the *2mit* mRNA decreased of ~85 %, reaching the 15% levels of *2mit* mRNA. We also demonstrated, by performing real-time PCR on L3 samples, that the transposon insertion in *PB2mit*^{c03963} strain did not modify the mRNA expression of *tim2* host gene and of the other internally transcribed sequences belonging to the *tim2* locus.
By performing preliminary mRNA *in situ* hybridization experiments on *PB2mit*^{c03963} adult brains, we found the *2mit* mRNA intensity staining was seriously reduced in correspondence to the *2mit* mRNA expression pattern detected in wild-type brains (mushroom bodies and ellipsoid-body). These achievements are consistent with real-time PCR results which displayed *2mit* mRNA reduced levels in *PB2mit*^{c03963} adult head samples, providing a confirmation of the *2mit* mRNA decreased levels characterizing the *PB2mit*^{c03963} strain.
Taken together, these data allow us to consider *c03963* insertional allele a hypomorphic allele of *2mit* gene and the *PB2mit*^{c03963} a suitable strain for the characterization of *2mit* role in *Drosophila melanogaster* adult flies.

2. Materials and Methods

2.1 Fly Stocks and Maintenance

2.1.1 Media and growth conditions

Flies were raised in vials containing a standard yeast/glucose/agar medium (Roberts and Standen, 1998) and were maintained in incubators at 18°C or at 23°C, 70% of relative humidity, on a 12:12 LD cycle.

2.1.2 Fly stocks

Wild-type strains
- ***white***^{1118}: used as control strain, it is characterized by the *white* (*w,* 1-1.5) recessive allele due to a deletion in the *white* locus (X chromosome). This deletion is responsible for the white eye phenotype (Zachar and Bingham, 1982). The *white* gene codes for a protein implicated in the translocation of both homocrome (brown) and pteridine (red) to compound eyes and ocelli of the adult individuals.

Transposon insertional strains (from Bloomington *Drosophila* stock center)
The following lines have been generated by the Exelixis Gene Disruption Project (Bellen et al., 2004) through the insertion of a transposon at level of *tim2* locus.
- ***PB2mit***^{c03963}: genotype: PBac{PB}timeout^{c03963}; insertion site: 87D14, 3R:8978167.
- ***f06803***: genotype: PBac{WH}timeout^{f06803}; insertion site: 87D13, 3R:8947626.

- ***f00075***: genotype: PBac{WH}timeout^{f00075}; insertion site: 87D14, 3R:8967122.
- ***MB08132*** (stock number #25366): genotype: w^{1118}; Mi{ET1}timeout^{MB08132}; insertion site: 87D13, 3R:8947607; comments: may be segregating TM6C, Sb[1].
- ***MB08962*** (stock number #26420): genotype: w^{1118}; Mi{ET1}timeout^{MB08962}; insertion site: 87D13, 3R:8954480; comments: may be segregating TM6C, Sb[1].
- ***MB03271***(stock number #24056): genotype: w^{1118}; Mi{ET1}timeout^{MB03271}; insertion site: 87D14, 3R:8966112; comments: may be segregating TM3, Sb[1] Ser[1].
- ***f00297***: genotype: PBac{WH}timeout^{f00297}; insertion site: 87D13, 3R:8935424.
- ***c06976*** (stock number #17793): genotype: w^{1118}; PBac{PB}timeout^{c06976}; insertion site: 87D12, 3R:8914606; comments: may be segregating TM6B, Tb[1].

2.2 mRNA *in situ* hybridization

mRNA *in situ* hybridization (ISH) is a type of hybridization that uses a labeled complementary mRNA strand, named probe, to localize a specific RNA sequence in a section or in the entire tissue. mRNA *in situ* hybridization experiments were performed on brains of 3-5 day-old flies, reared in 12:12 LD or in DD conditions, and collected at different time points. An antisense *2mit* mRNA was used as probe. Sample collection, tissue fixation and mRNA *in situ* hybridization procedures have been previously described in Wülbeck and Helfrich-Forster (2007), while the following steps were done according to the instructions reported in the TSATM Signal Amplification kit (PerkinElmer), with minor modifications.

2.2.1 Solutions

- 10X PBS (pH 7.4): 130 mM NaCl, 7 mM Na_2HPO_4, 3 mM NaH_2PO_4

- PBT: 1X PBS, 0.1% Tween®20

- 20X SSC: 150 mM NaCl, 15 mM Sodium citrate, adjusted to pH 7.0

- 2X SSCT: 2X SSC, 0.1% Tween®20

- 0.2X SSCT: 0.2X SSC, 0.1% Tween®20

- PFA solution: 4% Paraformaldehyde (PFA, from 20% stock), PBS

- PFA 20% (stock): 10 g PFA, 50 ml ddH_2O, 300 ml 5 M NaOH

- HB: 50% deionized formamide, 5X SSC, 0.1% Tween®20, ddH_2O

- Hybrix: 50% deionized formamide, 5X SSC, 100 mg/ml tRNA, 100 mg/ml ssDNA, 50 mg/ml heparin, 0.1% Tween®20, ddH_2O

- Blocking buffer reagent: 10X PBS, 1% nonfat milk powder, ddH_2O

- TNT: 0.1 M Tris-HCl pH 7.5, 0.15 M NaCl, 0.05% Tween®20

- TNB: 0.1 M Tris-HCl pH 7.5, 0.15 M NaCl, 0.5% Blocking buffer reagent

2.2.2 Preparation of the probes

For mRNA *in situ* hybridization on whole mount adult brains, Digoxigenin- (Dig) or Biotin- (Bio) labeled RNA probes were made using the Dig RNA Labelling Kit and Biotin RNA Labelling Mix (Roche). The Bio-labeled antisense and sense *2mit* RNA probes span 1680 bp (+1743 *SalI* rescriction site/+ 3423 stop) of *2mit* cDNA. *2mit* cDNA had been previously cloned in pBC® K/S vector (+/-; Invitrogen) and used as a template to synthetize the probes. The *2mit* sense probe was used as negative control. The Dig-labeled antisense *cryptocrome* (*cry*) RNA probe corresponds to the ~1.5 kb full-length *cry* cDNA and was used to mark the circadian clock neurons in the *Drosophila* brain. The Bio-labeled antisense *tim2* RNA probe spans ~1.6 kb (from 2665 to 4238 nt in AF279586).

2.2.2.1 Vector linearization and purification

The vector containing the DNA template for the probes was first linearized with an appropriate restriction enzyme cutting the multiple cloning site opposite to the transcription start site (T7 or T3), used subsequently for *in vitro* RNA transcription. The restriction enzyme *ClaI* was used to cut the pBC® K/S (+/-) + *2mit* polylinker downstream the T3 promoter in order to obtain the *2mit* antisense probe; *XhoI* was used to cut the polylinker downstream the T7 promoter in order to obtain the *2mit* sense probe used as negative control. Each digestion reaction was performed using a volume of vector+insert equivalent to 1 µg of insert, 5 U/µl *ClaI* or 10 U/µl *XhoI* in a final volume of 20 µl in ddH_20. The reaction was incubated at 37°C for 2 h. The digestion solution was then run on agarose gel and the band corresponding to the linearized vector+insert was cut and purified by using the QIAquick Spin Gel Extraction kit (Quiagen).

2.2.2.2 *In vitro* RNA transcription

The transcription reaction was performed in a final volume of 20 µl in DiEthyl PyroCarbonate (DEPC)-treated ddH_20 adding the following components: linear DNA equivalent to 1 µg of insert (1 mg of vector+insert), 4 µl 5X transcription buffer (400 mM Tris-HCl pH 8.0, 60 mM $MgCl_2$, 100 mM DTT, 60 mM spermidin; Promega), 2 µl 0.1 Dithiothreitol (DTT, supplied with RNA polymerase; Promega), 1 µl RNAs inhibitor (Promega), 2 µl 10X DIG or Biotin UTP RNA labeling mix (10 mM ATP, GTP and CTP, 6.5 mM UTP, 3.5 mM *UTP, pH 7.5; Roche), 40 U T7/T3/Sp6-RNA polymerase (Promega). The solution was mixed and incubated for 2 h at 37°C. 1 µl RNase-free DNase

(20U/µl; Promega) was added and the reaction was incubated for additional 30 min at 37°C to remove template DNA. The reaction was stopped by adding 2 µl of 0.2 M EDTA, pH 8.0. Then, 2.5 µl of 4 M LiCl and 75 µl of 100% ethanol were added and the obtained RNA was precipitated for 30 min at -80°C or for 2 h at -20°C followed by centrifugation at maximum speed for 15 min at 4°C. The supernatant was removed and the pellet was washed with -20°C of 75% ethanol followed by centrifugation at maximum speed at 4°C. The ethanol was removed and the pellet air-dried and then resuspended in 100 µl of Hybrix solution. Finally, amount, quality, and dimension of RNA transcripts were checked on a standard agarose gel.

2.2.3 Sample collection, dissection and fixation

After 12:12 LD entrainment, 3-5 days old flies were collected at the appropriate time point and fixed in 4% PFA in PBS by incubation on a rotating wheel for ~2 h at room temperature (RT). They were then washed three times for 15 min each in 1X PBS and then dissected in 1X PBS. During dissection brains were stored in 1X PBS on ice, in Eppendorf tubes. Afterwards, 1X PBS was removed and replaced with 325 µl of fresh PBT solution, 75 µl of 16% formaldehyde and 500 µl heptane. The mixture was shaken by hand for 30 to 45 s. When the foam set, the upper heptane phase and most of the aqueous phase were removed, leaving just enough to cover the tissue. 610 µl of fresh PBT, 150 µl of 16% formaldehyde and 40 µl DMSO were added. The brains were fixed for 20 min at RT on a rotating wheel. Then, two washes of 5 min each in 100% methanol were performed. The brains were stored in methanol at -20°C or immediately used.

2.2.4 Rehydration and Proteinase K treatment

The samples were rehydrated in a downgrading 90%, 70%, 50%, 30% methanol/PBT series lasting 5 min each followed by five washes for 5 min in PBT at RT. 1.25 µl proteinase K solution (10 mg/ml; Roche) was diluted in 500 µl of PBT and added to the sample in an Eppendorf tube. Proteinase K provides a solution to the problem of strong crosslinking of proteins after fixation which impairs probe penetration. Samples were incubated for 3 min at RT placing the tube horizontally without shaking. The reaction was stopped by adding 10 µl glycine stock solution. The samples were rinsed three times with 2 mg/ml glycine in PBT (1:100 dilution of the stock solution), that diluted any residual proteinase K. Two washes of 5 min each with PBT were performed placing the tube horizontally without shaking. The samples were fixed with 4% PFA in PBT for 20 min at RT, placing the tube horizontally without shaking. This step completely inhibits proteinase K and increases the stability of the sample. Five washes for 5 min each with PBT were performed on a rocking table.

2.2.5 Hybridization

RNA hybridization was performed at 60°C. The samples were incubated for 5 min in a 1:1 mixture of PBT:Hybrix at RT. The mix was replaced with Hybrix and incubated for 5 min at 60°C. The solution was replaced with 500 µl Hybrix used as blocking buffer and the samples were pre-hybridized for 2-4 h at 60°C. The riboprobes were diluted to the optimal concentration (50-100 ng) in Hybrix buffer (5 µl of each probe solutions diluted in Hybrix to a final volume of 100 µl), heated for 5 min at 70°C to remove RNA secondary structures and then put on ice immediately. The pre-hybridization buffer was removed and 100 µl riboprobe solution was added to the samples. Samples were incubated overnight at 60°C, sealing Eppendorf tubes with Parafilm.

2.2.6 Washes

The probe solution can be recycled 2-3 times. The following washes were performed:
- two washes for 20 min each with HB at 60°C.
- washes for 15 min each with a 3:2, 1:1, 2:3 ratio of HB: 2X SSCT at 60°C.
- one wash with 2X SSCT for 20 min at 60°C.
- two washes for 20 min each with 0.2X SSCT at 60°C.
- washes for 10 min each with a 3:2, 1:1, 2:3 ratio of 0.2X SSCT:PBT at RT
- three washes for 5 min each with PBT at RT.
- three washes for 5 min each with TNT at RT.

2.2.7 Detection

Samples were blocked in 500 µl TNB blocking solution for 2 h at RT. Then, they were incubated overnight at 4°C with streptavidin-Horseradish Peroxidase (HRP) primary antibody (provided by TSA PerkinElmer) diluted 1:100 in TNB. This antibody specifically recognizes Biotin-labeled probe. Samples were then washed for five times of 5 min each in TNT at RT. Samples were incubated with fluorescein fluorophore tyramide (green signal: excitation at 494 nm, emission at 517 nm; TSATM Fluorescein System PerkinElmer) for 3 h in darkness. The fluorescein fluorophore tyramide solution was diluted 1:50 using 1X amplification diluent to make 50 µl of working solution. The solution was changed twice. Activation and covalent binding of the Fluorophore Tyramides (Amplification Reagents) are catalyzed by HRP. Samples were then washed five times of 20 min each at RT in darkness. HRP activity was stopped by washing in 1% H_2O_2 in TNT for 20 min at RT. Three washes for 5 min each in TNT at RT, in darkness were performed. Samples were incubated for 45 min in TNB at RT in darkness and then incubated overnight at 4°C with anti-DIG-POD primary antibody (Roche Diagnostics), diluted 1:100 in TNB. This antibody specifically recognizes

Digoxigenin-labeled probe. Five washes for 5 min each in TNT were performed at RT in darkness. Samples were incubated with cyanine 3 fluorophore tyramide (red signal: excitation at 550 nm, emission at 570 nm; TSATM Cyanine 3 System PerkinElmer) for 3 h in darkness. The fluorophore tyramide solution was diluted 1:50 using 1X amplification diluent to make 50 µl working solution. The solution was changed twice. Five washes for 20 min each were performed at RT in darkness. Samples were mounted in Vectashield H-1000 (Vector Laboratories) and stored at 4°C.
Analyses of fluorescence detection were performed using Radians 2000, Bio-Rad (or Leica TCS SP5 X) laser scanning confocal microscope. For each brain 20 to 30 optical sections (Z-series) were taken. Post-acquisition analysis and Z-stack construction were performed with Image J (http://rsb.info.nih.gov/ij/).

2.3 RNA extraction and real-time PCR

2.3.1 RNA extraction

Total RNA was extracted from samples using Trizol Reagent (Invitrogen) as indicated in manifacturer data sheet instructions. The tissue samples (~100 mg), composed by either 10 L3 larvae or ~50 adult heads each, were grinded in 1 ml of Trizol Reagent using a power homogenizer. Samples were incubated for 5 min at RT. 0.2 ml of chloroform were added to samples that were vigorously mixed for 15 sec and incubated for 3 min at RT. Samples were centrifuged at 12000 g for 15 min at 4°C. Following centrifugation, the mixture separated into a lower red, phenol-chloroform phase, an interphase, and a colorless upper aqueous phase which contained the RNA. The aqueous phase was carefully transferred into a tube containing 0.5 ml of isopropyl alcohol. The mixture was incubated for 10 min at RT. Samples were centrifuged at 12000 g for 10 min at 4°C. The RNA precipitate formed a pellet on the side and bottom of the tube. The supernatant was completely removed and the RNA pellet was washed once with 1 ml of 75% ethanol. Samples were centrifuged at 7500 g for 5 min at RT. All ethanol was removed and the RNA pellet was air-dried for 15 min at RT and then resuspended in 20 µl of DEPC-treated ddH_2O (DEPC is an efficient and nonspecific inhibitor of RNAses).

2.3.2 Spectrophotometric analysis

1 µl RNA was diluted in 999 µl DEPC-treated ddH_2O (1:1000 dilution) for larval samples, and in 399 µl DEPC-treated ddH_2O (1:400 dilution) for adult head samples. Using the spectrophotometer (Beckman-Coulter DU530), Absorbance (A) at 260 nm and 280 nm was measured for each sample in order to determine sample concentration and purity.
a) A_{260}/A_{280} ratio indicates sample purity and should be between 1.7 and 2.

b) A_{260} permits to calculate RNA concentration, by using the formula:
[RNA] µl/ml = 40*A_{260} in which there is the applied convention that 1 A_{260} equals 40 µg/ml RNA. Finally, the real sample concentration is obtained by correcting the result of this formula with the dilution factor.

2.3.3 Retrotranscription

The first strand of cDNA was synthesized by reverse transcription RT-PCR on mRNA, employing SuperScript II (Invitrogen, USA) according to the manufacturer's instructions. A first reaction mix was obtained by diluting 1 µg RNA, 1 µl dNTPs (10 mM initial concentration) and 1 µl oligo-dT (17 polyT; 10 mM initial concentration) in DEPC-treated ddH_2O to a final volume of 12 µl. Samples were incubated 5 min at 70°C to denature RNA hairpins and other secondary structures. The following reagents were added in a total volume of 20 µl in DEPC-treated ddH_2O: 4 µl 1X First-Strand Buffer (Invitrogen, USA), 2 µl 0.1 M DiThioThreitol (DTT; Invitrogen, USA), 1 µl 40 U/ml RNaseOUT$_{TM}$ (Invitrogen, USA) and 1 µl 100 U/ml Superscript II. Samples were incubated 1 h at 42°C. Afterwards the enzyme was inactivated by 15 min incubation at 75°C.

2.3.4 Real-time PCR

The primers used for the real-time PCR were designed with the Primer 3 Software available at http://www.basic.nwu.edu/biotools/Primer3.html and are listed in Table 2.2.
For real-time PCR reaction, SYBR Green fluorescent marker was used to generate quantitative data and was included in PCR premix (Applied Biosystems, Foster City, CA) containing all reagents except target cDNAs. For each sample six amplification reactions were prepared: two replicates per three different amounts of total reverse transcribed RNA (54, 18 or 6 ng), according to Pfaffl (2001). Samples aliquots were prepared by a Robotic Liquid Handling System (CAS-1200, Corbett Robotics) into PCR tubes (Corbett Research). The real-time PCR reaction was carried out on Rotor Gene 3000 (Corbett Research) following the program:

95° for 10 min
95°C for 10 sec ┐
60°C for 15 sec ├ X 40 cycles
72°C for 45 sec ┘
72°C for 10 min.

Results were interpreted according to the mathematical model described in Pfaffl (2001), for relative quantification of a target transcript in comparison to a reference transcript. In the experiments, *rp49* transcripts were used as reference.

When real-time PCR was completed, a value, named "cycle threshold", had been measured for each amplification reaction. The "cycle threshold" represents the cycle in which the fluorescence emission of a sample overlapped a fixed value established as the threshold. The cycle thresholds, associated to the six amplification reactions per sample, were used to calculate the sample amplification efficiency using the formula: $E=10^{(-1/slope)}$. The amplification efficiency was used to estimate the relative level of expression between wild-type control samples chosen as reference (*white*^{1118} genotype or parental line) and unknown samples, through the equation:

$R=E_{target}^{\Delta Ct\ target}/E_{reference}^{\Delta Ct\ reference}$

where E_{target} is the amplification efficiency of the target mRNA; $E_{reference}$ is the amplification efficiency of reference *rp49* mRNA; ΔCt_{target} and $\Delta Ct_{reference}$ are the differences between cycle thresholds (Ct) of control and unknown samples for target mRNA and reference *rp49* mRNA respectively.

gene	position	RT-PCR primers	
2mit	43299-43318 (*449-468)	**forward**	5'-TCACCGCCATGGATCTGAGC-3'
	43101-43121 (*646-666)	**reverse**	5'-CAACTGAGGCAATCGCTGGGC-3'
tim2	73996-74015	**forward**	5'-AAAAGTCCAGAAGCGTCAGA-3'
	74739-74758	**reverse**	5'-TTGAGCGGCATTTGTTGACT-3'
CG34308	701-720	**forward**	5'-AAGGACAAACGAAACCCAAA-3'
	1277-1296	**reverse**	5'-GTGGAGATTTGTTGGGTGCT-3'
BK002510	3099-3118	**forward**	5'-ACGAGGATTTTTCCGCTTCT-3'
	3632-3651	**reverse**	5'-ATGGACACCCACTTCCACTC-3'
AY118619	44284-44303	**forward**	5'-TCGAGTTGAGTTGCGTTTTG-3'
	44136-44155	**reverse**	5'-GGGTCGACGTCGTCTGTTAT-3'
rp49	169-188	**forward**	5'-ATCGGTTACGGATCGAACAA-3'
	314-333	**reverse**	5'-GACAATCTCCTTGCGCTTCT-3'

Table 2.2 Real-time PCR Primers: position refers to *tim2* sequence. For *2mit* primers also the position referred to *2mit* cDNA sequence (*) is reported.

CHAPTER 3:

Effects of *2mit* mRNA depletion

3. Introduction

This chapter reports the phenotypical characterization of lines in which *2mit* mRNA levels are reduced. These lines are the *PB2mit*^{c03963} strain produced by transposon insertion mutagenesis and previously introduced (Chapter 2), and transgenic lines were *2mit* expression was knocked down by the specific activation of RNA interference machinery. The phenotypical analyses were conducted in order to elucidate *2mit* role in *Drosophila*, focusing in particular on the nervous system where we identified its mRNA expression.

3. Results

3.1 Vitality of the *PB2mit*^{c03963} strain

Albeit the *PB2mit*^{c03963} strain showed *2mit* mRNA decreased levels both at larval and adult stages, it was homozygous viable and without any morphological abnormality. This observation was not consistent with the results obtained when *2mit* KD was ubiquitously driven through the *ActGal4* driver. In fact, it was found that this latter condition led to lethality at late pupal stage with developmental impairments mainly observed in structures belonging to the abdominal region (description in paragraph 1.9.2 of the introduction). Thus, we performed vitality tests on the *PB2mit*^{c03963} strain in order to precisely evaluate whether *2mit* mRNA depletion caused milder effects on vitality, detectable only through a scrupulous analysis. Vitality tests were performed on individuals under 12:12 LD regime at 23°C and were based on the determination, for every developmental stage, of the amount of survived individuals with respect to both previous and embryonic stages (Table 3.1). The obtained results showed that for none of the developmental stages under analysis (embryonic, larval, pupal and adult stages) the *PB2mit*^{c03963} strain displayed a significant survival reduction with respect to the *white*^{1118}control. On the contrary, the percentages of survival were very similar to control for each analysed developmental stage, confirming that in the *PB2mit*^{c03963} strain the *2mit* mRNA decrement does not affect vitality during pre-adult instars and, in particular, does not cause defects in the body morphology.

Genotype	Embryos	Larvae	Pupae	Adults		
				♂	♀	Total
***white*^{1118}**	273	154 (54.4%)	125 [81.2%] (45.8%)	64 {51.2%}	61 {48.8%}	125 [100%] (45.8%)
***PB2mit*^{c03963}**	310	187 (60.3%)	163 [81.2%] (52.6%)	75 {53.6%}	65 {46.4%}	140 [85.9%] (45.2%)

Table 3.1 Vitality analyses of the *PB2mit*^{c03963} strain compared to *white*^{1118} control. Values in round brackets are calculated with respect to total layed embyos, values in square brackets are calculated with respect to the previous developmental stage, and values in curly brackets represent the percentage of males or females with respect to the totality of adult individuals.

3.2 Longevity of the *PB2mit*^{c03963} strain

The first investigations on ageing using *Drosophila melanogaster* as a model organism are dated almost 90 years ago with studies by Pearl and Parker (Lints et al., 1984). *Drosophila* has revealed to be a good model organism for longevity. Studies exploring flies lifespan have gained new interest in these last years because of the discovery that mutations affecting genes encoding components of the insulin/IGF signaling pathway enhance stress resistance and lead to an extension of lifespan in *Drosophila* (Tatar et al., 2001; Clancy et al., 2001; Broughton et al., 2005; Gronke et al., 2010; Partdrige et al., 2011). Ageing is genetically determined and environmentally modulated, and food availability, the nutritional status of the organism, and their effects upon reproductive rate play a key role in lifespan determination.

The idea to investigate the *PB2mit*^{c03963} flies lifespan developed because we found some inconsistencies comparing the results of *PB2mit*^{c03963} vitality during developmental stages with those achieved with *2mit* ubiquitous KD. In fact the vitality of *PB2mit*^{c03963} individuals during development resulted not to be affected by *2mit* mRNA decrement whereas *2mit* ubiquitous KD through RNAi had shown to lead to lethality at late pupal stage. Anyway, a preliminary Northern blot experiment performed on *ActGal4/2miti* samples had showed that in those lines *2mit* mRNA abatement during development was quite strong, while real-time PCR experiments performed on the *PB2mit*^{c03963} larval samples displayed a *2mit* mRNA decrement of ~50%. Unfortunately, real-time PCR experiments performed in same experimental conditions on *ActGal4/2miti* larvae did not give reproducible results, because in some replicates we obtained a strong *2mit* KD while in others a weak *2mit* mRNA decrement. We thought that this incapability to precisely determine the amount of *2mit* mRNA decrement in *ActGal4/2miti* lines via the real-time PCR technique was due to the fact that RNAi machinery may generate *2mit* mRNA fragments containing the sequence amplified in real-

time PCR experiments. In this case the effective transcript depletion would be masked and misrepresented. For this reason, Northern blot experiments will be performed on all lines, in order to make a direct comparison of *2mit* mRNA depleted levels among *PB2mit*^{c03963} strain and lines with general RNAi-mediated *2mit* KD. Therefore, up to now it is not possible to compare *2mit* mRNA depletion levels at larval stage among *PB2mit*^{c03963} insertional mutant strain and the *ActGal4/2miti* lines.

However, the 50% *2mit* mRNA depletion shown in *PB2mit*^{c03963} larvae could be sufficient to overcome the developmental stages but maybe affect viability later, at adult stage. Thus, in order to have a precise overview of the *PB2mit*^{c03963} genotype lifespan in comparison to the wild-type (*white*^{1118} genotype), longevity tests were performed. As in *Drosophila* the rate of development is greatly influenced by temperature, with increased temperature leading to a decreased lifespan (Miquel et al., 1976), the experiments were performed at a standard temperature of 23°C.

Fig.3.1a,b reports the results obtained for one replicate. The second replicate showed similar outcomes (not reported).

The *white*^{1118} control shared an overall survival profile similar to those described for wild-type strains in other works (Lints et al., 1984; Broughton et al., 2004). The 50% of *white*^{1118} males died 70 days after birth while the 50% of females died at about 60 days after birth. The maximum life expectancy, which is the age at which the oldest member has died in the population, was about 90-100 days old (Fig.3.1a,b).

On the contrary, for both *PB2mit*^{c03963} males and females, the lifespan was significantly reduced when compared to the correspondent sex of the *white*^{1118} control. Both *PB2mit*^{c03963} males and females showed premature mortality with flies starting to die from the first 10-12 days after birth. The 50% of both sexes died at about 30 days after birth. The maximum life expectancy was still 90-100 days after birth, similarly to *white*^{1118} controls, but the number of individuals able to reach this age was lower (Fig.3.1a,b).

The obtained results suggest that *2mit* mRNA depleted levels in *PB2mit*^{c03963} strain seem to induce a shortened lifespan for both males and females.

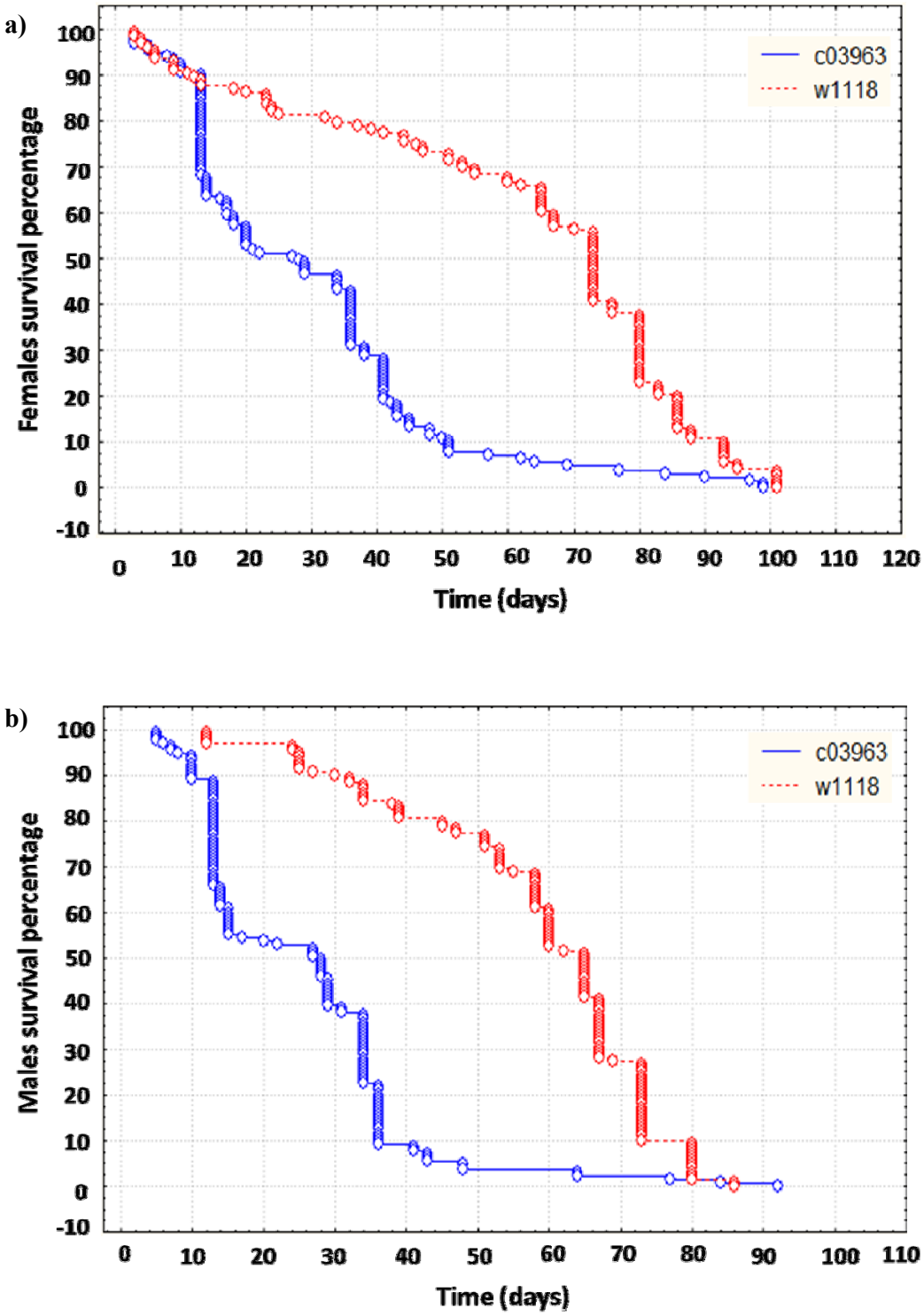

Fig.3.1 Longevity test showing survival curves of *PB2mit*^{c03963} mutant genotype compared to the *white*^{1118} control. **a)** Females: N=252; Z=-8.29 *p<0.00001. **b)** Males: N=257; Z=-10.88 *p<0.00001. *indicates a statistically significant difference.

3.3 Analyses of larval photophobic response

Since mRNA *is situ* hybridization experiments showed that *2mit* mRNA expression pattern in adult wild-type brains included a weak expression in optic lobes, we studied the effects of *2mit* mRNA depletion at level of the visual system, in order to elucidate whether *2mit* has a role in vision. Initially, we analysed the visual system integrity of the *2mit* mRNA depleted *PB2mit*^{c03963} strain focusing on L3 larval stage, investigating a typical larval behaviour related to the visual system, which is photophobicity.

Drosophila larvae present only a visual structure which is named Bolwig's Organ (BO), composed by 12 photoreceptors expressing *rhodopsin-5* (*rh5*) or *rhodopsin-6* (*rh6*) genes (Malpel et al., 2004). The BO is fundamental for photophobic behaviour of foraging larvae as well as for light synchronization of larval circadian clock (Sawin-McCormack et al., 1995; Malpel et al., 2002; 2004).

Photophobicity tests were performed at the same time of the day, at ZT6 and before testing all larvae had been entrained to 12:12 LD cycles at 23°C. Larval photophobic response can be determined by transferring larvae in the middle line of an agar petri dish presenting illuminated and dark halves. After 10 min wild-type larvae tend to move toward the dark side of the Petri dish, because of their light-avoidance behaviour (Mazzoni et al., 2005). We found that more than 80% of *PB2mit*^{c03963} larvae displayed a photophobic behaviour. This percentage was not statistically different from that of *white*^{1118} control larvae (Fig.3.2). The values observed for both genotypes are also similar to those reported for control strains in Mazzoni and colleagues (2005). So, these results suggest that *2mit* is not required for photophobic behaviour and light perception at larval stage.

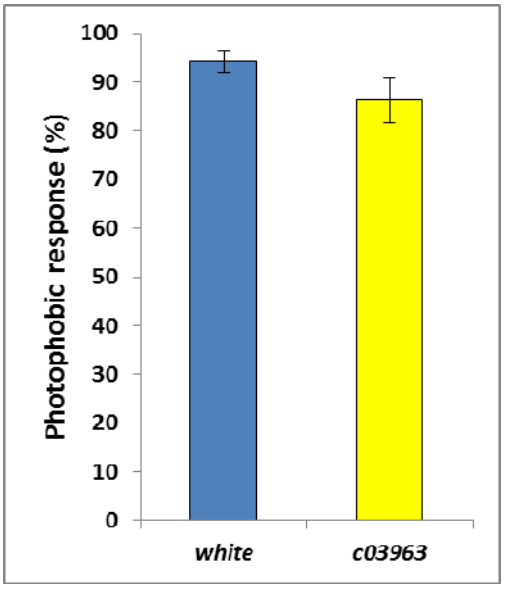

Fig.3.2 Photophobic response of *PB2mit*^{c03963} individuals (N=255) compared to *white*^{1118} controls (N=195). ANOVA: $F_{(1,21)}$=1.988 p=0.173 not significant.

3.4 Analyses of general locomotor activity at larval stage

Given *2mit* mRNA expression, in adult wild-type brains, in the ellipsoid-body of the central complex and in mushroom bodies, that are structures involved in the control of locomotor activity (Strauss, 1992; Strauss and Heisenberg, 1993; Martin et al., 1998; 1999a,b; 2001; Martin, 2004), we explored whether *2mit* has any involvement in this phenotype. Also for the general locomotor activity phenotype we started our analyses from the larval stage. During larval stage, movement and locomotion are very important for the survival of the individual. *Drosophila* larvae's movements over substrates are produced by rhythmic peristaltic waves of contraction and elongation of the body muscles. This locomotor behaviour, called telescopic peristalsis, depends on specialized neural circuits composing the central pattern generator (Marder and Bucher, 2001). Anyway, larval nervous system is simpler with respect to the adult stage and larval motor pattern seems to be distributed instead of having a precise localization within the larval nervous system (Suster et al., 2002).
We verified whether *2mit* mRNA depletion affected general locomotor activity during development by estimating different quantitative parameters: the total distance travelled, the number of inactivity episodes and the global immobility time. We tested general locomotor activity of L3 larvae because they are bigger and more manipulable with respect to individuals of previous larval instars. We studied the larval locomotor activity of $PB2mit^{c03963}$ individuals. We found that for the $PB2mit^{c03963}$ strain all larval locomotor activity parameters under investigation were very similar to those of the $white^{1118}$ control (Fig.3.3a-c). This suggests that 50% *2mit* mRNA depletion does not lead to any impairment in the estimated parameters concerning locomotor activity at larval stage and that *2mit* does not appear to be involved in the control of this phenotype during larval life.

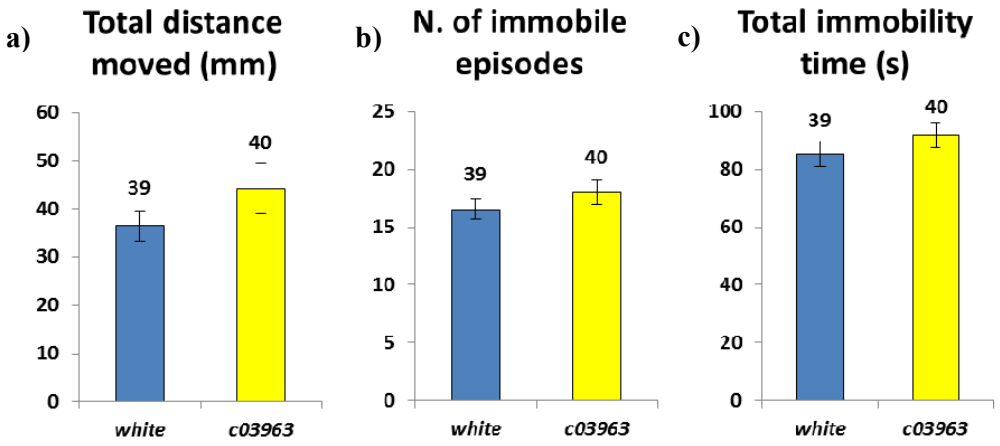

Fig.3.3 Locomotor activity parameters of third instar $PB2mit^{c03963}$ larvae compared to $white^{1118}$ control larvae. **a)** Total distance moved. ANOVA: $F_{(1,77)}=1.562$ p=0.215 n.s.. **b)** Number of immobile episodes. ANOVA: $F_{(1,77)}=1.183$ p=0.280 n.s.. **c)** Total immobility time. ANOVA: $F_{(1,77)}=1.147$ p=0.287 n.s..
n.s.=not significant. Values at the top of columns represent the number of tested individuals per genotype.

3.5 Analyses of the optomotor response

Given that *2mit* mRNA expression pattern in adult wild-type brains comprehends a weak expression in correspondence to optic lobes, we investigated whether *2mit* has a role in the visual system. We started from the larval stage but, as previously shown, no *2mit* involvement in vision was detected at this stage of development. The effects of *2mit* mRNA depletion at level of the visual system were also analysed at the adult stage.

In the *Drosophila* adult stage, visual system is composed by the retina of the compound eye and by optic lobes, constituted by lamina, medulla, lobula and lobula plate (Borst, 2010). In Insects, motion vision plays an important role as source of information about the surrounding environment and determines the motor response of the animal. A way to test fly visual system integrity, motion vision and following optic-motor coordination capabilities is provided by the "optomotor test", described by Burnet and Beck (1968). The *Drosophila* optomotor response starts to be processed from R1-6 retinal photoreceptors (Heisenberg and Buchner, 1977), involved in motion detection. Despite lobula plate tangential cells represent an important component for the optomotor response, because they integrate and transmit the motion information towards fly motor centers, so far it is not well elucidated which optic lobe neurons provide synaptic input to these lobula plate cells (Borst et al., 2010).

The visual system integrity of flies with decreased *2mit* mRNA levels was assayed through the "optomotor test". The analysed strains with depleted *2mit* mRNA expression were the $PB2mit^{c03963}$ strain and *2miti* lines in which the *2mit* silencing was driven in the whole nervous system (*elavGal4* driver), in mushroom bodies and optic lobes (*OK107Gal4*; Aso et al., 2009), in the eye R1-R8 photoreceptor cells (*GMRGal4* driver) and in medulla T1 basket cells of optic lobes (*T1Gal4* driver; Rister et al., 2007).

Fig.3.4a reports the optomotor results obtained for the $PB2mit^{c03963}$ strain compared to three control strains (*wt-ALA*, $white^{1118}$ and *Oregon-R/+* genotypes). In the optomotor assay, a fly perfomed a right optomotor response when turning in the same direction of a surrounding rotating drum representing a moving environment; otherwise, if the fly moved in the opposite direction, it did a wrong optomotor response. The control strains performances were characterized by a significant majority of right optomotor responses with respect to wrong ones: the *wt-ALA* individuals did the 80%, the *Oregon-R/+* the 75% and the $white^{1118}$ the 65% of right responses (Fig.3.4a). Anyway, in the $white^{1118}$ strain the percentage of right responses was lower with respect to the other two control strains. Specifically, the *white* mutation leads to an impaired function for the eye pigments translocator rendering the eyes of white instead of red wild-type color (Zachar and Bingham, 1982) and it is reported that in Insects white-eyed mutants present slight defects at level of the optomotor response (Kalmus, 1961). Therefore, we included a second control genotype represented by *Oregon-R/+*

line, characterized by having red eyes with a genetic background shared between the *white*^{1118} and the *Oregon-R* genotypes.

PB2mit^{c03963} individuals showed an optomotor response characterized by ~50% of right responses (Fig.3.4a), significantly decreased with respect to those of all three control strains. This means that *PB2mit*^{c03963} mutants made a random choice, independently to the direction of the drum rotation. This result suggests that *PB2mit*^{c03963} flies have defects at level of the visual system, in particular in optic-motor coordination abilities and in neuronal processing of motion vision, indicating a role for *2mit* in the visual system. It is important to underline that the optomotor response of *PB2mit*^{c03963} individuals, having orange eyes, was significantly different not only from those of the *wt-ALA* and the *Oregon-R/+* genotypes, having red eyes, but also from that of the *white*^{1118} strain, presenting white eyes. This observation indicates that *PB2mit*^{c03963} visual system defects are not due to orange instead of red eyes (the orange eyes phenotype is a consequence of the partial expression of the "*mini-white*" gene used as a marker for *PB2mit*^{c03963} transposon insertion in the *white*^{1118} genetic background).

Given *tim2* mRNA expression in the optic lobe (Benna et al., 2010), we evaluated whether also *2mit*'s host gene has a role in the optomotor response. Fig.3.4a illustrates the optomotor results obtained for two *tim2* insertional mutant strains with no perturbation of *2mit* mRNA expression levels: the *PBtim2*^{f00297}/+ and the *PBtim2*^{c06976}/+ strains. These two lines are heterozygous for a transposon insertion within *tim2* locus because this insertion leads to pupal lethality in homozygous individuals. *PBtim2*^{f00297}/+ mutants performed the 76% of right responses, similarly to *wt-ALA* and *Oregon-R/+* controls and significantly higher with respect to the *white*^{1118} control (Fig.3.4a). *PBtim2*^{c06976}/+ mutants did the 59% of correct responses, a value significantly lower with respect to *wt-ALA* and *Oregon-R/+* strains but comparable to that of *white*^{1118} control strain (Fig.3.5a). Probably the slight optomotor defects noticed in the *PBtim2*^{c06976}/+ mutant are due to its very bright orange eyes. Thus, unlike *2mit*, *tim2* does not seem to display a role in neural circuits involved in motion vision.

Fig.3.4b reports the optomotor results achieved for different *driverGal4/2miti* combinations. All lines in which *2mit* KD was driven either in the whole nervous system or in different visual system subregions showed optomotor responses not significantly different from those of their appropriate controls. The *elavGal4/6.1-2miti* individuals did the 87%, the *elavGal4/16.2-2miti* the 83%, the *OK107Gal4/6.1-2miti* the 77%, the *GMRGal4/6.1-2miti* the 83% and the *T1Gal4/6.1-2miti* the 77% of right responses while *elavGal4/+* controls performed the 80% and *GMRGal4* and *T1Gal4/+* controls the 70% of right responses. Thus, the obtained outcomes suggest that these lines with *2mit* silencing in different brain regions do not show any impairment in the optic-motor coordination phenotype.

In order to determine whether the defective optomotor behaviour observed in the *PB2mit*^{c03963} flies was due to impaired vision at level of the retina, the

electroretinogram (ERG) of *PB2mit*^{c03963} individuals was analysed. The ERG analyses, performed by Prof. Aram Megighian (Department of Physiology, University of Padova), showed that the electric activity of retinal photoreceptor cells of the eyes of 3-5 days old *PB2mit*^{c03963} individuals was similar to that of *white*^{1118} control flies of the same age (personal communication). These findings indicate that the *PB2mit*^{c03963} affected optomotor response is not due to impairments of photoreceptor cells.

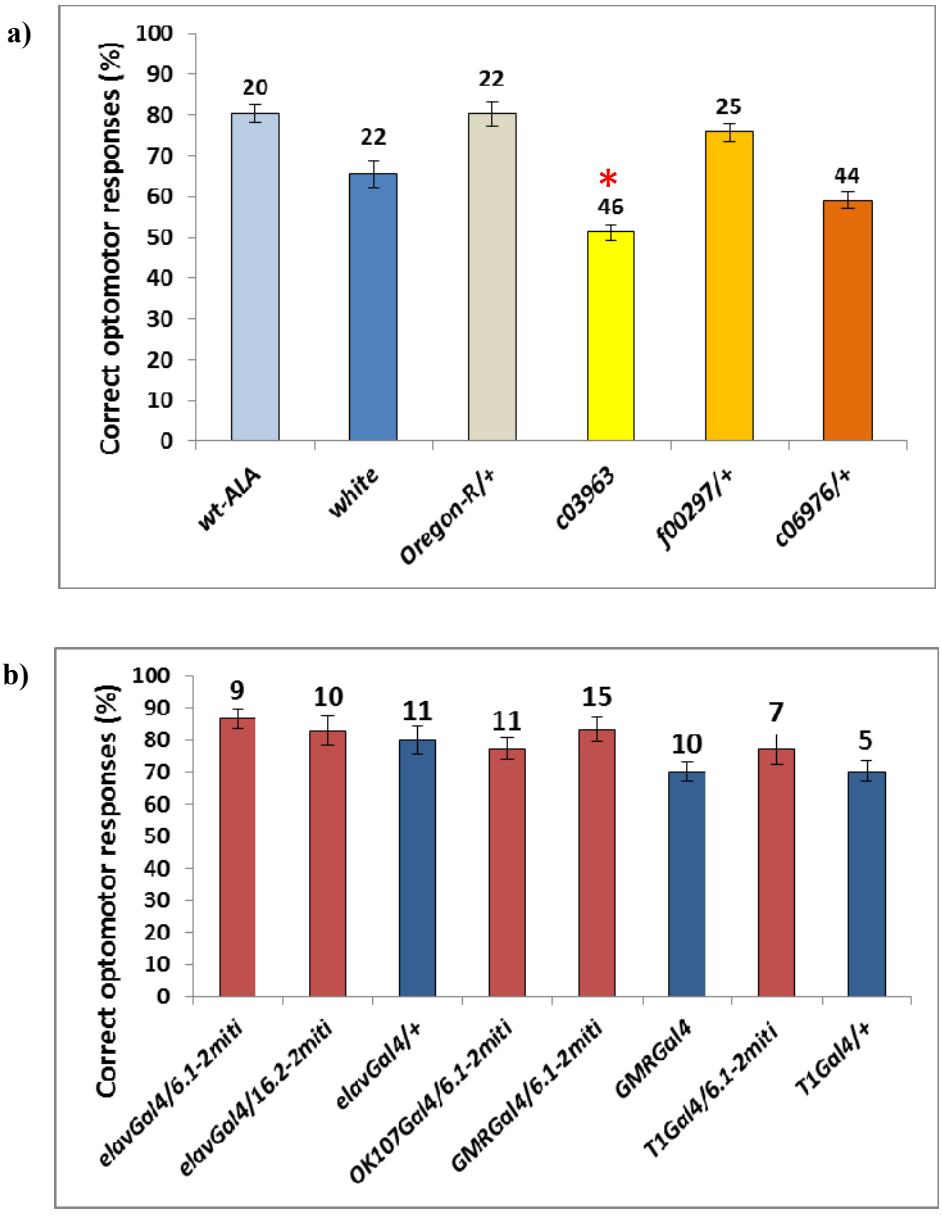

Fig.3.4 Optomotor response of **a)** *PB2mit*^{c03963}, *PBtim2*^{f00297}/+, *PBtim2*^{c06976}/+ and wild-type control strains (*wt-ALA*, *white*^{1118} and *Oregon-R*/+ genotypes). *ANOVA: $F_{(5,173)}$=27.555 p<<0.0001; test *post hoc* Newman-Keuls between *PB2mit*^{c03963} and: *wt-ALA* *p<0.0001; *white*^{1118} *p=0.0002; *Oregon-R*/+ *p<0.0001; test *post hoc* Newman-Keuls between *PBtim2*^{f00297}/+ and: *wt-ALA* p=0.394 n.s.; *white*^{1118} *p=0.004 but the optomotor response of the control is lower; *Oregon-R*/+ p=0.197 n.s.; test *post hoc* Newman-Keuls between *PBtim2*^{c06976}/+ and: *wt-ALA* *p<0.0001; *white*^{1118} p=0.067 n.s.; *Oregon-R*/+ *p<0.0001. **b)** *elav-,OK107-,GMR-,T1-Gal4/2miti* strains and control strains. ANOVA: $F_{(7,70)}$=2.058 p=0.060 n.s. Values at the top of

colums represent the number of individuals tested per genotype. * indicates a statistically significant difference. n.s.=not significant.

3.6 Circadian photoreception analyses

As reported in literature, intronic genes could present a functional correlation with their host genes (Gibson et al., 2005). Given *tim2* involvement in circadian photoreception in *Drosophila* adult brains (Benna et al., 2010), we investigated whether *2mit* shares the same function at the adult stage.

Circadian photoreception represents the capability of an endogenous circadian clock to be synchronized by external light stimuli. Circadian photoreception property of a clock can be investigated by the phase response curve (PRC), which provides a description of the phase dependent response of the clock to light.

Thus, with the purpose to determine whether *2mit* depletion gives some effects on the PRC, we tested the *PB2mit*^{c03963}strain for the behaviour related to circadian light entrainment. However, the *timeless1* (*tim1*) polymorphism, associated to the alternative *ls-tim1* and *s-tim1* alleles, significantly influences the capability of an endogenous circadian clock to be entrained to light cues, with *ls-tim1* allele less sensitive to light synchronization compared to *s-tim1* variant (Tauber et al., 2007; Sandrelli et al., 2007). So, it was necessary to determine the *ls-tim1/s-tim1* genotype in *PB2mit*^{c03963} flies.

We found that the *PB2mit*^{c03963} strain was homozygous for *ls-tim1* allele (Fig.3.5). Since the *white*^{1118} control is homozygous for the same *ls-tim1* polymorphism, it could be used as an appropriate control strain.

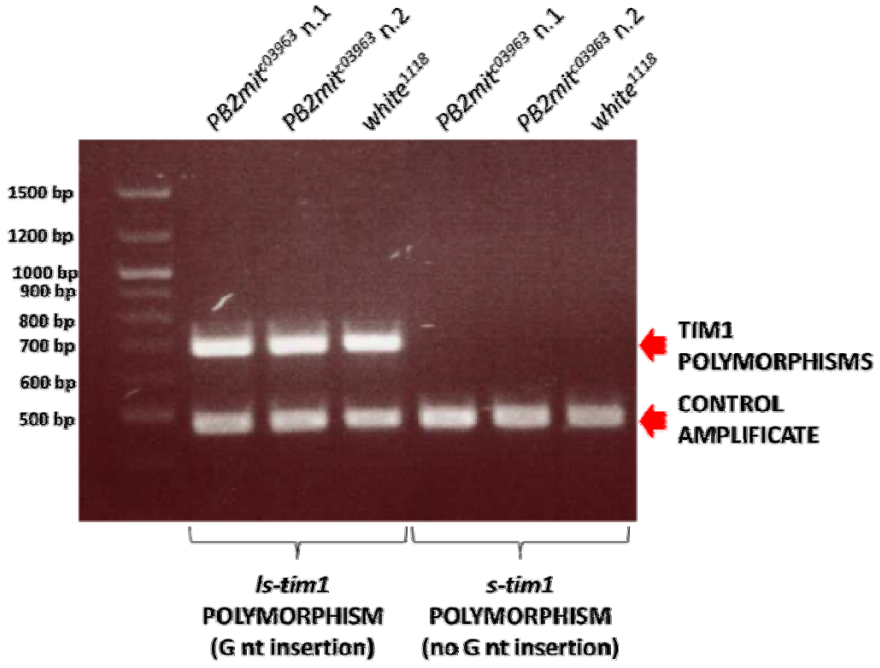

Fig.3.5 PCR amplificates obtained from two *PB2mit*^{c03963} and one *white*^{1118} control sample. The ~700 bp band represents the amplification product of the portion of *tim1* sequence containing the polymorphic site. For all the three reported samples, bands are present in correspondence to the *ls-tim1* polymorphism, characterized by G insertion. The ~500 bp band represents a control amplification product correspondent to another *tim1* region not characterized by polymorphisms.

Therefore, we studied the ability of 3-5 days old *PB2mit*^{c03963} flies to respond to a 20 min light pulse delivered at a precise time point during the night (ZT: 13; 15; 17; 19; 21; 23), after three days of entrainment under 12:12 LD regime at 23°C. The *white*^{1118} genotype was used as a wild-type control strain and was subjected to the same treatment. We denoted that for all the ZTs under investigation, the PRC profile of *PB2mit*^{c03963} individuals was not significantly different from that of the *white*^{1118}control (Fig.3.6). On the contrary, the PCR plot of heterozygous *tim2*$^{-}$ /+ mutants showed, in comparison to control, an enhanced response to light pulses administered late at night, in the advance zone at ZT19 and ZT21 (Benna et al., 2010), demonstrating a role for *tim2* in the entrainment of the circadian clock to environmental light cues.
These data suggest that *2mit* has not a function in light synchronization of adult circadian clock as *tim2*.

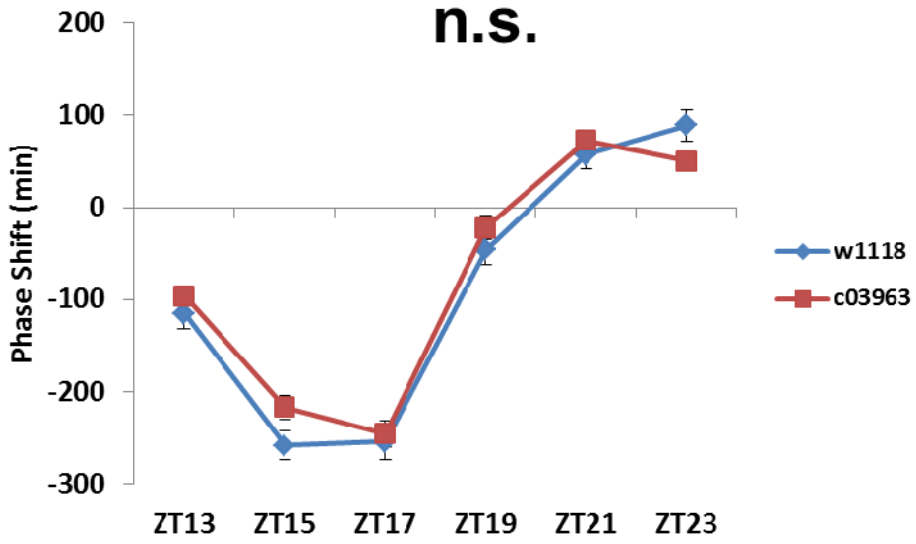

Fig.3.6 Phase-response curve (PRC) of *PB2mit*^{c03963} and *white*^{1118} control flies subjected to light pulses separately administered at different ZTs during night. ANOVA: $F_{(5,434)}$=1.760 p=0.120 not significant. Advances and delays in phase response are represented as positive and negative values, respectively.

3.7 Analyses of circadian rhythmicity

Although we found that *2mit* is not involved in circadian photoreception, we investigated whether *2mit* is somehow involved in other functions related to the establishment of the endogenous circadian rhythmicity. In *Drosophila* adult stage, the molecular and anatomical dissection of the endogenous circadian machinery and its relationship to other neural circuits in the fly brain relies on the analyses of

a clock-controlled behaviour which is locomotor activity along 24 h. Locomotor activity analyses, investigated under a variety of conditions, provide a relatively reliable, robust and easily interpretable output for the circadian clock.

To determine whether *2mit* has a role in circadian rhythmicity, we explored the effects of *2mit* mRNA depleted levels on *free running* periodicity of locomotor activity in DD at 23°C. The flies were first entrained for three days in12:12 LD regime and then kept in *free running* for seven days. In Chronobiology, periodicity in *free running* conditions (or tau) represents the length of the day cycle set by the endogenous clock. It is measured in constant conditions because in this way the endogenous clock is giving its rhythmicity spontaneously with no external stimuli influence.

The analysed *2mit* mRNA depleted flies were those belonging to outcrossed *PB2mit*^{c03963} strain and *2miti* lines in which *2mit* KD was driven in the whole nervous system (*elavGal4* driver), in circadian neurons (*timGal4* driver), in ellipsoid-body of the central complex (*c232Gal4*), in mushroom bodies and part of the optic lobe (*OK107Gal4* driver) and in the eye R1-R8 photoreceptors (*GMRGal4*).

Table 3.2 illustrates the circadian locomotor activity analyses in DD conditions of 3-5 days old outcrossed *PB2mit*^{c03963} strain, *white*^{1118}control and also *MB08132* and *MB08962* insertional strains presenting normal levels of *2mit* mRNA expression. Percentage of rhythmicity, periodicity in DD and percentage of flies with a periodicity over 25 h are reported. 3-5 days old *PB2mit*^{c03963} mutants showed a high rhythmicity percentage (over 95%), comparable to the one of *white*^{1118} control. Anyway, *PB2mit*^{c03963} individuals displayed a slight but significant increase of *free running* circadian periodicity of ~1 h with respect to the ~24 h tau values of the *white*^{1118} control (Table 3.2). In particular, ~40% of *PB2mit*^{c03963} flies had a tau over 25 h against ~10% of the *white*^{1118} strain. In parallel, *MB08132* and *MB08962* strains showed 100% of rhythmic individuals with a ~24 h circadian periodicity and less than 10% of flies with a tau over 25 h, similarly to what observed for the *white*^{1118} control (Table 3.2). These results suggest that the cause of the circadian phenotype observed in outcrossed *PB2mit*^{c03963} mutants seems to be *2mit* mRNA down-regulation.

With the aim of evaluating if the *PB2mit*^{c03963} circadian phenotype was enhanced by ageing, we examined circadian periodicity in 30 days old *PB2mit*^{c03963} flies, compared to *white*^{1118} flies of the same age. We found that a mild tau increase with ageing is a normal phenotype as noticed for 30 days old *white*^{1118} control flies (Table 3.2). Anyway, in 30 days old *PB2mit*^{c03963} individuals, this phenotype is emphasized with a tau almost 1 h and 30 min longer than the one of controls and with more than 80% of flies having a periodicity over 25 h while in the *white*^{1118} strain they were the ~20% (Table 3.2).

These results contribute to strengthen the indications regarding a possible *2mit* function in circadian periodicity.

Genotype	Age (days)	%R (R/N)	Tau in DD (mean±s.e.m.)	flies with tau>25h (%)
MB08132	3-5	100 (95/95)	23.995±0.073	9.47
MB08962	3-5	100 (93/93)	24.410±0.044	6.45
PB2mit^{c03963}	3-5	96.15 (125/130)	25.045±0.122	39.2
	30	92.31 (36/39)	25.683±0.222	80.56
white^{1118}	3-5	88.89 (24/27)	24.097±0.206	11.12
	30	92.21 (71/77)	24.324±0.072	19.72

Table 3.2 Locomotor activity analyses of 3-5 and 30 days old flies, reporting for each genotype: the percentage of rhythmicity R(%) calculated from number of rhythmic individuals (R), divided to the number of totally analysed individuals (N); the periodicity (tau) in DD; the percentage of rhythmic flies having a tau over 25 h.
ANOVA among 3-5 days old outcrossed *PB2mit^{c03963}*, *MB08132* and *MB08962* compared to the *white^{1118}* control: *$F_{(3,333)}$=22.962 p<<0.0001; test *post hoc* Newman-Keuls between *white^{1118}* and: outcrossed *PB2mit^{c03963}* *p<0.0001; *MB08132* p=0.579 n.s.; *MB08962* p=0.090 n.s.. ANOVA between 30 days old outcrossed *PB2mit^{c03963}* compared to the *white^{1118}* control: *$F_{(1,105)}$=52.668 p<0.0001. * indicates a statistically significant difference. n.s.=not significant.

Fig.3.7 reports representative locomotor activity profiles relative to 3-5 days old outcrossed *PB2mit^{c03963}* and *white^{1118}* control single flies. Both *PB2mit^{c03963}* and *white^{1118}* flies displayed a canonical rhythmic bimodal profile in 12:12 LD conditions with flies showing a peak of activity in correspondence to lights-on in the morning and lights-off in the evening as reported in literature (Allada and Chung, 2010). However, in DD conditions the *PB2mit^{c03963}* individual displays a shift in the locomotor activity profile in comparison to the *white^{1118}* fly. This shift indicates a lengthening of circadian periodicity in DD regime with respect to ~24 h periodicity of *white^{1118}* control.

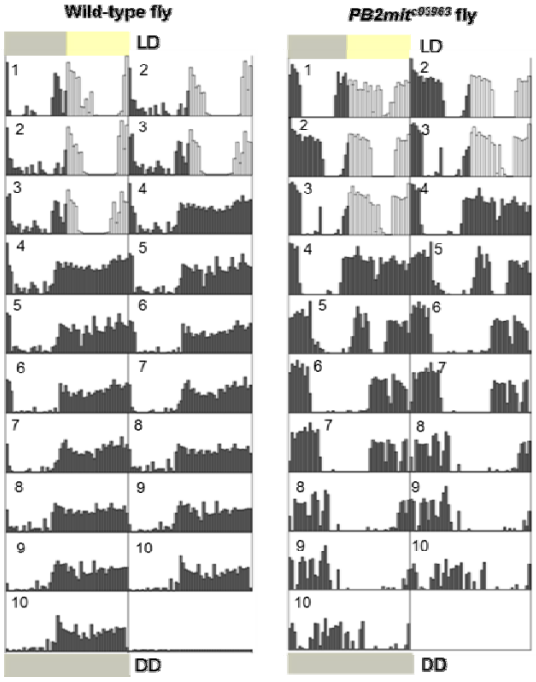

Fig.3.7 Representative activity plots, or actograms, of single *white^{1118}* control and *PB2mit^{c03963}* flies. The height of vertical bars indicates level of activity during a 30-min interval, or bin. Activity (Y-axis) is given as a function of time (X-axis). The flies have been monitored for 3 days in 12:12 LD and 7 days in DD. After day 3 the light was turned off permanently (DD). The *PB2mit^{c03963}* fly shows a shift in the locomotor activity profile that corresponds to an endogenous period longer than 24 h.
The yellow and grey bars on top represent day and night, respectively. Each horizontal line contains 48 h of activity data (double-plotted plot), with the second day on one line repeated on the following line as being the first day, in order to ease visualization of the circadian period. Numbers indicate the days order.

Table 3.3 reports circadian locomotor activity analyses in DD conditions of 3-5 and >20 days old individuals with pan-neuronal *2mit* RNAi (through *elavGal4* driver) compared to appropriate controls. *6.1-2miti*, *16.2-2miti* and *61.1-2miti* lines were employed to drive RNAi-mediated *2mit* down-regulation through UAS-GAL4 binary system. Percentage of rhythmicity, periodicity in DD and percentage of flies with a periodicity over 25 h are reported. 3-5 days old individuals belonging to all the lines having *2mit* down-regulation in the whole nervous system showed a percentage of rhythmicity (~95%) comparable to that of respective controls. Anyway the three lines showed a slight but significant ~30 min increase of circadian periodicity in *free running* conditions in comparison to the ~24-24.5 h values of controls, with percentages of individuals with a tau over 25 h being over ~40% whereas controls displayed ~10-25% (Table 3.3).

For *elavGal4/6.1-2miti* and *elavGal4/61.1-2miti* genotypes, circadian periodicity was evaluated in older flies, which were more than 20 days old (Table 3.3). >20 days old individuals of these two lines did not show a significant increase of circadian periodicity with respect to appropriate controls. However, in the *elavGal4/61.1-2miti* line the percentage of rhythmic individuals in the totality of tested flies was significantly reduced to ~50% compared to the ~95% of controls. In the *elavGal4/6.1-2miti* line, despite this strong effect is not detected, there is also a mild reduction of rhythmicity to ~75% against the ~95% of controls, and the number of individuals tested is not so far sufficiently representative (Table 3.3).

The results obtained with 3-5 days old *elavGal4/2miti* flies are in accordance to those previously described for the $PB2mit^{c03963}$ strain. *2mit* mRNA depletion due to both insertional mutation and pan-neuronal KD seems to lead to a slight increase in circadian tau in DD. Anyway, with ageing the effects of *2mit* mRNA depletion are different between the $PB2mit^{c03963}$, with enhanced increase of circadian tau, and *elavGal4/2miti* lines, with decreased percentage of rhythmicity.

In order to precisely map the eye or brain structures in which *2mit* KD could be responsible for the observed effects on circadian periodicity, circadian locomotor activity analyses were performed in 3-5 days old individuals with *2mit* KD specifically driven in circadian clock neurons (*timGal4* driver), in ellipsoid-body (*c232Gal4*), in mushroom bodies and optic lobes (*OK107Gal4* driver) or in eye R1-R8 photoreceptors (*GMRGal4* driver). Table 3.3 reports the results obtained for all these lines. In all *driverGal4/2miti* combinations, the percentage of rhythmicity and the circadian periodicity values were not significantly different when compared to those of corresponding controls (Table 3.3).

Genotype	Age (days)	%R (R/N)	Tau in DD (mean±s.e.m.)	flies with tau>25h (%)
elavGal4/6.1-2miti	3-5	95.24 (20/21)	25.128±0.204	55
	>20	76.92 (10/13)	24.251±0.226	20
elavGal4/16.2-2miti	3-5	97.56 (40/41)	24.942±0.093	40
	>20	-	-	-
elavGal4/61.1-2miti	3-5	95.74 (45/47)	24.799±0.077	42.22
	>20	52.31 (34/65)	23.643±0.118	5.88
elavGal4/+	3-5	87.10 (27/31)	24.173±0.106	7.41
	>20	96.00 (48/50)	24.004±0.109	14.58
timGal4/6.1-2miti	3-5	100 (6/6)	24.475±0.173	16.67
timGal4/16.2-2miti	3-5	95.00 (57/60)	23.734±0.063	0
timGal4/61.1-2miti	3-5	95.56 (43/45)	23.964±0.063	0
timGal4/+	3-5	80 (24/30)	23.494±0.102	0
c232Gal4/6.1-2miti	3-5	82.76 (24/29)	24.285±0.087	0
c232Gal4/16.2-2miti	3-5	98.59 (70/71)	24.059±0.040	1.43
c232Gal4/61.1-2miti	3-5	98.59 (70/71)	23.848±0.042	0
c232Gal4/+	3-5	100 (44/44)	23.805±0.059	0
OK107Gal4/6.1-2miti	3-5	94 (67/71)	24.47 ± 0.06	13.43
OK107Gal4/16.2-2miti	3-5	84 (63/75)	24.59 ± 0.05	22.62
OK107Gal4/61.1-2miti	3-5	90 (84/93)	24.21 ± 0.06	5.08
OK107Gal4/+	3-5	88 (23/26)	24.41 ± 0.12	17.39
GMRGal4/6.1-2miti	3-5	-	-	-
GMRGal4/16.2-2miti	3-5	71.88 (23/32)	23.888±0.160	0
GMRGal4/61.1-2miti	3-5	96.15 (25/26)	23.590±0.127	0
GMRGal4/+	3-5	95.12 (39/41)	23.761±0.120	5.13
6.1-2miti/+	3-5	88.89 (16/18)	24.513±0.164	18.75
	>20	97.37 (37/38)	24.549±0.080	29.73
16.2-2miti/+	3-5	85.71 (12/14)	24.605±0.192	25
	>20	-	-	-
61.1-2miti/+	3-5	94.44 (17/18)	24.181±0.128	5.88
	>20	93.54 (87/93)	24.002±0.057	6.90

Table 3.3 Locomotor activity analyses of 3-5 and >20 days old flies reporting for each genotype: the percentage of rhythmicity R(%) calculated from number of rhythmic individuals (R) divided to the number of totally analysed individuals (N); the periodicity (tau) in DD; the percentage of rhythmic flies having a tau over 25 h. Statistic support is made considering the *6.1-2miti*, *16.2-2miti* and *61.1-2miti* lines separately.

- *2miti* driven with *elavGal4* driver.
3-5 days old flies: ANOVA:*$F_{(6,169)}$=8.354 p<0.0001; test *post hoc* Newman-Keuls between *elavGal4/6.1-2miti* and: *elavGal4/+* *p<0.0001; *6.1-2miti/+* *p=0.003; test *post hoc* Newman-Keuls between *elavGal4/16.2-2miti* and: *elavGal4/+* *p<0.0001; *16.2-2miti/+* p<0.011 n.s.; test *post hoc* Newman-Keuls between *elavGal4/61.1-2miti* and: *elavGal4/+* *p<0.0001; *61.1-2miti/+* *p=0.0005.
>20 days old flies: ANOVA:*$F_{(4,211)}$=10.268 p<0.0001; test *post hoc* Newman-Keuls between *elavGal4/6.1-2miti* and: *elavGal4/+* p=0.143 n.s.; *6.1-2miti/+* p=0.078 n.s.; test *post hoc* Newman-Keuls between *elavGal4/61.1-2miti* and: *elavGal4/+* p=0.083 n.s.; *61.1-2miti/+* *p=0.033.
- *2miti* driven with *timGal4* driver:
3-5 days old flies: ANOVA:*$F_{(6,167)}$=13.277 p<0.0001; test *post hoc* Newman-Keuls between *timGal4/6.1-2miti* and: *timGal4/+* *p<0.0001; *6.1-2miti/+* p=0.834 n.s.; test *post hoc* Newman-Keuls between *timGal4/16.2-2miti* and: *timGal4/+* p<0.0187 n.s.; *16.2-2miti/+* *p<0.0001; test *post hoc* Newman-Keuls between *timGal4/61.1-2miti* and: *timGal4/+* *p=0.026; *61.1-2miti/+* p=0.234 n.s..
The *timGal4/2miti* lines are significantly different only to one of the controls.
- *2miti* driven with *c232Gal4* driver: ANOVA:*$F_{(6,245)}$=13.501 p<0.0001; test *post hoc* Newman-Keuls between *c232Gal4/6.1-2miti* and: *c232Gal4/+* *p=0.0008; *6.1-2miti/+* p=0.062 n.s.; test *post hoc* Newman-Keuls between c232*Gal4/16.2-2miti* and: *c232Gal4/+* p=0.095 n.s.; *16.2-2miti/+* *p<0.0001 n.s.; test *post hoc* Newman-Keuls between c232*Gal4/61.1-2miti* and: *c232Gal4/+* p=0.727 n.s.; *61.1-2miti/+* *p=0.018.
The *c232Gal4/2miti* lines are significantly different only to one of the controls.
- *2miti* driven with *OK107Gal4* driver:
ANOVA:*$F_{(6,270)}$=3.983 p=0.0007; test *post hoc* Newman-Keuls between *OK107Gal4/6.1-2miti* and: *OK107Gal4/+* p=0.639 n.s.; *6.1-2miti/+* p=0.781 n.s.; test *post hoc* Newman-Keuls between *OK107Gal4/16.2-2miti* and: *OK107Gal4/+* p=0.135 n.s.; *16.2-2miti/+* p=0.969 n.s.; test *post hoc* Newman-Keuls between *OK107Gal4/61.1-2miti* and: *OK107Gal4/+* p=0.133 n.s.; *61.1-2miti/+* p=0.807 n.s..
The *OK107Gal4/2miti* lines are significantly different only to one of the controls.
- *2miti* driven with *GMRGal4* driver:
ANOVA:*$F_{(6,130)}$=6.371 p<0.0001; test *post hoc* Newman-Keuls between *GMRGal4/6.1-2miti* and: *GMRGal4/+* p=0.551 n.s.; *6.1-2miti/+* *p=0.0006; test *post hoc* Newman-Keuls between *GMRGal4/16.2-2miti* and: *GMRGal4/+* p=0.607 n.s.; *16.2-2miti/+* *p=0.019; test *post hoc* Newman-Keuls between *GMRGal4/61.1-2miti* and: *GMRGal4/+* p=0.487 n.s.; *61.1-2miti/+* p=0.077 n.s..
The *GMRGal4/2miti* lines are significantly different only to one of the controls.
*indicates a statistically significant difference. n.s.=not significant.

3.8 Determination of PERIOD protein kinetics in circadian clock neurons

Drosophila circadian clock, which controls locomotor activity rhythms, is located in the brain and relies of about 70 clock neurons for each brain hemisphere (Peschel and Helfrich-Forster, 2011). PER and TIM1 proteins, being fundamental components of the circadian machinery, are expressed in circadian clock neurons, and their levels oscillate during the 24 h, with a maximum at around ZT0 and a minimum at around ZT12 (Shafer et al., 2002).
Since we achieved that in the outcrossed *PB2mit*^{c03963} strain the circadian periodicity was lengthening with respect to the *white*^{1118} control strain, we inquired whether at the molecular level there was a corresponding modification in the circadian pacemaker mechanisms, allowing the explanation of this phenotype. Therefore we performed immunocytochemical experiments (ICC) focusing on the oscillation and on the nuclear accumulation kinetics during the 24 h of the PER clock protein in specific clusters of clock neurons, the small (four out of five) and the large ventrolateral neurons (s- and l-LNvs), which play a central role in the control of circadian behavioural rhythms. These neurons were chosen because they express the neuropeptide Pigment dispersing factor (PDF), with specific and

exclusive cytoplasmic localization, which was used as cytoplasmic marker, allowing us to delineate the nuclei in both s- and l-LNvs cell bodies.
ICC assay was performed on dissected brains of 3-5 days old *PB2mit*^{c03963} and *white*^{1118} control flies entrained for at least three days in 12:12 LD conditions. The flies were collected at different ZTs (ZT: 18; 20; 22; 24; 2; 4) choosing a time window in which PER levels are the highest along the 24 h and during which the protein shuttles from the cytoplasm to the nucleus (Shafer et al., 2002). The ICC experiments were repeated twice. Fig.3.8a reports an example of PER (in green) and PDF (in red) staining in s-LNvs (but not the 5th s-LNv) and l-LNvs of one hemisphere in a wild-type fly at ZT22.

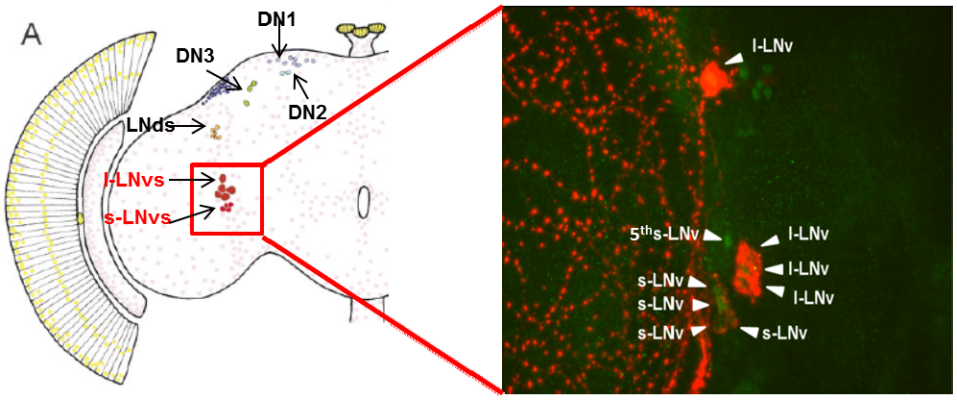

Fig.3.8 Representative picture of circadian neurons in one brain hemisphere (left, modified from Helfrich-Forster, 2003) and an example of ICC PER-PDF double staining (PER in green, PDF in red) in one brain hemisphere of a *white*^{1118} wild-type individual collected at ZT22 (right).

The PER signal in correspondence to the nucleus of clock neurons belonging to these two clusters was quantified and plotted (Fig.3.9a,b). As expected, in both s- and l-LNvs of *white*^{1118} wild-type brains, PER expression reached a maximum peak at ZT0 (Shafer et al., 2002). The *PB2mit*^{c03963} mutant displayed, for both s- and l-LNvs, PER intensity values significantly different from those of the controls. In particular, in s-LNvs of *PB2mit*^{c03963} individuals, PER levels were higher compared to those of the controls in the time window including the last part of the night and the first hours of the day (from ZT 22 to ZT 2). In l-LNvs of *PB2mit*^{c03963} strain, the peak of PER expression was not well defined specifically at ZT0, but it was broadly distributed between ZT0 and ZT2, when PER levels in control brains were lower.
These data indicate, in both s-LNvs and l-LNvs of *PB2mit*^{c03963} mutant flies, a different PER protein nuclear kinetics (higher nuclear accumulation or slower degradation), compared to those of *white*^{1118} controls.
These achievements suggest that probably the slight but significant modification in PER nuclear accumulation of *PB2mit*^{c03963} brains could be responsible for the increased tau seen in this *2mit* mutant strain.

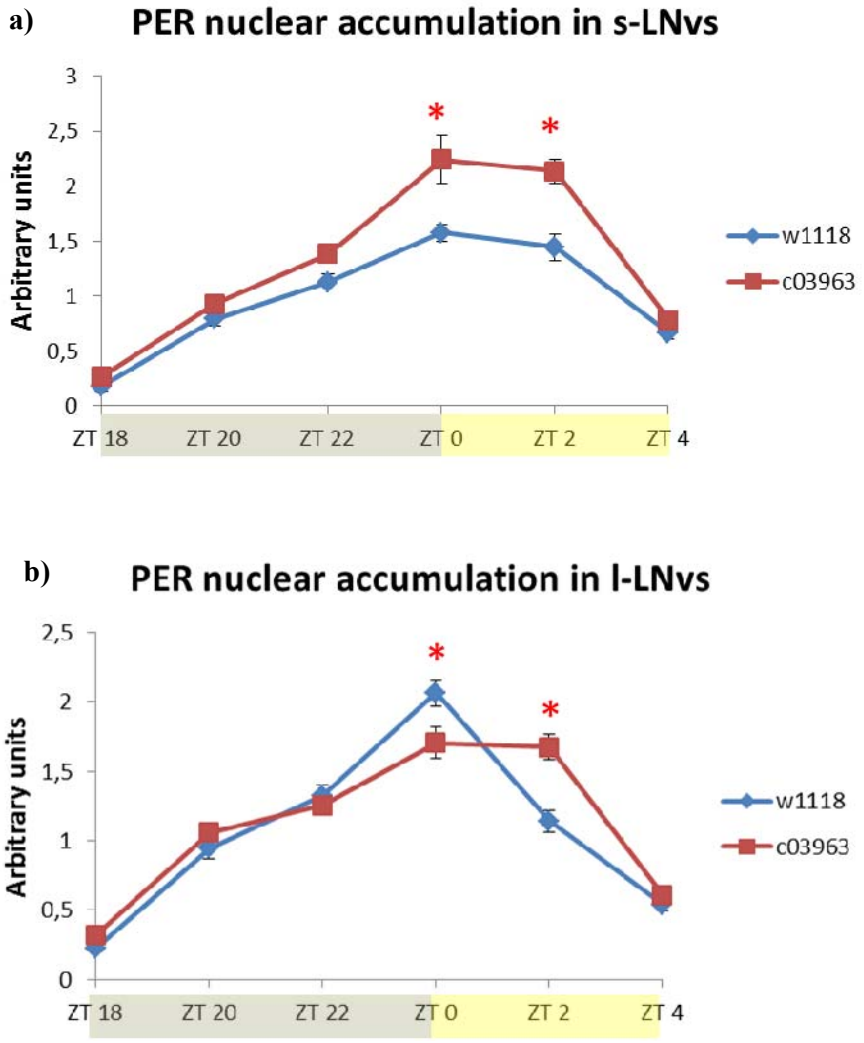

Fig.3.9 One replicate of PER relative levels of nuclear accumulation between ZT18 and ZT4, after 3-5 days of entrainment in 12:12 LD regime in *PB2mit*^{c03963} brains compared to *white*^{1118} control brains. **a)** 4 pdf-positive s-LNvs. ANOVA: *$F_{(5,688)}$=4.791 p=0.0003; test *post hoc* Newman-Keuls between *PB2mit*^{c03963} and *white*^{1118} at: ZT18 p=0.517 n.s.; ZT20 p=0.332 n.s.; ZT22 p=0.594 n.s.; *ZT0 p<0.0001; * ZT2 p<0.0001; ZT4 p=0.396 n.s. **b)** l-LNvs. ANOVA: *$F_{(5,818)}$=9.045 p<0.0001; test *post hoc* Newman-Keuls between *PB2mit*^{c03963} and *white*^{1118} at: ZT18 p=0.365 n.s.; ZT20 p=0.280 n.s.; ZT22 p=0.507 n.s.; *ZT0 p=0.0006; *ZT2 p<0.0001; ZT4 p=0.533 n.s.. For each genotype, at least 10 brain lobes per time point were tested.
*indicates a statistically significant difference. n.s.=not significant.

3.9 Analyses of general locomotor activity at adult stage

Since *2mit* mRNA is expressed in structures involved in the control of locomotor activity, we investigated whether *2mit* has any involvement in the control of general locomotor activity. We started from the larval stage but, as previously described, *2mit* does not seem to have a role in larval locomotor activity. Effects of *2mit* mRNA depletion on general locomotor activity were analysed at the adult stage by estimating the same quantitative parameters considered also at the larval

stage: the total distance travelled, the number of inactivity episodes and the global immobility time. In addition, also the overall average speed was measured. Since in *Drosophila* locomotor activity at adult stage is sexually dimorphic (Martin et al., 1999a; Martin, 2004) those parameters were evaluated for males and females separately. 3-7 days old individuals, entrained for at least three days in 12:12 LD conditions, were tested.

The analysed strains, characterized by *2mit* mRNA reduced expression levels, were the outcrossed *PB2mit*^{c03963} strain and *2miti* lines in which *2mit* was silenced in the whole nervous system (*elavGal4* driver) or in mushroom bodies (*OK107Gal4* driver).

At first, the effect of *2mit* mRNA decreased levels in general locomotor activity was analysed in 3-7 days old outcrossed *PB2mit*^{c03963} individuals. The results showed that for all the analysed locomotor activity parameters, the values obtained from this strain were not significantly different with respect to other strains analysed, such as *white*^{1118} and *wt-ALA* wild-type strains, *MB08962* insertional strain with no *2mit* mRNA depletion and the *tim*^{01} clock mutant (Fig.3.10a-d; the only significant difference regarded *tim*^{01} average speed that was slightly higher with respect to the one of all other strains).

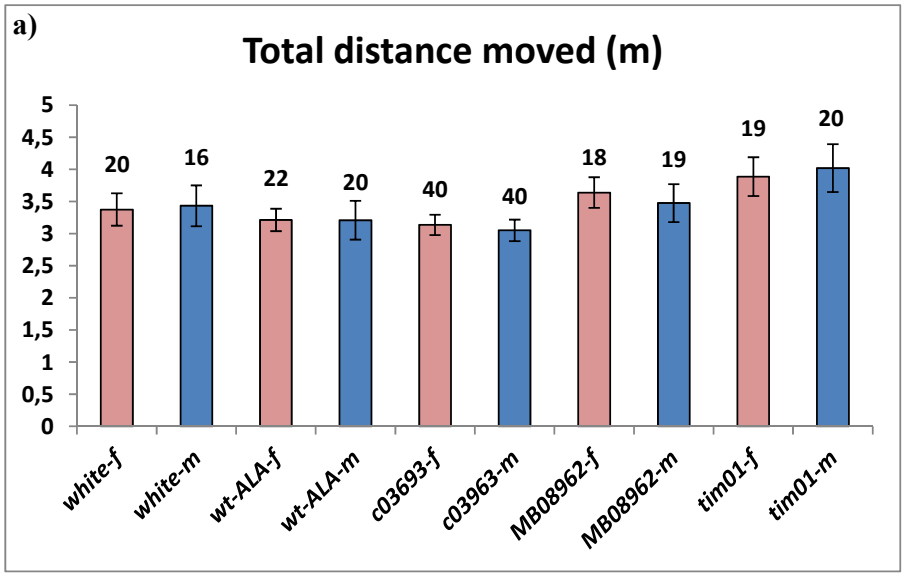

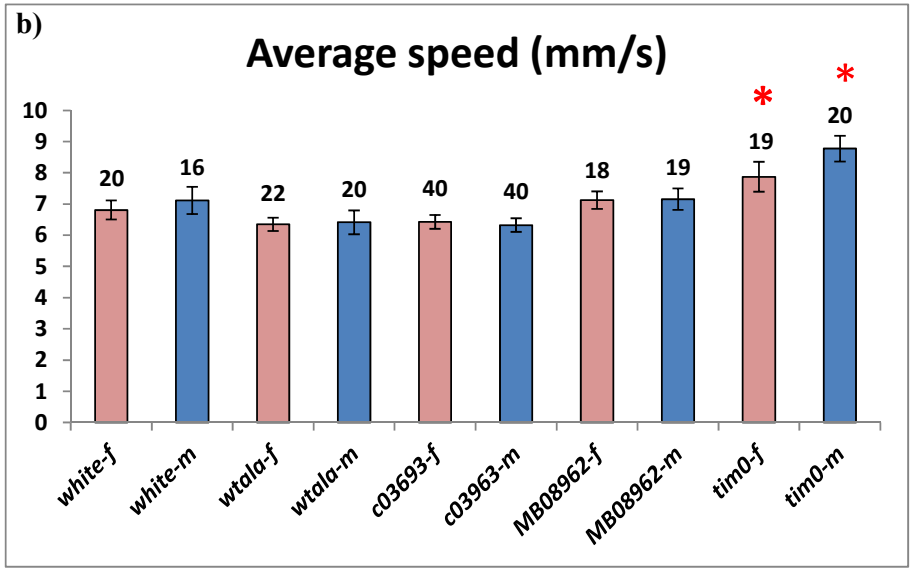
b)
Average speed (mm/s)
10
9
8
7
6
5
4
3
2
1
0
20
16
22
20
40
40
18
19
19
20
*
*
white-f
white-m
wtala-f
wtala-m
c03693-f
c03963-m
MB08962-f
MB08962-m
tim0-f
tim0-m

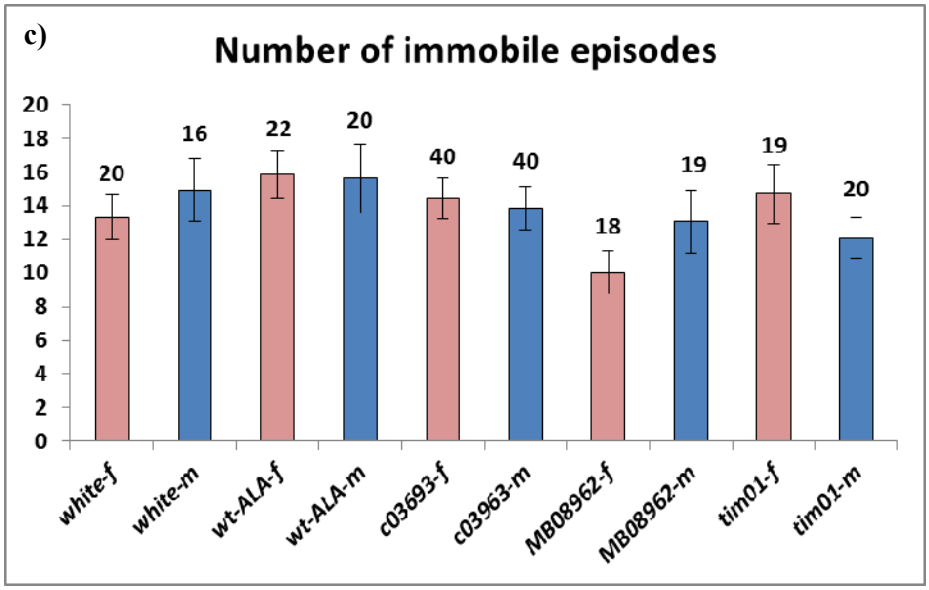
c)
Number of immobile episodes
20
18
16
14
12
10
8
6
4
2
0
20
16
22
20
40
40
18
19
19
20
white-f
white-m
wt-ALA-f
wt-ALA-m
c03693-f
c03963-m
MB08962-f
MB08962-m
tim01-f
tim01-m

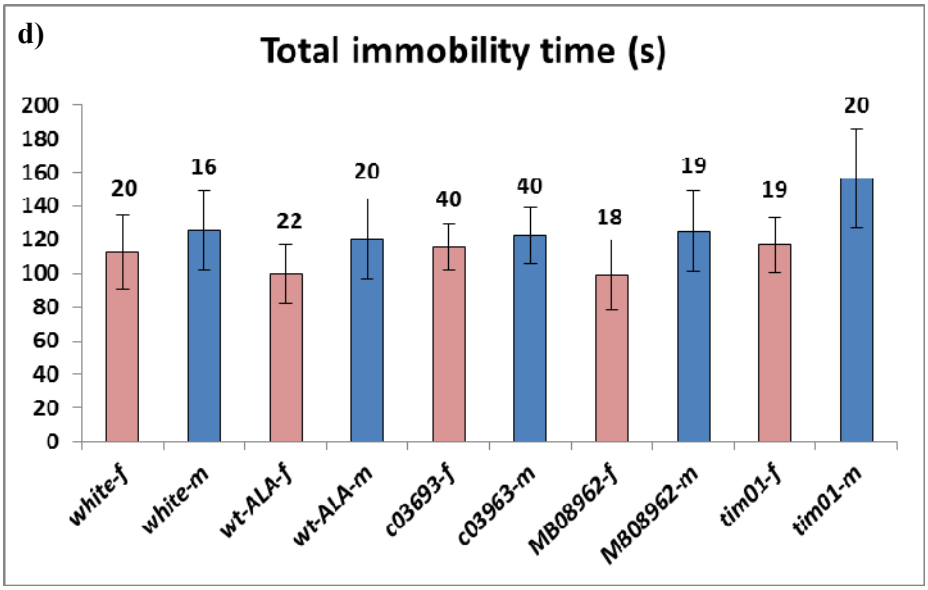

Fig.3.10 General locomotor activity parameters of 3-7 days old *PB2mit*^{c03963}, *MB08962* and *tim*^{01} individuals compared to *white*^{1118} and *wt-ALA* controls. f=females (pink); m=males (blue). **a)** Total distance moved. ANOVA: females: $F_{(4,114)}$=2.071 p=0.089 n.s.; males: $F_{(4,110)}$=1.964 p=0.105 n.s.. **b)** Average speed. ANOVA: females: *$F_{(4,114)}$=4.106 p=0.004, test post hoc Newman-Keuls between: *white*^{1118} and *tim*^{01}: *p=0.041; and *wt-ALA* and *tim*^{01}: *p=0.006; males: *$F_{(4,110)}$=8.687 p<0.0001, test post hoc Newman-Keuls between: *white*^{1118} and *tim*^{01}: *p=0.003; and *wt-ALA* and *tim*^{01}: *p=0.0002. **c)** Number of immobile episodes. ANOVA: females: $F_{(4,114)}$=1.944 p=0.108 n.s.; males: $F_{(4,110)}$=0.634 p=0.639 n.s.. **d)** Total immobility time. ANOVA: females: $F_{(4,114)}$=0.235 p=0.918 n.s.; males: $F_{(4,110)}$=0.383 p=0.820 n.s..
*indicates a statistically significant difference. n.s.=not significant. Values at the top of colums represent the number of individuals tested per genotype.

In parallel, we found that all tested locomotor activity parameters of lines with RNAi-mediated *2mit* KD driven in the whole nervous system (*elavGal4* driver) and in mushroom bodies (*OK107Gal4* driver) did not display, again, any significant difference with respect to those of appropriate controls (data not shown).

These findings indicate that *2mit* does not seem to have a role in general locomotor activity.

With the aim to analyse whether *2mit* depletion affected general locomotor behaviour of aged flies, we tested 30 days old outcrossed *PB2mit*^{c03963} individuals. However, their survival was seriously compromised following the protocol steps regarding CO_2-anasthesia and overnight incubation in starvation conditions and most of the individuals died before the test. So, we analysed ~20 days old outcrossed *PB2mit*^{c03963} flies and, again, we did not find any statistically significant difference in comparison to *white*^{1118} control flies of the same age (Fig.3.11a-d). With those further results, the overall conclusion is that *2mit* does not seem to have a role in the control of general locomotor activity paradigm.

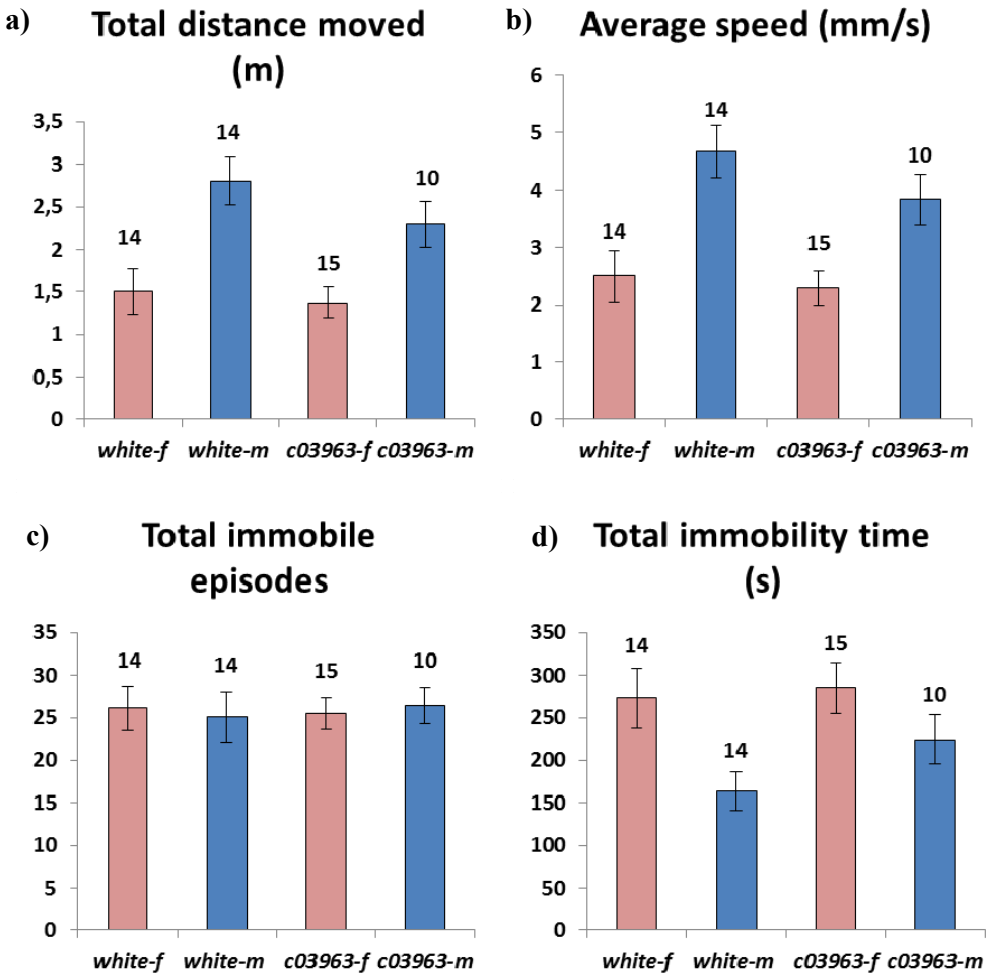

Fig.3.11 General locomotor activity parameters of 20 days old *PB2mit*^{c03963} individuals compared to *white*^{1118} controls. f=females (pink); m=males (blue). **A)** Total distance moved. ANOVA: females: $F_{(1,27)}$=0.161 p=0.691 n.s.; males: $F_{(1,22)}$=1.641 p=0.213 n.s.. **b)** Average speed. ANOVA: females: $F_{(1,27)}$=0.0002 p=0.989 n.s.; males: $F_{(1,22)}$=0.118 p=0.734 n.s.. **c)** Number of immobile episodes. ANOVA: females: $F_{(1,27)}$=0.039 p=0.845 n.s.; males: $F_{(1,22)}$=0.115 p=0.737 n.s.. **d)** Total immobility time. ANOVA: females: $F_{(1,27)}$=0.062 p=0.805 n.s.; males: $F_{(1,22)}$=2.884 p=0.104 n.s.. n.s.=not significant. Values at the top of colums represent the number of individuals tested per genotype.

3.10 Analyses of short-term memory

From mRNA *in situ* hybridization experiments, among the adult brain regions characterized by *2mit* mRNA expression, we identified the mushroom bodies and the ellipsoid-body of the central complex. Mushroom bodies primarily, and the central complex in minor contribution, are brain components involved in learning and memory (Heisenberg, 1998; Heisenberg, 2003; Zars et al., 2000; Pascual and Preat, 2001; Sitnik, 2003; Joiner and Griffith, 1999).

Even if learning and memory have been mainly studied through classical paradigms directly testing their association to olfactory pathways (odor-shock associative paradigm), there are also other approaches that study the olfactory

implication on learning and memory in an indirect way. For instance courtship behaviour represents a valid tool for this kind of analyses.

Drosophila courtship in characterized by a sequence of innate behaviours based on a set of stimuli belonging to different sensory modalities (Ejima et al., 2005; Ejima and Griffith, 2008). First, the male orientates towards the female and follows her, being able, in this way, to smell low volatily pheromones (Ferveur, 2005). Subsequently, the male taps the courtee abdomen with his forelegs, and again this behaviour allows to sniff cuticular non-volatile pheromones (Bray and Amrein, 2003). Then, the male extends and vibrates one of its wings to produce a courtship song, which is species-specific allowing the female to recognize males belonging to the same species (Tauber and Eberl, 2003). Finally the male licks her genitalia sensing again non-volatile pheromones and attempts copulation (Bastock and Manning, 1955), that provides a mechanosensory stimulation for both sexes (Ejima and Griffith, 2008).

Although courtship is an inborn behaviour, it can modify in an experience-dependent way. One assay based on this assumption is the classical courtship conditioning (Mehren et al., 2004; Griffith and Ejima, 2009), that is composed by a training and a test period. During the training period, males are singly placed with mated females that refuse their courtship both by emitting aversive pheromones and by extruding their ovipositor (Tompkins et al., 1983; Ackerman and Siegel, 1986). During the test period, these "conditioned" males are placed in presence of a virgin female and levels of courtship are measured and compared to those of "sham" males, which belong to the same genotype but do not have had the previous negative courtship experience. In wild-type strains, the courtship level of "conditioned" males is lower compared to that of "sham" controls. The reason of the "conditioned male" behaviour is the memory of its previous failed attempted copulation. Therefore, "courtship conditioning", also defined as "conditioned courtship suppression", is a form of associative memory, in which the association is between the female and an aversive olfactory stimulus, acting as an unconditioned stimulus (US). The effect of this association is the decreased level of courtship toward a virgin female despite its production of attractive pheromones providing a conditioned stimulus (CS; Tompkins et al., 1983; Joiner and Griffith, 1999; Mehren et al., 2004). Courtship conditioning represents a valid method to measure both associative learning and memory. Learning is determined by measuring the change in the amount of courtship towards a mated female during the training period, while memory is defined by the suppression of subsequent courtship towards a virgin female (Mehren et al., 2004). Memory can be distinguished in different phases and in our experiments we focused at the moment on short-term memory (STM). In courtship conditioning, STM is analysed with training sessions having low behavioural intervals. It lasts 2-3 h and does not imply transcriptional or translational changes in the cell (Siegel and Hall, 1979).

Courtship conditioning assay was applied to study short-term associative memory of *PB2mit*^{c03963} strain in order to explore whether a *2mit* mRNA general depletion, including brain structures with a role in memory formation, affects STM phenotype. The *PB2mit*^{c03963} strain was compared to two wild-type control strains, the *Oregon-R* and the *white*^{1118} strains, and to a classic memory mutant, the *dunce* (*dnc*) strain. *dunce* (*dnc*) gene codes for a cAMP- phosphodiesterase with a role in memory (Byers et al., 1981). For each genotype, courtship levels of "conditioned" and "sham" males were compared. From the examination of the results, in the two wild-type control strains the "conditioned" males courted significantly less with respect to the corresponding "sham" controls, indicating memory formation (Fig.3.12). On the contrary, the *dunce* memory mutant control, characterized by memory impairments, did not show, as expected, any significant difference between the two subgroups of conditioned and "sham" males (Fig.3.12). *PB2mit*^{c03963} males did not show statistically significant reduced levels of courtship of conditioned males with respect to sham controls (Fig.3.12). This suggests that *PB2mit*^{c03963} males present memory defects and that *2mit* appears to have a function in short-term associative memory.

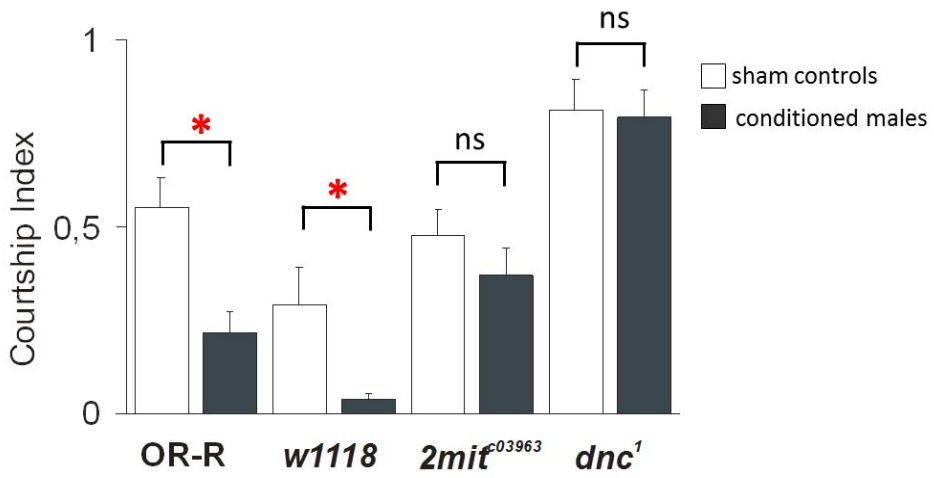

Fig.3.12 Courtship conditioning assay to test short-term associative memory of *PB2mit*^{c03963} strain compared to *Oregon-R* and *white*^{1118} wild-type controls and *dunce*^{1} memory mutant control. ANOVA: comparison between conditioned males vs sham controls for each genotype: *Oregon-R:* ANOVA: *$F_{(1,46)}$=12.022 p=0.001; *white*^{1118}: ANOVA: *$F_{(1,17)}$=5.551 p=0.031; PB2*mit*^{c03963}: ANOVA: $F_{(1,51)}$=1.149 p=0.289 n.s.; *dunce*^{1}: ANOVA: $F_{(1,12)}$=0.025 p=0.887 n.s.. *indicates a statistically significant difference. n.s.=not significant.

3. Discussion

This chapter reports the phenotypical and behavioural characterization of *2mit* mRNA depleted lines, performed in order to identify the role of *2mit* gene in *Drosophila*. The *2mit* mRNA depleted lines under analysis were the *PB2mit*^{c03963} insertional mutant strain and *driverGal4/2miti* lines, in which *2mit* KD was

specifically driven in the whole nervous system or in specific subregions of the adult brain.

In previous experiments it had been reported that a RNAi-mediated *2mit* ubiquitous KD leads to lethality at late pupal stage with main defects at level of the abdominal region, suggesting a role for *2mit* in metamorphosis and an essential function for survival during developmental stages. Northern blot experiments on pupal samples with ubiquitous *2mit* RNAi detected a strong *2mit* abatement with a smeared lane probably corresponding to *2mit* mRNA degraded fragments.

2mit mRNA depleted levels in $PB2mit^{c03963}$ strain did not lead to the pupal lethality phenotype. In fact, $PB2mit^{c03963}$ individuals displayed homozygous viability and no defects in their body morphology. Real-time PCR assays in $PB2mit^{c03963}$ larval samples revealed a 50% *2mit* mRNA decrement, thus mimicking a heterozygous condition. In $PB2mit^{c03963}$ adult heads, *2mit* mRNA levels were 15% compared to controls. It is interesting to note that both $PB2mit^{c03963}$ adult males and females showed a significantly reduced lifespan compared to controls. Even if we cannot completely exclude that the lethal phenotype shown in *2mit* KD pupae is due to off-target effects, one possible hypothesis is that *2mit* has a general role during postembryonic development. Levels of *2mit* expression in the $PB2mit^{c03963}$ larvae are likely sufficient for developmental completion and metamorphosis overcoming. To check this hypothesis Northern blot experiments will be performed on all RNAi-mediated general *2mit* KD lines and $PB2mit^{c03963}$ strain in order to make a direct comparison between the effects that the two strategies have on the reduction of *2mit* mRNA expression. However, in $PB2mit^{c03963}$ adults the strong *2mit* mRNA decrement impairs viability. This reduced longevity could be explainable as premature ageing, for example due to impairments at level of stress resistance, organism physiology and/or metabolism.

Given *2mit* slight expression in optic lobes of the adult brain, we tested *2mit* involvement in the visual system at both larval and adult stages, analysing the $PB2mit^{c03963}$ mutant strain. We found that at larval stage the typical light-avoidance behaviour, which is related to vision capabilities, is not affected in $PB2mit^{c30963}$ individuals, characterized by ~50% of *2mit* mRNA level. In $PB2mit^{c03963}$adults, which showed ~85% *2mit* mRNA decreased in adult heads expression compared to controls, we found impairments in the optomotor response, indicating in these flies a loss of integrity occurring at level of the adult visual system. These results suggest that *2mit* exerts a role in neural circuits involved in the processing of motion vision of the adult. However, we cannot exclude an involvement of *2mit* in light perception during preadult stages, because the ~50% of *2mit* mRNA level in $PB2mit^{c30963}$ larvae might guarantee a photophobic behaviour similar to that of the wild-type.

Despite the positive results observed for insertional mutant, we have shown that the optomotor response was not perturbed by *2mit* KD driven in the whole

nervous system or in specific compartments of the visual system. A possible hypothesis, explaining this difference between the two strategies adopted to down-regulate *2mit* mRNA, could be that, when *2mit* KD was driven in the nervous system, it was not sufficiently abating *2mit* mRNA levels as in the $PB2mit^{c03963}$ strain to cause a defective optomotor response. Given that in *Drosophila* the optomotor response processing begins at level of R1-6 retinal photoreceptors (Heisenberg and Buchner, 1977), which are involved in motion detection, $PB2mit^{c03963}$ individuals were tested for their electrical activity at level of the retina showing that in these mutant flies no alterations at level of the eye were evident (personal communication by Prof. Aram Megighian, Department of Physiology, University of Padova, Italy). This indicated that the defective optomotor behaviour in $2mit^{-}$ adult mutants was not due to impaired vision at level of retina photoreceptor cells but rather to optic lobes components involved in the processing and integration of motion information. Different optic lobe neuronal pathways involved in the transfer of motion information have been identified and, so far, are not completely defined. For example Rister and co-workers (2007) published that L1 and L2 monopolar cells and, at minor level and under particular environmental conditions, T1 basket cells are implicated in motion detection. Lobula plate tangential neurons are asserted to be important components for the optomotor response representing the final step, in the optic lobe, for the transmission of motion information to fly motor centers (Borst et al., 2010). Moreover, outside the optic lobe, also postsynaptic descending neurons (Haag et al., 2007; Wertz et al., 2008; Borst et al., 2010) and motor centers in the thoracic ganglion are implicated in the elaboration of the motion vision response and, as far as we know, *2mit* may exert its function also in those districts.

We have also found that *2mit*'s host gene *tim2*, which is also expressed in optic lobes (Benna et al., 2010), did not seem to exhibit a functional correlation with *2mit* at level of motion vision, given the correct optomotor responses detected in two $tim2^{-}/+$ heterozygous mutant lines tested at the same conditions of $PB2mit^{c03963}$ individuals.

Despite nested intronic genes could share same or correlated functions with respect to their host genes (Gibson et al., 2005), we found that *2mit* is not involved in circadian photoreception at the adult stage as *tim2* (Benna et al., 2010). The role of *tim2* in the modulation of this phenotype was related to its expression at level of medulla T1-basket cells in the optic lobe. For problems related to the mRNA *in situ* hybridization technique, we were not able to determine at the molecular level whether *2mit* mRNA expression co-localized with that of *tim2* mRNA in the optic lobe of adult brains. However, analyses of our behavioural data suggest that in the optic lobe *2mit* and its host gene *tim2* exert different functions, with *2mit* implicated in optomotor response and its host gene *tim2* in circadian photoreception.

Anyway, if *2mit* is not involved in light entrainment of the circadian clock, we have shown an increased circadian periodicity in constant conditions in 3-5 days

old flies belonging to both the *PB2mit*^{c03963} mutant and pan-neuronal *2miti* lines. The two strategies applied to obtain *2mit* down-regulation appeared to share overlapping effects in young flies. Furthermore, we have also shown that with ageing the phenomenon of circadian periodicity lengthening in *free running* conditions became more prominent only in the *PB2mit*^{c03963} mutant, whereas a pan-neuronal *2mit* KD led to increased arhythmicity in one of the tested lines, with no modification of circadian tau. One interpretation that could link together these apparently different results could be that, with ageing, *2mit* mRNA depletion might enhance impairments to circadian rhythmicity and the phenotypical effect could be either represented by rhythmicity alteration, with a further lengthening of circadian tau in DD, or rhythmicity loss.

In addition to behavioural data, we found that, in *PB2mit*^{c03963} mutant brains, the PER protein nuclear accumulation kinetics was different from that of the controls. In fact, in *PB2mit*^{c03963} mutant brains PER seemed to accumulate in the nuclei of s- and l-LNvs circadian neurons at higher levels and for a longer period with respect to controls, indicating that in *PB2mit*^{c03963} mutants PER has altered stability or degradation kinetics. PER protein nuclear entry and accumulation is critical for clock dinamics and the establishment of circadian rhythmicity (Curtin et al., 1995). In Curtin et al. (1995) it is reported that in long-period mutants PER nuclear entry is delayed and it is suggested, in a more general sight, that the alteration of periodicity is a direct consequence of a general change in PER activity. In our case, molecular results seem to mimic what was detected at behavioural point of view in *PB2mit*^{c03963} mutants, which was the lengthening of circadian periodicity. These data seem to suggest that *2mit* mRNA depletion is the reason of the observed modified circadian phenotype and that *2mit* has a role in the control of circadian periodicity.

Nevertheless, experiments, led to map the putative cerebral regions in which *2mit* would exert this function, have not been exhaustive. In fact, none of the lines where *2mit* KD was driven in eye, ellipsoid body, mushroom bodies or circadian neurons displayed a significant increase of the circadian periodicity in DD. These results might be explained hypothesizing that none of the cerebral subregions where *2mit* KD was induced were important for the putative control of the circadian phenotype. Alternatively, these negative results might be due to an ineffective *2mit* mRNA depletion in the analysed lines.

PB2mit^{c03963} mutants did not show any impairment in general locomotor activity both at larval and adult stages. At the adult stage this result was observed also in lines with *2mit* KD induced by RNAi, indicating that *2mit* does not have any role in the control of general locomotor activity at adult stage. However, we cannot exclude an involvement of *2mit* in the control of general parameters of locomotor activity during larval stages, because the ~50% of *2mit* mRNA level in *PB2mit*^{c30963} larvae might be sufficient to exhibit a wild-type behaviour. These findings also prove that the alterations on adult circadian locomotor activity in *2mit*$^{-}$ mutants are not a consequence of general locomotor activity impairments.

In agreement with the *2mit* mRNA expression pattern in brain mushroom bodies, structures mainly involved in memory formation, and in the ellipsoid-body of the central complex, also implicated in memory (Heisenberg, 2003; Zars et al., 2000; Pascual and Preat, 2001; Mehren et al., 2004), we have demonstrated that *2mit* plays a role in short-term associative memory formation. In fact $PB2mit^{c03963}$ mutants exhibited memory impairments on courtship conditioning assay.
The results reported in this chapter allow us to hypothesize that *2mit* depletion could provoke defects at level of the nervous system affecting normal neural functions related to the motion vision, establishment of daily rhythmicity and memory and could also cause precocious death. So we have identified different phenotypes in which *2mit* might be involved but we need to confirm all of them through rescue experiments analysing for the same phenotypes transgenic lines overexpressing 2MIT in $PB2mit^{c03963}$ background. In addition, regarding the *2mit* role in memory formation phenotype, we have to see whether it is a specific function of this gene or somehow related to the *tim2* host gene. Anyway, preliminary results obtained by testing a $tim2^{-}$/+ heterozygous mutant strain for the same phenotype showed no impairments in memory formation, indicating that probably the role in memory is peculiar of *2mit* gene.

3. Materials and Methods

3.1 Fly Stocks and UAS-GAL4 binary system

3.1.1 The UAS-GAL4 binary system

The *Drosophila* GAL4-UAS binary system was first described by Brand and Perrimon in 1993. This technique represents a powerful tool that allows the spatial and temporal control of the ectopic selective activation of a transgenic construct bearing a specific target gene or a sequence. Using this strategy, it is possible to drive the expression of a target sequence in specific tissues or cells and/or in specific developmetal stages of *Drosophila melanogaster*, in the same expression pattern established by a promoter sequence (Brand and Perrimon, 1993; O'Kane, 1998). This technique is based on the contemporary activation of two transgenic constructs that are first separated in two distinct parental lines. One of these transgenic constructs carries the sequence encoding the *Saccharomyces cerevisiae* GAL4 transcriptional factor, able to bind specific enhancer regions defined as Upstream Activation Sequences (UAS). The expression of GAL4 is tissue- and/or development-specific and depends on an upstream promoter regulatory region driving its specific expression pattern. The second construct is composed by the UAS, recognized by the GAL4, fused to a target sequence, which is silent in absence of GAL4. When a fly carrying the UAS-target sequence is crossed to another one bearing the promoter-*Gal4* construct, in the progeny all individuals will carry both constructs. As consequence, the UAS-GAL4 system will be

activated allowing the expression of the target sequence in the same expression pattern of the GAL4 factor.

The UAS-GAL4 method is advantageous for multiple reasons. Through the separation in independent lines of the target gene from the construct for its activation, problems due to the toxicity of a gene product are overcome. This allows parental lines to be viable and lethality events to be easily studied. In addition, a target transgene can be expressed in numerous distinct patterns by crossing it with different driver lines (Brand and Perrimon, 1993) and conversely, different target genes can be activated in the same cells and tissue pattern, by crossing them with the same driver line. The UAS-GAL4 tool is particularly advantageous for example to alter or ablate cell function by driving the expression of specific elements. Fig.3.13 provides a schematic description of the UAS-GAL4 binary system strategy.

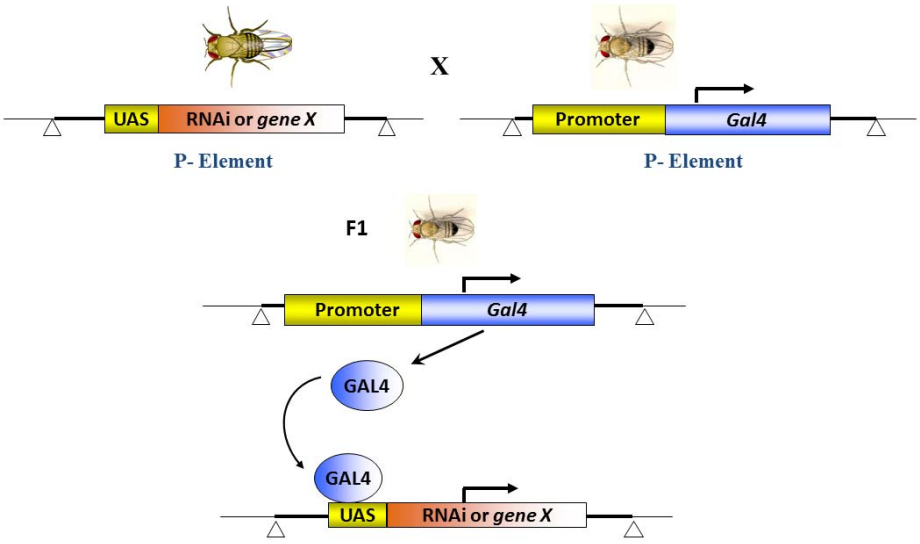

Fig.3.13 Schematic representation of *Drosophila* UAS-GAL4 binary system. A female carrying the construct for RNA interference (RNAi) or of a target *gene X* is crossed to a male expressing GAL4 yeast transcriptional factor under the control of a tissue-specific promoter. In the progeny (F1), in cells where GAL4 is expressed, the UAS-RNAi/*gene X* construct is activated and it is possible to observe the effects of this targeted expression (modified from Brand and Perrimon, 1993).

3.1.2 Fly stocks

Wild-type strains

- ***white*^{1118}**: described in Chapter 2
- ***Oregon-R***: used as control strain, it derives from a wild-type strain sampled in Oregon (USA).
- ***wt-ALA***: used as control strain, this line was founded in 2004 from wild-type females from Alto Adige (latitude: 46°N). The strain was stabilized in 2007.

Transposon insertional strains (from Bloomington *Drosophila* stock center)
- ***PB2mit^{c03963}*** (outcrossed), ***MB08132***, ***MB08962***, ***f00297*** and ***c06976*** , described in Chapter 2.

***Gal4* driver lines**:
- ***w^{+}; elavGal4/CyO*** (stock number #8765): genotype: P{GAL4-elav.L}2/CyO; insertion chromosome: 2; comments: expresses GAL4 in the nervous system (from Bloomington *Drosophila* stock center).
- ***GMRGal4*** (stock number #1104): genotype: w*; P{GAL4-ninaE.GMR}12; insertion chromosome: 2; comments: glass enhancer driving GAL4 in the eye disc, provides strong expression in all cells behind the morphogenetic furrow (from Bloomington *Drosophila* stock center).
- ***OK107Gal4*** (stock number #854): genotype: w*; P{GawB}ey^{OK107}; insertion chromosome: 4; comments: GAL4 expressed in mushroom bodies (from Bloomington *Drosophila* stock center).
- ***T1Gal4*** (stock number #103879): genotype: y[*]w[*]P{w[+mW.hs]=GawB} CG14200[NP1086]/FM7c; insertion chromosome: 1; insertion site: 18C8 (from *Drosophila* Genetics Resource Center (DGRC) Kyoto Institute of Technology, Kyoto stock center).
- ***c232Gal4*** (stock number #30828): genotype: w*; P{GawB}Aph-4^{c232}; insertion chromosome: 3; comments: expresses GAL4 in ring neurons, malpighian tubules, large field neurons of the ellipsoid-body (from Bloomington *Drosophila* stock center).
- ***timGal4*** (a gift by M. Young): genotype: y^{1} w*; P{UAS-tim-GAL4}; *Gal4* is under the control of the *timeless* (*tim*) promoter. *tim* is a circadian gene displaying an oscillating expression profile during the 24 h. This driver is expressed in circadian clock neurons (Emery et al., 1998) and elements of the pheripheral clock (Plautz et al, 1997).

***UAS-2mitRNAi* lines:**
- ***6.1-2miti*:** insertion site: 3R 95D.
- ***16.2-2miti*:** insertion site: 2L 35E-F.
- ***61.1-2miti*:** insertion site: 2L 28A-B.

These three lines were generated in the laboratory for *2miti* KD. They carry the same construct to drive RNA interference (RNAi) against *2mit.* This construct is composed by UAS fused to a 1223 bp portion of *2mit* cDNA (position:1471-2693) separated by a linker from its reverse complement. In Fig.3.14 a schematic representation of the *2mit* RNAi construct is reported. In Table 3.4 the *2mit* sequence used as reference is reported.

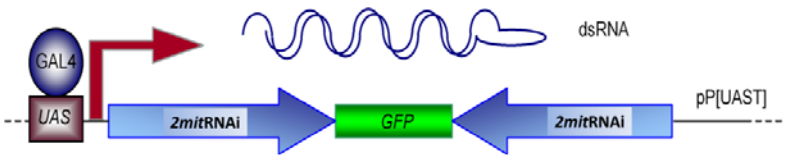

Fig.3.14 Schematic representation of the *Drosophila 2mit* RNA interference construct.

***UAS-2mit-*RNAi (*UAS-2miti*) lines**	***2mit* RNAi sequence**
UAS-6.1-2miti	CGCGTGGATTTGAAGACGGAGTATCTGCAATTCCACAATTTTTACGAAAACT TCAGCAGCCGAGAGTGTGGTATAAGAAAACCGGAAAATGACACAAAGCCG CCTTCTTGCAGCCTAACAAGGGCATCAGCTACATTAACAACAACACCCAGA AGTATGTCAAAAGTTGAAAAGTCACAAGAAGCACAAGCAACAGCAACATC AGTGGAAGTAGCAGCGGCAACAGCAGCAACATCAGAAAAAACAGGCATAC AAGCAACATCAGCAGCACAGTCGACTGCGGCGGCAACAACAGCAGAAAGA GAAGCAATTGCAACAGCAACATCAAGCGACACCACAGCAACACCAACACTC GCAGCAGCAGCAGCAATACAATCAGCTGGCAACATCCCTGCCCAGTTAACC ACAAAAACGTTGCGGCCCACAGAAACAACTTCGTTAGCGCAACTGCAGCGT CGGCAACAAATGCCTGGCATGCCGGCCAAAACAACAGAAACGCCAGCAAA GAACCTGCCAAGTTTGGCCCAGACAAAGGCAACAACAGCGCTTCCCATTTT GGCAACACGAGATGCTGCCACAGCAACAACGGAAATAAATTCCGACAAGC CAACGAACATTAGCGGTGCCACAAAAACAGTAGCAACATCAGCTGCAGAA ATAGCAACACCACCAGCAATTGAAGTGCCACAAACCATTTTGGCCGGCAAA AAATCTGACAAAATGCCAGCCGATAAGGCACACGAGACTTTATTAAAATAC CCAACAAGGGACACATCCGGTCAAGTTGCAACAACGCCACACAAACATGCA ACACTGCAGCTGCACGTTAAGGATCGACATCTAATTGGCACACCGCTGCTG ATGCACAAGGGCGATGTCCTATTGGTGGATGCCGAGCAGTTGTTGCTGCCTG GTACGGCCACCGTGGCGGATGCGGATTCGGAAGTTCTGGACCCGAGCCAAC AACATCAGTCAGCGGAGCAGGAAAAGCACCAGTCAGCGACTGATAAGCGG CAAGCGGATGCAATAAACGGCGACACGAAGTCGCCGGCGAAAGGCCACAA AAAGAAACCATCGCTGAGCATCAAGAAGATGACCTACAGTACCAAACACGC GGCAAAAACCGTGGAGGATATGGCAGCCACCTCGAAGACACCGCAACACC AACATAGCAGTGTGAACACACCCAAAGAGGCTGCTCCCGAGGAGTTGAGCA CCTTTGC
UAS-16.2-2miti	
UAS-61.1-2miti	

Table 3.4 Sequence of *2mit* cDNA portion used as reference to generate *2mit* RNAi construct.

Other mutant lines:

- ***tim*^{01}**: homozygous line, characterized by a 64 bp deletion in exon 7 (4937-5000 position) of the *timeless* gene (Myers et al., 1995) that leads to an arhythmic circadian phenotype.

3.2 Vitality test from embryonic to adult stage

Vitality test experiments were performed in 12:12 LD conditions at 23°C. Flies were left from 6 to 24 h in a cylinder plastic container (provided with holes to keep the air flow) having on the bottom a petri dish (50 mm diameter x 12 mm) filled with standard medium. Then, flies were removed and the number of fertilized egg (embryos) in the plate was counted. In general from 50 to 200 embryos were counted. The number of embryos reaching the third instar larval stage was counted. Larvae were transferred in a clean vial with food. The number

of larvae reaching the pupal stage was determined. Finally the number of pupae eclosing to adult stage was defined (distinguishing by gender). The relative percentages of survived individuals for each developmental stage were calculated with respect to the previous stage and to embryonic stage. At least three replicates per genotype were performed.

3.3 Longevity Tests

For each genotype, ~130 females and ~130 males were tested. 1 day old flies were collected and maintained in clean vials (~6 flies per vial). The amount of dead individuals was recorded every two days. The flies were transferred to fresh medium every 2-5 days, without CO_2-anesthesia. The experiments were perfomed in 12:12 LD conditions at 23 °C. At least two replicates per genotype were achieved.

3.4 Larval photophobicity test

Larval light-avoidance behaviour was tested as described in Mazzoni et al. (2005), with minor modifications. A 10 cm Petri dish and its lid were half-covered with black electric tape. The Petri was filled with 15 ml of 1.5% Bactoagar.
Third instar larvae were removed from vial internal walls and were washed with PBS (for 1 l: 200 g NaCl; 5 g KCl; 5 g KH_2PO_4; 27.8 g $Na_2HPO_4 \cdot 2H_2O$, pH 7.4). 20-25 larvae were distributed along the junction between light and dark. At least 10 replicates per genotype were analysed. Illumination of the plates was provided from above by using a light lamp. After 10 min at room temperature (RT), the number of larvae in each half plate was counted. Wild-type larvae, given their photophobic behaviour, tend to distribute in the dark side of the petri dish. Larvae with affected visual system and/or circadian synchronization distribute in a random manner (Mazzoni et al., 2005). Larvae climbing on the plates walls were excluded. Petri dishes with larvae penetrating into agar were discarded. Given circadian variation in light sensitivity the experiments were conducted at the same time interval of day around ZT6 (15:00 pm).

3.5 Analysis of general locomotor activity behaviour

3.5.1 Larval stage

For each genotype, locomotor activity of third instar larvae, entrained to 12:12 LD conditions at 23°C, was recorded for 2 min period using a video tracking system. Individual larvae were selected among those emerging from the food and were placed in the middle of a Petri dish (15 cm in diameter) filled with a thin layer of agar gel 1%. The Petri dish, representing a circular “arena”, was placed inside a box characterized by black internal walls and by uniform white light illumination.

Locomotor activity was videotaped by using a Canon digital video camera. Video recordings were transferred to a computer and were converted in locomotor activity data by the AnyMaze software (Stoelting, USA). The software reproduced the path travelled by the moving animal during the recording and determined different general locomotor parameters:

- the **total distance moved (mm)**: representing the length of the path travelled expressed as the sum of the distance between each point in the track.
- the **total number of immobile episodes**: determined by counting the number of transitions from a mobile state to an immobile state during the test. Every inactivity period exceeding 2 s was considered as an immobility episode.
- the **total immobility time (s)**: defined as the sum of the duration of each immobile episode in the test.

A total number of 50 larvae were analysed for each genotype. All strains were tested at the same time interval of the day at RT.

3.5.2 Adult stage

For each genotype both males and females were analysed, ~10 individuals per sex. Either 3-5 or 20 days old flies, entrained in 12:12 LD conditions at 23°C, were subjected to CO_2-anesthesia and single individuals were transferred inside transparent vials (1.5 cm in diameter and 4.5 cm in length) without food but containing a piece of paper soaked in water inserted beside the vial plug. In this way the following day, during the recording period, the fly was stimulated to move for searching food. Flies were tested after at least 10 h in order to have a complete recovery from CO_2-anesthesia. Locomotor activity of each adult individual was singly recorded for 10 min by the video-tracking apparatus, similarly to the protocol described for locomotor activity recording at larval stage.
5 min before the test, the wet paper was removed from each vial. Each vial was placed inside a box characterized by black internal walls and by uniform white light illumination. Locomotor activity was videotaped by using a Canon digital video camera. Video recordings were transferred to a computer and converted in general locomotor activity data by the AnyMaze software (Stoelting, USA). The software reproduced the path travelled by the moving animal during the recording and the following parameters were considered:

- the **total distance moved (mm)**.
- the **average speed (mm/s)**: calculated by dividing the total distance travelled with the total movement duration.
- the **total number of immobile episodes**.
- the **total immobility time (s)**.

The characteristics of the total distance moved, the total number of immobile episodes and the total immobility time are the same as described for the larval stage. Given the circadian fluctuations of *Drosophila* locomotor activity

phenotype, all strains were tested at the same time interval of the day, from ZT1.5 (10:00 am) to ZT7 (16:00 pm). The recordings were performed at RT.

3.6 Optomotor test

The optomotor response, evaluated in adult flies, represents a reaction to the motion of the surrounding environment. The optomotor response was assayed as described in Sandrelli et al. (2001). The test was performed at RT on 3-7 days old males entrained for at least 3 days in a 12:12 LD regime at 23°C. Each fly was singly placed inside a T-shaped glass tube, precisely in the dark side of the tube represented by the longer arm painted black (while the other two shorter arms of the tube were transparent). The tube was held stationary in the center of rotating drum whose internal walls were painted with black and white stripes alternatively. The drum was open on the top and was illuminated from above thought a white light source. The drum rotated clockwise or counter-clockwise and flies, being attracted by light, exited from the darkened arm of the T-tube and moved inside one of the two transparent arms. Wild-type individuals, which can detect the rotating stripes, in most of the cases tend to follow the direction of the rotation by entering the correspondent arm. Individuals with defects in the visual system move in random manner, independently from the direction of the drum rotation. Approximately 20 individuals were tested for each genotype. Every single individual was tested for ten trials with one of more pauses during the test. Given circadian variation of *Drosophila* locomotor activity, all tests were performed at the same time interval of the day, from ZT1 (10:00 am) to ZT4 (13:00 pm), when flies were more reactive to light stimuli (Sandrelli et al., 2001; Borst et al., 2010).

3.7 Analyses and determination of *timeless1* polymorphisms (*ls-tim1* vs *s-tim1*)

Two different allelic variants had been recognized in *Drosophila timeless1* (*tim1*) gene: *ls-tim1* and *s-tim1* (Rosato et al., 1997). These alleles differ on the G insertion/deletion in 294 site (GenBank U37018) of *tim1* gene.

3.7.1 Single-fly genomic DNA extraction and PCR amplification

Each fly, following CO_2-anesthesia, was singly placed into an Eppendorf tube (0.5 ml): 50 µl Buffer A (10 mM Tris-HCl pH 8.2, 2 mM EDTA, 25 mM NaCl) was added to each sample. Each individual was homogenized by using pipette tip and 1 µl Proteinase K (10 mg/ml; Roche) was added. The mixture was incubated for 45 min at 37°C and then for 3 min at 100°C to inactivate Proteinase K. Samples were centrifuged for 1 min at maximum speed at RT to pull down the fly homogenized tissues and were stored at -20°C.

PCR reactions were performed by following the ARMS (Amplification Refractory Mutation System) strategy applied for the amplification of a portion of the *timeless1* gene containing the 294 site, characterized by the nucleotide polymorphism (Myers et al., 1995; Ousley et al., 1998; Rosato et al., 1997).
For each sample two different PCR reactions were performed, each amplifying only one of the two alternative *ls-tim1*/*s-tim1* polymorphisms, through the use of two alternative *tim1* allele-specific forward primes (GA or AT). The primers used are listed in Table 3.5.
Each amplification reaction contained two couples of primers:
- alternatively, GA or TA forward primes coupled with the TIM-3' reverse primer.
- TIM-C5' forward and TIM-C3' reverse primers, amplifying another *tim1* region considered as a control sequence to test PCR efficiency.

position	**PCR primers**		
3262-3281	**GA**	**forward**	5'-TGGAATAATCAGAACTTTGA-3'
3262-3280	**AT**	**forward**	5'-TGGAATAATCAGAACTTTAT-3'
3935-3954	**TIM-3'**	**reverse**	5'-AGATTCCACAAGATCGTGTT-3'
6015-6034	**TIM-C5' (control)**	**forward**	5'-CATTCATTCCAAGCAGTATC-3'
6482-6501	**TIM-C3' (control)**	**reverse**	5'-TATTCATGAACTTGTGAATC-3'

Table 3.5 List of primers used for ARMS. The primer positions are referred to the *tim1* genomic sequence reported in Flybase (http://flybase.org/).

PCRs were performed in a 20 µl reaction mixture containing:
- 2.5 µl 10 mM dNTPs (Promega)
- 1 µl *tim* allele-specific forward primer (GA or TA)
- 1 µl TIM-3' reverse primer
- 1 µl TIM-C5' forward control primer
- 1 µl TIM-C3' reverse control primer
- 2 µl 10X Taq buffer (provided with $MgCl_2$, Euroclone;)
- 2 µl genomic DNA (of a single individual)
- 0.4 µl Taq polymerase (5U/ µl; Euroclone)
- 9.1 µl ddH_20

Amplification program:
first denaturation step: 95° for 2 min
denaturation: 95°C for 1 min
annealing: 52°C for 1 min } X 30 cycles
extension: 72°C for 45 sec
final elongation step: 72°C for 10 min.

Amplification products were visualized after electrophoretic separation in 2% w/w agarose gel.

3.8 Analysis of circadian photoreception: the phase response curve

The phase of a clock refers to the temporal relationship between a reference point in the activity profile, as for example the morning peak of activity, and an external reference point, as for instance the lights-on time (either actual or subjective) (Rosato and Kyriacou, 2006). Short light pulses can provoke phase shifts of the circadian clock causing its resetting. These phase shifts are measured by the phase response curve (PRC), which illustrates the effect of a light pulse delivered during the dark period of the LD regime. For each genotype, 3-5 days old males were entrained in 12:12 LD conditions for three days and then transferred in DD condition, at 23°C. During the first night in DD, individuals were subjected to a 20 min light pulse delivered at different moments of the night (ZT13; ZT15; ZT17; ZT19; ZT21 or ZT23). For each individual, the phase shift response was determined subtracting the mean phase of non-pulsed individuals. A PRC was generated by plotting the phase shift as a function of the time at which the light pulse was administrated. Generally, in wild-type strains, a light pulse delivered early at night generates a delay in the activity. On the contrary, a light pulse late at night causes an advance in the activity. The middle of the night and the day are defined as “dead” zones, with no effects due to a light pulse. Flies mutants in the circadian photoreception phenotypes are characterized by a different PRC plot with respect to a wild-type control, reflecting an impaired response to a light pulse of the endogenous clock.

3.9 Circadian locomotor activity analysis

3.9.1 Locomotor activity recording

The analyses of *Drosophila* circadian locomotor rhythms were performed as described in Zordan et al. (2007) with minor modifications. Circadian locomotor activity of either 3-5 or 20-30 days old males was recorded through *Drosophila* Activity Monitoring System© (DAMSystem©) provided by Trikinetics Inc, (Waltham, MA, USA). Each male was singly entered in a small glass tube (0.4 cm

in diameter and 6.5 cm in length) filled with standard medium from one of its extremities. The tubes were inserted inside *Drosophila* activity monitors, named DAM2, provided by DAMSystem© and harboring the place for 32 tubes each. DAM2 monitors were connected to a computer equipped with the TriKinetics software (DAMsystem 2.1.0). The TriKinetics software allowed to program the experimental conditions and stored locomotor activity recorded data. Flies were previously entrained for at least 3 days 12:12 LD cycles and then kept for 7 days in DD conditions. Experiments were performed at 23°C. Within DAM2 monitors, an infra-red beam was passing through the middle part of each tube and every time a male interrupted it by moving along the tube, the system recorded a locomotor activity event. Locomotor activity events were first clustered in 5 min intervals. Then, during the following data processing, they were summed in 30 min time windows, called bins, they were analysed through the Phyton software and were plotted in locomotor activity profiles defined as Actograms. In Actograms, levels of activity (Y-axis) were given as a function of time (X-axis), with 1 bin in the locomotor activity plot corresponding to a 30 min recording.

3.9.2 Data analysis

The calculation of periodicity (tau) in *free running* conditions (DD; when the endogenous circadian clock is not influenced by external light stimuli) was possible through two different and complementary statistical tests (Fig.3.15):
- autocorrelation: a function resolving the periodicity in the data by comparing a time series with a time-shifted version of itself.
- CLEAN algorithm (Zordan et al., 2007): a spectral analysis employing an iterative procedure based upon deconvolution of the Fourier transform (from Dr. J. Lehar, MIT, Cambridge, Mass., USA). This method decomposes data in a reduced number of sinusoidal functions and allows the identification of harmonic components in data belonging to rhythmic behaviours. The highest peak over the significativity range obtained from CLEAN analysis was considered as the fly periodicity.

Both autocorrelation and CLEAN spectral analysis were executed by the Python software (http://www.python.org/). Ranges of significativity of 95% and 99% (red lines in Fig.3.15) were provided by both statistical tests to estimate significantly rhythmic data.
For each individual, locomotor activity was considered as being rhythmic if both statistical tests revealed the presence of significant periodicity peaks. On the contrary, flies with no peaks of significance were considered as being arhythmic.

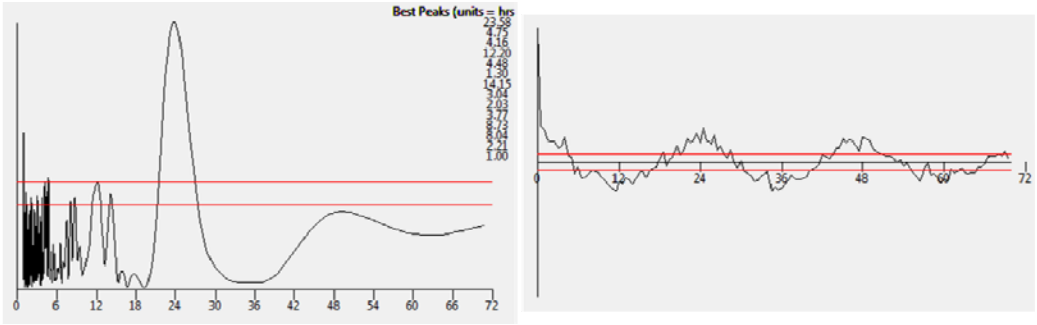

Fig.3.15 Example of a single fly graphs obtained from CLEAN spectral analyses (left) and autocorrelation analyses (right).

3.10 Immunocytochemistry

Immunocytochemical experiments (ICC) were performed on adult *Drosophila* brains in order to quantify, at different time points, the nuclear accumulation kinetics of the PER protein in two subgroups of circadian clock neurons, the small and large ventrolateral neurons (s- and l- LNvs). In parallel the localization of Pigment dispersing factor (PDF) was used to mark the two clock cell clusters under analysis.

3.10.1 Solutions and antibodies

- 10X PBS (pH 7.4): 130 mM NaCl, 7 mM Na_2HPO_4, 3 mM NaH_2PO_4

- 0.3% PBS-T: 1X PBS, 0.3% Triton X-100

- 1% PBS-T: 1X PBS, 1% Triton X-100

- PFA solution: 4% Paraformaldehyde (PFA from 20% stock), 1X PBS

- PFA 20% (stock): 10 g PFA, 50 ml ddH_2O, 300 ml 5M NaOH

- BSA (Bovine serum albumin): 1% or 0.1% of BSA solution (from 10% stock)

Primary antibody	Protein detected	Origin	Working concentration	Provenience
α-PER	PERIOD	Rabbit	1:2500	R. Stanewsky (London)
α-PDF	PIGMET DISPERSING FACTOR	Mouse	1:5000	Hybridoma Bank

Table 3.6 Primary antibodies employed.

Secondary antibody	IgG detected	Origin	Working concentration	Provenience
Alexa 488 (green)	Rabbit	Goat	1:250	Invitrogen
Alexa 568 (red)	Mouse			

Table 3.7 Secondary antibodies employed.

3.10.2 Sample preparation

For each genotype, 3-5 days old individuals were first entrained in 12:12 LD conditions at 23°C and then were collected at precise time points (ZTs: 18; 20; 22; 24; 2; 4). At least 10 flies (both males and females) were collected and dissected per time point. Two replicates were performed for each genotype tested. Flies were harvested in ethanol 100%, which was immediately removed to avoid excessive tissues dehydration. Flies were incubated in 4% PFA for 2 h at RT on a rotating wheel (or alternatively overnight at 4°C) and washed for three times of 5 min each in 1X PBS. Brains were dissected in 1X PBS.
Afterwards, brains were treated as follows:
- fixation in 4% PFA for 1 h at RT;
- six washes of 5 min each in 0.3% PBS-T at RT;
- permeabilization in 1% PBS-T for 10 min at RT;
- blockage in 1% BSA, 0.3% PBS-T for 2 h at RT (or alternatively overnight at 4°C);
- incubation in primary antibody solution: both primary antibodies were diluted, as indicated in Table 3.6, in 0.1% BSA, 0.3% PBS-T for 3-5 days at 4°C (or alternatively overnight at RT);
- six washes of 10 min each in 0.3% PBS-T at RT;
- blockage in 1% BSA, 0.3% PBS-T for 1 h at RT;
- incubation in secondary antibody solution: both secondary antibodies were diluted, as indicated in Table 3.7, in 0.1% BSA, 0.3% PBS-T, overnight at 4°C (or alternatively 3 h at RT);
- six washes of 5 min each in 1X PBS at RT;
- brains were mounted between slides and coverslides with Vectashield (Vector Laboratories, Inc.);
- storage at -20°C until observation.

3.10.3 Visualization and quantification of staining intensity

Slides were examined using the semiconfocal microscope Nikon Eclipse 80i equipped with a QiCAM Fast Camera, using the Image ProPlus software (Department of Biology, University of Padova, Italy).

For each brain, the two brain hemispheres were separately acquired and images were obtained from different sections forming a Z-series. The size of each section, was approximately 1.2/1.4 μm. PER fluorescence staining intensities were quantified from digital images with the ImageJ software (freely available at http://rsbweb.nih.gov/ij/) and calculation were made employing Microsoft Excel.
To quantify the staining intensity, a 9 pixel square selection area was applied to each nucleus of the two subgroups of circadian neurons, s- (the 4 PDF+) and l-LNvs, in which the nuclear accumulation kinetics of PER protein had to be quantified. Being careful not to select cytoplasmic regions, selection areas of the same dimensions were used to randomly quantify the aspecific staining of the background regions adjacent to the neurons of interest. In this way, for each nucleus a background value was associated. Then, for each clusters of neurons, the collected values of background intensities were mediated and this average value was used to normalize the single values of nuclear staining intensity, through the formula: I=(S-Bavg)/Bavg, where S represents the fluorescence intensity of a specific clock nucleus and Bavg represents the average background intensity of areas adjacent to a cluster of positive cells.

3.11 Courtship conditioning memory test

Courtship conditioning assay was performed as described in Mehren and Griffith (2004) with minor modifications. Memory test experiment was performed at RT. Virgin males were harvested as soon as they eclosed and were kept alone for 4 days. Two subgroups of males were analysed per genotype: the conditioned males and the sham controls. Regarding the conditioned males, single 4 days old individuals were tracked with a wild-type *Oregon-R* mated female for 1 h in Plexiglas mating chambers (8 mm diameter, 3 mm high). Subsequently, conditioned males were transferred to a new mating chamber with a wild-type virgin female for a 10 min test period. The virgin female was collected the same day and had been previously CO_2-anesthetized for 1 h. Sham controls were placed alone in a mating chamber during the training period and then they were treated as the conditioned males during the test period.
The first and last 10 min of the 1 h training period, and the 10 min test period were videotaped. For each tested male, a courtship index (CI), which is the amount of time the male spent courting during an observation period of 10 min, was measured. For each genotype, memory was calculated by statistically comparing the mean CI during test period of conditioned males with the mean CI during test period of sham controls. If the two values were not statistically different, no memory was formed, whereas a significantly reduction of mean CI in conditioned males with respect to that of sham controls indicated memory formation. Males who copulated during training period or had courted less than 1 min were excluded from the analysis. If males copulated during the test period or

an anesthetized virgin awakened from anesthesia, the observation period had to be considered concluded.

3.12 Statistical analyses

Data were statistically analysed by ANOVA Test and when appropriated with the post-hoc Newman-Keuls Test, by using the software Statistica 5.0 package (Statsoft Inc.).

CHAPTER 4:

Characterization of transgenic flies overexpressing 2MIT in *PB2mit*^{c03963} mutant genetic background

4. Introduction

We have shown that the *PB2mit*^{c03963} strain, characterized by *2mit* mRNA decremented levels, presented behavioural defects related to the optomotor response and memory formation, a decreased longevity at adult stage and a slightly altered phenotype regarding the lengthening of circadian periodicity in DD conditions. In this chapter we describe rescue experiments performed in order to confirm whether these *PB2mit*^{c03963} phenotypical impairments are effectively a consequence of *2mit* mRNA depletion. These experiments were based on generation and analysis of transgenic lines overexpressing a 2MIT-HA chimeric protein (with HA representing the haemagglutinin tag), in *PB2mit*^{c03963} background. After a molecular characterization performed to demonstrate *2mitHA* cDNA expression, these lines have been tested for those phenotypes which resulted affected in *PB2mit*^{c03963} mutant strain.

4. Results

4.1 Generation of transgenic lines for *2mit* overexpression

In the laboratory we I did my PhD, *2mit* cDNA had been previously cloned in a pBluescript vector. As described in details in the Materials and Methods section of this chapter, from this construct we added a HA tag (haemagglutinin tag) in frame in 3' *2mit* full-lenght cDNA. Subsequently, the *2mitHA* cDNA was transferred in pUAST, which is the typical vector used in *Drosophila* transgenesis. Three independent *2mitHA* transgenic lines have been obtained. These lines were marked as: *M4-2mitHA*, *M14-2mitHA* and *F8-2mitHA*. *M4-2mitHA* and *M14-2mitHA* carried the *2mitHA* construct on the second chromosome, whereas *F8-2mitHA* carried this construct on the third chromosome. These lines were used for molecular and behavioural characterization of 2MIT overexpression in both wild-type and *PB2mit*^{c03963} genetic background.

4.2 2MIT-HA protein expression in wild-type background

Initially, for the three selected *2mitHA* lines, we performed Western blot experiments in order to evaluate whether the 2MIT-HA protein was effectively expressed in individuals *ActGal4*/*2mitHA,* generally overexpressing the *2mitHA* construct. The presence of the HA tag in 2MIT-HA chimeric protein was evaluated using different α-HA commercial antibodies. In fact, different *2mit* anti-serums had been previously produced, either in rabbit or in rat, but no one resulted to specifically recognize 2MIT protein, in both Western blot and immunocytochemical experiments. Furthermore, being 2MIT a transmembrane

protein, the protocol applied to extract 2MIT-HA was the result of various modifications on protein extraction step, based on the use of specific detergents.
Fig.4.1a-d illustrates Western blot assays characterized by different combinations of protein extraction conditions and α-HA antibodies used (produced in mouse or in rabbit). Protein extracts were obtained from whole adult bodies samples, collected from individuals in which 2MIT-HA overexpression was ubiquitously driven, through the *ActGal4* driver, in the wild-type genetic background. These samples were compared to a negative control (*ActGal4/CyO*).
In Fig.4.1a,b Western blot results are reported for samples in which protein extraction was performed using the β-dodecyl maltopyranoside detergent and the employed antibody was α-HA produced in mouse. A band in correspondence to ~150 kDa was present in 2MIT-HA-expressing samples but not in the negative control.
In Fig.4.1c it is reported a Western blot experiment performed on samples treated with β-dodecyl maltopyranoside detergent, as done for the previously described conditions, and with sodium deoxycholate detergent, in order to try to increase the efficiency of transmembrane proteins extraction. As for previous conditions, the antibody used for membrane hybridization was α-HA produced in mouse. Also in this case, a ~150 kDa band was present only in *ActGal4/2mitHA* samples and not in the negative control. However, from a comparison with Fig.4.1a,b, it seemed that the further treatment with sodium deoxycholate detergent, combined with the use of α-HA produced in mouse, did not lead to any improvement in the ~150 kDa band resolution.
Fig.4.1d reports Western blot results in which protein extraction was executed using both β-dodecyl maltopyranoside and sodium deoxycholate detergents as done for experiments in Fig.4.1c, in combination to membrane hybridization with α-HA produced in rabbit. This combination seems to lead to an improvement with an increased intensity and resolution of the identified ~150 kDa band.
Despite the putative expected 2MIT-HA molecular weight is 125.84 kDa, in Western blot experiments performed with both α-HA produced in mouse and α-HA produced in rabbit the only band, in proximity to the putative molecular weight and present specifically in *ActGal4/2mitHA* samples and not in the negative control, was in correspondence to ~150 kDa. Anyway, in the troubleshooting guide of the pre-cast gel used to perform SDS-PAGE (NuPAGE® Invitrogen), it is reported that there could be a disparity between the real molecular weight of a protein and its apparent molecular weight established on the basis of relative mobility on the gel. This disparity could depend for example on the buffer system or to retention of varying degrees of secondary structure in the protein despite SDS and denaturation step, phenomenon that is also observed in highly hydrophobic membrane proteins. Moreover it has been reported that detergents, used during the transmenbrane protein extraction procedure, modify the SDS-PAGE migration of membrane proteins (Rath et al., 2009). On the basis of these information we identified the 150 kDa band as representing 2MIT-HA

protein. Thus, the selected lines seemed to express 2MIT-HA protein at different level. In particular, the *ActGal4/F8-2mitHA* appeared to express higher level of 2MIT-HA protein, because in each experimental condition tested, *ActGal4/F8-2mitHA* samples showed the 150 kDa 2MIT-HA band. Respect to *ActGal4/F8-2mitHA, ActGal4/M4-2mitHA* and *ActGal4/M14-2mitHA* individuals resulted to express lower 2MIT-HA levels.

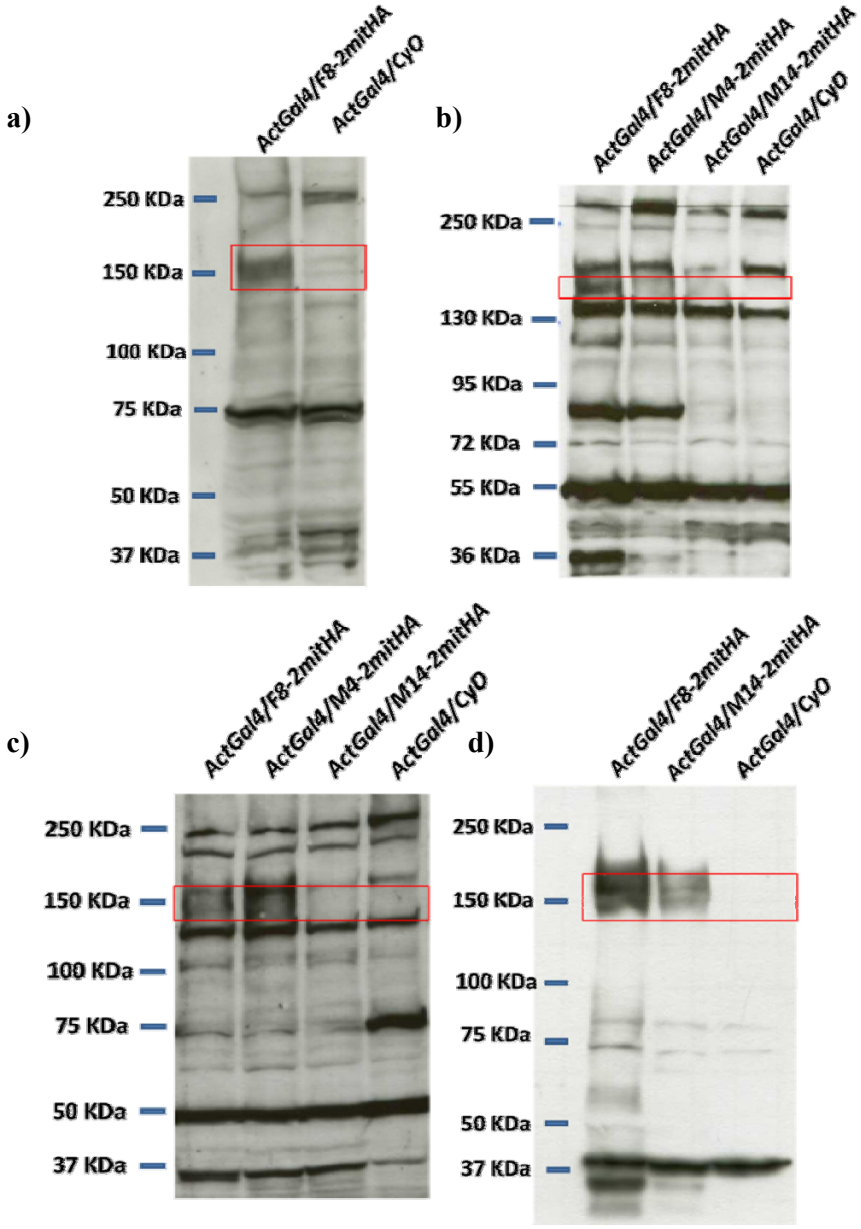

Fig.4.1 Western blot experiments, performed on entire adult bodies extracts, to test different lines carrying the *2mitHA* construct for *2mit* overexpression. **a)** treatment with β-dodecyl maltopyranoside; 1:1000 α-HA in mouse. **b)** treatment with β-dodecyl maltopyranoside; 1:1000 α-HA in mouse. **c)** treatment with β-dodecyl maltopyranoside and with sodium deoxycholate; 1:1000 α-HA in mouse. **d)** treatment with β-dodecyl maltopyranoside and with sodium deoxycholate; 1:1000 α-HA in rabbit. Bands at ~150 kDa, thought to represent 2MIT-HA protein, are evidenced by a red square.

4.3 Generation of lines carrying the *2mitHA* construct in *PB2mit^{c03963}* genetic background

In order to execute rescue experiments, we generated lines in which *2mitHA* overexpression was driven in *PB2mit^{c03963}* mutant genetic background. Since the *PB2mit^{c03963}* mutation is given by a transposon insertion on third chromosome, in proximity of *2mit* coding region, by genetic crossings we produced lines presenting a *2mitHA* (for *M4-* and *M14-2mitHA* lines) transgene or *Gal4* driver constructs (for *ActGal4* and *elavGal4* lines) on the second chromosome and the third chromosome carrying the *c03963* transposon insertional mutation.
Regarding the *F8-2mitHA* line, the localization of *2mitHA* construct was on the third chromosome, the same of transposon insertion in *PB2mit^{c03963}* strain. Therefore, individuals carrying both *F8-2mitHA* construct and *c03963* trasposon insertion were produced by genetic recombination. The presence of both constructs on the same homologue was checked via PCR. In fact, it was not possible to select recombinant individuals only on the basis of their phenotypical characteristics. Specifically, the *F8-2mitHA* construct, carrying the "*mini-white*" gene, conferred red eyes, whereas the *c03963* insertion gave orange eyes. Thus, after occurrence of recombination events between *2mitHA* and *c03963* constructs, in the following generations, individuals carrying only *c03963* transposon were easily recognized because of their orange eyes and could be excluded as non-recombinant. On the contrary, individuals carrying only the *F8-2mitHA* construct, having red eyes, were not distinguishable from the ones containing both insertions. 40 red-eyed individuals were used as founders of 40 independent lines. PCR experiments were executed on single individuals belonging to each founded line, using primers which gave rise to a 663 bp amplification product only when recombination events have not occurred.
Fig.4.2 reports the results for the first nine lines. Those displaying a 663 bp amplification product were the non-recombinant ones. On the contrary, those lines not displaying this 663 bp amplificate were selected as recombinant. In fact the presence of the 7.257 kb *PiggyBac* transposon prevented the amplification of the sequence flanking its insertion site. We chose the line n.6 (w;; *F8-2mitHA-c03963*) to proceed with rescue experiments.

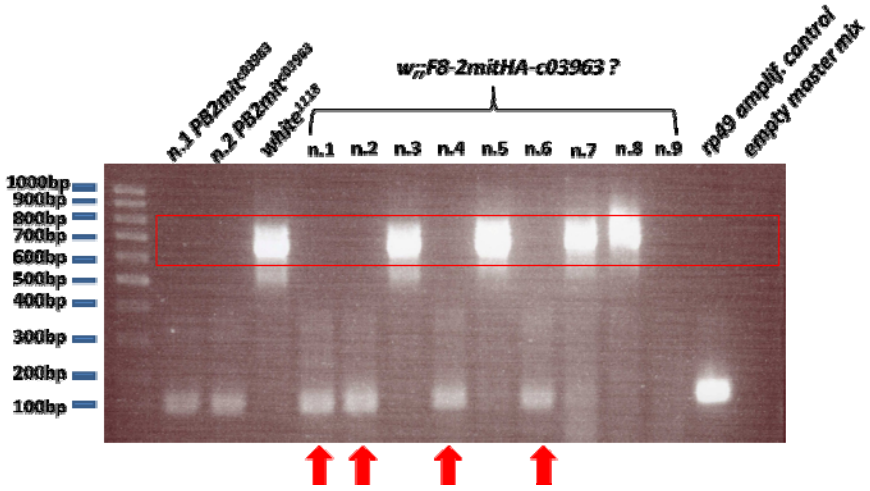

Fig.4.2 PCR experiments to identify the *F8-2mitHA-c03963* recombinant lines. *PB2mit*^{c03963} (n.1 and n.2), *white*^{1118}, *rp29* products and empty master mix are reaction controls. Recombinant lines (n.1; 2; 4; 6) do not show the 663 bp amplification product.

4.4 *2mitHA* mRNA overexpression in *PB2mit*^{c03963} background

Real-time PCR experiments were performed to check whether lines activating the *2mitHA* construct in the *PB2mit*^{c03963} background were effectively overexpressing *2mit* mRNA. The *2mitHA; PB2mit*^{c03963} lines were crossed with *ActGal4; PB2mit*^{c03963} stock and real-time PCR assays were performed on adult whole body samples, in which the *2mitHA* transgene expression was generally activated using *ActGal4* driver in the *PB2mit*^{c03963} mutant genetic background. The results indicated that in the *ActGal4/M14-2mitHA; PB2mit*^{c03963} line *2mit* mRNA is expressed ~50-fold with respect to the *white*^{1118} control strain, while in *ActGal4/M4-2mitHA; PB2mit*^{c03963} and *ActGal4; F8-2mitHA-PB2mit*^{c03963} lines *2mit* mRNA levels are ~150 and ~200-fold higher than those of the *white*^{1118} control, respectively (Fig.4.3).

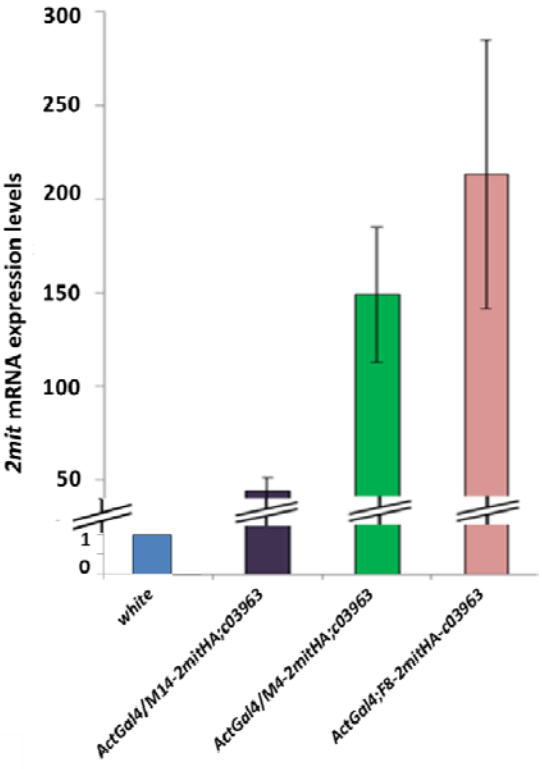

Fig.4.3 Real-time PCR values of *2mit* mRNA expression levels in *ActGal4/M14-2mitHA; PB2mit*^{c03963}, *ActGal4/M4-2mitHA; PB2mit*^{c03963} and *ActGal4; F8-2mitHA-PB2mit*^{c03963} with respect to the *white*^{1118} wild-type control whose *2mit* mRNA levels were considered equal to 1.

The real-time PCR results, demonstrating that *ActGal4/M14-, M4-* and *F8-2mitHA* lines effectively overexpressed *2mit* mRNA levels, indicate that all these three lines could be used for rescue experiments of *PB2mit*^{c03963} mutant phenotypes.

4.5 Rescue of the *PB2mit*^{c03963} optomotor response

PB2mit^{c03963} individuals exhibited an affected optomotor response suggesting that *2mit* is involved in the optic-motor coordination phenotype. In order to confirm these indications, we tested whether the overexpression of *2mit* mRNA specifically driven in the whole nervous system (through *elavGal4* driver), in *PB2mit*^{c03963} background, restored or improved the optomotor response.
Therefore *elavGal4/M14-2mitHA; PB2mit*^{c03963}, *elavGal4/M4-2mitHA; PB2mit*^{c03963} and *elavGal4; F8-2mitHA-PB2mit*^{c03963} individuals were evaluated via optomotor test and results were compared to those obtained for their appropriate negative controls (*M14-2mitHA/+; PB2mit*^{c03963}, *M4-2mitHA/+; PB2mit*^{c03963} and *F8-2mitHA-PB2mit*^{c03963} respectively and *elavGal4/+; PB2mit*^{c03963} lines). Negative controls presented only either the *2mitHA* or the *elavGal4* construct in the *2mit* mRNA depleted *PB2mit*^{c03963} genetic background. Therefore, in all these *PB2mit*^{c03963} controls no *2mit* overexpression is expected. The optomotor analyses of negative controls showed that their responses were all comprises between the 50% and 58%, meaning that they still had defects in the visual system in association to the neuronal processing of motion vision, confirming the likelihood of the optomotor impairments seen in the *PB2mit*^{c03963} strain. Regarding lines where *2mitHA* was activated in the nervous system, we noticed that in only one of them, the *elavGal4/M14-2mitHA; PB2mit*^{c03963}, positive optomotor responses were the ~70%, significantly higher with respect to those of both negative controls (Fig.4.4a). The *elavGal4/M4-2mitHA; PB2mit*^{c03963} and *elavGal4; F8-2mitHA-PB2mit*^{c03963} individuals showed the 56% and 60% of correct optomotor response values respectively, not significantly different with respect to those of negative controls (Fig.4.4b,c).

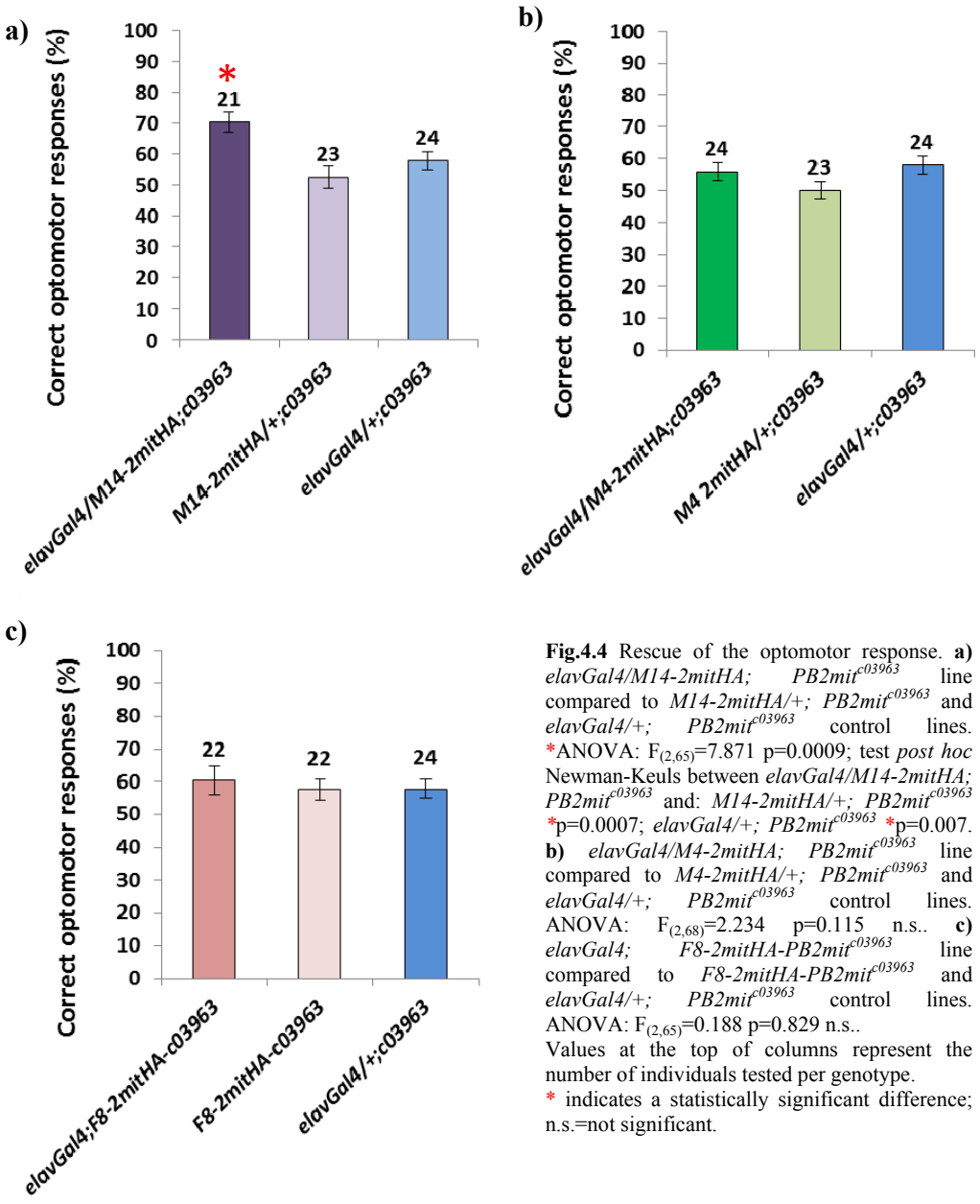

Fig.4.4 Rescue of the optomotor response. **a)** *elavGal4/M14-2mitHA; PB2mit^{c03963}* line compared to *M14-2mitHA/+; PB2mit^{c03963}* and *elavGal4/+; PB2mit^{c03963}* control lines. *ANOVA: $F_{(2,65)}$=7.871 p=0.0009; test *post hoc* Newman-Keuls between *elavGal4/M14-2mitHA; PB2mit^{c03963}* and: *M14-2mitHA/+; PB2mit^{c03963}* *p=0.0007; *elavGal4/+; PB2mit^{c03963}* *p=0.007. **b)** *elavGal4/M4-2mitHA; PB2mit^{c03963}* line compared to *M4-2mitHA/+; PB2mit^{c03963}* and *elavGal4/+; PB2mit^{c03963}* control lines. ANOVA: $F_{(2,68)}$=2.234 p=0.115 n.s.. **c)** *elavGal4; F8-2mitHA-PB2mit^{c03963}* line compared to *F8-2mitHA-PB2mit^{c03963}* and *elavGal4/+; PB2mit^{c03963}* control lines. ANOVA: $F_{(2,65)}$=0.188 p=0.829 n.s.. Values at the top of columns represent the number of individuals tested per genotype. * indicates a statistically significant difference; n.s.=not significant.

4.6 Failed rescue of the *PB2mit^{c03963}* phenotype related to circadian rhythmicity

PB2mit^{c03963} individuals displayed a mild but significant lengthening of circadian periodicity in DD conditions. This phenotype was emphasized by ageing. In order to verify whether *2mit* was really implicated in the control of circadian periodicity, we performed rescue experiments based on *2mit* mRNA overexpression specifically driven in the whole nervous system (through *elavGal4* driver), in the *PB2mit^{c03963}* mutant background. We expected that, if *2mit* depletion was responsable to the lengthening of circadian tau in *PB2mit^{c03963}*

mutant individuals, 2MIT-HA overexpression in *PB2mit*^{c03963} mutant genotype will recover the circadian tau to wild-type values. Since we obtained stronger results in 30 days old *PB2mit*^{c03963} flies with respect to younger ones, we performed rescue experiments on 30 days old individuals. Circadian locomotor activity was examined for *elavGal4/M14-2mitHA; PB2mit*^{c03963}, *elavGal4/M4-2mitHA; PB2mit*^{c03963} and *elavGal4; F8-2mitHA-PB2mit*^{c03963} lines, compared to their appropriate negative controls (*M14-2mitHA/+; PB2mit*^{c03963}, *M4-2mitHA/+; PB2mit*^{c03963} and *F8-2mitHA-PB2mit*^{c03963} respectively and *elavGal4/+; PB2mit*^{c03963} lines).

Results are illustrated in Table 4.1. Individuals belonging to all *elavGal4/2mitHA; PB2mit*^{c03963} overexpressing lines displayed tau values around 24 h, not showing the characteristic lengthening in periodicity seen in *PB2mit*^{c03963} strain. However, negative controls, carrying either *elavGal4* or *2mitHA* construct singly in the *PB2mit*^{c03963} mutant background, displayed a ~24 h circadian periodicity. These data indicate that in negative controls the phenotype observed originally in *PB2mit*^{c03963} strain was not maintained.

Genotype	Age (days)	%R (R/N)	Tau in DD (mean±s.e.m.)	flies with tau>25h (%)
elavGal4/M14-2mitHA;c03963	30	67.86 (19/28)	23.847±0.089	0
elavGal4/M4-2mitHA;c03963	30	85.19 (23/27)	24.153±0.133	4.35
elavGal4;F8-2mitHA-c03963	30	61.54 (24/39)	24.657±0.130	20.51
M14-2mitHA/+;c03963	30	93.10 (27/29)	23.874±0.117	3.70
M4-2mitHA/+;c03963	30	81.01 (64/79)	24.121±0.083	12.50
F8-2mitiHA-c03963	30	82.56 (71/86)	24.221±0.075	15.49
elavGal4/+;c03963	30	76.71 (56/73)	23.876±0.077	5.36

Table 4.1 Analyses of circadian locomotor activity of 30 days old flies overexpressing *2mit* in *PB2mit*^{c03963} genetic background, compared to respective controls. For each genotype are reported: the percentage of rhythmicity R(%) calculated from number of rhythmic individuals (R) divided to the number of totally analysed individuals (N); the periodicity (tau) in DD; the percentage of rhythmic flies having a tau over 25 h. Statistic support is made considering *M14-2mitHA*, *M4-2mitHA* and *F8-2mitHA* lines separately.
ANOVA: *$F_{(6,276)}$=6.191 p<0.0001; test *post hoc* Newman-Keuls between *elavGal4/M14-2mitHA; PB2mit*^{c03963} and: *M14-2mitHA/+; PB2mit*^{c03963} p=0.865 n.s.; *elavGal4/+; PB2mit*^{c03963} p=0.982 n.s.; test *post hoc* Newman-Keuls between *elavGal4/M4-2mitHA; PB2mit*^{c03963} and: *M4-2mitHA/+; PB2mit*^{c03963} p=0.840 n.s.; *elavGal4/+; PB2mit*^{c03963} p=0.175 n.s.; test *post hoc* Newman-Keuls between *elavGal4; F8-2mitHA-PB2mit*^{c03963} and: *F8-2mitHA-PB2mit*^{c03963}/+ *p=0.005; *elavGal4/+;PB2mit*^{c03963} *p<0.0001.
* indicates a statistically significant difference; n.s.=not significant.

4.7 Rescue of the *PB2mit*^{c03963} memory phenotype

PB2mit^{c03963} mutant flies showed defects at level of short-term associative memory, suggesting a role for *2mit* in memory formation.

In order to confirm *2mit* putative role in this phenotype, we analysed associative memory in individuals overexpressing *2mit* in *PB2mit*^{c03963} mutant background. Currently, we have performed the rescue of courtship conditioning test only on *elavGal4/M14-2mitHA; PB2mit*^{c03963} line compared to its appropriate *M14-2mitHA/+; PB2mit*^{c03963} and *elavGal4/+; PB2mit*^{c03963} negative controls.
Results, reported in Fig.4.5, indicate that *elavGal4/M14-2mitHA; PB2mit*^{c03963} individuals showed a rescue of memory phenotype while both negative controls did not. In fact *elavGal4/M14-2mitHA; PB2mit*^{c03963} conditioned males displayed a statistically significant lowering of courtship index in comparison to that of sham males (Fig.4.5), indicating an occurrence of memory recovery.
On the contrary, negative controls did not display any statistically significant difference in courtship index between conditioned and sham control males, indicating that they still present the memory defects detected in *PB2mit*^{c03963} individuals (Fig.4.5).
Although these results regard only one *2mitHA* overexpressing line, they suggest that the memory impaired phenotype observed in the *PB2mit*^{c03963} strain is specifically a consequence of *2mit* mRNA decremented expression levels.

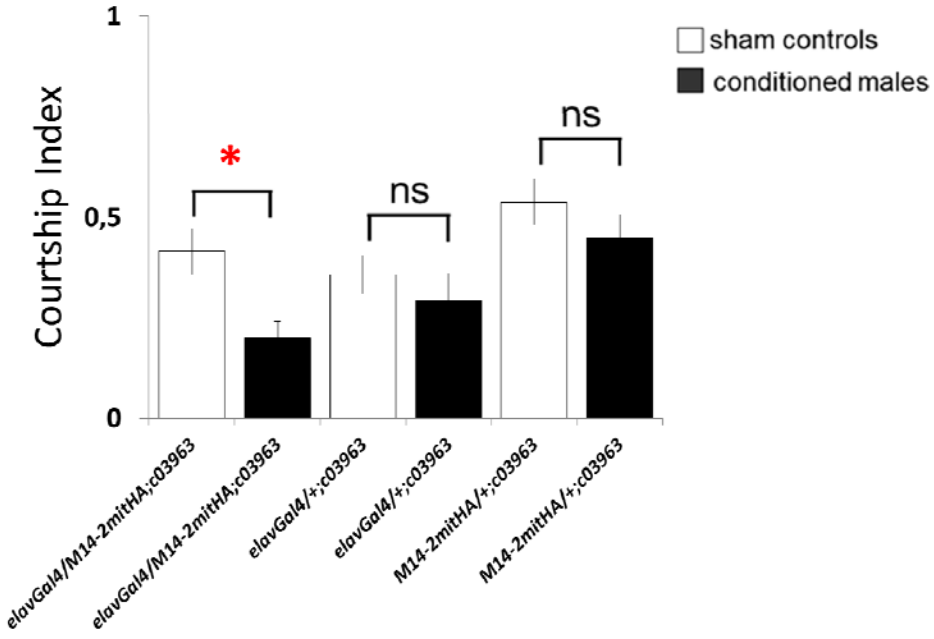

Fig.4.5 Rescue of short-term associative memory in courtship conditioning assay of *elavGal4/M14-2mitHA; PB2mit*^{c03963} line compared to *M14-2mitHA/+; PB2mit*^{c03963} and *elavGal4/+; PB2mit*^{c03963} negative controls. ANOVA: comparison between conditioned males vs sham controls for each genotype: *elavGal4/M14-2mitHA; PB2mit*^{c03963}: ANOVA: *$F_{(1,30)}$=8.868 p<0.01; *M14-2mitHA/+; PB2mit*^{c03963}: ANOVA: $F_{(1,44)}$=1.13 p=0.29 n.s.; *elavGal4/+; PB2mit*^{c03963}: ANOVA: $F_{(1,44)}$=1.540 p=0.466 n.s..
*indicates a statistically significant difference. n.s.=not significant.

4. Discussion

This chapter reports rescue experiments performed in order to verify the reliability of the mutant phenotypes observed in the *PB2mit*^{c03963} strain.

To perform this kind of experiments, three lines carrying the *2mitHA* construct for *2mit* overexpression were generated. These lines were checked for *2mit* overexpression. Their *2mitHA* expression, ubiquitously driven, was shown both at protein level by Western blot experiments (in a wild-type genetic background), and at mRNA level by real-time PCR experiments (in the *PB2mit*^{c03963} mutant genetic background).

However, since 2MIT has been predicted to be a transmembrane protein, 2MIT-HA signals revealed by Western Blot might underestimate the real 2MIT-HA overexpression levels, probably because of difficulties found in the identification of the optimal extraction conditions for a transmembrane protein.

The three independent *2mitHA* transgenic lines, with pan-neuronal overexpression of the *2mitHA* transgenic construct in the *PB2mit*^{c03963} mutant genetic background, were tested to analyse whether phenotypes impaired in *PB2mit*^{c03963} strains (optomotor response, circadian periodicity and memory) recovered to wild-type characteristics.

We have demonstrated that in one out of three lines, the pan-neuronal *2mit* mRNA overexpression in *PB2mit*^{c03963} mutant genetic background (*elavGal4/M14-2mitHA; PB2mit*^{c03963}) lead to a recovery of the optomotor response. This achievement argues in favor of a role for *2mit* in the visual system, specifically in neural mechanisms involved in optic-motor coordination. No significant rescue in the optomotor response was demonstrated in the other two 2MIT overexpressing lines (*elavGal4/M4-2mitHA; PB2mit*^{c03963} and *elavGal4; F8-2mitHA-PB2mit*^{c03963}). These flies carried transgenes *M4-* and F8- *2mitHA* which, when ubiquitously activated (using *ActGal4* driver), caused strong increments in *2mit* mRNA expression (150/200-folds compared to wild-type). This excessive *2mit* mRNA expression might be present also using *elavGal4* driver and cause deleterious effects on the normal neuronal cell functions which disturb the optomotor phenotype recovery. This hypothesis will be tested analysing the optomotor response of individuals overexpressing *2mitHA* construct in *2mit*$^{+}$ wild-type background. In fact, if this hypothesis is correct, we might expect a normal optomotor response in *elavGal4/M14-2mitHA; 2mit*$^{+}$ individuals, which showed the "milder" *2mitHA* overexpression, and an impaired optomotor phenotype in *elavGal4/M4-2mitHA; 2mit*$^{+}$ and *elavGal4; F8-2mitHA-2mit*$^{+}$ flies, characterized by the strongest *2mitHA* overexpression.

Investigating the possible phenotypes affected in *PB2mit*^{c03963} mutant strain, we found that *PB2mit*^{c03963} individuals were characterized by a longer circadian periodicity in constant conditions compared to that of *white*^{1118} controls (Chapter 3). In addition, in *PB2mit*^{c03963} flies the tau increment strongly increased with age, involving the 80% of old *PB2mit*^{c03963} flies compared to the 20% of *white*^{1118}

controls at the same age (Chapter 3). However, when this phenotype was tested in the three *elavGal4/2mitHA; PB2mit*^{c03963} lines and the specific negative controls, carrying *elavGal4* driver alone or non activated *2mitHA* constructs in *PB2mit*^{c03963} background, tau values around 23-24 h were displayed by all analysed genotypes and no tau increment related with age was noticed. Specifically, the negative controls showed a circadian rhythmicity similar to the wild-type instead to the expected *PB2mit*^{c03963} one. On the consequence, these data do not support the hypothesis in which *2mit* is directly involved in the control of circadian rhythmicity. We can hypothesize that, in *2mit* depleted lines (*PB2mit*^{c03963} and *elavGal4/2miti* lines) the modification of circadian periodicity (Chapter 3) was due to a mild and unstable phenotype, detectable depending on the genetic background in which the *c03963* insertion is located. So, *2mit* might exert just an ancillary and marginal role on the control of circadian rhythmicity and/or may need other elements in the genome exercising a synergistic role complementing its own one.

Regarding the rescue of the memory phenotype, so far we have tested only the *elavGal4/M14-2mitHA; PB2mit*^{c03963} line. We have shown that individuals belonging to this line displayed a recovery of short-term associative memory in the courtship conditioning assay. Interestingly, this line is the same displaying the recovery of the optomotor response, strengthening the reliability of results obtained for both phenotypes. This result supports the hypothesis in which *2mit* plays a role in the neural circuits implicated in memory formation. Further experiments will be performed evaluating memory phenotype in *elavGal4/M4-2mitHA; PB2mit*^{c03963} and *elavGal4; F8-2mitHA-PB2mit*^{c03963} lines.

As *PB2mit*^{c03963} exhibited an affected longevity profile, we are planning to perform rescue experiments to verify also this phenotype.

To conclude, these rescue experiments confirm a role for *2mit* in motion vision and in memory but not in circadian rhythmicity.

4. Materials and Methods

4.1 Generation of pUAST vector carrying *2mitHA* construct

In the laboratory, we already disposed of pBluescript® II S/K (+/-) vector (Invitrogen) containing the *2mit* cDNA complete sequence with *NotI* and *XhoI* extremities. Starting with this available plasmid we performed cloning and restriction reactions in order to add in frame HA (haemagglutinin) tag nucleotide sequence in 3' *2mit* cDNA. A 261 bp sequence of *2mit* cDNA comprising its 3' was amplified by using a primer internal to *2mit* cDNA sequence upstream the *NarI* restriction site (5'-GATGACAGCTACTATATAGA-3') and a primer pairing with 3' *2mit* cDNA, composed by the HA nucleotide sequence followed by a *XhoI* restriction site tail (*XhoI*-HA-R 5'-

AGGCCTCGAGAGCGTAATCTGGAACATCGTATGGGTACATGGTCCAGAT GTTCAGCCTCCGCGAA-3'). The amplification reaction was purified after gel electrophoresis by using Wizard® SV Gel and PCR Clean-Up System kit (Promega). *2mit* portion+HA was cut with *NarI* and *XhoI* restriction enzymes. The *2mitHA* sequence carrying *NarI-XhoI* extremities was gel purified.
The pBluescript II S/K-*2mit* full-length cDNA plasmid was linearized with *NarI* and *XhoI* enzymes. Then the 261 bp 3' *2mitHA* sequence carrying *NarI-XhoI* extremities was sub-cloned into the linearized pBluescript II S/K-*2mit* cDNA plasmid at level of *NarI* and *XhoI* restriction sites through ligation (3 h at room temperature, RT).
Ligation reagents to final 15 µl volume:
- 2 µl 3' *2mitHA* insert (50 ng/µl)
- 2 µl pBluescript II S/K-*2mit* cDNA plasmid (20 ng/µl)
- 3 µl 5X ligation buffer (Invitrogen)
- 1 µl T4 DNA ligasi (1U/µl) (Invitrogen)
- 8 µl ddH_2O

2.5 µl ligation reaction were used to transform 40 µl One Shot® TOP10 Chemically Competent *E. coli* bacteria (Invitrogen) using standard procedures. 15 µl ligation reaction was added to the TOP10 cells maintained on ice for 30 min. The cells were heat-shocked at 42 °C for 45 sec and then placed on ice for 2 min. Then, 500 µl of SOC medium were added and the cells were incubated for 1 h at 37 °C. Cells were plated in 100 mm petri dishes provided with Luria-Bertani (LB) medium (1% Bactotryptone, 0.5% yeast extract, 1% NaCl, 2% Agar) supplemented with ampicillin (50 µg/ml) and were incubated overnight at 37 °C.
Positive clones were selected and the plasmids were purified by using the PureYield™ Plasmid Miniprep System (Promega). To verify whether ligation reaction correctly assembled the two *2mit* cDNA portions, the whole insert was sequenced (BMR Genomics S.r.l., Padova, Italy). The plasmid was purified through Maxi-preps protocol (described in the following paragraph).
The *2mitHA* cDNA in pBluescript II S/K was then sub-cloned in pUAST *Drosophila* vector (Invitrogen), using *NotI* and *XhoI* restriction sites. The *2mitHA* insert was extracted from pBluescript II S/K plasmid by employing *NotI* and *XhoI* restriction enzymes and purified after gel electrophoresis using Wizard® SV Gel and PCR Clean-Up System kit (Promega). pUAST vector was digested with *NotI* and *XhoI* and then its extremities were dephosphorylated to avoid self-circularization. The linearized vector was gel-purified using the Wizard® SV Gel and PCR Clean-Up System kit (Promega). *2mitHA* sequence carrying *NotI-XhoI* extremities was ligated into the linearized pUAST plasmid (overnight at 4°C)
Ligation reagents to final 15 µl volume:
- 10 µl *2mitHA* insert (10 ng/µl)
- 2 µl pUAST vector (20 ng/µl; Invitrogen)
- 3 µl 5X ligation buffer (Invitrogen)

- 1 µl T4 DNA ligasi (1U/µl; Invitrogen)
- 8 µl ddH_2O

40 µl One Shot® TOP10 Chemically Competent *E. coli* bacteria (Invitrogen) were then transformed using the procedures previously described.
Plasmid carrying the *2mitHA* was purified from one of the positives clones by performing mini-preps through PureYield™ Plasmid Miniprep System (Promega). The *2mitHA* sequence in pUAST vector was checked by sequencing (BRM Genomics S.r.l, Padova, Italy).
The UAS-*2mitHA* construct plasmid was used for generation of *Drosophila* transgenic lines using the *Drosophila* Embryo Injection Service (Transflier, University of Ferrara, Italy). Three transgenic lines were obtained. The line names were: *M4-2mitHA*, *M14-2mitHA* and *F8-2mitHA*.
In Fig.4.6 there is a schematic representation of pBluescript II S/K and pUAST vectors.

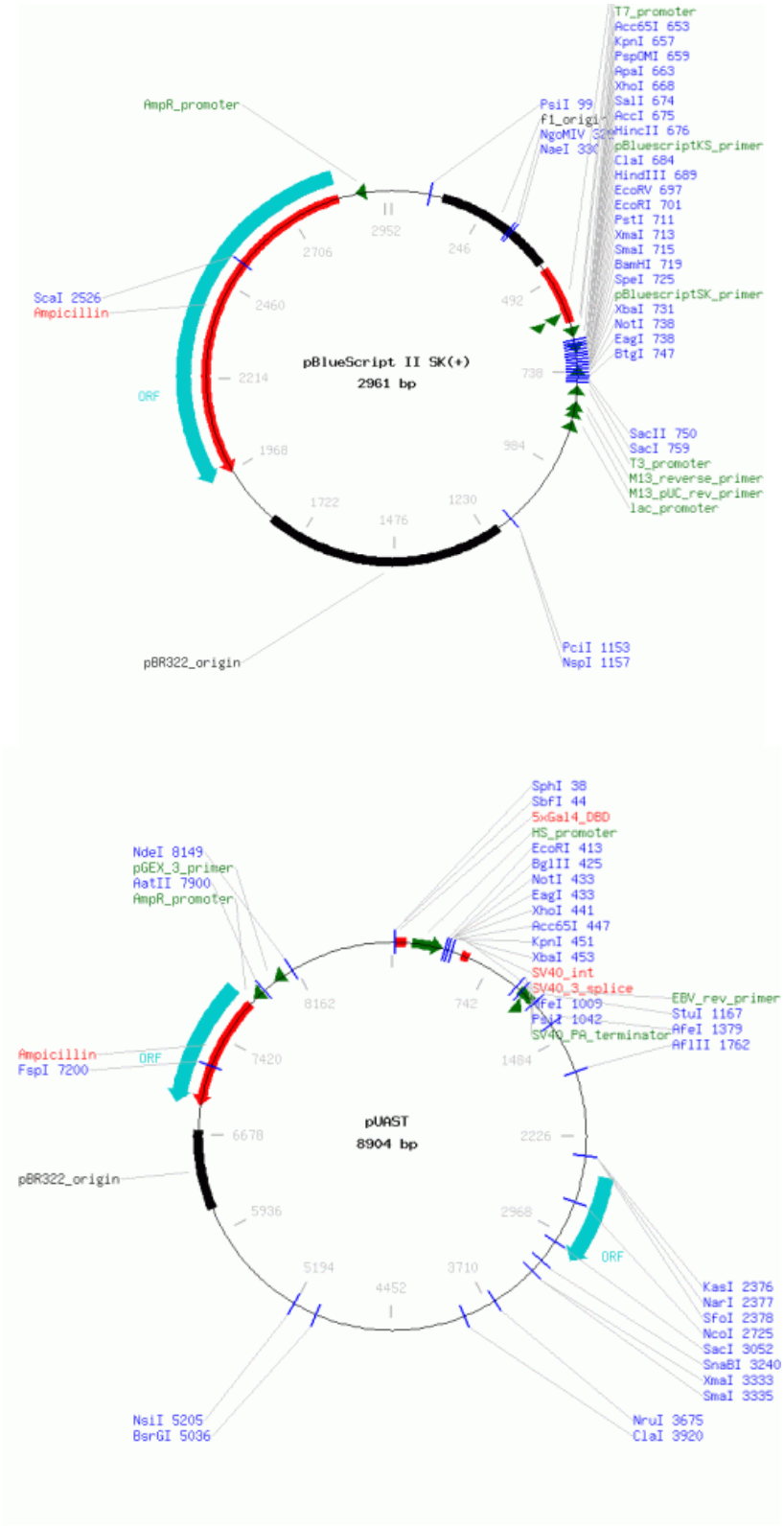

Fig.4.6 Schematic representation of the pBluescript II S/K and the pUAST vectors used to generate UAS-*2mitHA* construct (from http://www.lablife.org/).

4.2 Maxi-Preps

This method allows the obtaining of large-scale extraction of DNA plasmid from bacterial cultures and it is based on the protocol described by Feliciello and Chinali (1993). 100-200 ml cell culture was centrifuged at 5000 rpm for 15 min at 4°C. The cell pellet was resuspended in 20 ml STE solution (0.1 M NaCl, 10 mM Tris-HCl, 1 mM EDTA pH 8) and then centrifuged at 5000 rpm for 15 min at 4°C. After discarding supernatant, the cell pellet was resuspended in 4 ml solution n.1 (50 mM glucose, 10 mM Tris-HCl, 1 mM EDTA pH 8). The cell lysis was obtained by adding 8 ml solution n.2 (0.2 M NaOH, 1% SDS). Then 12 ml solution n.3 (4 M CH_3CO_2K, 2 M CH_3COOH) were added to neutralize the reaction. The mixture was centrifuged at 13000 rpm for 30 min at 4°C and the supernatant was filtered and precipitated with isopropyl alcohol. The mixture was centrifuged at 13000 rpm for 30 min at 4°C. 250 µl TE (10 mM Tris-HCl pH 8, 1 mM EDTA pH 8) + RNAsi solution were added to the air-dried DNA pellet. Following 20-30 min incubation at RT, 600 µl of 88% isopropyl alcohol and 0.2 M CH_3CO_2K solution were added. The mixture was centrifuged at 14000 rpm for 15 min at RT and the supernatant was discarded. 80% ethanol was added to the DNA pellet and, following centrifugation at 14000 rpm for 5 min at RT, the DNA pellet was finally resuspended in 300 µl TE solution and freezed at -20°C.

4.3 Generation of lines carrying the *2mitHA* construct in the *PB2mit^{c03963}* genetic background

The generation of lines in which *2mitHA* overexpression was driven in the *2mit* mutant *PB2mit^{c03963}* genetic background required different crossings. First, it was necessary to obtain lines in which *2mitHA* (*M4*, *M14* and *F8* lines) and driver constructs (*ActGal4* and *elavGal4* lines) were transferred in the *PB2mit^{c03963}* mutant background.

In order to obtain these lines we used a conventional strategy based on the use of Balancing stocks, characterized by the presence of Balancer chromosomes. Balancer chromosomes have three important properties: they prevent genetic recombination between homologous chromosomes, they carry dominant markers (as *Cy* on Balancer *CyO* for second chromosome, *Tb* on Balancer *TM6B* for third chromosome) and are lethal when homozygously carried.

The schemes of the genetic crossings followed to obtain the lines necessary for rescue experiments are reported in Fig.4.7a-d.

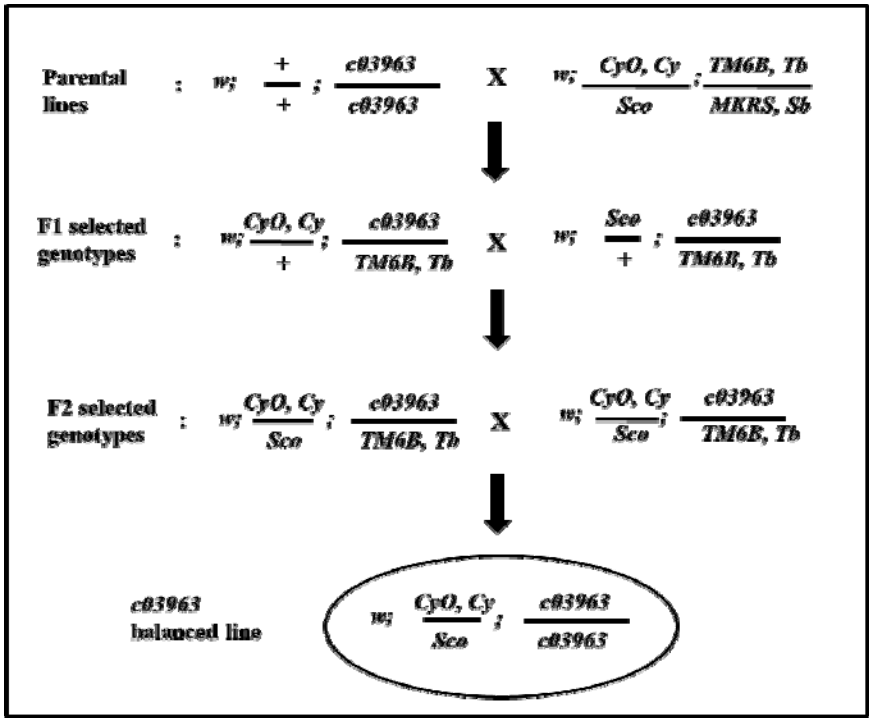
Parental lines : w; + / + ; c03963 / c03963 X w; CyO, Cy / Sco ; TM6B, Tb / MKRS, Sb
F1 selected genotypes : w; CyO, Cy / + ; c03963 / TM6B, Tb X w; Sco / + ; c03963 / TM6B, Tb
F2 selected genotypes : w; CyO, Cy / Sco ; c03963 / TM6B, Tb X w; CyO, Cy / Sco ; c03963 / TM6B, Tb
c03963 balanced line
w; CyO, Cy / Sco ; c03963 / c03963

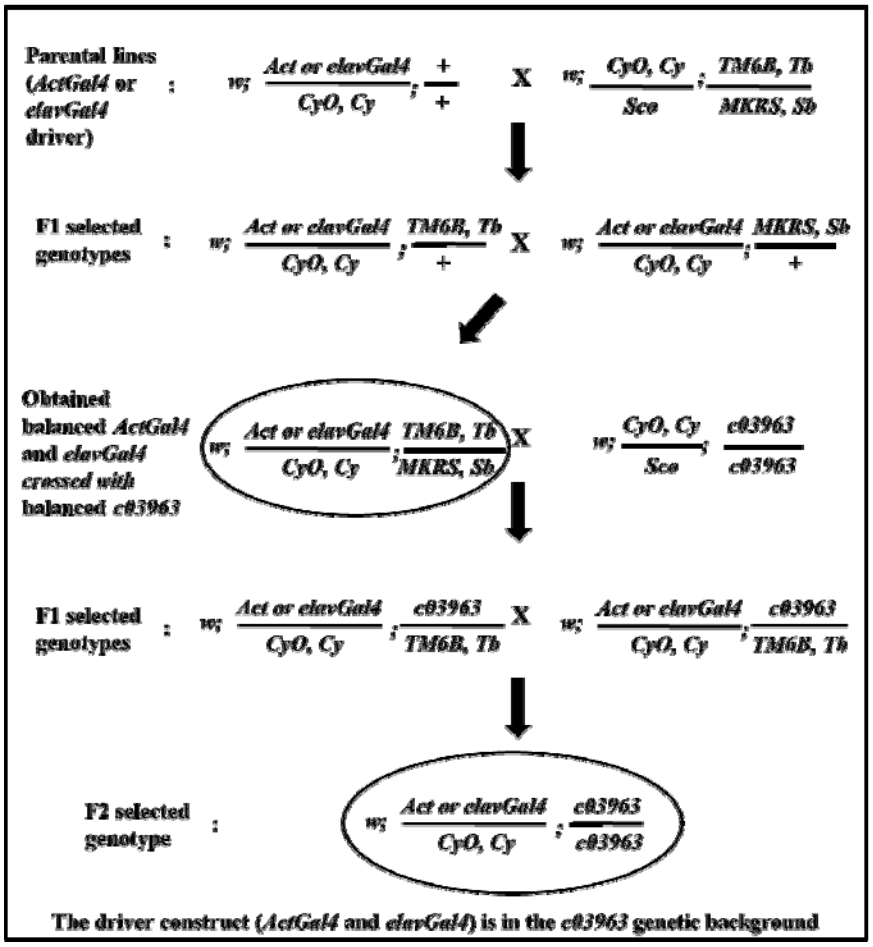
Parental lines (ActGal4 or elavGal4 driver) : w; Act or elavGal4 / CyO, Cy ; + / + X w; CyO, Cy / Sco ; TM6B, Tb / MKRS, Sb
F1 selected genotypes : w; Act or elavGal4 / CyO, Cy ; TM6B, Tb / + X w; Act or elavGal4 / CyO, Cy ; MKRS, Sb / +
Obtained balanced ActGal4 and elavGal4 crossed with balanced c03963
w; Act or elavGal4 / CyO, Cy ; TM6B, Tb / MKRS, Sb X w; CyO, Cy / Sco ; c03963 / c03963
F1 selected genotypes : w; Act or elavGal4 / CyO, Cy ; c03963 / TM6B, Tb X w; Act or elavGal4 / CyO, Cy ; c03963 / TM6B, Tb
F2 selected genotype :
w; Act or elavGal4 / CyO, Cy ; c03963 / c03963
The driver construct (ActGal4 and elavGal4) is in the c03963 genetic background

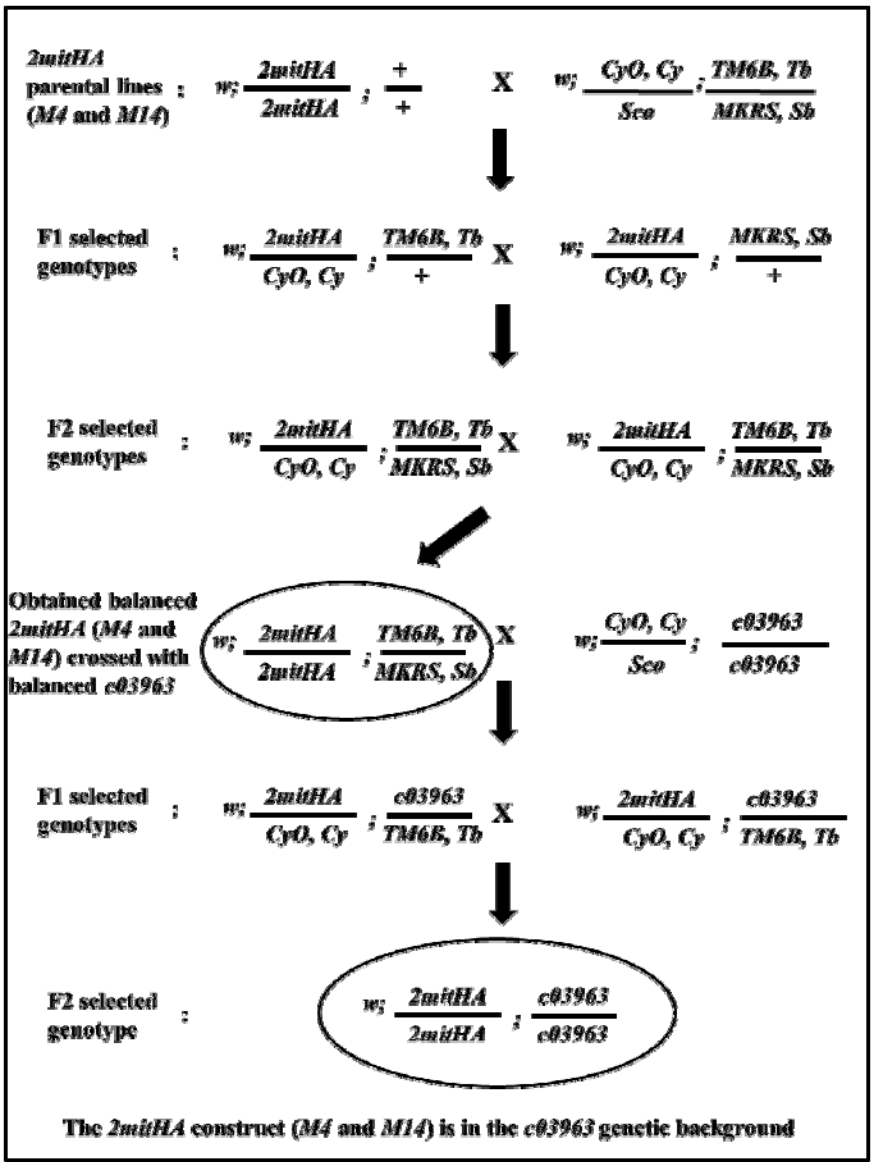
2mitHA parental lines (M4 and M14) : w; 2mitHA/2mitHA ; +/+ X w; CyO, Cy/Sco ; TM6B, Tb/MKRS, Sb
F1 selected genotypes : w; 2mitHA/CyO, Cy ; TM6B, Tb/+ X w; 2mitHA/CyO, Cy ; MKRS, Sb/+
F2 selected genotypes : w; 2mitHA/CyO, Cy ; TM6B, Tb/MKRS, Sb X w; 2mitHA/CyO, Cy ; TM6B, Tb/MKRS, Sb
Obtained balanced 2mitHA (M4 and M14) crossed with balanced c03963
w; 2mitHA/2mitHA ; TM6B, Tb/MKRS, Sb X w; CyO, Cy/Sco ; c03963/c03963
F1 selected genotypes : w; 2mitHA/CyO, Cy ; c03963/TM6B, Tb X w; 2mitHA/CyO, Cy ; c03963/TM6B, Tb
F2 selected genotype : w; 2mitHA/2mitHA ; c03963/c03963
The 2mitHA construct (M4 and M14) is in the c03963 genetic background

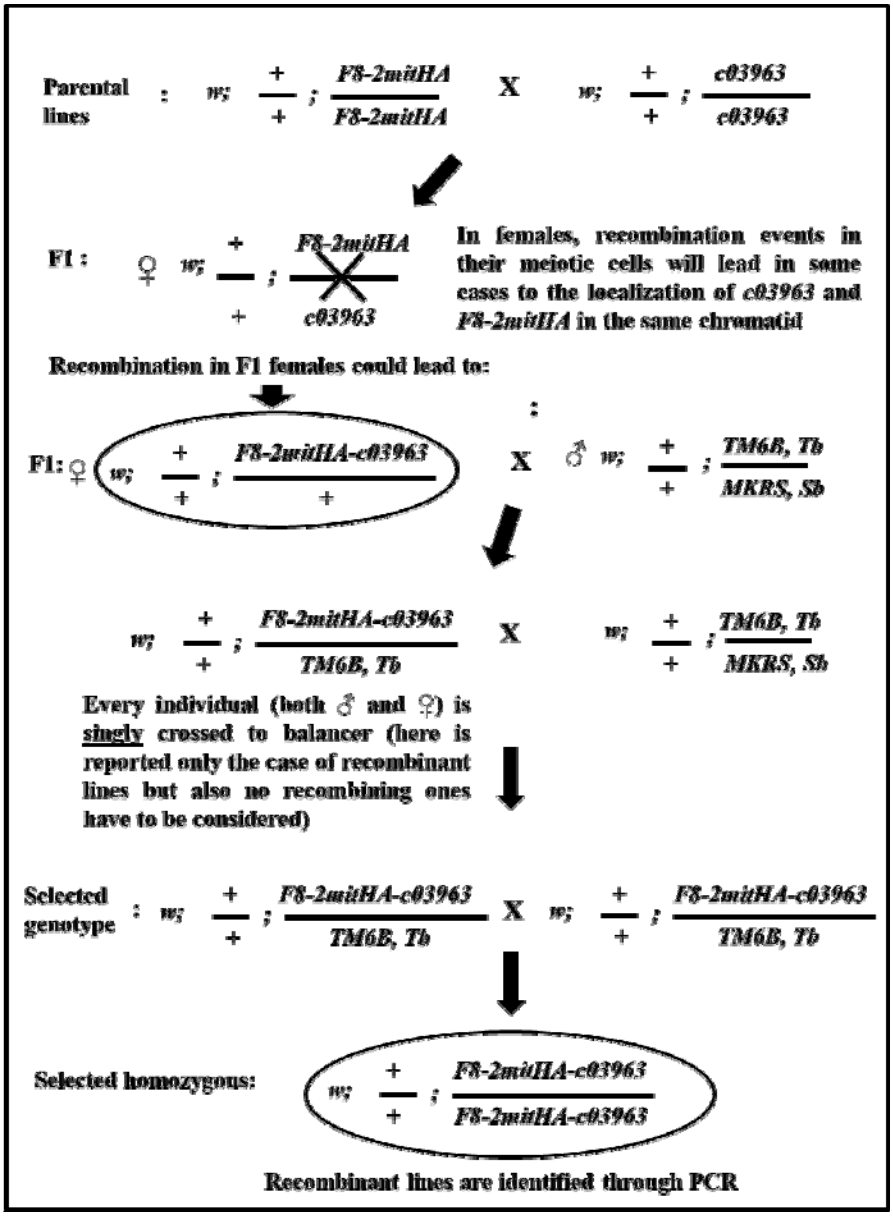

Fig.4.7 Schemes of crossings performed to obtain lines carrying *2mitHA* or driver (*ActGal4* or *elavGal4*) constructs in the *PB2mit*^{c03963} genetic background. **a)** balancing of *PB2mit*^{c03963} strain **b)** balancing and *c03963* insertion in drivers lines (*ActGal4* and *elavGal4*). **c)** balancing and *c03963* insertion in *M4-2mitHA* and *M14-2mitHA* lines. **d)** recombination among *F8-2mitHA* and *c03963* constructs, and following balancing.

Fly stocks used for crossings (from Bloomington *Drosophila* stock center)

- ***y, w; ActGal4/CyO*** (stock number #4414): genotype: y^1 w^*; P{Act5C-GAL4}25FO1/CyO, y^+; insertion chromosome: 2; comments: ubiquitous expression of GAL4 (from Bloomington *Drosophila* stock center).
- ***w*$^+$*; elavGal4/CyO*** (stock number #8765): described in Chapter 3.
- ***w; CyO, Cy/Sco; TM6B, Tb/MKRS, Sb***: double Balancer strain.
- ***PB2mit*^{c03963}** (outcrossed): described in Chapter 2.

4.4 PCR experiments to determine *c03963* transposon insertion

In the obtained lines (*ActGal4/CyO; PB2mit*^{c03963}, *elavGal4/CyO; PB2mit*^{c03963}, *M14-2mitHA; PB2mit*^{c03963}, *M4-2mitHA; PB2mit*^{c03963} and *F8-2mitHA-PB2mit*^{c03963}) the presence of *c03963* transposon insertion was checked by PCR.
Solutions, DNA extraction and agarose gel electrophoresis procedures were the same as described in the paragraph 3.7 of the Chapter 3.
Primers (Table 4.2) were designed, using the Primer 3 Software, in the flanking sequence of the *c03963* transposon insertion site, located in the 11th intron of *tim2* locus (3R: 8978167).
The 164 bp *rp49* fragment was obtained using specific primers (Table 4.2), in order to check the amplification reaction.

gene	position	PCR primers	
tim2	63597-63616	**forward**	5'-TTAACAAACATGCGGAGTGC-3'
	64240-64259	**reverse**	5'-CCGAAAAGCCATAAAGTCCA-3'
rp49	169-188	**forward**	5'-ATCGGTTACGGATCGAACAA-3'
	314-333	**reverse**	5'-GACAATCTCCTTGCGCTTCT-3'

Table 4.2 List of primers used to detect *c03963* transposon insertion.

PCRs were performed in a 20 µl reaction mixture containing:
- 0.6 µl of 10 mM dNTPs (Promega)
- 1 µl of 10 mM forward primer
- 1 µl of 10 mM reverse primer
- 4 µl green 5X Taq buffer (provided with $MgCl_2$, Promega)
- 2 µl genomic DNA (of a single individual)
- 0.4 µl Taq polymerase (5 U/µl; Promega)
- 11 µl ddH_20

PCR amplification conditions:
Initial Denaturation: 94°C for 2 min
Denaturation: 94°C for 30 sec
Annealing: 57°C for 30 sec
Elongation: 72°C for 1 min
} X 40 cycles
Final Elongation: 72°C for 10 min

4.5 Western blot experiments

ActGal4/2mitHA samples, generally expressing 2MIT full-length protein fused to a HA tag, were used for Western blot experiments. The presence of HA tag allowed us to use commercial α-HA antibodies in order to identify 2MIT protein by Western blot. Different α-HA commercial antibodies used in this group of experiments are listed in Table 4.3

4.5.1 Solutions and antibodies

- Extraction buffer: 20 mM Hepes pH 7.5, 50 mM KCl, 10 mM EDTA pH 8.15, 5% Glycerol, 0.1% Triton X-100

- 20X Running Buffer (pH 8.24): 50 mM Tricine, 50 mM Tris Base, 0.1% SDS

- 20X Transfer Buffer (pH 7.2): 25 mM Bicine, 25 mM Bis-Tris (free base), 1 mM EDTA pH 7.2

- NuPAGE® LDS Sample Buffer (pH 8.5): 106 mM Tris HCl, 141 mM Tris Base, 2% LDS, 10% Glycerol, 0.51 mM EDTA, 0.22 mM SERVA Blue G250, 0.175 mM Phenol Red

- 0.05% TBST: 100 mM Tris-HCl pH 7.5, 140 mM NaCl, 0.05% Tween®20

- Blocking Buffer: 0.05% TBST, 5% milk (Carnation NonFat Dry Milk)

- Detection Solution: 2.25 mM luminol, 0.2 mM p-coumaric acid, 0.1 M Tris-HCl pH 8.5, 0.01% H_2O_2

- Sodium deoxycholate solution: 5% Sodium deoxycholate, 20 mM Hepes pH 7.5, 50 mM KCl, 10 mM EDTA pH 8.15

Primary antibody	Origin	Working concentration	Provenience
α-HA	Mouse	1:1000	Sigma Aldrich
α-HA	Rabbit	1:1000	Sigma Aldrich

Table 4.3 Primary antibodies employed in Western blot experiments.

Secondary antibody	Origin	Working concentration	Provenience
α-mouse	Goat	1:1000 or 1:2500	Santa Cruz Biotecnology Inc.
α-rabbit	Goat	1:1000	Santa Cruz Biotecnology Inc.

Table 4.4 Secondary antibodies employed in Western blot experiments

4.5.2 Protein extraction

Protein extraction was performed on samples collected from 3-6 days old transgenic individuals entrained at 12:12 LD cycles for at least three days at 23 °C. For each *ActGal4/2mitHA* line, samples of at least 10 adult bodies each were collected. *ActGal4/CyO* driver line represented the negative control, not expressing 2MIT-HA chimeric protein.

Each sample was homogenized in 100 µl ice-cold extraction buffer added with the protease inhibitors and DTT reducing agent (per 1 ml extraction buffer: 2 µl apoprotinin, 5 µl pepstatinA, 2 µl leupeptin, 50 µl PMSF (phenylmethylsulfonyl fluoride) and 1 µl 1 M DTT). Following homogenization, other 40 µl ice-cold extraction buffer (+protease inhibitors and DTT) were added. After 2 min sonication, 10 µl of 15% β-dodecyl maltopyranoside detergent solution were added (in this way the final concentration of β-dodecyl maltopyranoside detergent was 1%) and the mixture was incubated for 1 h at 4°C on a rotating wheel.

A variation to the protocol consisted on addition of 30 µl of 5% sodium deoxycholate solution (1/5 of the sample volume) and on incubation on ice for 10 min (Cavallari et al., 2011). Sodium deoxycholate is an ionic detergent used for isolation of membrane proteins and for dissociation of protein interactions.

The samples were centrifuged at 2800 g for 10 min at 4°C and the supernatants were collected and placed in clean 1.5 ml tubes. The supernatants were then centrifuged at 2800 g for 5 min at 4°C and the supernatants were collected and placed in clean 0.5 ml tubes. The protein quantification, through Bradford method, was performed only to approximately determine the protein extract quantity for each sample but the values obtained were not used to estimate the loading volumes. For each sample, 10.71 µl (2.8X) LDS loading buffer solution (Invitrogen) and 2.14 µl (14X) DTT 1 M were added to 30 µl protein extract. Samples were denatured at 70°C for 10 min prior SDS polyacrylamide gel electrophoresis (SDS-PAGE).

4.5.3 Gel electrophoresis, transfer, blocking and detection

Protein extracts were separated according to their molecular weight by SDS-PAGE using a gel electrophoresis apparatus (Invitrogen). The electrophoretic chamber containing the running gel was filled with running buffer. 400 µl antioxidant solution (Invitrogen) was added in the running buffer before loading samples. 22 µl protein extract samples (with LDS and DTT) were loaded into wells of a 3-8% NuPAGE® Tris-Acetate pre-cast gel (Invitrogen). 8 µl of 10-250 kDa protein ladder (New England Biolabs) or of 11-250 kDa protein ladder (Invitrogen) were used as marker of molecular weight. Electrophoretic run was performed at 80 V for the first 30 min and then at 105 V. The gel was blotted on a nitrocellulose membrane for 1 h at 30 V in transfer buffer using a blotting apparatus (Invitrogen). Transfer of proteins was controlled by Ponceau staining (Sigma). For blockage step, the nitrocellulose membrane was incubated for 1 h in blocking buffer. The membrane was then incubated overnight at 4°C with α-HA primary antibody (produced in mouse or in rabbit) diluted as reported in Table 4.3 in 1% milk 0.05% TBST. The membrane was washed for three times of 10 min each in 0.05% TBST at RT and incubated for 2 h at RT with Horse Radish Peroxidase (HRP)-conjugated secondary antibody (α-mouse or α-rabbit) diluted as reported in Table 4.4 in 1% milk 0.05% TBST solution. Then, it was washed for three times of 10 min each in 0.05% TBST at RT. HRP activity was revealed with an ECL (enhanced chemioluminescence) system. The membrane was incubated for 1 min with the detection solution, then it was wrapped in a transparent plastic film and in darkness condition it was placed in contact with a BioMax film (Kodak), which was impressed by photons emitted from the reaction between peroxidase and luminol.

4.6 Real-time PCR experiments

Samples were collected from 3-6 days old individuals entrained at 12:12 LD cycles for at least three days at 23 °C. Each sample was composed by 10 entire frozen adult bodies. Four replicates per lines were analysed.
mRNA extraction and retrotranscription procedures are described in paragraph 2.3 of Chapter 2. 20 µl cDNA obtained from retrotranscritption were precipitated and resuspended in 10 µl of DEPC-treated ddH_20. mRNA quantification was performed by using the NanoDrop fluorospectrometer (Thermo scientific). The Agilent 2100 Bioanalyzer (Agilent Technologies) was employed to ascertain the integrity of the extracted mRNA. Real-time PCR experiments were performed by using a 96-plate apparatus available at the MicroCribi service (University of Padova, Italy). The amplification conditions were the same as described in paragraph 2.3 of Chapter 2. A first real-time PCR, perfomed on progressive dilutions of a cDNA mixture composed by all samples, was necessary to calculate the primers efficiency (absolute efficiency quantification), determining the

optimal cDNA concentration to be used for the following analyses led on single samples. The chosen cDNA concentration was 5 ng/µl. A second real-time PCR (relative efficiency quantification) was then performed on single samples diluted 5 ng/µl. Primers used were the *2mit* and *rp49* (as control) real-time PCR primers reported in Table 2.3 of Chapter 2. *white*^{1118} genotype was employed as control strain.

A 10 µl real-time PCR reaction was composed by:
- 5 µl of 2X Master Mix (Promega)
- 0.2 µl of 10 mM Forward primer
- 0.2 µl of 10 mM Reverse primer
- 1 µl sample cDNA (5 ng/µl)
- 3.6 µl ddH_20

The mathematical model applied to determine the mRNA levels is reported in Chapter 2.

4.7 Behavioural experiments and statistical analyses

The optomotor test, the analyses of circadian rhythmicity and the memory test based on courtship conditioning were performed according to corresponding protocols described in Chapter 3. Statistical analyses were led as reported in Chapter 2.

4. Appendix

***2mitHA* cDNA sequence** (3453 bp)

1 **atg**gtgaaaa tcgtgaacca acactgtgat ctaggcctgg cccttctcct ggcctggacg
61 tggctaacaa ggctggtggt ggcggcccat ctggtcgaca tccccacctc atcacgcctg
121 gccgctgaac gggaggagca gcagttgtcc cggcaggacg taggacggct cagctaccag
181 agtatccatc gtatgctgag ggacgaaaac gaaccggata gctttcgggg ggaattgcga
241 taccaacaga aacgccacaa aagggagctg gagctgaatg cgccggccaa caagcttaat
301 ctcacccacc gcgatttgag gacattcaat agcactggtg gtcagtggaa gggcgacttt
361 caagtgatca ccgccatgga tctgagcagc aatcaactgg agagcctcag cttggacaac
421 ttcaatcaac tgaggcagct ggacttggga aataactccc tggaggtaat acccttgagt
481 ttggcagaca ccaatatgtc actacccttt gtgacgctcg atctttcctg caacaaattc
541 agccaaattt ctacgagctt ttttgcccag cgattgcctc agttgaaaaa tctgaatctg
601 gctcacaatg aattgctaaa tatttcccgg gaatcattct ataatttatt ggaactacaa
661 acgttagttc tcagtcacaa caacatctcg gatattgact atgaaacatt tttggcacta
721 ccgaatctgc aatatctgga tttatcccat aaccgcttga gtggatccgc tattcgtgct
781 ctgcaaggaa ttccggattt ggtcagcctt tccatcgctt acaatccaga tgtgggagtg
841 gcgatgcagg agttcgttgc ttcctggagc ctaaaggagt tggatgccag tggcactgga
901 ttgtgtcagg tgcctgcagc tctagcccaa tccgtgagga ctctcaagtt gtccgacaac
961 tggctcaagg caattaattg cggtgacatg gacagctatc cgctgctgca gtatcttgat
1021 ctctcgcact cccgcattgc ccaagtggag gacgatgcct tgggacgatt ggagctcctc
1081 gaatcccttt tcctagaccg taatctactg atgcgagtgc caagtagtct gccgccatcg
1141 ctggaacact tatttctgca gcacaatcag ataatggagc ttccgccaca ggcttttgtg
1201 ggattggtca atctacagac tctggactta tccaacaatc gattgatctt cctgcccccg
1261 ctatcgctcc ccaaattgct caccctgaat ctggaatcgt caggggtgga gagcgttagc
1321 caatcgatag tgcacacact gccacagtta agggatcttc tactggagga caaccccatt
1381 aagtgcagcg atttgctggg cattgccgaa tgggccagtc cttgcaggtc agtggatgcg
1441 ggtcaatcga atggggcaag tgtaagtggg cgcgtggatt tgaagacgga gtatctgcaa
1501 ttccacaatt tttacgaaaa cttcagcagc cgagagtgtg gtataagaaa accggaaaat
1561 gacacaaagc cgccttcttg cagcctaaca agggcatcag ctacattaac aacaacaccc
1621 agaagtatgt caaaagttga aaagtcacaa gaagcacaag caacagcaac atcagtggaa
1681 gtagcagcgg caacagcagc aacatcagaa aaaacaggca tacaagcaac atcagcagca
1741 cagtcgactg cggcggcaac aacagcagaa agagaagcaa ttgcaacagc aacatcaagc
1801 gacaccacag caacaccaac actcgcagca gcagcagcaa tacaatcagc tggcaacatc
1861 cctgcccagt taaccacaaa aacgttgcgg cccacagaaa caacttcgtt agcgcaactg
1921 cagcgtcggc aacaaatgcc tggcatgccg gccaaaacaa cagaaacgcc agcaaagaac
1981 ctgccaagtt tggcccagac aaaggcaaca acagcgcttc ccattttggc aacacgagat
2041 gctgccacag caacaacgga aataaattcc gacaagccaa cgaacattag cggtgccaca
2101 aaaacagtag caacatcagc tgcagaaata gcaacaccac cagcaattga agtgccacaa
2161 accattttgg ccggcaaaaa atctgacaaa atgccagccg ataaggcaca cgagacttta
2221 ttaaaatacc caacaaggga cacatccggt caagttgcaa caacgccaca caaacatgca
2281 acactgcagc tgcacgttaa ggatcgacat ctaattggca caccgctgct gatgcacaag

2341 ggcgatgtcc tattggtgga tgccgagcag ttgttgctgc ctggtacggc caccgtggcg
2401 gatgcggatt cggaagttct ggacccgagc caacaacatc agtcagcgga gcaggaaaag
2461 caccagtcag cgactgataa gcggcaagcg gatgcaataa acggcgacac gaagtcgccg
2521 gcgaaaggcc acaaaaagaa accatcgctg agcatcaaga agatgaccta cagtaccaaa
2581 cacgcggcaa aaaccgtgga ggatatggca gccacctcga agacaccgca acaccaacat
2641 agcagtgtga acacacccaa agaggctgct cccgaggagt tgagcacctt tgcgcagctt
2701 aaagcctatg tggagctaaa gagcgaatcg aaaccggaac acctaatgga ccagcgggag
2761 gaaaaccatc ataatcttac aggaaatcat ccaggagtca tgctcctggt ggcctgcgtt
2821 ttgttcatcg tcctgctcgc cggtttggcc cacgtctatc gctgtgaatt gccttggcaa
2881 aggagcaacc gctctggtca attgcgaccg catcatcaaa gacacctaaa cgaaaccgat
2941 gatgcgcaca gcttcctgca ctatcaggga tctgtgaact ccaatggcgg tgatccggct
3001 cgcctgcaaa agtggcacca cagcacgcgg agagaagcac cctacagctc cccgctgcac
3061 aatctacaag cgcgggaact gcaacagcaa cgctgccagc aattctatag ctcctcgctg
3121 gcggacaaga gctcctccac ctcgtcttcc tcgtcgggaa gcagtcgcag tagcctgcac
3181 tcgcccagca gagatgacag ctactatata gagatggcgc ccagtagtcc accagcagcc
3241 aacctgccca gtttgcccat ggaacttttg ggcagccgga gtaatgccct cggatgccgg
3301 acggatcgag tggcagccac cgatctgggc ggtacgacag aggcggtacc ctcttcggcg
3361 gcggccatca agtcggtgag cagcagactg atgacgccca gttcgcggag gctgaacatc
3421 tggtaccct acgatgtgcc cgattacgcc **tga**

*Met and the stop codons are in bold; the HA-tag nucleotide sequence is underlined

CHAPTER 5:

Search for 2MIT protein molecular partners

5. Introduction

In order to elucidate the molecular role of 2MIT protein, in this chapter we describe the research of 2MIT putative molecular partners. The identification of 2MIT interactors is important because it allows 2MIT protein characterization at anatomical and temporal levels, and permits to obtain information about mechanisms and/or molecular pathways in which 2MIT is involved. This search has been performed by screening a *Drosophila* cDNA library in the yeast-two hybrid assay.
Then, identified candidates have been critically analysed on the basis of what reported in literature, in order to determine if their interactions with 2MIT could effectively occur *in vivo*.

5. Results

5.1 Principles of the search for 2MIT protein molecular partners in the yeast-two hybrid system

We looked for 2MIT interactors through the yeast two-hybrid (Y2H) system, by screening a commercial *Drosophila* cDNA library (Mate & Plate™ Library) provided by the Matchmaker™ Gold Yeast Two-Hybrid System (Clontech). This library was produced from a collection of all mRNAs, expressed in the whole organism, during different developmental stages (embryonic, larval and adult stage), allowing the search for putative 2MIT partners throughout development. The investigation on 2MIT putative partners was possible by taken the advantages of mating between two *Saccharomyces cerevisiae* strains of opposite mating type: the Y2HGold and the Y187 strains, genetically engineered in order to be unable to biosynthesize specific nutrients (tryptophan, leucine, histidine and adenine). The Y2HGold strain was transformed with the pGBKT7 vector containing the sequence expressing the 2MIT bait as a fusion with GAL4 yeast transcriptional factor DNA-binding domain (BD), responsible for binding to UAS sequences. The pGBKT7 plasmid also carried the *TRP1* gene allowing the survival in media in which the tryptophan amino acid was absent. The Y187 strain was commercially available transformed with the pGADT7 RecAB vector carrying the prey, constituted by a normalized *Drosophila* cDNA library expressed as fusions to GAL4 activation domain (AD). The pGADT7 plasmid also contained the *LEU2* gene permitting the growth in media where leucine amino acid was lacking. After mating between these two transformed strains, diploid cells carrying both plasmids were obtained. The milestone of this technique is based on the fact that, in diploids characterized by interaction between bait and prey fusion proteins, the GAL4 transcriptional factor DNA-BD and AD are connected and brought into proximity. On the consequence, the assembly of the chimeric GAL4

transcriptional factor, previously split into two separate fragments, leads to the expression of four reporter genes (*HIS3*, *ADE2*, *MEL1*, and *AUR1-C)* by binding to their specifically recognized promoter regions carrying the UAS sequence. The reporter genes allow diploids growth onto selective medium. The *HIS3* and *ADE2* genes permit diploids to grow in media lacking histidine and adenine respectively; the *MEL1* gene codes for α-galactosidase that makes colonies to turn blue in presence of the X-α-Gal substrate; the *AUR1-C* gene confers resistance to the Aureobasidin A drug. On the contrary, if bait and prey proteins do not interact, no transcription of reporter genes is occurring and diploids do not survive in selective media. Therefore, the presence of blue colonies is strictly related to a successful interaction between two fusion proteins.

5.2 Generation of 2MIT bait constructs

In Y2H screening, the bait was represented by the 2MIT protein. Bioinformatic predictions indicated that 2MIT is a transmembrane protein, carrying a 23 aa transmembrane domain (AA 931-953) and a 28 aa N-terminal signal peptide, driving protein insertion into the plasma membrane. In particular, being the Y2H test based on interactions occurring at level of the nucleus, we projected 2MIT bait plasmids characterized by the absence of the transmembrane domain and/or by the deletion of the N-terminal signal peptide.
Three different 2MIT baits were generated (Fig.5.1):
1) 2MIT ΔTM: 2MIT full-length protein mutagenized in order to eliminate the transmembrane domain. In this bait, used for the first Y2H experiments, the 28 aa N-terminal signal peptide was kept.
2) 2MIT ED: 2MIT extracellular portion alone, not comprising the N-terminal 28 aa signal peptide necessary for localization. In this bait the signal peptide was deleted, as suggested in Wright (2009), to avoid 2MIT protein targeting through the export pathway.
3) 2MIT ID: 2MIT intracellular portion alone.

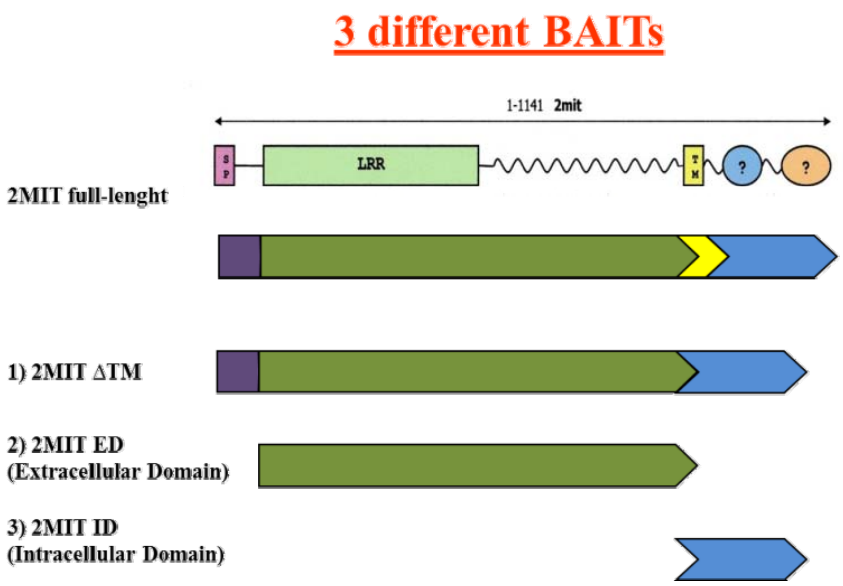

Fig.5.1 Schematic representation of the bait constructs generated for the Y2H screening: 2MIT ΔTM, 2MIT ED and 2MIT ID.

Specifically, *2mit* bait constructs were obtained from an available sub-cloned *2mit* cDNA sequence belonging to the *white*^{1118} strain. In order to establish whether the *white*^{1118} *2mit* genomic sequence could be generally representative as a *2mit* wild-type sequence, we evaluated the degree of similarity of *2mit* cDNA sequence belonging to the *white*^{1118} strain with respect to the *Oregon-R* wild-type sequence reported in Flybase (http://flybase.org/). By comparing the two sequences we found eight synonymous nucleotide substitutions, not modifying the 2MIT protein sequence (Table 5.1). We also detected five non-synonymous nucleotide substitutions, leading to amino acid substitutions at the protein level (Table 5.1). We verified whether the non-synonymous substitutions were mutations, which would not allow us to keep this *2mit* sequence as a reference for baits realization, or polymorphisms. *2mit* sequences of five different individuals, belonging to the wild-type *wt-ALA* strain, were analysed. Some of them presented, homozygously or heterozygously, the same non-synonymous substitutions detected in the *white*^{1118} *2mit* sequence, indicating that these non-synonymous substitutions were polymorphisms. Moreover, novel *2mit* synonymous and non-synonymous substitution sites were identified in the *wt-ALA* strain (Table 5.1). So, the *2mit* cDNA from *white*^{1118} genotype was used as template for the production of 2MIT baits.

After *2mit* bait sequences had been separately cloned into the pGBKT7 vector, fusion junctions with the segments conding for the GAL4 DNA-BD were sequenced showing that all the three bait insertions occurred in frame with respect to the GAL4 DNA-BD sequence.

	Position	Substitution	AA	*white*^{1118} Clone ΔTM	*O-R*	*wt-ALA* (Female n.1)	*wt-ALA* (Female n.2)	*wt-ALA* (Male n.1)	*wt-ALA* (Male n.2)	*wt-ALA* (Male n.3)
1	1100	A→G	Arg→His	X	/	X	/	nd	nd	X
2	1227	C→T	Asp synonymous	X	/	nd	nd	nd	nd	nd
3	1541	G→A	Gly→Asp	X	/	/	/	/	/	X
4	1606	T→A	Leu→Ile	X	/	/	/	/	/	X-eter
5	1619	C→A	Pro→His	X	/	/	/	/	/	X-eter
6						1684-eter (G-A) A-T				
7	2082	G→A	Thr synonymous	X	/	X	/	X-eter	X-eter	
8										2145 (G-C) A-P
9	2247	C→T	Ser synonymous	X	/	X	/	/	/	X-eter
10	2352	A→T	Leu synonymous	X	/	X	nd	/	/	/
11	2358	G→A	Val synonymous	X	/	X-eter	nd	/	/	/
12	2527	G→A	Gly→Ser	X	/	X	/	/	/	X eter
13	2547	G→A	Ser synonymous	X	/	X-eter	/	/	/	/
14							2585-eter (C-T)syn	/	/	/
15	2680	T→C	Leu synonymous	X	/	nd	nd	/	/	/
16	2730	G→A	Ser synonymous	X	/	nd	nd	nd	nd	nd

Table 5.1 Map of the polymorphic sites in *2mit* genomic sequence. Comparisons among *2mit* ΔTM sequence used (green) for baits generation (belonging to the *white*^{1118} genotype), *Oregon-R* (*O-R*) and five *wt-ALA* individuals. In pink the non-synonymous substitutions in the *2mit* ΔTM sequence. nd: not determined.

5.3 2MIT baits expression in the Y2HGold strain

Y2HGold strain was transformed with bait plasmids in which *2mit* ΔTM, *2mit* ED or *2mit* ID bait cDNA sequences had been sub-cloned in pGBKT7 vector and consequently fused to the GAL4 DNA-BD nucleotide sequence. Transformed Y2HGold colonies were selected in SD/-Trp medium, given that the pGBKT7 allows the growth in media not provided with the tryptophan amino acid.
Before proceeding with the library screening, we confirmed, by Western blot experiments, that the three 2MIT bait constructs were effectively expressed in the Y2HGold strain. In the pGBKT7 vector the *2mit* bait sequences were fused to a c-

Myc epitope tag that allowed the use of a commercial α-c-Myc monoclonal antibody for the detection of bait proteins. For each 2MIT bait, Western blot experiments were conducted by employing protein extracts from six independent transformed clones.

Fig.5.2a reports Western blot results obtained for six Y2HGold clones transformed with the pGBKT7-2MIT ΔTM plasmid. The GAL4 BD-2MIT ΔTM-cMyc fusion protein molecular weight is 140.38 kDa. Given that a band at almost ~150 kDa, in correspondence to the expected molecular weight, was specifically detected only in these clones but not in negative control, we concluded that this band represented 2MIT ΔTM bait fusion protein. All six tested clones expressed the 2MIT ΔTM bait.

Fig.5.2b reports the Western blot results obtained for six Y2HGold clones transformed with the pGBKT7-2MIT ED plasmid. The GAL4 BD-2MIT ED-cMyc fusion protein molecular weight is 116.53 kDa. Given that a band at ~120 kDa, in range with the expected molecular weight, was specifically detected in only these clones but not in negative control, we concluded that it represented 2MIT ED bait fusion protein. All six tested clones expressed the 2MIT ED bait. In addition, in the positive control the expected band at ~57 kDa was detected.

Fig.5.2c reports the Western blot results obtained for six Y2HGold clones transformed with the pGBKT7-2MIT ID plasmid. The GAL4 BD-2MIT ID-cMyc fusion protein molecular weight is 38.73 kDa. Since a band at ~40 kDa, in range with the expected molecular weight, was specifically detected in only these clones but not in negative control, we concluded that it represented 2MIT ID bait fusion protein. Also in this case, all six tested clones expressed the 2MIT ID bait.

These experiments confirmed that all the three 2MIT baits, integrated in the pGBKT7 plasmid, were expressed in the Y2HGold strain and could be used for the following procedures.

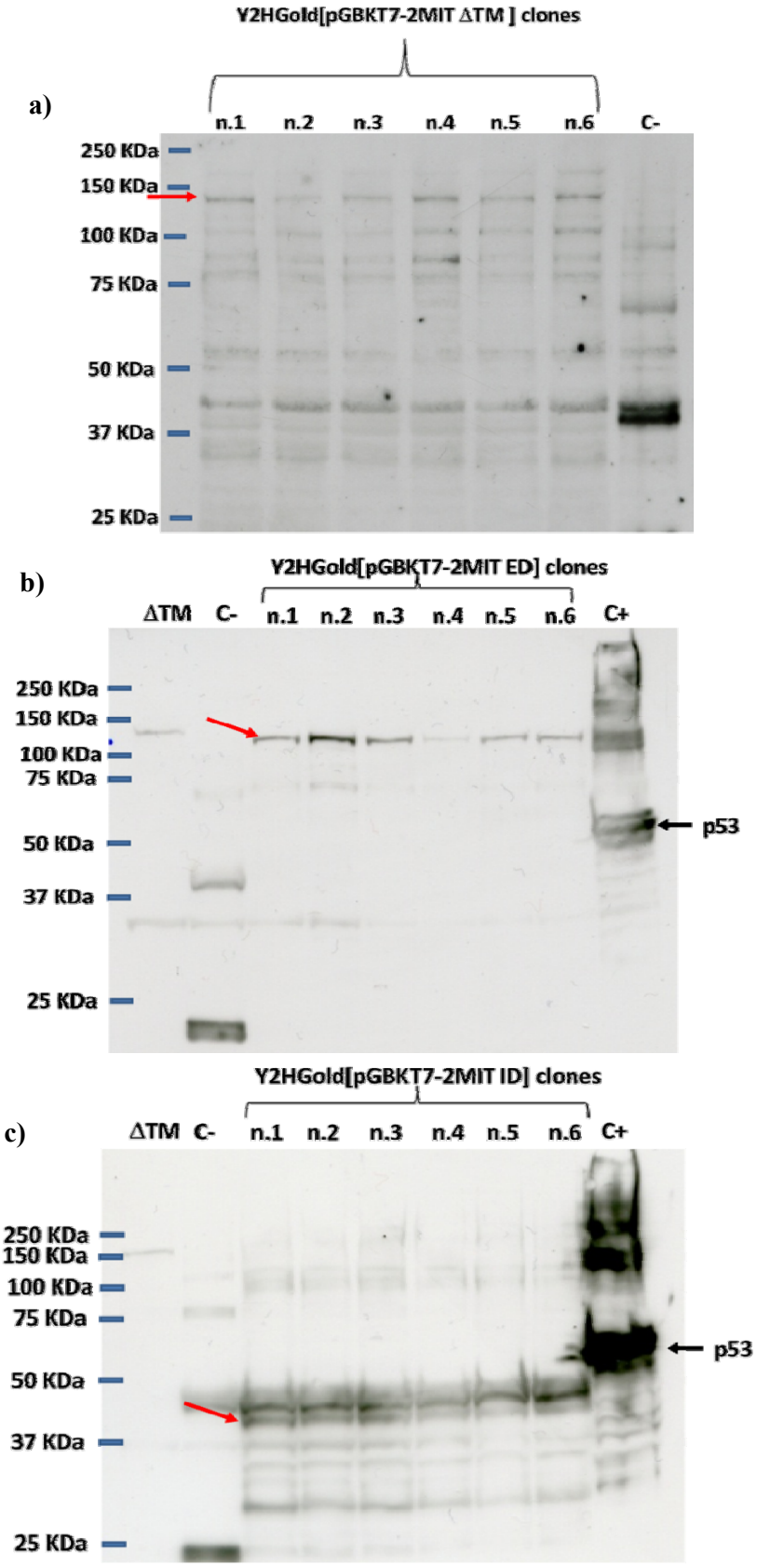
a)
Y2HGold[pGBKT7-2MIT ΔTM] clones
n.1
n.2
n.3
n.4
n.5
n.6
C-
250 KDa
150 KDa
100 KDa
75 KDa
50 KDa
37 KDa
25 KDa
b)
Y2HGold[pGBKT7-2MIT ED] clones
ΔTM
C-
n.1
n.2
n.3
n.4
n.5
n.6
C+
250 KDa
150 KDa
100 KDa
75 KDa
50 KDa
37 KDa
25 KDa
p53
c)
Y2HGold[pGBKT7-2MIT ID] clones
ΔTM
C-
n.1
n.2
n.3
n.4
n.5
n.6
C+
250 KDa
150 KDa
100 KDa
75 KDa
50 KDa
37 KDa
25 KDa
p53

Fig.5.2 Western blot experiments to detect 2MIT-c-Myc baits (red arrows), by using 1:1000 α-c-Myc antibody, in protein extracts from Y2HGold strain transformed with **a)** pGBKT7-2MIT ΔTM vector; **b)** pGBKT7-2MIT ED vector; **c)** pGBKT7-2MIT ID vector. The positive control (C+) is provided by protein extracts fromY2HGold cells transformed with the pGBKT7-53 vector expressing the 57 kDa murine p53 protein fused to GAL4 BD. The negative control (C-) represents protein extracts from Y2HGold cells transformed with the pGBKT7 empty vector. ΔTM: Y2HGold[pGKT7-2MIT ΔTM] protein extracts.

5.4 Preliminary experiments

The search for 2MIT interactors, through the screening of a library in the Y2H system, had to be preceded by a series of preliminary experiments based on:
- positive and negative control experiments in order to establish the feasibility and the reliability of the Y2H technique and materials. The positive control was based on mating between a bait and a prey proteins which interaction is known to occur in Y2H, in order to verify whether in diploid cells carrying these fusion proteins reporter genes were activated. The negative control was represented by mating between a bait and a prey proteins that do not interact in Y2H, in order to check if in diploids reporter genes were not activated.
- experiments to test the 2MIT baits for autoactivation and toxicity.

5.4.1 Control mating tests

In the positive control mating between Y2HGold[pGBKT7-53] and Y187[pGADT7-T] strains, the interaction between murine p53 and T-antigen fusions proteins effectively occurred leading to reporter genes activation in appropriate selective media. In the negative control mating between Y2HGold[pGBKT7-Lam] and Y187[pGADT7-T] strains, Lam and T-antigen chimeric proteins did not interact, as expected, and on the consequence reporter genes were not activated in appropriate selective media (data not shown).
These preliminary experiments gave a positive outcome and permitted to continue with following experiments based on testing bait contructs.

5.4.2 Baits autoactivation test

An important step was represented by the bait autoactivation test. In fact, it was fundamental to confirm that the bait alone, without the prey presence, did not autonomously activate the reporter genes in the Y2HGold strain.
Ten independent positive Y2HGold clones for each 2MIT bait (2MIT ΔTM, 2MIT ED, 2MIT ID) were spreaded in different selective media.
The results reported in Fig.5.3 were obtained by plating bait clones in a medium (SDO/X) lacking tryptophan amino acid and containing the chromogenic substrate X-α-Gal. All the tested clones were expected to grow because they presented the pGBKT7 vector conferring survival capability in a medium lacking tryptophan. The tested clones were also expected to be white, because, despite the presence of the chromogenic substrate X-α-Gal, the bait alone was not awaited to activate the reporter gene encoding for the α-galactosidase, which converts this X-α-Gal

substrate in a blue product. The expected results were confirmed for Y2HGold clones transformed with the pGBKT7 plasmid carrying the 2MIT ΔTM and 2MIT ED baits (Fig.5.3), but were not confirmed for Y2HGold clones carrying the pGBKT7 plasmid with the 2MIT ID bait (Fig.5.3). In fact these latter ones were blue meaning that the bait protein 2MIT ID alone, in absence of the prey protein, activated the *MEL1* reporter gene.
Therefore, the 2MIT ID bait was excluded for the library screening, whereas 2MIT ΔTM and 2MIT ED, not autoactivating the reporter genes, were used for the following experiments.

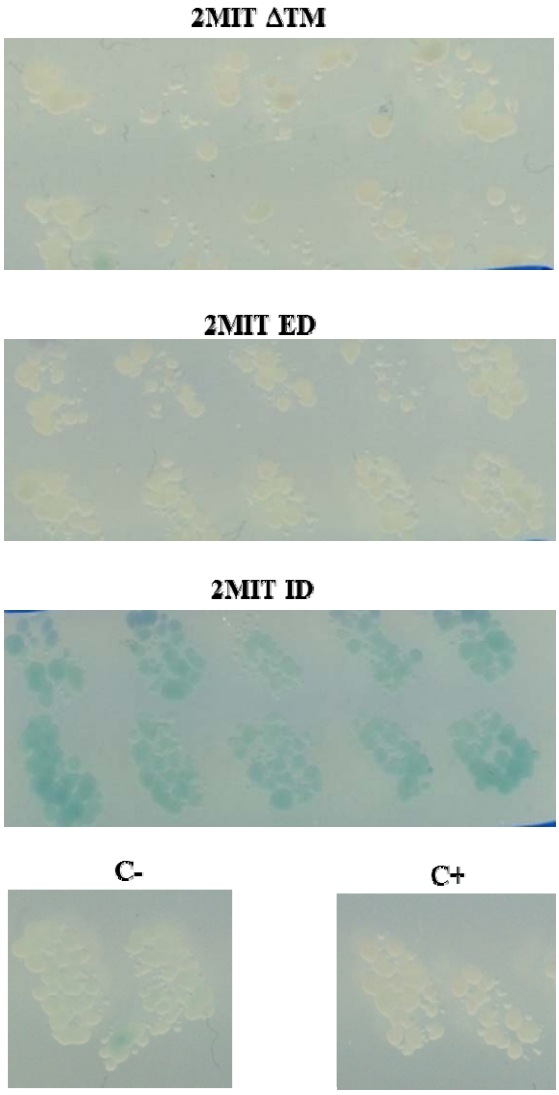

Fig.5.3 Autoactivation test, performed on SD/–Trp/X-α-Gal (SDO/X) agar plates, for 2YHGold strain transformed with pGBKT7-2MIT ΔTM, pGBKT7-2MIT ED or pGBKT7-2MIT ID plasmids, and with pGBKT7-53 vector (positive control, C+) and pGBKT7 empty vector (negative control, C-). Both positive and negative controls are expected to grow and to be white because they do not autoactivate the *MEL1* reporter gene.

5.4.3 Baits toxicity test

Another important phase of control experiments was represented by the bait toxicity test, necessary to confirm that bait proteins were not toxic for the yeast strains in which they were expressed. Generally, a bait protein is considered as being toxic when both solid and liquid cultures of bait transformed yeast cells grow slowler compared to cells transformed with the pGBKT7 empty vector.
To check for possible 2MIT ΔTM and 2MIT ED baits toxic effects, Y2HGold clones transformed with pGBKT7 plasmid carrying 2MIT ΔTM or 2MIT ED baits were compared to the Y2HGold strain containing the empty pGBKT7 vector and used as negative control.
The results, reported in Fig.5.4, showed that both Y2HGold grown colonies carrying 2MIT ΔTM or 2MIT ED baits were similar in size relative to colonies containing the empty pGBKT7 vector (negative control, C-). This means that both 2MIT ΔTM and 2MIT ED bait proteins were not toxic for the Y2HGold strain and could be eventually used for the library screening.
Moreover, the non-toxic effects of the 2MIT ΔTM bait for the Y2HGold strain were also demonstrated on liquid cultures (data not shown).

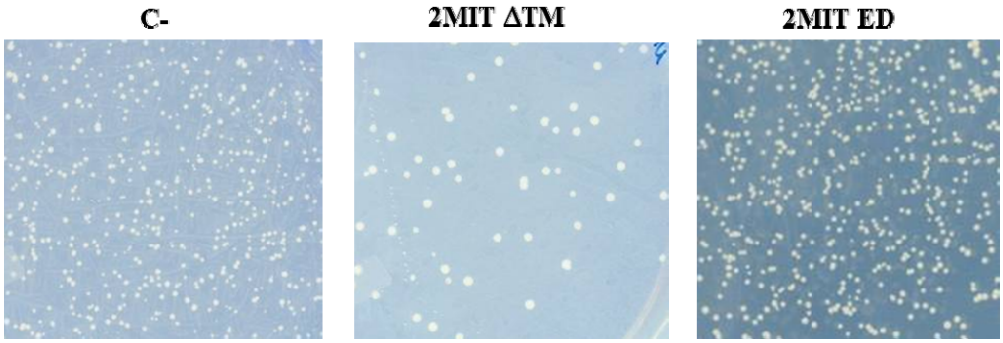

Fig.5.4 Toxicity test, performed on SD/-Trp (SDO) agar plates, for 2YHGold clones transformed with pGKT7-2MIT ΔTM or pGKT7-2MIT ED plasmids, compared to 2YHGold strain transformed with pGBKT7 empty vector (C-).

5.5 The two-hybrid library screening using yeast mating

For the Y2H screening, cultures belonging to the Y2HGold and Y187 transformed strains, of opposite mating type, were mixed together, allowing their mating to occur. Mating events generated diploid cells containing four reporter genes: *HIS3*, *ADE2*, *MEL1* and *AUR1-C*. Since reporter genes are activated in response to two-hybrid interactions, only the diploid cells carrying the putative 2MIT interactor proteins were supposed to grow onto high selective medium (QDO/X/A). Performing the Y2H screening, the mating efficiency was a critical parameter that was kept in consideration. A good mating efficiency, over a defined threshold value, was necessary to screen a representative number of library clones.

After several attempts to obtain a good mating efficiency by following the Manual protocol, based on mating on liquid culture, we turned to a protocol based on mating occurring on solid agar plates (Bendixen et al., 1994).
We first analysed the 2MIT ΔTM bait. We obtained a prey viability of $1.7x10^7$ and a 2.35% mating efficiency, value that was in range with that suggested by the protocol (2% mating efficiency). The number of screened clones was good ($4.53x10^6$) compared to the ~$1x10^6$ diploid clones indicated by the protocol for a good chance to get interactors. However, we did not obtain positive clones.
A possible explanation was based on bait protein topology. The 2MIT ΔTM construct represents the first attempt of a 2MIT bait to be used in the *Drosophila* library screening. In order to not strongly modify 2MIT protein of the bait, this construct was characterized by the lack of the trasmembrane domain, but by the presence of the N-terminal signal peptide. The deletion of the transmembrane domain was planned in order to avoid the incorporation of 2MIT ΔTM protein into the yeast membrane. We decided not to further modify the 2MIT ΔTM protein, maintaining the rest of the protein intact and therefore leaving the N-terminal signal peptide. In fact, although the N-terminal signal peptide is conserved among Eukaryotes, that one of heterologous type I transmembrane proteins (as *Drosophila* 2MIT is) might not be recognized as N-terminal cleavable signal sequence by the yeast system.
Anyway, in the first screening of the *Drosophila* library with 2MIT ΔTM bait, we did not found any interactor. The reasons of these negative results might therefore be due to the absence of transmembrane region, which might have caused a misfolding of the protein compromising its interaction, as well as to the presence of the N-terminal signal peptide, recognized by the yeast export pathway.
Therefore, we decided to separately screen the extracellular and the intracellual 2MIT domains, and to delete the signal peptide in the 2MIT extracellular domain. As already described, we could use only the 2MIT ED bait with the N-terminal signal peptide deletion, but not the 2MIT ID bait, excluded from the screening because it gave autoactivation during control experiments.
Two independent Y2H screenings were performed by using the 2MIT ED bait. From the first screening the prey viability was $8x10^6$, in conformity with the manual values. However, both 0.215% mating efficiency and ~$2.4x10^4$ screened clones were lower respect to protocol indications. Anyway, we achieved the growth of eight positive clones on high-stringency patching QDO/X/A medium, used to select bait and prey interactions. Then, we pursued with steps to confirm the positive interactions, performing segregation procedure, rescue and isolation of library plasmids and their co-transformation in Y2HGold strain with the pGBKT7-2MIT ED bait vector. From these confirmation experiments we distinguished one (out of eight) positive interactor with 2MIT extracellular domain. The other previously positive preys did not interact anymore with 2MIT ED, leading to lack of clones growth in selective agar plates. Moreover, this interactor seemed to be genuine because, when co-transformed with the pGBKT7

empty vector, so in absence of 2MIT ED prey, it did not activate the reporter genes. The sequencing of the cDNA prey regarding the confirmed Y2H candidate allowed the identification of a portion localized in the 3' region of the sequence coding for FLAMINGO protein (Fig.5.5a)

A second independent screen, using again 2MIT ED as bait protein, gave prey viability of $1.4x10^6$, a very high mating efficiency of 12.1% and a number of screened clones overcoming $\sim 1x10^6$ ($1.87\ 10^6$). In this case we obtained four positive clones in QDO/X/A high-stringency medium. For the identification of potential binding partners, we accomplished the same confirmation steps done in the previous screening. Only one of the putative candidates was identified as being a real 2MIT ED interactor in Y2H. cDNA prey sequence analyses allowed us to identify a fragment at 3' region of the sequence conding for the NCKX30C protein (Fig.5.5b).

Fig.5.5 reports plates showing both FLAMINGO- and NCKX30C-2MIT ED interactions. The high-stringency selective medium permitted only the growth of clones expressing all reporter genes, which were the ones co-transformed with both 2MIT ED bait and FLAMINGO or NCKX30C preys. No clones grew in Y2HGold cells co-transformed with pGADT7-FLAMINGO or -NCKX30C and with pGBKT7 empty vector, confirming that the two prey proteins were not false positives able to activate alone the reporter genes.

Via *in silico* analyses we found that the portion codified by *Flamingo* cDNA, which was interacting with 2MIT extracellular portion, was intracellular. On the consequence, we had to exclude FLAMINGO, because 2MIT-FLAMINGO interaction probably does not occur *in vivo*. NCKX30C protein is much less characterized with respect to FLAMINGO and, as far as we know, NCKX30C fragment interacting with 2MIT ED could share the same extracellular localization.

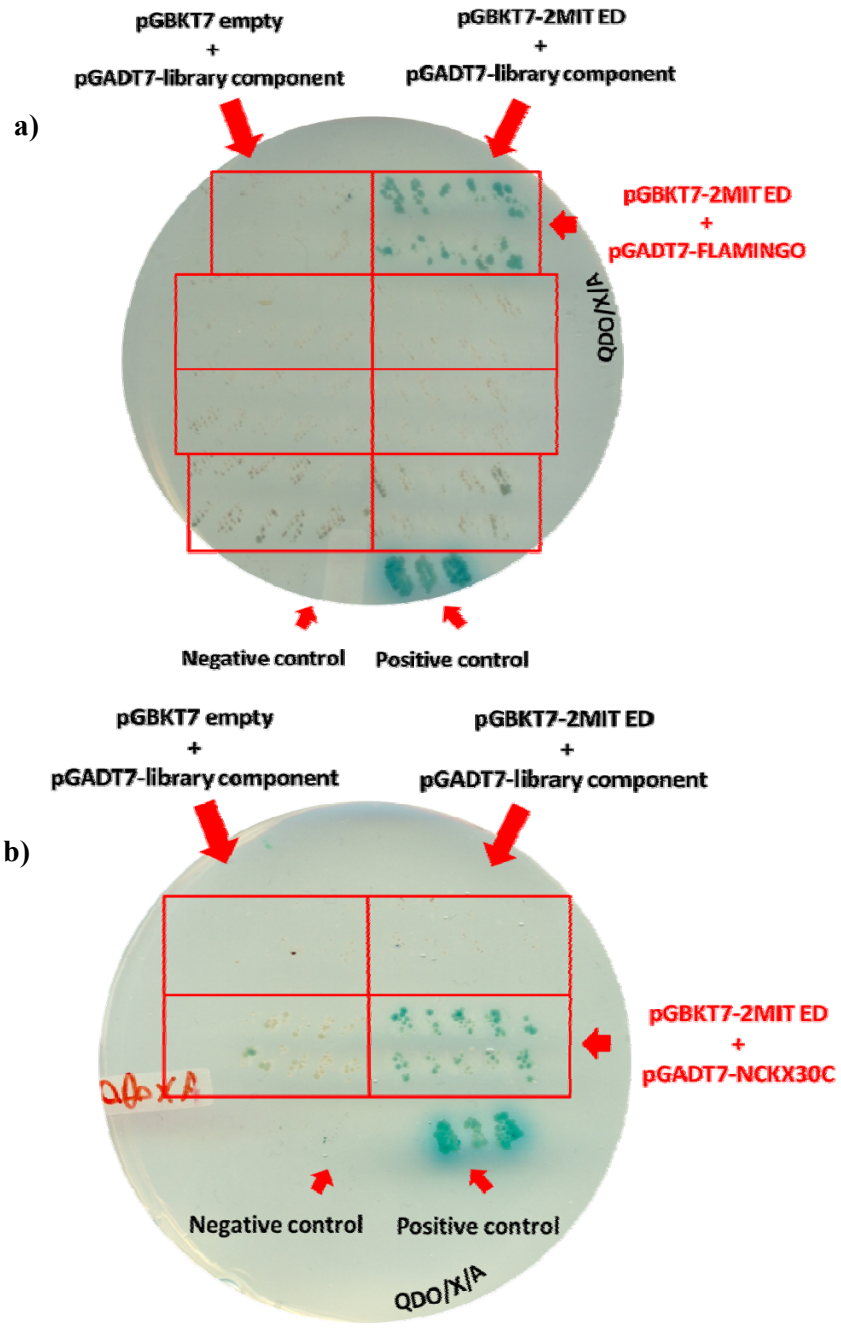

Fig.5.5 Plates allowing the identification of 2MIT effective interactors in Y2H by co-transformation of Y2HGold cells with both bait and prey constructs. The blue growing clones represent the positive Y2HGold clones in which the interaction between 2MIT and **a)** FLAMINGO or **b)** NCKX30C occurs activating the four reporter genes. QDO/A/X medium: quadruple dropout (-His, -Leu, -Ade, -Trp) with Aureobasidin A (A) and X-α-Gal (X). Positive control is represented by the grown blue Y2HGold clones co-transformed with pGBKT7-53 and pGADT7-T vectors, whereas negative control is represented by Y2HGold clones co-transformed with pGBKT7 and pGADT7 empty vectors.

5. Discussion

In this chapter we described the search for 2MIT protein molecular partners by screening a *Drosophila* cDNA library in the yeast-two hybrid system. We generated three distinct 2MIT baits from a *2mit* cDNA sequence obtained from the *white*^{1118} genotype. Although this sequence revealed non-synonymous substitutions when compared to those of the *Oregon-R* wild-type genotype, we ascertain that these substitutions were polymorphisms.

The first Y2H screens were performed using the 2MIT ΔTM bait, composed by *2mit* full-length cDNA lacking the sequence coding for the transmembrane domain, which was hypothesized to interfere with the test efficiency. Anyway, using this bait no 2MIT interactors were identified. We hypothesized that it was probably due to the transmembrane domain absence, which led to protein misfolding, and/or of the presence of the *Drosophila* 2MIT N-terminal signal peptide, that might have been recognized by the yeast targeting pathway, transporting the chimeric protein to the membrane. In fact, the Y2H system necessitates that both binding partners interact within the nucleus.

The other two 2MIT baits were the 2MIT extracellular portion (2MIT ED) and the 2MIT intracellular portion (2MIT ID) alone.

The 2MIT ID bait could not be used for the Y2H screening because autonomously self-activated the reporter genes during control experiments.

We managed to identify 2MIT putative molecular partners only by employing 2MIT ED as bait. This bait was generated with the deletion of the N-terminal signal peptide for membrane localization, that might had interfered with the nuclear localization of Y2H proteins interactions in previous experiments led with 2MIT ΔTM bait. We have shown that, in Y2H system, 2MIT ED interacts with the protocadherin FLAMINGO and with the antiporter NCKX30C.

FLAMINGO is a non-classic protocadherin with functions in signal reception, in establishment of tissue polarity (Usui et al., 1999; Lu et al., 1999; Chae et al., 1999) and in neural morphogenesis (Kimura et al., 2006; Matsubara et al., 2011; Reuter et al., 2003; Lee et al., 2003; Senti et al., 2003). It is expressed during all developmental stages in epitelia, nervous system and photoreceptor cells.

NCKX30C is a K^+-dependent Na^+/Ca^{2+} exchanger involved in modulation of Ca^{2+} in signaling events occurring during developmental stages and in Ca^{2+} removal and maintenance of Ca^{2+} homeostasis during signaling at adult stage, in particular in phototransduction. It is expressed during all developmental stages, in particular in embryonic ventral nerve cord, in larval imaginal discs (mainly eye-antennal disc), and in adult nervous system and photoreceptor cells (Haug-Collet et al., 1999; Webel et al., 2002).

Therefore, we found that 2MIT trasmembrane protein interacts in yeast with other two transmembrane proteins, which interestingly share with 2MIT common expression pattern regions. Both FLAMINGO and NCKX30C are expressed

during all developmental stages, in the nervous system and in photoreceptor cells. Focusing on the adult stage, it appears that FLAMINGO shares, in comparison to 2MIT, the same expression pattern in mushroom bodies and, given *2mit* mRNA expression in optic lobes, in the visual system. On the other hand, in the adult brain NCKX30C is also expressed in the visual system (photoreceptors and optic lobes).

In silico analyses showed that the portion codified by *Flamingo* cDNA, which was interacting with 2MIT extracellular portion, was intracellular. The FLAMINGO structural model might be not definitive and other FLAMINGO protein isoforms, carrying the C-terminal region in the extrernal part of the cell, might be present in *Drosophila* (http://flybase.org/). However, currently we will not progress with the *in vivo* analysis, in order to verify FLAMINGO as possible 2MIT interactor in *Drosophila* head.

NCKX30C protein is much less characterized with respect to FLAMINGO and, as far as we know, NCKX30C fragment interacting with 2MIT ED could share the same extracellular localization. Anyway, further analyses need to be performed in order to verify 2MIT-NCKX30C interaction *in vivo*.

In addition, from Bloomington Stock Center we obtained the *#17853 Nckx30C* strain, carrying a transposon insertion within *Nckx30c* locus. The molecular and phenotypical characterization of this mutant strain will give information on the putative interaction between NCKX30C and 2MIT trasnmembrane proteins.

5. Materials and methods

5.1 Analyses of *2mit* polymorphisms

5.1.1 PCR of sequences belonging to *2mit* gene

PCR amplification reactions were perfomed on four different portions of *2mit* genomic DNA, containing the polymorphic sites under analyses.

Solutions, DNA extraction and agarose gel electrophoresis procedures were the same as described in the paragraph 3.7 of the Chapter 3. The primers used are listed in Table 5.2.

gene	position	PCR primers		
2mit	970-989	Primer n.1_F	**forward**	5'-GCAATTAATTGCGGTGACAT-3'
	1271-1290	Primer n.1_R	**reverse**	5'-ATTCAGGGTGAGCAATTTGG-3'
2mit	1271-1290	Primer n.2_F	**forward**	5'-CCAAATTGCTCACCCTGAAT-3'
	1801-1820	Primer n.2_R	**reverse**	5'-GTTGGTGTTGCTGTGGTGTC-3'
2mit	2290-2309	Primer n.3_F	**forward**	5'-CTGCACGTTAAGGATCGACA-3'
	2674-2693	Primer n.3_R	**reverse**	5'-GCAAAGGTGCTCAACTCCTC-3'
2mit	1801-1820	Primer n.4_F	**forward**	5'-GACACCACAGCAACACCAAC-3'
	2335-2354	Primer n.4_R	**reverse**	5'-AATAGGACATCGCCCTTGTG-3'

Table 5.2 Primers used for analyses of nucleotide substitutions in *2mit* genomic sequence. Positions are referred to *2mit* cDNA sequence.

PCRs were performed in a 20 µl reaction mixture containing:
- 0.5 µl of 10 mM dNTPs (Promega)
- 0.5 µl of 10 mM forward primer
- 0.5 µl of 10 mM reverse primer
- 2 µl 10X buffer (Invitrogen)
- 1.2 µl $MgCl_2$ (Invitrogen)
- 2 µl genomic DNA (of a single individual)
- 0.4 µl Taq polymerase (5U/ µl) (Invitrogen)
- 12.9 µl ddH_20

PCR amplification conditions:
Initial Denaturation: 94°C for 2 min
Denaturation: 94°C for 30 sec
Annealing: 61.5°C for 30 sec
Elongation: 72°C for 1 min
} X 40 cycles
Final Elongation: 72°C for 10 min

5.1.2 PCR products sequencing

5 µl amplification product was added to 5 µl ExoSAP mix (1 µl Exonuclease I 10U/µl, 1 µl Shrimp Alkaline Phosphatase 2U/µl (Promega), 3 µl ddH_2O). The SAP program (37°C for 15 min; 80°C for 15 min; 4°C) was run. Then, 0.5 µl of

the appropriate forward or reverse primer was added. The DNA was dried and sequenced (BMR genomics S.r.l., Padova, Italy).

5.2 Speedy-preps

Independent bacterial colonies were placed into selective liquid medium at 37°C for ~16 h. For each colony, 1.5 ml culture was collected and centrifuged at 14000 rpm for 30 sec at room temperature (RT). The cell pellet was resuspended in 100 µl of A solution (50 mM Tris-HCl pH 8.0, 4% TritonX-100, 2.5 M LiCl, 62.5 mM EDTA), that led to bacterial lysis. 100 µl phenol/chloroform solution was added, in order to denature and precipitate proteins. The mixture was centrifuged at 14000 rpm for 5 min at RT. Following centrifugation the solution separated in two distinct phases: an aqueous upper phase, containing nucleic acids, and a lower one containing proteins. The upper phase was collected and 300 µl of 100% ethanol were added to precipitate the DNA. The mixture was incubated at -80°C for at least 20 min and was centrifuged at 14000 rpm for 15 min at RT. After supernatant removal, the DNA pellet was washed in 250 µl of 75% ethanol. The mixture was centrifuged at 14000 rpm for 5 min at RT. After supernatant removal, the DNA pellet was air-dried and then resuspended in 10 µl ddH_20.

5.3 Yeast cells transformation

A single yeast colony was inoculated into 5 ml complete YPG liquid medium (yeast extract, peptone, and dextrose) and grown overnight at 30°C. 1.5 ml culture was centrifuged at maximum speed for 3 min at RT. 2 µg plasmid DNA, 50 µg carrier DNA (salmon DNA sperm denatured at 100°C for 10 min) and 100 µl transformation solution (40% PEG3350, 0.2 M LiAc pH 7.5, 0.1 M DTT) were added to the cell pellet. The cells were resuspended by vigorous shaking and then they were subjected to heat shock at 45°C for 30 min. Following centrifugation at maximum speed for 3 min at RT and supernatant removal, the cell pellet was resuspended in 200 µl ddH_20. 100 µl solution was plated on the appropriate minimal selective medium. The petri dishes were incubated at 30°C for 48-72 h.

5.4 Yeast-Two Hybrid System

The Yeast-Two Hybrid System technique was performed in order to search for 2MIT protein interactors by applying the Matchmaker Gold Yeast Two-Hybrid System provided by Clontech Laboratories Inc. (CA). The technique was based on the screening of a *Drosophila* cDNA library in order to find which proteins, expressed from the cDNA constructs, interact with 2MIT protein.
This two-hybrid assay is based on the generation in *Saccharomyces cerevisiae* of a chimeric GAL4 yeast transcriptional factor, in which 2MIT represents the BAIT

protein that is expressed fused to the GAL4 DNA-binding domain (BD) and transformed in the yeast strain Y2HGold, whereas the library of proteins constitutes the PREY, and each protein is expressed fused to the GAL4 activation domain (AD) and transformed in the yeast strain Y187 (Fields and Song, 1989; Chien et al., 1991). When cell cultures of the two transformed strains are mix together, mating events occur generating diploid cells containing both bait and prey constructs. The interaction between bait (2MIT) and prey (a component of the library) fusion proteins allows the obtaining of complete chimeric GAL4 transcriptional factor by assembling its GAL4 DNA-BD and AD. The assembled GAL4 activates the expression of four independent reporter genes, located downstream GAL4-responsive promoters:

- ***AUR1-C***, a dominant mutant allele of the *AUR1* gene that codes for the inositol phosphoryl ceramide synthase. This enzyme confers resistance to the highly toxic drug Aureobasidin A.
- ***HIS3***, allowing Y2HGold cells to biosynthesize histidine and grow on -His minimal medium, given that this strain is unable to synthesize histidine and to grow on media that do not contain histidine.
- ***ADE2***, permitting Y2HGold cells to grow on -Ade minimal medium since this strain is unable to grow on minimal media lacking adenine.
- ***MEL1***, coding for α-galactosidase, which is expressed and secreted by the yeast cells and makes them to turn blue in presence of the chromagenic substrate X-α-Gal.

5.4.1 Strains, media and other materials

Matchmaker Vectors (Matchmaker™ Gold Yeast Two-Hybrid System)
- pGBKT7 DNA-BD Cloning Vector (0.1 μg/μl)
- pGADT7 AD Cloning Vector (0.1 μg/μl)
- pGBKT7-53 Control Vector (0.1 μg/μl)
- pGADT7-T Control Vector (0.1 μg/μl)
- pGBKT7-Lam Control Vector (0.1 μg/μl)

Matchmaker Yeast Strains (Matchmaker™ Gold Yeast Two-Hybrid System)
- Y2HGold Yeast Strain (*MATa, trp1-901, leu2-3, 112, ura3-52, his3-200, gal4Δ, gal80Δ, LYS2::GAL1UAS–Gal1TATA–His3, GAL2UAS–Gal2TATA–Ade2 URA3::MEL1UAS–Mel1TATA AUR1-C MEL1*) is the bait strain.
- Y187 Yeast Strain (*MAT*α, *ura3-52, his3-200, ade2-101, trp1-901, leu2-3, 112, gal4*D, *gal80*D, *met–, URA3::GAL1UAS-GAL1TATA-LacZ, MEL1*) is the prey strain.

Mate & Plate™ Library (Matchmaker™ Gold Yeast Two-Hybrid System)
1.0 ml Library Aliquots

Yeast Media

- SD medium (synthetically defined medium): minimal medium for yeast supplying everything a yeast cell needs to survive; it comprises a nitrogen base, a carbon source (glucose), and a DO supplement.

- 6.7 g/l yeast nitrogen base without amino acids
- 20 g/l glucose
- 100 ml of the appropriate sterile 10X DO Solution
- 0.003% Ade (by adding 15 ml of 0.2% adenine hemisulfate solution per liter of medium)
- only for plates: 20 g/l agar

- 10X DO (Dropout supplement or solution), a mixture of specific amino acids and nucleosides used to supplement SD base to make SD medium. A 10X Dropout Solution contains all but one or more of these nutrients required by untransformed yeast to grow on SD medium. Ser, Asp and Glu are excluded because they make the medium too acidic and yeast cells are able to synthesize these amino acids endogenously.

- **Nutrient 10X Concentration**

L-Adenine hemisulfate salt	200 mg/L
L-Arginine HCl	200 mg/L
L-Histidine HCl monohydrate	200 mg/L
L-Isoleucine	300 mg/L
L-Leucine	1000 mg/L
L-Lysine HCl	300 mg/L
L-Methionine	200 mg/L
L-Phenylalanine	500 mg/L
L-Threonine	2000 mg/L
L-Tryptophan	200 mg/L
L-Tyrosine	300 mg/L
L-Uracil	200 mg/L
L-Valine	1500 mg/L

According to which nutrients are missing and which substrates are present, the following media are produced (with addiction of 20 g/l agar for plates):

- SDO (single dropout medium): SD/-Leu or **SD/-Trp.** Cells containing prey plasmid are able to grow in SD/-Leu medium, being this vector encoding for a gene necessary for leucine biosynthesis. Cells containing bait plasmid are able to grow in SD/-Trp medium, being this vector encoding for a gene necessary for tryptophan biosynthesis.

- SDO/X: SD/-Trp supplemented with X-α-Gal.

- SDO/X/A: SD/-Trp supplemented with X-α-Gal and Aureobasidin A.

- **DDO (Double dropout medium): SD/–Leu/–Trp**, used to select for the bait and prey plasmids. SD/–Leu/–Trp dropout is composed by every essential amino acid except leucine and tryptophan. Cells containing bait and prey plasmids are able to grow because these vectors codes for tryptophan and leucine biosynthesis genes, respectively. The endogenous genome of the cell does not present those genes.
- **DDO/X: SD/–Leu/–Trp supplemented with X-α-Gal.**
- **DDO/X/A: SD/–Leu/–Trp supplemented with X-α-Gal and Aureobasidin A.**
- **TDO (Triple dropout medium): SD/–His/–Leu/–Trp** or **SD/–Ade/–Leu/–Trp.**
- **QDO (Quadruple dropout medium): SD/–Ade/–His/–Leu/–Trp**. It allows bait and prey plasmids selection and, in addition, activation of *HIS3* and *ADE2* reporter genes. It is used the end of the screening to confirm interactions.
- **QDO/X/A: SD/–Ade/–His/–Leu/–Trp supplemented with X-α-Gal and Aureobasidin A.**

- YPDA: complete medium, composed by yeast extract, peptone, and dextrose, supplemented with adenine hemisulfate.

- 20 g/l Difco peptone
- 10 g/l Yeast extract
- 0.003% Ade (by adding 15 ml of a 0.2% adenine hemisulfate solution per liter of medium)
- only for plates: 20 g/l agar

- X-α-Gal (5-bromo-4-chloro-3-indolyl α-D-galactopyranoside), a chromogenic substrate used to detect α-galactosidase activity.
Stock concentration: 20 mg/ml in N,N-dimethylformamide
Working concentration: 0.04 mg/ml

- Aerobasidin-A (AbA), a cyclic depsipeptide antibiotic, isolated from the filamentous fungus *Aureobasidium pullulans* R106. It is toxic to yeast at low concentrations (0.1-0.5 µg/ml).
Stock concentration: 500 µg/ml in 100% ethanol
Working concentration: 80 ng/ml

- Kanamycin sulfate. The bait plasmid contains a gene conferring resistance to kanamycin to avoid bacterial contamination.
Stock concentration: 50 mg/ml
Working concentration: 50 µg/ml

- Ampicillin. The prey plasmid contains a gene conferring resistance to ampicillin to avoid bacterial contamination.
Stock solution: 50 mg/ml
Working concentration: 50 µg/ml

5.4.2 Cloning vectors

pGBKT7: BAIT vector

The pGBKT7 vector (Fig.5.6) was used in order to generate the GAL4 DNA-BD/BAIT construct. The pGBKT7 vector allows the expression of the BAIT protein fused in frame to the 1–147 aa of the GAL4 DNA binding domain (AA 1-147; DNA-BD). In addition the pGBKT7 vector contains:

- the constitutive *ADH1* (alchool dehydrogenease) gene promoter (P_{ADH1}), upstream the GAL4-DB-BAIT sequence encoding for the fusion protein.
- T7 and *ADH1* transcription termination signals ($T_{T7\ \&\ ADH1}$ terminators), which are sequences located downstream the construct for the fusion protein.
- pUC the and 2 μ ori plasmid replication origin, sequences for the autonomous pGBKT7 replication in both *E. coli* and *S. cerevisiae*, respectively.
- Kanamycin resistance gene (*Kan*^{r}), conferring resistance to the antibiotic Kanamycin for selection in *E. coli.*
- *TRP1* nutritional marker, for selection in yeast in a medium lacking tryptophan.
- MCS (multiple cloning site), a polylinker containing unique restriction sites in frame with the 3' end of the GAL4 DNA-BD, for constructing fusion proteins with a bait protein.
- c-Myc epitope tag. The bait protein is also expressed as a fusion to a c-Myc tag allowing its identification with antibodies recognizing this common epitope.
- T7 RNA polymerase promoter, used for *in vitro* transcription and translation of the epitope tagged fusion protein (GAL4-BD is not expressed from the T7 promoter).

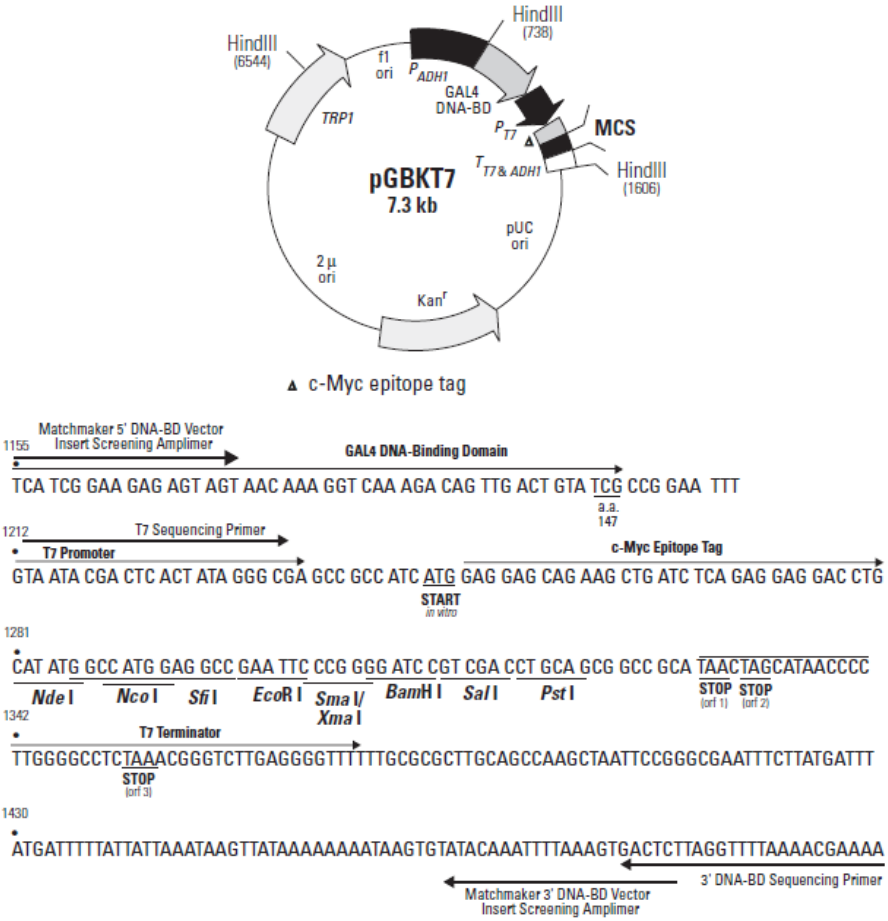

Fig.5.6 The pGBKT7 vector and the restriction map of its multiple cloning site (MCS).

pGADT7-RecAB: PREY vector

The pGADT7-RecAB vector (Fig.5.7) was used in order to generate the GAL4-AD/PREY construct through the cloning of the *Drosophila* cDNA library components. The pGADT7-RecAB vector allows the expression of the PREY protein fused in frame to the 768-881 aa of the GAL4 activation domain (AA 768-881; GAL4-AD). In addition the pGADT7-RecAB vector contains:

- the constitutive *ADH1* (alchool dehydrogenease) gene promoter (P_{ADH1}), upstream the GAL4-AD-PREY sequence encoding for the fusion protein
- the *ADH1* transcription terminator (T_{ADH1}), located downstream the construct for the fusion protein.
- the SV40 nuclear localization signal (SV40 NLS), included in the GAL4-AD sequence, so that fusions translocates to the yeast nucleus.
- pUC the and 2 µ ori plasmid replication origin, sequences for the autonomous pGBKT7 replication in both *E. coli* and *S. cerevisiae*, respectively.
- Ampicillin resistance gene (*Amp^r*), conferring resistance to the antibiotic Ampicillin for selection in *E. coli.*

- *LEU2* nutritional marker, for selection in yeast in a medium lacking leucine.
- *SfiI* sites (*SfiI*A and *SfiI*B) allowing that the GAL4-AD /cDNA fusion library can be generated *in vitro* through the SMART™ method. Following *SfiI* digestion the cDNAs of the library are ligated maintaining their directionality in the *SfiI*-digested pGADT7-RecAB vector.
- a hemagglutinin (HA) epitope tag, allowing identification of HA tagged proteins with antibodies recognizing this common epitope.
- T7 promoter, used for *in vitro* transcription and translation of the epitope tagged fusion protein (GAL4-AD is not expressed from the T7 promoter).

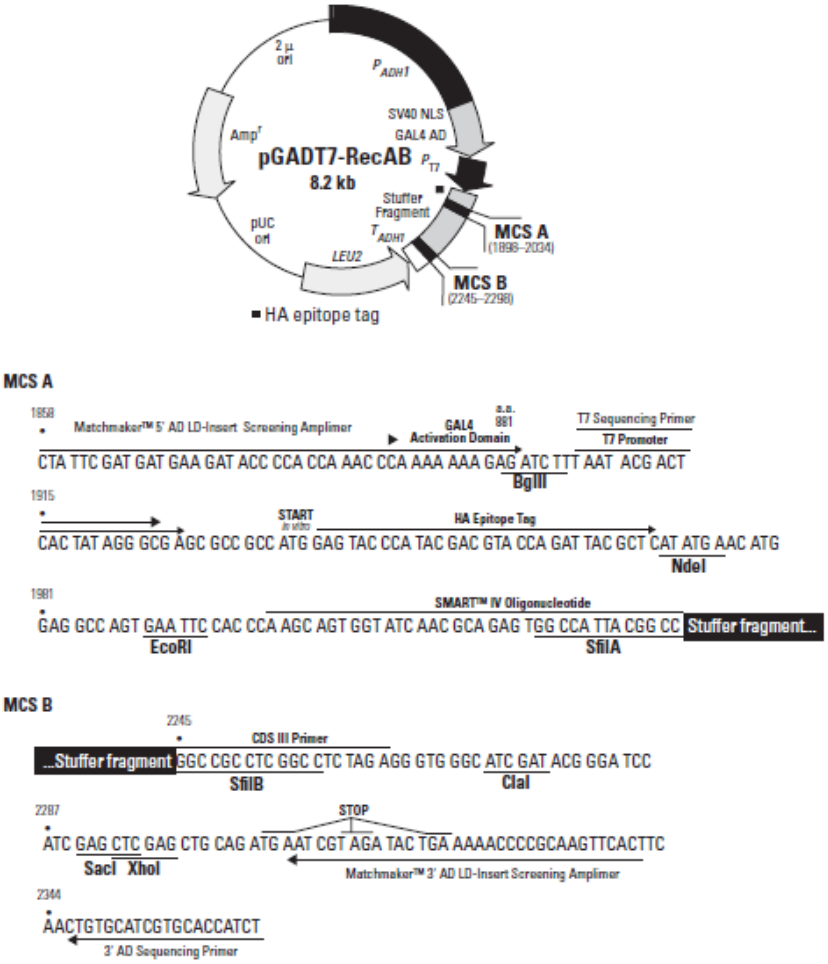

Fig.5.7 The pGADT7-RecAB vector with its restriction map and cloning sites.

5.4.3 The PREY: Mate & Plate™ *Drosophila* cDNA library

To perform the yeast-two hybrid screening we already disposed of aliquots (provided by Clontech) of Y187 yeast cells in which the cDNA library had been transformed. Y2H Mate & Plate™ library was constructed in pGADT7-RecAB vector from mRNAs isolated from *Drosophila melanogaster*. Specifically, the

mRNA source was composed by equal quantities of poly A+ RNAs isolated from embryonic (~20 h), larval and adult stages. The cDNA was synthesized using the SMART™ technology and was normalized prior to library construction in order to reduce the proportion of the most abundant mRNAs derived from highly represented transcripts, increasing the representation of low copy number. The normalization process was based on a combination between SMART™ technology and a Duplex-Specific Nuclease (DSN) treatment. In this way the number of clones to be screened was reduced facilitating the analyses at the level of interactors identification. Once normalized, the cDNAs were *SfiI* digested and cloned into the *SfiI* A/B sites of pGADT7-RecAB (PT3718-5) vector. Then the library was amplified in *E. coli* and transformed into the Y187 yeast strain. The MATα Y187 strain, containing the library, has to be mated to a *MATa* GAL4 Y2HGold reporter strain for screening.

5.4.4 The BAIT: 2MIT constructs

5.4.4.1 Generation of GAL4-BD/2MIT ΔTM BAIT:

For the generation of the 2MIT ΔTM bait, the sequence coding for the transmembrane domain (TM) was deleted. Once generated, the 2MIT ΔTM sequence was amplified and subsequently cloned into the pGBKT7 vector in order to obtain the GAL4-BD/2MIT ΔTM fusion bait construct.

PCR mutagenesis to generate 2mit ΔTM sequence

This method of PCR mutagenesis was used to produce, in the *2mit* full-length cDNA, a specific deletion in its portion coding for the transmembrane domain. The *2mit* sequence conding for the extracellular and the one coding for the intracellular portion were amplified in separate PCRs by using specific couples of primers. Primers flanking the transmembrane region, one of them used to amplify the extracellular the other one the intracellular portion, were designed with a 5' tail corresponding to the fusion flanking sequence of the opposite fragment and were complementary to each other (inverted tail-to-tail directions). Aliquots of the two initial PCR reactions were mixed together in a fusion PCR reaction exploiting the outer primers complementary tails in order to induce fusion between extracellular and intracellular portions and, on the consequence, generating the *2mit* cDNA sequence with the defined transmembrane deletion.

The following primers were used to amplify *2mit* extracellular sequence (the *NdeI* restriction site is underlined)

5'NdeI: 5'- CCCATATGATGGTGAAAATCGTGAACCAA-3'

3'Δ_TM: 5'-AAGGCAATTCACAGCGATAATGATTTCCTGTAAGATTATG-3'

The following primers were used to amplify *2mit* intracellular sequence (the *EcoRI* restriction sites is underlined)

5'Δ_TM: 5'-CATAATCTTACAGGAAATCATTATCGCTGTGAATTGCTT-3'
3' *EcoRI*: 5'-GGGAATTCCCAGATGTTCAGCCTCCGCGA-3'

PCR reagents:
- 4 µl 5X Buffer (Promega)
- 0.5 µl of 10 mM dNTPs
- 0.4 µl Taq Polimerase (Promega)
- 1 µl of 10 mM primer 2mitED_F
- 1 µl of 10 mM primer 2mitED_R
- 4 µl template DNA (10 ng/µl)
- 9 µl ddH_2O

PCR amplification conditions:
Initial Denaturation: 95°C for 1 min
Denaturation: 95°C for 45 sec
Annealing: 62°C for 45 sec
Elongation: 72°C for 45 sec
} X 35 cycles
Final Elongation: 72°C for 10 min

Ligation and cloning in the pGBKT7 vector

The amplified *2mit* sequence coding for the 2MIT ΔTM (AA 1-930/954-1141) was subsequently cloned into the pGBKT7 vector in order to obtain the GAL4-BD/2MIT ΔTM bait construct. Poly-A tails were added to *2mit* ΔTM PCR products (tailing: added 0.5 µl GoTaq and incubation at 72°C for 15 min). Then, PCR products were purified by using the Wizard® SV Gel and PCR Clean-Up System kit (Promega). 3 µl of PCR fragments were ligated into 1 µl pGEM-T-Easy vector (Promega) for 3 h at RT. The obtained vectors were transformed into One Shot® TOP10 Chemically Competent *E. coli* (Invitrogen). The cells were plated onto LB agar plates. Positive clones for 2MIT ΔTM were selected by digesting with *NdeI* (the *EcoRI* site could not be used because a restriction site is present within *2mit* sequence). The DNA was finally checked by sequencing (BRM Genomics S.r.l., Padova, Italy). Maxi-preps were performed to isolate a high amount of pGEM-T-Easy-2MIT ΔTM vector from *E.coli* cells. Then, pGEM-T-Easy-2MIT ΔTM was digested with *NdeI* and *ScaI* enzymes in order to extract *2mit* ΔTM from the vector. *2mit* ΔTM sequence was ligated into pGBKT7 vector: the *NdeI*-*NdeI 2mit* ΔTM fragment was gel-purified and ligated into *NdeI* digested pGBKT7 vector, while *ScaI* was used to disrupt the pGEM-T-Easy vector and to subsequently distinguish the vector from the insert.

5.4.4.2 Generation of GAL4-BD/2MIT ED BAIT

For the generation of the 2MIT ED bait, the sequence coding for the N-terminal signal peptide was excluded. The *2mit* sequence coding for the 2MIT ED (AA 29-930, without the signal peptide) was amplified and subsequently cloned into the pGBKT7 vector in order to obtain the GAL4-BD/2MIT ED BAIT construct.

PCR to generate 2mit ED sequence

For the amplification of *2mit* extracellular region, the template was *2mit* full-length cDNA fused with the HA tag, cloned in the pUAST plasmid (the same construct was used to generate *Drosophila melanogaster* transgenic lines described in Chapter 4).
The following primers were used:
2mitED_F: CATCATATGGCCCATCTGGTCGACATC
2mitED_R: TTGGGCCATATGGGCCATGATTTCCTGTAAGATT

PCR reagents:
- 2.5 µl primer 10 mM 2mitED_F
- 2.5 µl primer 10 mM 2mitED_R
- 2 µl template DNA (2 ng/µl)
- 25 µl Fusion Mix (Finnzymes)
- 18 µl ddH_2O

PCR amplification conditions:
Initial Denaturation: 98°C for 30 sec
Denaturation: 98°C for 20 sec
Annealing: 65°C for 30 sec
Elongation: 72°C for 15 sec
} X 35 cycles
Final Elongation: 72°C for 10 min

Ligation and cloning in the pGBKT7 vector

Poly-A tails were added to *2mit* ED PCR products (tailing: added 0.5 µl GoTaq and incubation at 72°C for 15 min). Then PCR products were purified by using the Wizard® SV Gel and PCR Clean-Up System kit (Promega). 3 µl PCR fragments were ligated into 1 µl pGEM-T-Easy vector (Promega) for 3 h at RT. The obtained plasmids were transformed into One Shot® TOP10 Chemically Competent *E. coli* (Invitrogen). The cells were plated onto LB agar plates. Mini-preps were performed through the PureYield™ Plasmid Miniprep System kit (Promega) from small liquid cultures of the colonies. Positive clones for *2mit* ED were selected by digesting with *BamHI* and the DNA was finally checked by sequencing (BRM Genomics S.r.l., Padova, Italy).

Then, pGEM-T-Easy-2MIT ED was digested with *NdeI* and *ScaI* enzymes in order to extract *2mit* ED from the vector. The *NdeI-NdeI* 3 kb fragment corresponding to *2mit* ED was gel-purified and ligated into *NdeI* digested pGBKT7 vector. *ScaI* was used in order to disrupt the vector and to subsequently distinguish the pGEM-T-Easy vector from the insert. Positive pGBKT7-2MIT ED clones were selected by digestion of DNA extracted though speedy-preps with *BamHI*: this enzyme permitted to check the correct insertion direction.

5.5.4.3 Generation of GAL4-BD/2MIT ID BAIT

For the generation of the 2MIT ID BAIT (AA 954-1141) the *2mit* sequence coding for the 2MIT intracellular portion (ID) was amplified and subsequently cloned into the pGBKT7 vector in order to obtain the GAL4-BD/2MIT ID BAIT construct.

PCR to generate 2mit ID sequence

For the amplification of *2mit* intracellular region the template was the same used for the 2MIT ED.
The following primers were used:
2mitID_F: CATCATATCGCTGTGAATTGCCTTGG
2mitID_R: TTGGGATCCTCACCAGATGTTCAGCCT
PCR reagents and amplification conditions were also the same used for 2MIT ED.

Ligation and cloning in the pGBKT7 vector

The procedure was the same described for 2MIT ED. After transformation of TOP10 cells with pGEM-T-Easy-2MIT ID plasmid, the positive clones for *2mit* ID were selected through *NdeI* digestion and the DNA was finally checked by sequencing (BRM Genomics S.r.l., Padova, Italy).
Then, pGEM-T-Easy-2MIT ID was digested with *NdeI* and *BamHI* enzymes in order to extract *2mit* ID from the vector. The *NdeI-BamHI* 0.5 kb fragment corresponding to *2mit* ID was gel-purified and ligated into *NdeI-BamHI* digested pGBKT7 vector. Positive pGBKT7-2MIT ID clones were selected by digestion of DNA extracted through speedy-preps with *NdeI*.

5.4.5 Western blot to detect baits expression

Western blot experiments were performed on samples composed by Y2HGold cells that had been previously transformed with pGBKT7-2MIT ΔTM, pGBKT7-2MIT ED or pGBKT7-2MIT ID bait plasmids, in order to determine whether these baits were expressed in yeast. Y2HGold clones carrying one of these bait constructs were selected among the grown clones plated onto SD/-Trp selective medium. Y2HGold[pGBKT7-53] strain, which expresses a 57 kDa protein, was

used as a positive control, whereas the Y2HGold[pGBKT7] strain, carrying the pGBKT7 empty vector, represented the negative control. Commercial antibodies used in these experiments are listed in Table 5.3 and 5.4.

5.4.5.1 Solutions and antibodies

- 20X MOPS Running Buffer (pH 7.7): 50 mM MOPS, 50 mM Tris Base, 0.1% SDS, 2% LDS, 1 mM EDTA

- 20X Transfer Buffer (pH 7.2): 25 mM Bicine, 25 mM Bis-Tris (free base), 1 mM EDTA pH 7.2

- NuPAGE® LDS Sample Buffer (pH 8.5): 106 mM Tris HCl, 141 mM Tris Base, 2% LDS, 10% Glycerol, 0.51 mM EDTA, 0.22 mM SERVA Blue G250, 0.175 mM Phenol Red

- 0.05% TBST: 100 mM Tris-HCl pH 7.5, 140 mM NaCl, 0.05% Tween®20

- Blocking Buffer: 0.05% TBST**,** 5% milk (Carnation NonFat Dry Milk)

- Detection Solution: 2.25 mM luminol, 0.2 mM p-coumaric acid, 0.1 M Tris-HCl pH 8.5, 0.01% H_2O_2

Primary antibody	Origin	Working concentration	Provenience
α-c-Myc	Mouse	1:1000 or 1:2000	Clontech

Table 5.3 Primary antibody employed in Western blot experiments related to the yeast-two hybrid system.

Secondary antibody	Origin	Working concentration	Provenience
α-mouse	Goat	1:5000	Santa Cruz Biotecnology Inc.

Table 5.4 Secondary antibody employed in Western blot experiments related to the yeast-two hybrid system.

5.4.5.2 Protein extraction

Independent *S. cerevisiae* colonies were inoculated into 5 ml selective minimal medium and incubated at 30°C for 48-72 h, until the phase of exponential growth (OD600=1.5). 2 ml culture was centrifuged at 13200 rpm for 3 min at RT and the supernatant was removed. 20 µl LDS Nupage 4X and 5 µl of 1M DTT were added to the cell pellet. The samples were vortexed, frozen in liquid nitrogen and incubated at 100°C for 5 min, causing the rupture of the cell wall. Samples were

centrifuged at 13200 rpm for 1 min at RT and the supernatant was recovered. On the basis of the optical density of cultures, for each sample comparable amounts of lysate protein were loaded.

5.4.5.3 Gel electrophoresis, transfer, blocking and detection

The procedure was the same of the one reported for Western blot experiments described in paragraph 4.5 of Chapter 4 with minor modifications.
Gel electrophoresis apparatus (Invitrogen) was filled with MOPS running buffer and 400 µl antioxidant solution (Invitrogen) was added in the running buffer. Protein extracts were loaded into wells of a 4-12% NuPAGE® pre-cast gel (Invitrogen). 8 µl of 10-250 kDa protein ladder (New England Biolabs) were loaded as molecular weight marker. Gel was blotted on a nitrocellulose membrane for 1 h at 30 V by using a blotting apparatus (Invitrogen) provided with transfer buffer. Equal transfer of proteins was controlled by Ponceau staining (Sigma). The nitrocellulose membrane was incubated for 1 h in blocking buffer. Then it was incubated overnight at 4°C with α-c-Myc primary monoclonal antibody (produced in mouse) diluted as reported in Table 5.3, in 1% milk 0.05% TBST. α-ARP7 antibody recognizing a constitutive protein of *S. cerevisiae* cytoskeleton was used as control. The membrane was washed for three times of 10 min each in 0.05% TBST at RT. It was incubated for 2 h at RT with HRP-conjugated secondary antibody diluted as reported in Table 5.4 in 1% milk 0.05% TBST. Then it was washed for three times of 10 min each in 0.05% TBST at RT. HRP activity was revealed with an ECL system.

5.4.6 Matchmaker screening control experiments

Before screening the library, control mating experiments were performed. The following vectors containing known bait or prey proteins were used:
- pGBKT7-53, positive control bait plasmid encoding the GAL4 DNA-BD fused with murine p53.
- pGADT7-T, positive control prey plasmid encoding the GAL4-AD fused with SV40 large T-antigen.
- pGADT7-Lam, negative control bait plasmid encoding the GAL4-BD fused with lamin.

The pGBKT7-53 and pGBKT7-Lam vectors were transformed into the Y2HGold strain, while the pGADT7-T was transformed into the Y187 strain. After three days at 30°C, colonies of each type were used for control matings:
positive control mating: mating betweenY2HGold[pGBKT7-53] with Y187 [pGADT7-T]. SV40 large T-antigen is known to interact with p53 in Y2H (Li and Fields, 1993; Iwabuchi et al., 1993).

Negative control mating: mating between Y2HGold[pGBKT7-Lam] with Y187 [pGADT7-T].
For each mating, both colonies were placed in a tube containing 500 µl 2X YPDA and were incubated at 200 rpm at 30°C for 20-24 h. Then, from the mated culture, 100 µl of 1/10, 1/100, and 1/1000 dilutions were spread on different selective agar plates: SD/–Trp, SD/–Leu, SD/–Leu/–Trp (DDO), SD/–Leu/–Trp/X-α-Gal/AbA (DDO/X/A). The plates were incubated at 30°C for 3-5 days.
Positive control diploids, carrying both plasmids that can activate all four reporter genes, were expected to give a similar number of colonies on DDO and DDO/X/A selective media (with blue colonies). Negative control diploids, containing both plasmids that do not activate reporter genes, were expected to grow on DDO but not on DDO/X/A selective media.

5.4.7 Testing baits for autoactivation

The autoactivation test was performed in order to verify that, before mating, the baits did not autonomously activate the reporter genes in Y2HGold strain, when the prey protein was not present. 100 µl Y2HGold cells, transformed with pGBKT7-2MIT ΔTM, pGBKT7-2MIT ED or pGBKT7-2MIT ID bait plasmids, were spread in 1/10 and 1/100 dilutions onto different selective media: SD/–Trp plates (SDO), SD/–Trp/X-α-Gal (SDO/X) and SD/–Trp/X-α-Gal/AbA (SDO/X/A) plates. The same procedure was conducted for Y2HGold cells transformed with the pGBKT7 empty vector, considered as negative control, and with Y2HGold cells transformed with the pGBKT7-53 vector, employed as positive control. The plates were incubated for 3-5 days at 30°C. The expected results are listed in Table 5.5.

Selective medium	Colony growth	Color
SDO	Yes	white
SDO/X	Yes	white or pale blue
SDO/X/A	No	-

Table 5.5 Expected results from the bait autoactivation test.

5.4.8 Testing baits for toxicity

The toxicity test was performed to demonstrate whether the 2MIT bait proteins were not toxic when expressed in yeast. 100 µl Y2HGold cells, transformed with pGBKT7-2MIT ΔTM, pGBKT7-2MIT ED or pGBKT7-2MIT ID bait plasmids, were spread in 1/10 and 1/100 dilutions onto SD/–Trp (SDO) agar plates. The same procedure was conducted for Y2HGold cells transformed with the pGBKT7 empty vector, considered as negative control. The plates were incubated for 3-5

days at 30°C. Each bait was considered as being toxic whether colonies containing it were significantly smaller than colonies containing the empty pGBKT7 vector.

5.4.9 Two-hybrid library screening using yeast mating

After several attempts to obtain a good mating efficiency by following the mating protocol described in the Matchmaker^{TM} Gold Yeast Two-Hybrid System User Manual, a different protocol, suggested in the manual troubleshooting guide, was performed. The followed protocol was based on a variation from the procedure described in the manual: the mating between strains carrying bait and prey was conducted on solid agar plates (Bendixen et al., 1994) instead of liquid culture.
A concentrated culture of Y2HGold[pGBKT7-2MIT ΔTM] or Y2HGold [pGBKT7-2MIT ED] bait strains was prepared by inoculating, for each of them, one fresh and large colony into 30 ml of SD/–Trp liquid medium. The culture was incubated overnight at 30°C. Then the culture was centrifuged at 1000 g for 5 min at RT to pellet the cells and discard the supernatant. The cell pellet was resuspended with 70 ml liquid YPDA and incubated at 250-270 rpm shaking at 30°C until the OD600 reached 0.8 (after ~ 4 h). 1 ml aliquot of library strain was thawed in a RT water bath for 2 min. Then, the library strain was combined with 70 ml bait culture but, before mixing, 10 µl library strain was removed for titering. Specifically, 10 µl library strain was used for spreading 100 µl of 1/100, 1/1000 and 1/10000 dilutions onto 100 mm SD/–Leu agar plates. Given that 1 ml library aliquot should contain >$2x10^7$ cells (titer of $2x10^7$ cells/ml), 200 colonies should be obtained on the 1/10000 dilution plate. The bait and prey mixture was incubated for 10 minutes at 30°C with shaking. Then, it was centrifuged at 1000 g for 5 min to pellet the cells and discard the supernatant. The cell pellet was resuspended with 2 ml YPDA and plated onto a 150 mm YPDA agar plate, which was incubated for ~ 4-6 h at 30°C. From time to time it was important to check a small sample of the culture under a phase contrast microscope (40X). If zygotes were present, the following step was carried on, if not, mating was allowed to continue. A zygote typically has a 3-lobed structure. The lobes represent the two haploid parental cells and the budding diploid cell. Some zygotes may resemble a clover leaf, while others may take on a shape similar to a “Mickey Mouse” face. In the following step, the mated cells were scraped by adding SD/-Leu-Trp liquid medium to the YPDA plate. The plate was rinsed many times obtaining a final volume of 11 ml liquid medium. For titering (calculate the number of screened clones), from the mated culture 100 µl of 1/10, 1/100, 1/1000 and 1/10000 dilutions were spread onto each of 100 mm SD/–Trp, SD/–Leu and SD/–Leu/–Trp (DDO) agar plates and incubated at 30°C for 3-5 days. The remainder of the culture was plated, spreading 200 µl of mated culture per 150 mm DDO/X/A agar plate. The obtained 50–55 plates were incubated at 30°C for 3-5 days.

For titering the colonies grown after 3-5 days were counted from the SD/–Trp, SD/–Leu and SD/–Leu/–Trp DDO plates.

Determination of the number of screened clones (diploids)

Number of Screened Clones=cfu/ml of diploids x resuspension volume (ml)

Per single plate: cfu/ml of diploids= n. of colonies x plating volume x dilution

It was fundament to obtain at least 1 million diploids to be screened, as less diploids would mean less chance of detecting genuine interactions on DDO/X/A plates.

Determination of the mating efficiency

In order to calculate the mating efficiency it was necessary to determine the viability of the prey library, the bait and the diploids.

Measure of viabilities:

• viability of the prey library= n. of cfu/ml on SD/–Leu

• viability of bait= n. of cfu/ml on SD/–Trp

• viability of diploids= n. of cfu/ml on SD/–Leu/–Trp

The strain (bait or prey) with the lower viability was considered as the "limiting partner", employed for the following formula used for the determination of mating efficiency.

Mating Efficiency (percentage of diploids):

n. of cfu/ml of diploids x 100/ n. of cfu/ml of limiting partner=% diploids

Mating efficiency had not to be less than 2% in order to screen 1 million diploids.

By using a sterile toothpick, all blue colonies that grew on DDO/X/A medium were picked and scraped onto medium stringency media (TDO-His/X/A, TDO-Ade/X/A) agar plates and high stringency medium (QDO/X/A) agar plates. For each selective medium, different replica plates were obtained for the selected clones. All the QDO/X/A positive interactions had to be further analysed to identify duplicates and to verify that the interactions were genuine.

5.4.10 Confirmation of positive interactions and rescue of the prey plasmid

Once identified positive clones in the library screening assay, it was necessary to confirm that the positive interactions were genuine. This was possible by performing experiments based on rescue and isolation of the library plasmids responsible for activation of reporters, and by distinguishing genuine positive from false positive interactions.

5.4.10.1 Segregation of library plasmid in yeast

Transformed yeast cells can contain more than one version of a specific plasmid. This means that they may contain, in addition to a prey vector expressing a

protein leading to reporter genes activation, also one or more prey plasmids that do not express an interacting protein. So, it was fundamental to perform segregation of yeast plasmids, increasing the probability of rescuing a positive prey interactor. For the segregation procedure, positive clones were streak 2-3 times on DDO/X, each time picking a single blue colony for re-streaking. After, only blue colonies should be seen.

5.4.10.2 Extraction of the library plasmid from yeast for use in the transformation of *E. coli*

For rescuing the prey plasmid from yeast, the following procedure was adopted as modification of the protocol described by Polaina and Adam (1991).
A positive yeast colony was isolated from QDO/X medium and resuspended on 1 ml SD/-Trp-Leu liquid medium. The cell culture was incubated at 30°C for ~24 h at 285 rpm shaking. Then, it was centrifuged at 14000 g for 30 sec at RT to pellet the cells and discard the supernatant. The cell pellet was resuspended in 100 µl freshly prepared 3% sodium dodecyl sulfate (SDS), 0.2 N NaOH solution. The mixture was incubated for 15 min at RT with occasional mixing by rapid inversions. 500 µl TE (10 mM Tris-HCl pH 7.5, 1 mM EDTA) were added, mixing by rapid inversions. Then, 60 µl of 3 M sodium acetate were added, mixing by rapid inversions. 600 µl phenol (saturated with 10 mM Tris-HCl pH 8.0, 1 mM EDTA):chloroform:isoamyl alcohol, 25:24:1 were added. The mixture was vortexed for 2 min at full speed and then centrifuged at 14000 g for 2 min. The upper aqueous phase was transferred to a new tube, vortexed for 2 min at full speed and centrifuged at 14000 g for 2 min. Again, the upper aqueous phase was transferred to a new tube. 650 µl ice-cold isopropanol were added and mixed by rapid inversions. The mixture was incubated at -20°C for at least 20 min and subsequently centrifuged at 14000 g for 5 min at RT, discarding the supernatant. After centrifugation for 10 sec and removal of all residual supernatant, 100 µl of 70% ethanol were added. After a first centrifugation at 14000 g for 5 min, discarding the supernatant, and a second one for 10 sec, to remove all residual supernatant, the pellet was suspended in 10 µl TE solution. 1 µl of the extracted DNA was used to electroporate *E. coli* ElectroMAX™ DH10B™ cells. For the selection of *E. coli* transformants containing the prey plasmid, given that the bait is cloned in the pGBKT7 which contains a Kanamycin resistance gene, the transformation mixture was plated in LB+100 µg/ml Ampicillin.

5.4.10.3 Retransformation Test: distinguishing genuine positive from false positive interactions

The DNA prey plasmid was extracted from *E. coli* colonies grown in the selective medium by using the Wizard® Plus Minipreps DNA Purification System (Promega). 100 ng pGADT7-prey plasmid, extracted from bacteria, and 100 ng

pGBKT7-bait (2MIT ED) plasmid were used to co-transform competent Y2HGold cells. As negative control the pGADT7-prey was also co-transformed into competent Y2HGold cells with the pGBKT7 empty vector. Y2HGold[pGBKT7-53]xY187[pGADT7-T] positive and Y2HGold [pGBKT7]xY187[pGADT7] negative mating controls were used for this test.
1/10 and 1/100 dilutions of 100 µl Y2HGold transformed cells of each combination were spread onto DDO/X and QDO/X/A agar plates. The plates were incubated for 3-5 days at 30°C. In a genuine positive interaction both bait and prey are required to activate the reporter genes whereas in false positives the prey can activate the reported genes in the absence of the bait.
The key for the interpretation of the results is reported in Table 5.6.
The confirmed genuine positive interactors were identified by sequencing (BMR Genomics S.r.l., Padova, Italy) from the T7 promoter localized in the pGADT7 vector, upstream the prey insertion site.

Interaction	Sample	Selective medium	Colony growth	Color
GENUINE INTERACTOR	pGBKT7-bait + pGADT7-prey	DDO/X	yes	blue
		QDO/X/A	yes	blue
	pGBKT7 empty + pGADT7-prey	DDO/X	yes	white
		QDO/X/A	no	-
FALSE POSITIVE	pGBKT7-bait + pGADT7-prey	DDO/X	yes	blue
		QDO/X/A	yes	blue
	pGBKT7 empty + pGADT7-prey	DDO/X	yes	blue
		QDO/X/A	yes	blue

Table 5.6 Interpretation of the results obtained from the yeast re-transformation tests. In false positive interactions, all plates display similar numbers of blue colonies.

CHAPTER 6:

Conclusions

Drosophila melanogaster 2mit gene is localized within the longest intron (11th) of the 75 kb *tim2* locus, in the opposite transcriptional orientation (Benna at al., 2010). Despite *tim2* locus contains other intronic sequences, *2mit* seems to be the only one to be translated, given the presence of a canonical translation start sequence in correspondence of the AUG start codon of its longest predicted ORF (Benna et al., 2010; Cavener and Ray, 1991). *In silico* translation of *2mit* sequence gives rise to a putative 1141 aa 2MIT protein characterized by a main extracellular portion, carrying a LRR motif important for protein-protein interaction (Kajava, 1998; Kobe and Kajava, 2001; Dolan et al., 2007), a transmembrane domain and a smaller intracellular portion, characterized by a region rich in serine amino acids (1037-1076 aa) that could provide phosphorylation sites, generally important for signaling transduction pathways. Therefore, the 2MIT protein predicted topology leads to the assumption that this protein may exert a membrane receptor function.

Phylogenetic analyses have revealed that 2MIT protein is conserved in all the other *Drosophila* species and also in other Insects (*Culex quinquefasciatus*, *Apis mellifera*, *Pediculus humanus* and *Acyrthosiphon pisum*). *2mit* orthologues in all Drosophilid species display also conserved synteny, with *2mit* sequence intronic of *tim2* locus.

On the basis of the data available before my PhD project, *2mit* mRNA is expressed from early embryonic stages, mainly concentrating in the developing nervous system. Moreover, an early *2mit* KD, dsRNAi-mediated using *ActGal4* driver, caused lethality at late pupal stage, with developmental defects regarding the abdominal region. These previous findings suggested that *2mit* might play an essential role during development, in particular during metamorphosis.

Since the *2mit*'s host gene *tim2* has a pleiotropic role, with functions in both chromosome stability (fundamental during development) and light synchronization of the circadian clock in adult (Benna et al., 2010), my PhD project was developed to explore the role of *2mit* in *Drosophila*, paying particular attention on the adult stage. This study was performed also with the aim to evaluate the possible relationship between *2mit* nested and *tim2* host genes. In fact, an intronic gene can present co-regulated expression and/or correlated function with respect to its host gene (Gibson et al., 2005).

We have found that, in adult wild-type heads, *2mit* mRNA levels show a slight 24 h daily oscillation in 12:12 LD regime. In DD regime mRNA expression became constitutive, meaning that *2mit* is not subjected to a circadian regulation, as it was previously demonstrated for *tim2* mRNA (Benna et al., 2010).

Comparing the *2mit* and *tim2* mRNAs expression profiles in wild-type heads in 12:12 LD, the 24 h *2mit* mRNA kinetics was different from that of *tim2*, with *2mit* mRNA peaking around the end of the night, and *tim2* mRNA around the end of the day/beginning of the night. The difference between the two peaks was 8 h, a value which is neither in phase nor in anti-phase. However, *Drosophila* adult head is composed by different tissues (being mainly formed by brain and compound

eyes). Therefore, the absence of a *2mit-tim2* co-regulation in this kind of sample might be not representative of a hypothetical tissue-specific co-regulation at level of single organs. Therefore we analysed *2mit* mRNA expression and its possible co-regulation with that of *tim2* at level of adult brain. We have shown that in this organ *2mit* mRNA is mainly expressed in the ellipsoid-body and in mushroom bodies. The ellipsoid-body is part of the central complex, which is the brain structure involved in the control of locomotor activity in *Drosophila* adult stage (Strauss and Heisenberg, 1993; Strauss, 2002), exerting also an auxiliary role in memory (Joiner and Griffith, 1999; Sitnik et al., 2003; Neuser et al., 2008; Liu et al., 2006). Concerning mushroom bodies, their main function is related to olfactory learning and memory (de Belle and Heisenberg, 1994; Heisenberg, 2003; Zars et al., 2000; Pascual and Preat, 2001; Blum et al., 2009) even if they also influence locomotor activity behaviour (Martin et al., 1998). In addition, *2mit* mRNA was weakly detected in correspondence to optic lobes. It is therefore interesting to note that in the adult brain *2mit* and *tim2* expression patterns appear to be complementary. In fact, Benna and colleagues (2010) demonstrated a strong *tim2* mRNA expression at level of optic lobe and a weak *tim2* mRNA presence in mushroom bodies and ellipsoid-body. It might therefore exist a sort of tissue specific regulation between *tim2* and *2mit* mRNA expressions, responsible of a weak *2mit* transcription in the regions where *tim2* host gene expression is prominent and *viceversa*.

Subsequently, by determining the *2mit* mRNA expression levels in six strains carrying a transposon insertion in proximity or inside *2mit* locus, we identified a *2mit* hypomorphic strain, $PB2mit^{c03963}$, whose *PB* transposon insertion causes a *2mit* mRNA expression of 50% in larvae and 15% in adult heads compared to wild-type. These *2mit* mRNA decremented levels in the $PB2mit^{c03963}$ strain were confirmed after outcrossing. In the $PB2mit^{c03963}$ strain the transposon insertion is localized within *tim2*'s 11^{th} intron at ~20 kb upstream *2mit* locus with respect to *2mit* orientation, probably in correspondence to an enhancer region required for *2mit* expression. Importantly, this insertion does not influence the expression levels of *tim2* mRNA and of the other transcribed sequences belonging to the *tim2* locus. The *2mit* mRNA depletion in the $PB2mit^{c03963}$ strain was also confirmed by *in situ* mRNA hybridization experiments showing that, in this mutant, *2mit* mRNA expression in mushroom bodies and in the ellipsoid-body of the adult brain was seriously reduced.

Afterwards, in order to determine *2mit* role in *Drosophila* adult nervous system, *2mit* functional characterization was conducted through phenotypical analyses on $PB2mit^{c03963}$ insertional mutants and on *2miti* lines with dsRNAi-mediated *2mit* KD driven in whole nervous system or in different regions of the adult brain.

We have found that, contrarily to previous experiments, showing that dsRNAi-mediated ubiquitous *2mit* KD leads to pupal lethality with defects in abdomen morphology, $PB2mit^{c03963}$ individuals were homozygous viable and without any morphological abnormality. Anyway, the reduced longevity at adult stage of

PB2mit^{c03963} individuals suggested that *2mit* mRNA decrement in the adult may cause impairments affecting flies lifespan. So, the effects of pupal lethality seen in the *ActGal4/2miti* lines seem to have been postponed to the adult stage in the *PB2mit*^{c03963} mutants. The 50% *2mit* mRNA decrement showed in *PB2mit*^{c03963} individuals at larval stage, represents a heterozygous condition that allows individuals to overcome metamorphosis and reach the adult stage. The putative stronger *2mit* down-regulation in *ActGal4/2miti* lines appears to have a greater impact during development. To test this hypothesis, Northern blot experiments will be performed in order to directly compare the relative amounts of *2mit* mRNA between the *PB2mit*^{c03963} insertional mutant and lines with *2mit* KD due to RNAi machinery activation. Moreover, rescue experiments overexpressing 2MIT-HA in *PB2mit*^{c03963} background have to be performed in order to verify *2mit* effective involvement in lifespan.

In wild-type brains at level optic lobes, we noticed the presence of a *2mit* mRNA hybridization signal, even if weak. With the aim to determine whether *2mit* transcription in these brain regions might have a functional meaning, we analysed the optomotor response of *2mit* KD induced by either insertional mutation (*PB2mit*^{c03963}) or RNAi induction (*driverGal4/2miti* lines).We have found that *PB2mit*^{c03963} flies showed a defective optomotor response, meaning that they presented impairments in optic-motor coordination capabilities. Anyway, the optomotor response was not affected by RNAi-mediated *2mit* down-regulation driven in the whole nervous system or in specific compartments of the visual system. A possible explanation could be that the pan-neuronal *2mit* KD was not enough sufficient to decrease *2mit* mRNA levels till those of the *PB2mit*^{c03963} strain, and consequently to elicit a defective optomotor response. In addition, when we performed rescue experiments evaluating the optomotor response in transgenic lines, carrying constructs for pan-neuronal *2mit* overexpression in the *PB2mit*^{c03963} mutant genetic background, we demonstrated a recovery of the optomotor response in one out of the three analysed lines. Despite we have to explore the reason of absent recovery of the optomotor phenotype in the remaining two *2mit* overexpressing lines, these data strongly indicate a role of *2mit* gene in neuronal pathways which mediate the motion vision in optic lobes. Albeit the optomotor response processing starts at the level of R1-6 retinal photoreceptors (Heisenberg and Buchner, 1977; Borst et al., 2010), in collaboration with Prof. Aram Megighian (Derpartment of Physiology, University of Padova, Italy) it was demonstrated that *2mit* function in motion vision does not localize in the retina. Its role has therefore to be searched in optic lobe structures involved in the motion visual response. However, in optic lobes there are different neuronal pathways mediating inputs underlying motion vision, and so far these pathways are not clearly defined. For example it is reported that the two most prominent pathways are mediated by L1 and L2 monopolar cells of the lamina and that T1 basket cells are implicated in motion detection at particular environmental conditions (Rister et al., 2007). Despite also *tim2* is expressed in

optic lobes (Benna et al., 2010), we have shown that the function in motion vision seems to be characteristic of *2mit* and not of its host gene *tim2*. Lobula plate tangential neurons are reported to represent the final step, in the optic lobe, for the transmission of motion information to fly motor centers (Hausen, 1984; Hengstenberg et al., 1982; Douglass and Strausfeld, 1996; Borst et al., 2010). Therefore, one of our future goals is to elucidate which optic lobe neurons could be considered as candidates for *2mit* expression and its subsequent implication in motion vision. This might be investigated mapping the recovery of the optomotor response in lines overexpressing 2MIT in specific optic lobe subregions in the $PB2mit^{c03963}$ mutant background.

Consistently with *2mit* mRNA expression pattern in mushroom bodies, playing a key role in memory formation (Heisenberg, 1998; Heisenberg, 2003; Zars et al., 2000; Pascual and Preat, 2001; Blum et al., 2009), and in the ellipsoid-body of the central complex, also implicated in memory (Sitnik, 2003; Joiner and Griffith, 1999), our results argue in favor of *2mit* role in short-term associative memory. In fact $PB2mit^{c03963}$ mutants exhibited memory impairments on courtship conditioning assay and this behaviour has been restored to wild-type characteristics in rescue experiments, through pan-neuronal *2mit* overexpression in the $PB2mit^{c03963}$ mutant background. Interestingly, the same line that had showed rescue of optomotor response displayed also recovery of the short-term associative memory phenotype. Anyway, until now, rescue experiments of the memory phenotype have been performed for only one of three available lines, and have to be repeated for the two missing ones. Moreover, given *tim2* slight expression in mushroom bodies and ellipsoid-body, it is important to establish whether *tim2* shares with its intronic gene *2mit* the same involvement in the memory phenotype. Currently, preliminary courtship conditioning experiments performed on a $tim2^{-}/+$ mutant strain, showed that these mutants do not show any impairment in the memory phenotype, suggesting that *tim2* is not involved in the control of this phenotype.

On the basis of the data available so far, it is not easy to localize 2MIT protein in a putative model for memory formation. Anyway, in literature it is reported that mushroom bodies anatomical components present a functional specialization, being γ lobes responsible for short-term memory and α/β lobes for long-term memory phenotype (Zars et al., 2000; Pascual and Preat, 2001; Fahrbach, 2006; Blum et al., 2009). Given *2mit* role in short-term memory, further analyses need to be performed in order to identify a possible functional correlation at level of mushroom bodies γ lobes, with proteins having known roles in the synaptic circuits elaborating short-term memory. In fact, *Drosophila* memory formation has been extensively explored, demonstrating that several proteins contribute to the occurrence of this phenotype. For example, proteins belonging to the cAMP signaling pathway (*dunce*, *rutabaga* and *amnesiac*), the Calcium/calmodulin-dependent protein kinase II (CaMKII), ion channels and ion channels-related proteins, and the protein kinase C (PKC) (Griffith et al., 1994; O'Dell et al., 1999;

Kane et al., 1997; Cowan and Siegel, 1984; Mehren et al., 2004) are important in the short-term memory formation. One possible strategy might be to analyse the memory phenotype in double mutant strains, carrying mutations on *2mit* gene and on each of the other genes involved in the memory phenotype. From these analyses it will be possible to dissect the memory pathway in which *2mit* gene seems to be involved.

Our data have displayed that *2mit* is not involved in adult circadian photoreception as *tim2* host gene (Benna et al., 2010). Anyway, our initial results supported the existence of a role for *2mit* in the control of circadian rhythmicity. In fact both $PB2mit^{c03963}$ insertional mutant and pan-neuronal *2mit* RNAi young flies showed a lengthening in *free running* circadian periodicity. Interestingly, at molecular level young $PB2mit^{c03963}$ flies showed an altered PER protein nuclear accumulation profile, accordingly to the increased periodicity in their circadian locomotor behaviour. In older $PB2mit^{c03963}$ insertional mutants, this phenotype was emphasized, while pan-neuronal *2mit* KD individuals displayed an increased arhythmic behaviour. Nevertheless, in rescue experiments, performed to verify the effective *2mit* role in the control of this phenotype, negative controls (characterized by inactive *2mitHA* transgene or by the driver construct alone, in $PB2mit^{c03963}$ mutant background), did not maintain the altered phenotype, behaving as wild-type. So, *2mit* involvement in the control of circadian rhythmicity was not confirmed. One hypothesis explaining the instability of this phenotype deals with a possible *2mit* auxiliary and/or dispensable role in circadian rhythmicity. Moreover, *2mit* may need to interact with other elements in the genome exercising a complementary or a synergistic role. In addition, mRNA *in situ* hybridization experiments displayed that *2mit* mRNA is not expressed in circadian clock neurons. Therefore, if *2mit* gene is really responsible of somehow effects on circadian behaviour, probably this function has to be indirect.

Furthermore, despite a strong *2mit* mRNA expression in the ellipsoid-body of the central complex, our results did not address a role for *2mit* in the control of general locomotor activity at adult stage.

By screening a *Drosophila* cDNA library in the yeast-two hybrid system we demonstrated that 2MIT extracellular portion (2MIT ED) interacts with the K^+-dependent NA^+:Ca^{2+} exchanger NCKX30C (Haug-Collet et al., 1999; Webel et al., 2002). We found as putative 2MIT ED interactor also the protocadherin FLAMINGO, but it was subsequently excluded, because we found that the interaction occurred between 2MIT ED and FLAMINGO C-terminal portion, reported to be intracellular (Chae et al., 1999; Usui et al., 1999; Liu et al., 1999).

As 2MIT, also NCKX30C antiporter is a transmembrane protein expressed during all developmental stages and localized in photoreceptor cells and optic lobes of the adult nervous system (Haug-Collet et al., 1999). So, the two proteins may co-localize or be in proximity within optic lobes. Anyhow, it will be necessary to verify 2MIT-NCKX30C interaction *in vivo* through co-immunoprecipitation experiments. If the interaction is confirmed, the molecular and behavioural

characterization of strains, presenting *Nckx30C* depleted levels, has to be performed in order to evaluate if the two proteins display functional correlation.

In conclusion, on the basis of the results obtained, 2MIT protein might act as a brain membrane receptor in the adult nervous system of *Drosophila*, with an involvement in different neuronal circuits. Specifically, our data support a role of 2MIT in the neural processing of motion vision and of short-term associative memory. Therefore, in the adult nervous system of *Drosophila melanogaster*, *2mit* intronic gene exerts a different function with respect to its host gene *tim2*. In fact, *2mit* is not involved in circadian photoreception as *tim2*; on the other hand, *tim2* is not involved in motion vision response and preliminary experiments seem to suggest that it is not involved in the memory phenotype. If a relation between these two genes exists, it seems to be at level of mRNA expression, which in the adult brain appeared to be complementary. Anyway, an aspect that is shared between *tim2* and *2mit* genes is their pleiotropic roles. *tim2* is involved in chromosome stability and circadian photoreception (Benna et al., 2010) and we demonstrated an involvement of *2mit* in vision and memory in adults. In addition, *2mit* could exert different functions depending on the developmental stage in which it is expressed. So, once completed the analyses regarding the elucidation of *2mit* function at the adult stage, it would be interesting to shift our attention to developmental stages, in order to establish if *2mit* might have a role also in preadult life. This putative role has also been suggested by the phenotypical effects of pupal lethality caused by a general *2mit* RNAi-mediated down-regulation, which indicated an essential role for *2mit* during development.

Moreover, in a wider perspective, the elucidation of *2mit* role in *Drosophila melanogaster* contributes to shed light on functions of *2mit* homologue sequences identified in other Insects.

References

Ackerman SL and Siegel RW (1986). Chemically reinforced conditioned courtship in *Drosophila*: responses of wild-type and the *dunce*, *amnesiac* and *don giovanni* mutants. *J Neurogenet* 3:111-123.

Adams MD et al. (2000). The genome sequence of *Drosophila melanogaster*. *Science* 287(5461):2185-95.

Allada R, White NE, So WV, Hall JC, Rosbash M (1998). A mutant *Drosophila* homolog of mammalian Clock disrupts circadian rhythms and transcription of *period* and *timeless*. *Cell* 93:791-804.

Allada R and Chung BY (2010). Circadian organization of behavior and physiology in *Drosophila*. *Annu Rev Physiol.* 72:605-24.

Aso Y, Grübel K, Busch S, Friedrich AB, Siwanowicz I, Tanimoto H (2009). The mushroom body of adult *Drosophila* characterized by GAL4 drivers. *J Neurogenet* 23:156-72.

Assis R, Kondrashov AS, Koonin EV, Kondrashov FA (2008). Nested genes and increasing organizational complexity of metazoan genomes. *Trends Genet.* 24:475-478.

Bastock M, Manning A (1955). The courtship of *Drosophila melanogaster*. *Behavior* 8:85-111.

Bell JK, Botos I, Hall PR, Askins J, Shiloach J, Segal DM, Davies DR (2005). The molecular structure of the Toll-like receptor 3 ligand-binding domain. *Proc Natl Acad Sci USA*. 102:10976-80.

Bella J, Hindle KL, McEwan PA, Lovell SC (2008). The leucine-rich repeat structure. *Cell Mol Life Sci.* 65:2307-33.

Bellen HJ, Levis RW, Liao G, He Y, Carlson JW, Tsang G, Evans-Holm M, Hiesinger PR, Schulze KL, Rubin GM, Hoskins RA, Spradling AC (2004). The BDGP gene disruption project: single transposon insertions associated with 40% of *Drosophila* genes. *Genetics.* 167(2):761-81.

Bendixen C, Gangloff S, Rothstein R (1994). A yeast mating-selection scheme for detection of protein-protein interactions. *Nucleic Acids Res.* 22:1778-1779.

Benna C, Scannapieco P, Piccin A, Sandrelli F, Zordan M, Rosato E, Kyriacou CP, Valle G, Costa R (2000). A second *timeless* gene in *Drosophila* shares greater sequence similarity with mammalian *tim*. *Curr Biol* 10R:512-513.

Benna C, Bonaccorsi S, Wülbeck C, Helfrich-Förster C, Gatti M, Kyriacou CP, Costa R, Sandrelli F (2010). *Drosophila timeless2* is required for chromosome stability and circadian photoreception. *Curr Biol.* 20(4):346-52.

Besson M and Martin JR (2005). Centrophobism/thigmotaxis, a new role for the mushroom bodies in *Drosophila*. *J Neurobiol.* 62(3):386-96.

Blondeau J and Heisenberg M (1982). The three-dimensional optomotor torque system of *Drosophila melanogaster*. *J. Comp. Physiol. A* 145:321-329.

Blum AL, Li W, Cressy M, Dubnau J (2009). Short- and long-term memory in *Drosophila* require cAMP signaling in distinct neuron types. *Curr Biol.* 19(16):1341-50.

Borst A (2009). *Drosophila*'s view on insect vision. *Curr Biol.* 19(1):R36-47.

Borst A, Haag J, Reiff DF (2010). Fly motion vision. *Annu Rev Neurosci.* 33:49-70.

Brand AH and Perrimon N (1993). Targeted gene expression as a means of altering cell fates and generating dominant phenotypes. *Development* 118:401-415.

Bray S and Amrein H (2003). A putative *Drosophila* pheromone receptor expressed in male-specific taste neurons is required for efficient courtship. *Neuron* 39:1019-1029.

Brotz T and Borst A (1996). Cholinergic and GABAergic receptors on fly tangential cells and their role in visual motion detection. *J. Neurophysiol.* 76:1786-99.

Broughton SJ, Piper MD, Ikeya T, Bass TM, Jacobson J, Driege Y, Martinez P, Hafen E, Withers DJ, Leevers SJ, Partridge L (2005). Longer lifespan, altered metabolism, and stress resistance in *Drosophila* from ablation of cells making insulin-like ligands. *Proc. Natl. Acad. Sci. USA.* 102:3105–3110.

Burnet B and Beck J (1968). Phenogenetic studies on visual acuity in *Drosophila melanogaster*. *J. Insect Physiol.* 57:855-860.

Byers D, Davis RL, Kiger JA Jr (1981). Defect in cyclic AMP phosphodiesterase due to the *dunce* mutation of learning in *Drosophila melanogaster*. *Nature* 289(5793):79-81.

Cavallari N, Frigato E, Vallone D, Fröhlich N, Lopez-Olmeda JF, Foà A, Berti R, Sánchez-Vázquez FJ, Bertolucci C, Foulkes NS (2011). A blind circadian clock in cavefish reveals that opsins mediate peripheral clock photoreception. *PLoS Biol.* 9(9):e1001142.

Cavener DR and Ray SC (1991). Eukaryotic start and stop translation sites. *Nucleic Acids Res* 19:3185-92.

Cawthon RM, O'Connell P, Buchberg AM, Viskochil D, Weiss RB, Culver M, Stevens J, Jenkins NA, Copeland NG, White R (1990). Identification and characterization of transcripts from the *neurofibromatosis 1* region: the sequence and genomic structure of *EVI2* and mapping of other transcripts. *Genomics.* 7(4):555-65.

Chae J, Kim MJ, Goo JH, Collier S, Gubb D, Charlton J, Adler PN, Park WJ (1999). The *Drosophila* tissue polarity gene *starry night* encodes a member of the protocadherin family. *Development* 126(23):5421-9.

Chen CN, Malone T, Beckendorf SK, Davis RL (1987). At least two genes reside within a large intron of the *dunce* gene of *Drosophila*. *Nature* 329:721-724.

Chien CT, Bartel PL, Sternglanz R, Fields S (1991). The two-hybrid system: A method to identify and clone genes for proteins that interact with a protein of interest. Proc. Nat. Acad. Sci. USA 88:9578-9582.

Clancy DJ, Gems D, Harshman LG, Oldham S, Stocker H, Hafen E, Leevers SJ, Partridge L (2001). Extension of life-span by loss of CHICO, a *Drosophila* insulin receptor substrate protein. *Science* 292:104-106.

Coelho PS, Bryan AC, Kumar A, Shadel GS, Snyder M (2002). A novel mitochondrial protein, Tar1p, is encoded on the antisense strand of the nuclear 25S rDNA. *Genes Dev.* 16**:**2755-2760.

Coggshall JC, Boschek CB, Buchner SM (1973). Preliminary investigations on a pair of giant fibers in the central nervous system of dipteran flies. *Z. Naturforsch.* 28c:783-784.

Cowan TM and Siegel RW (1984). Mutational and pharmacological alterations of neuronal membrane function disrupt conditioning in *Drosophila*. *J Neurogenet* 1:333-344.

Crittenden JR, Skoulakis EM, Han KA, Kalderon D, Davis RL (1998). Tripartite mushroom body architecture revealed by antigenic markers. *Learn Mem.* 5(1-2):38-51.

Curtin KD, Huang ZJ, Rosbash M (1995). Temporally regulated nuclear entry of the *Drosophila* period protein contributes to the circadian clock. *Neuron* 14:365-372.

Cyran SA, Buchsbaum AM, Reddy KL, Lin MC, Glossop NR, Hardin PE, Young MW, Storti RV, Blau J (2003). vrille, Pdp1, and dClock form a second feedback loop in the *Drosophila* circadian clock. *Cell* 112(3):329-41.

Darlington TK, Wager-Smith K, Ceriani MF, Staknis D, Gekakis N, Steeves TD, Weitz CJ, Takahashi JS, Kay SA (1998). Closing the circadian loop: CLOCK-induced transcription of its own inhibitors per and *tim*. *Science.* 280(5369):1599-603.

Davis RL (2005). Olfactory memory formation in *Drosophila*: from molecular to systems neuroscience. *Annu Rev Neurosci.* 28:275-302.

de Belle JS, Heisenberg M (1994). Associative odor learning in *Drosophila* abolished by chemical ablation of mushroom bodies. *Science* 263(5147):692-5.

Dolan J, Walshe K, Alsbury S, Hokamp K, O'Keeffe S, Okafuji T, Miller SF, Tear G, Mitchell KJ (2007). The extracellular leucine-rich repeat superfamily; a comparative survey and analysis of evolutionary relationships and expression patterns. *BMC Genomics.* 14:8-320.

Douglass JK and Strausfeld NJ (1996). Visual motion-detection circuits in flies: parallel direction- and non-direction-sensitive pathways between the medulla and lobula plate. *J. Neurosci.* 16:4551-4562.

Ejima A, Smith BP, Lucas C, Levine JD, Griffith LC (2005). Sequential learning of pheromonal cues modulates memory consolidation in trainer-specific associative courtship conditioning. *Curr Biol* 15:194-206.

Ejima A and Griffith LC (2008). Courtship initiation is stimulated by acoustic signals in *Drosophila melanogaster*. *PLoS One* 3: e3246. doi: 10.1371/journal.pone.0003246.

Emery P, So WV, Kaneko M, Hall JC, Rosbash M (1998). CRY, a *Drosophila* clock and light-regulated cryptochrome, is a major contributor to circadian rhythm resetting and photosensitivity. *Cell* 95(5):669-79.

Fahrbach SE (2006). Structure of the mushroom bodies of the insect brain. *Annu Rev Entomol.* 51:209-32.

Feany MB and Quinn WG (1995). A neuropeptide gene defined by the *Drosophila* memory mutant *amnesiac*. *Science* 268(5212):869-73.

Feliciello I and Chinali G (1993). A modified alkaline lysis method for the preparation of highly purified plasmid DNA from *Escherichia coli*. *Anal. Biochem*. 212:394-401.

Ferveur JF (2005). Cuticular hydrocarbons: Their evolution and roles in *Drosophila* pheromonal communication. *Behav Genet* 35:279-295.

Fields S and Song O (1989). A novel genetic system to detect protein-protein interactions. *Nature* 340:245-247.

Fischbach KF and Dittrich APM (1989). The optic lobe of *Drosophila melanogaster*. A Golgi analysis of wild-type structure. *Cell Tissue Res.* 258:441-475.

Franceschini N, Riehle A, Le Nestour A (1989). Directionally selective motion detection by insect neurons. In: Stavenga DG, Hardie RC, editors. Facets of vision. Heidelberg: Springer; pp. 360–90.

Furia M, D'Avino PP, Crispi S, Artiaco D, Polito LC (1993). Dense cluster of genes is located at the ecdysone-regulated 3C puff of *Drosophila melanogaster*. *J Mol Biol.* 231(2):531-8.

Gibson CW, Thomson NH, Abrams WR, Kirkham J (2005). Nested genes: biological implications and use of AFM for analysis. *Gene* 350**:**15-23.

Gorczyca MG, Phillis RW, Budnik V (1994). The role of *tinman*, a mesodermal cell fate gene, in axon pathfinding during the development of the transverse nerve in *Drosophila*. *Development.*120:2143-2152.

Gotter AL, Mangarano T, Weave DR, Kolakowsky LF Jr, Possidente B, Sriram S, MacLaughlin DT, Reppert SM (2000). A time-less function for mouse Timeless. *Nature Neurosci* 3:755-756.

Griffith LC, Wang J, Zhong Y, Wu C-F, Greenspan RJ (1994). Calcium/calmodulin-dependent protein kinase II and potassium channel subunit Eag similarly affect plasticity in *Drosophila*. *Proc Natl Acad Sci USA* 91:10044-10048.

Griffith LC and Ejima A (2009). Courtship learning in *Drosophila melanogaster*: diverse plasticity of a reproductive behavior. *Learn Mem.* 16(12):743-50.

Grima B, Lamouroux A, Chelot E, Papin C, Limbourg-Bouchon B, Rouyer F (2002). The F-box protein slimb controls the levels of clock proteins period and timeless. *Nature* 420:178-182.

Grima B, Chélot E, Xia R, Rouyer F (2004). Morning and evening peaks of activity rely on different clock neurons of the *Drosophila* brain. *Nature* 431(7010):869-73.

Gronke S, Clarke DF, Broughton S, Andrews TD, Partridge L (2010). Molecular evolution and functional characterization of *Drosophila* insulin-like peptides. *PLoS Genet.* 6:e1000857.

Guindon S and Gascuel O (2003). A simple, fast, and accurate algorithm to estimate large phylogenies by maximum likelihood. *Syst Biol.* 52(5):696-704.

Haag J, Wertz A, Borst A (2007). Integration of lobula plate output signals by DNOVS1, an identified premotor descending neuron. *J. Neurosci.* 27:1992-2000.

Habib AA, Gulcher JR, Högnason T, Zheng L, Stefánsson K (1998a). The *OMgp* gene, a second growth suppressor within the NF1 gene. *Oncogene* 16(12):1525-31.

Habib AA, Marton LS, Allwardt B, Gulcher JR, Mikol DD, Högnason T, Chattopadhyay N, Stefansson K (1998b). Expression of the oligodendrocyte-myelin glycoprotein by neurons in the mouse central nervous system. *J Neurochem.* 70(4):1704-11.

Hall JC (2003). Genetics and molecular biology of rhythms in *Drosophila* and other insects. *Adv. Genet* 48:1-208.

Halligan DL and Keightley PD (2006). Ubiquitous selective constraints in the *Drosophila* genome revealed by a genome-wide interspecies comparison. *Genome Res.* 16(7):875-84.

Hanesch U, Fischbach KF, Heisenberg M (1989). Neuronal architecture of the central complex in *Drosophila melanogaster*. *Cell Tissue Res*. 257:343-366.

Hardie RC(1989). A histamine-activated chloride channel involved in neurotransmission at a photoreceptor synapse. *Nature* 339:704-706.

Haug-Collet K, Pearson B, Webel R, Szerencsei RT, Winkfein RJ, Schnetkamp PP, Colley NJ (1999). Cloning and characterization of a potassium-dependent sodium/calcium exchanger in *Drosophila*. *J Cell Biol.* 147(3):659-70.

Hausen K (1984). The lobula-complex of the fly: Structure, function and significance in visual behaviour. In Photoreception and Vision in Invertebrates, M.A. Ali, ed. (New York, London: Plenum Press), pp. 523–559.

He XL, Bazan JF, McDermott G, Park JB, Wang K, Tessier-Lavigne M, He Z, Garcia KC (2003). Structure of the Nogo receptor ectodomain: a recognition module implicated in myelin inhibition. *Neuron.* 38:177-85.

Heisenberg M and Buchner E (1977). The role of retinula cell types in visual behavior of *Drosophila melanogaster*. *J. Comp. Physiol. A* 117:127-162.

Heisenberg, M., Wonneberger, R., and Wolf, R. (1978). Optomotor-blind (H31) - a *Drosophila* mutant of the *lobula plate* giant neurons. *J. Comp. Physiol.A* 124:287-296.

Heisenberg M (1998). What do the mushroom bodies do for the insect brain? An introduction. *Learn. Mem.* 5:1-10.

Heisenberg M (2003). Mushroom body memoir: from maps to models. *Nat Rev Neurosci.* 4:266-275.

Helfrich-Forster C (2003). The neuroarchitecture of the circadian clock in the brain of *Drosophila* melanogaster. *Microsc. Res. Tech.* 62(2): 94-102.

Helfrich-Förster C, Yoshii T, Wülbeck C, Grieshaber E, Rieger D, Bachleitner W, Cusamano P, Rouyer F (2007). The lateral and dorsal neurons of *Drosophila melanogaster*: new insights about their morphology and function. *Cold Spring Harb Symp Quant Biol.*72:517-25.

Hengstenberg R, Hausen K, Hengstenberg B (1982). The number and structure of giant vertical cells (VS) in the lobula plate of the blowfly *Calliphora erytrocephala*. *J. Comp. Physiol. A* 149:163-177.

Henikoff S, Keene MA, Fechtel K, Fristrom JM (1986). Gene within a gene: nested *Drosophila* genes encode unrelated proteins on opposite DNA strands. *Cell* 44**:**33-42.

Henikoff S, Eghtedarzadeh MK (1987). Conserved arrangement of nested genes at the *Drosophila Gart* locus. *Genetics* 117:711-725.

Hofbauer A and Campos-Ortega JA (1990). Proliferation pattern and early differentiation of the optic lobes in *Drosophila melanogaster*. *Roux's Arch Dev Biol.* 198:264-74.

Homberg U. (1987) Structure and functions of the central complex in insects. In *Arthropod brain, its evolution, development, structure and function*s. Gupta, A.P. (ed) (John Wiley and Sons, New York), pp. 347-367.

Iwabuchi K, Li B, Bartel P, Fields S (1993). Use of the two-hybrid system to identify the domain of p53 involved in oligomerization. *Oncogene* 8:1693-1696.

Joesch M, Plett J, Borst A, Reiff DF (2008). Response properties of motion-sensitive visual interneurons in the lobula plate of *Drosophila melanogaster*. *Curr. Biol.* 18:368-374.

Johnstonen ME, Nash D, Naguib NF (1985). Three purine auxotrophic loci on the second chromosome of *Drosophila melanogaster*. *Biochem. Genet.* 23:539-555.

Joiner MA and Griffith LC (1999). Mapping of the anatomical circuit of CaM kinase-dependent courtship conditioning in *Drosophila*. *Learn Mem* 6:177-192.

Kajava A V (1998). Structural diversity of leucine-richrepeat proteins. *J. Mol. Biol.* 277:519-527.

Kalmus H (1961). The attenuation of optomotor responses in white-eyed mutants of *musca domestica* and of *coelopa frigida*. *Vision Research*, Volume 1, Issues 1-2, pp 192-197 IN9-IN10.

Kane NS, Robichon A, Dickinson JA, Greenspan RJ (1997). Learning without performance in PKC-deficient *Drosophila*. *Neuron* 18:307-314.

Kaneko M and Hall JC (2000). Neuroanatomy of cells expressing clock genes in *Drosophila*: transgenic manipulation of the *period* and *timeless* genes to mark the perikarya of circadian pacemaker neurons and their projections. *J Comp Neurol* 422(1):66-94.

Kaufmann D, Gruener S, Braun F, Stark M, Griesser J, Hoffmeyer S, Bartelt B (1999). *EVI2B*, a gene lying in an intron of the *neurofibromatosis type 1* (NF1) gene, is as the *NF1* gene involved in differentiation of melanocytes and keratinocytes and is overexpressed in cells derived from NF1 neurofibromas. *DNA Cell Biol.* 18(5):345-56.

Kimura H, Usui T, Tsubouchi A, Uemura T (2006). Potential dual molecular interaction of the *Drosophila* 7-pass transmembrane cadherin Flamingo in dendritic morphogenesis. *J Cell Sci.* 119(Pt 6):1118-29.

Klarsfeld A, Malpel S, Michard-Vanhée C, Picot M, Chélot E, Rouyer F (2004). Novel features of cryptochrome-mediated photoreception in the brain circadian clock of *Drosophila*. *J Neurosci* 24(6):1468-77.

Kobe B and Deisenhofer J (1993). Crystal structure of porcine ribonuclease inhibitor, a protein with leucine-rich repeats. *Nature* 366(6457):751-6.

Kobe B and Kajava AV (2001). The leucine-rich repeat as a protein recognition motif. *Curr Opin Struct Biol.* 11:725-32.

Koh K, Zheng X, Sehgal A (2006). JETLAG resets the *Drosophila* circadian clock by promoting light-induced degradation of TIMELESS. *Science* 312:1809-1812.

Kumar A (2009). An overview of nested genes in eukaryotic genomes. *Eukaryot Cell* 8:1321-1329.

Lee C, Parikh V, Itsukaichi T, Bae K, Edery I (1996). Resetting the *Drosophila* clock by photic regulation of PER and a PER-TIM complex. *Science* 271(5256):1740-4.

Lee T, Lee A, Luo L (1999a). Development of the *Drosophila* mushroom bodies: sequential generation of three distinct types of neurons from a neuroblast. *Development* 126:4065-4076.

Lee C, Bae K, Edery I (1999b). PER and TIM inhibit the DNA binding activity of a *Drosophila* CLOCK-CYC/dBMAL1 heterodimer without disrupting formation of the heterodimer: a basis for circadian transcription. *Mol. Cell. Biol.* 19:5316-5325.

Lee RC, Clandinin TR, Lee CH, Chen PL, Meinertzhagen IA, Zipursky SL (2003). The protocadherin Flamingo is required for axon target selection in the *Drosophila* visual system. *Nat Neurosci.* 6(6):557-63.

Leonardi E, Andreazza S, Vanin S, Busolin G, Nobile C, Tosatto SC (2011). A computational model of the LGI1 protein suggests a common binding site for ADAM proteins. *PLoS One.* 6(3):e18142.

Levin LR, Han PL, Hwang PM, Feinstein PG, Davis RL, Reed RR (1992). The *Drosophila* learning and memory gene *rutabaga* encodes a Ca2+/Calmodulin-responsive adenylyl cyclase. *Cell* 68(3):479-89.

Levine JD, Casey CI, Kalderon DD, Jackson FR (1994). Altered circadian pacemaker functions and cyclic AMP rhythms in the *Drosophila* learning mutant *dunce*. *Neuron* 13(4):967-74.

Li B and Fields S (1993). Identification of mutations in p53 that affect its binding to SV40 T antigen by using the yeast two-hybrid system. *FASEB J.* 7:957-963.

Lints FA, Le Bourg E, Lints CV (1984). Spontaneous locomotor activity and lifespan. A test of the rate of living theory in *Drosophila melanogaster. Gerontology* 30:376-87.

Liu G, Seiler H, Wen A, Zars T, Ito K, Wolf R, Heisenberg M, Liu L (2006). Distinct memory traces for two visual features in the *Drosophila* brain. *Nature* 439:551-556.

Lu B, Usui T, Uemura T, Jan L, Jan YN (1999). Flamingo controls the planar polarity of sensory bristles and asymmetric division of sensory organ precursors in *Drosophila*. *Curr Biol.* 9(21):1247-50.

Lynch M (2002). Intron evolution as a population-genetic process. *Proc. Natl. Acad. Sci. USA* 99**:**6118-6123.

Lynch M and Conery JS (2003). The origins of genome complexity. *Science* 302**:**1401-1404.

Ma J, Dobry CJ, Krysan DJ, Kumar A (2008). Unconventional genomic architecture in the budding yeast *Saccharomyces cerevisiae* masks the nested antisense gene *NAG1*. *Eukaryot. Cell* 7:1289-1298.

Malpel S, Klarsfeld A, Rouyer F (2002). Larval optic nerve and adult extra-retinal photoreceptors sequentially associate with clock neurons during *Drosophila* brain development. *Development* 129(6):1443-53.

Malpel S, Klarsfeld A, Rouyer F (2004). Circadian synchronization and rhythmicity in larval photoperception-defective mutants of *Drosophila*. *J Biol Rhythms.* 19(1):10-21.

Marder E and Bucher D (2001). Central pattern generators and the control of rhythmic movements. *Curr Biol.* 11(23):R986-96.

Margulies C, Tully T, Dubnau J (2005). Deconstructing memory in *Drosophila*. *Curr Biol.* 15(17):R700-13.

Marin EC, Jefferis GS, Komiyama T, Zhu H, Luo L (2002). Representation of the glomerular olfactory map in the *Drosophila* brain. *Cell* 109:243-255.

Martin JR, Ernst R, Heisenberg M (1998). Mushroom bodies suppress locomotor activity in *Drosophila melanogaster*. *Learn Mem.* 5(1-2):179-91.

Martin JR, Ernst R, Heisenberg M (1999a). Temporal pattern of locomotor activity in *Drosophila melanogaste*r. *J. Comp. Physiol. A* 184:73-84.

Martin JR, Raabe T, Heisenberg M (1999b). Central complex substructures are required for the maintenance of locomotor activity in *Drosophila melanogaster. J. Comp. Physiol. A*.185: 277-288.

Martin JR, Faure F, Ernst R (2001). The power law distribution for walking-time intervals correlates with the ellipsoid-body in *Drosophila*. *J. Neurogenet*. 15(3-4):205-19.

Martin JR (2003). Locomotor activity: a complex behavioural trait to unravel. *Behav. Process*. 64:145-160.

Martin JR (2004). A portrait of locomotor behaviour in *Drosophila* determined by a video-tracking paradigm. *Behav. Process.* 67:207-219.

Matsubara D, Horiuchi SY, Shimono K, Usui T, Uemura T (2011). The seven-pass transmembrane cadherin Flamingo controls dendritic self-avoidance via its binding to a LIM domain protein, Espinas, in *Drosophila* sensory neurons. *Genes Dev.* 25(18):1982-96.

Mazzoni EO, Desplan C, Blau J (2005). Circadian pacemaker neurons transmit and modulate visual information to control a rapid behavioral response. *Neuron* 45(2):293-300.

Mehren JE, Ejima A, Griffith LC (2004). Unconventional sex: fresh approaches to courtship learning. *Curr Opin Neurobiol.* 14:745-50.

Mehren JE and Griffith LC (2004). Calcium-independent calcium/calmodulin-dependent protein kinase II in the adult *Drosophila* CNS enhances the training of pheromonal cues. *J Neurosci.* 24(47):10584-93.

Meinertzhagen IA and O'Neil SD (1991). Synaptic organization of columnar elements in the lamina of the wild type in *Drosophila melanogaster*. *J. Comp. Neurol.* 305:232–263.

Meyer P, Saez L, Young MW (2006). PER-TIM interactions in living *Drosophila* cells: an interval timer for the circadian clock. *Science* 311(5758):226-9.

Miquel J, Lundgren PR, Bensch KG, Atlan H (1976). Effects of temperature on the life span, vitality and fine structure of *Drosophila melanogaster*. *Mech Ageing Dev.* 5(5):347-70.

Misra S et al. (2002). Annotation of the *Drosophila melanogaster* euchromatic genome: a systematic review. *Genome Biol.* 3(12):RESEARCH0083.

Miyasako Y, Umezaki Y, Tomioka K (2007). Separate sets of cerebral clock neurons are responsible for light and temperature entrainment of *Drosophila* circadian locomotor rhythms. *J Biol Rhythms* 22:115-126.

Morante J and Desplan C (2004). Building a projection map for photoreceptor neurons in the *Drosophila* optic lobes. *Semin Cell Dev Biol.* 15(1):137-43.

Mosyak L, Wood A, Dwyer B, Buddha M, Johnson M, Aulabaugh A, Zhong X, Presman E, Murad A, Emery-Le M, Emery P (2007). A subset of dorsal neurons modulates circadian behavior and light responses in *Drosophila*. *Neuron* 53:689-701.

Myers MP, Wager-Smith K, Wesley CS, Young MW, Sehgal A (1995). Positional cloning and sequence analysis of the *Drosophila* clock gene*, timeless*. *Science* 270(5237):805-8.

Neuser K, Triphan T, Mronz M, Poeck B, Strauss R (2008). Analysis of a spatial orientation memory in *Drosophila*. *Nature* 453:1244-1247.

Nitabach MN and Taghert PH (2008). Organization of the *Drosophila* circadian control circuit. *Curr Biol.* 18(2):R84-93.

O'Dell KMC, Jamieson D, Goodwin SF, Kaiser K (1999). Abnormal courtship conditioning in males mutant for the RI regulatory subunit of *Drosophila* protein kinase A. *J Neurogenet* 13:105-118.

O'Kane CJ (1998). Enhancer traps. In *Drosophila, a practical approach.* Series Editor: B. D. Hames, second edition. Edited by D. B. Roberts. pp 131-178.

Ousley A, Zafarullah K, Chen Y, Emerson M, Hickman L, Sehgal A (1998). Conserved regions of the *timeless* (*tim*) clock gene in *Drosophila* analyzed through phylogenetic and functional studies. *Genetics.* 148(2):815-25.

Partridge L, Alic N, Bjedov I, Piper MD (2011). Ageing in *Drosophila*: the role of the insulin/Igf and TOR signalling network. *Exp Gerontol.* 46(5):376-81.

Pascual A and Preat T (2001). Localization of long-term memory within the *Drosophila* mushroom body. *Science.* 294:1115-1117.

Peschel N, Veleri S, Stanewsky R (2006). Veela defines a molecular link between Cryptochrome and Timeless in the light-input pathway to *Drosophila*'s circadian clock. *Proc. Natl. Acad. Sci. USA* 103:17313-17318.

Peschel N and Helfrich-Förster C (2011). Setting the clock by nature: circadian rhythm in the fruitfly *Drosophila melanogaster*. *FEBS Lett.* 585(10):1435-42.

Pfaffl MW (2001). A new mathematical model for relative quantification in real-time RT-PCR. *Nucleic Acids Res.* 29(9):e45.

Pichaud F, Briscoe A, Desplan C (1999). Evolution of color vision. *Curr Opin Neurobiol.* 9(5):622-7.

Plautz JD, Kaneko M, Hall JC, Kay SA (1997). Independent photoreceptive circadian clocks throughout *Drosophila*. *Science.* 278(5343):1632-5.

Polaina J and Adam AC (1991). A fast procedure for yeast DNA purification. *Nucleic Acids Res.* 19(19):5443.

Price JL, Blau J, Rothenfluh A, Abodeely M, Kloss B, Young MW (1998). *Double-time* is a novel *Drosophila* clock gene that regulates PERIOD protein accumulation. *Cell* 94:83-95.

Qiu Y and Davis RL (1993). Genetic dissection of the learning/memory gene *dunce* of *Drosophila melanogaster*. *Genes Dev.* 7(7B):1447-58.

Raghu SV, Joesch M, Borst A, Reiff DF (2007). Synaptic organization of lobula plate tangential cells in *Drosophila*: GABA-receptors and chemical release sites. *J. Comp. Neurol.* 502:598-610.

Raghu SV, Joesch M, Sigrist S, Borst A, Reiff DF (2009). Synaptic organization of lobula plate tangential cells in *Drosophila*: Dα7 cholinergic receptors. *J. Neurogenetics* 23:200-9.

Rak B, Lusky M, Hable M (1982). Expression of two proteins from overlapping and oppositely oriented genes on transposable DNA insertion element IS5. *Nature* 297**:**124-128.

Rath A, Glibowicka M, Nadeau VG, Chen G, Deber CM (2009). Detergent binding explains anomalous SDS-PAGE migration of membrane proteins. *Proc Natl Acad Sci U SA* 106(6):1760-5.

Reiter LT, Potocki L, Chien S, Gribskov M, Bier E (2001). A systematic analysis of human disease-associated gene sequences in *Drosophila melanogaster*. *Genome Res.* 11(6):1114-25.

Renn SC, Armstrong JD, Yang M, Wang Z, An X, Kaiser K, Taghert PH (1999). Genetic analysis of the *Drosophila* ellipsoid body neuropil: organization and development of the central complex. *J Neurobiol.* 41(2):189-207.

Reuter JE, Nardine TM, Penton A, Billuart P, Scott EK, Usui T, Uemura T, Luo L (2003). A mosaic genetic screen for genes necessary for *Drosophila* mushroom body neuronal morphogenesis. *Development.* 130(6):1203-13.

Rister J, Pauls D, Schnell B, Ting CY, Lee CH, Sinakevitch I, Morante J, Strausfeld NJ, Ito K, Heisenberg M (2007). Dissection of the peripheral motion channel in the visual system of *Drosophila melanogaster*. *Neuron* 56:155-170.

Roberts DB and Standen GN (1998). The elements of *Drosophila* biology and genetics. pp.1-54 in *Drosophila: A Practical Approach*, edited by D. B. Roberts. IRL Press, Oxford.

Rosato E and Kyriacou CP (2006). Analysis of locomotor activity rhythms in *Drosophila*. *Nat Protoc.* 1(2):559-68.

Rutila JE, Suri V, Le M, So WV, Rosbash M, Hall JC (1998). CYCLE is a second bHLH-PAS clock protein essential for circadian rhythmicity and transcription of *Drosophila period* and *timeless*. *Cell* 93:805–814.

Sandrelli F, Campesan S, Rossetto M, Benna C, Zieger E, Megighian A, Couchman M, Kyriacou C, Costa R (2001). Molecular Dissection of the 5' Region of *no-on-transientA* of *Drosophila melanogaster* Reveals cis-Regulation by Adjacent *dGpi1* Sequences.. *Genetics.* 157(2):765-75.

Sandrelli F, Tauber E, Pegoraro M, Mazzotta G, Cisotto P, Landskron J, Stanewsky R, Piccin A, Rosato E, Zordan M, Costa R, Kyriacou CP (2007). A molecular basis for natural selection at the timeless locus in *Drosophila melanogaster*. *Science* 316(5833):1898-900.

Sanna CR, Li WH, Zhang L (2008). Overlapping genes in the human and mouse genomes. *BMC Genomics* 9**:**169.

Sawers RG (2005). Transcript analysis of *Escherichia coli* K-12 insertion element IS5. *FEMS Microbiol. Lett.* 244**:**397-401.

Sawin-McCormack EP, Sokolowski MB, Campos AR (1995). Characterization and genetic analysis of *Drosophila melanogaster* photobehavior during larval development. *J. Neurogenet.* 10:119-135.

Schwaerzel M, Monastirioti M, Scholz H, Friggi-Grelin F, Birman S, Heisenberg M (2003). Dopamine and octopamine differentiate between aversive and appetitive olfactory memories in *Drosophila*. *J Neurosci.* 23:10495-10502.

Scott EK, Raabe T, Luo L (2002). Structure of the vertical and horizontal system neurons of the lobula plate in *Drosophila*. *J. Comp. Neurol.* 454:470-481.

Sehgal A, Price JL, Man B, Young MW (1994). Loss of circadian behavioral rhythms and *per* RNA oscillations in the *Drosophila* mutant *timeless*. *Science* 263:1603-1606.

Senti KA, Usui T, Boucke K, Greber U, Uemura T, Dickson BJ (2003). Flamingo regulates R8 axon-axon and axon-target interactions in the *Drosophila* visual system. *Curr Biol.* 13(10):828-32.

Shafer OT, Rosbash M, Truman JW (2002). Sequential nuclear accumulation of the clock proteins period and timeless in the pacemaker neurons of *Drosophila melanogaster*. *J Neurosci* 22:5946-5954.

Shafer OT, Helfrich-Förster C, Renn SC, Taghert PH (2006). Reevaluation of *Drosophila melanogaster*'s neuronal circadian pacemakers reveals new neuronal classes. *J Comp Neurol.* 498(2):180-93.

Sheeba V, Fogle KJ, Kaneko M, Rashid S, Chou YT, Sharma VK, Holmes TC (2008). Large ventral lateral neurons modulate arousal and sleep in *Drosophila*. *Curr Biol* 18:1537-1545.

Siegel RW and Hall JC (1979). Conditioned responses in courtship behavior of normal and mutant *Drosophila*. *Proc Natl Acad Sci U S A* 76(7):3430-4.

Sitnik NA, Tokmacheva EV, Savvateeva-Popova EV (2003). The ability of *Drosophila* mutants with defects in the central complex and mushroom bodies to learn and form memories. *Neurosci Behav Physiol* 33:67-71.

Stoleru D, Peng Y, Agosto J, Rosbash M (2004). Coupled oscillators control morning and evening locomotor behaviour of *Drosophila. Nature* 431:862-868.

Stoleru D, Nawathean P, Fernandez MP, Menet JS, Ceriani MF, Rosbash M (2007). The *Drosophila* circadian network is a seasonal timer. *Cell* 129:207-219.

Strausfeld NJ (1976). Mosaic organizations, layers, and visual pathways in the insect brain. In: Zettler F, Weiler R, editors. Neural principles in vision. Berlin: Springer-Verlag; pp. 245-79.

Strausfeld NJ and Lee JK (1991). Neuronal basis for parallel visual processing in the fly. *Vis. Neurosci.* 7:13-33.

Strauss R, Hanesch U, Kinkelin M, Wolf R, Heisenberg M (1992). *No-bridge* of *Drosophila melanogaster*: portrait of a structural brain mutant of the central complex. *J. Neurogenet*. 8:125-155.

Strauss R and Heisenberg M (1993). A higher control center of locomotor behavior in the *Drosophila* brain. *J. Neurosci*. 13:1852-1861.

Strauss R (2002). The central complex and the genetic dissection of locomotor behaviour. *Curr. Opin. Neurobiol.* 12:633-638.

Suster ML, Martin JR, Sung C, Robinow S (2003). Targeted expression of tetanus toxin reveals sets of neurons involved in larval locomotion in *Drosophila. J Neurobiol.* 55(2):233-46.

Takemura SY, Lu Z, Meinertzhagen IA (2008). Synaptic circuits of the *Drosophila* optic lobe: the input terminals to the medulla. *J. Comp. Neurol.* 509:493–513.

Tatar M, Kopelman A, Epstein D, Tu MP, Yin CM, Garofalo RS (2001). A mutant *Drosophila* insulin receptor homolog that extends life-span and impairs neuroendocrine function. *Science* 292:107-110.

Tauber E and Eberl DF (2003). Acoustic communication in *Drosophila*. *Behav Processes* 64:197-210.

Tauber E, Zordan M, Sandrelli F, Pegoraro M, Osterwalder N, Breda C, Daga A, Selmin A, Monger K, Benna C, Rosato E, Kyriacou CP, Costa R (2007). Natural selection favors a newly derived *timeless* allele in *Drosophila melanogaster*. *Science* 316(5833):1895-8.

Ting CY and Lee CH (2007). Visual circuit development in *Drosophila*. *Curr Opin Neurobiol.* 17(1):65-72.

Tiong, S Y and Nash D (1990). Genetic analysis of the *adenosine3* (*Gart*) region of the second chromosome of *Drosophila melanogaster*. *Genetics* 124:889-897.

Tompkins L, Siegel RW, Gailey DA, Hall JC (1983). Conditioned courtship in *Drosophila* and its mediation by association of chemical cues. *Behav. Genet.* 13:565-578.

Tully T, Preat T, Boynton SC, Del Vecchio M (1994). Genetic dissection of consolidated memory in *Drosophila*. *Cell* 79:35-47.

Uptain SM, Kane CM, Chamberlin MJ (1997). Basic mechanisms of transcript elongation and its regulation. *Ann. Rev. Biochem.* 66:117-172

Usui T, Shima Y, Shimada Y, Hirano S, Burgess RW, Schwarz TL, Takeichi M, Uemura T (1999). Flamingo, a seven-pass transmembrane cadherin, regulates planar cell polarity under the control of Frizzled. *Cell* 98(5):585-95.

Veleri S, Brandes C, Helfrich-Forster C, Hall JC, Stanewsky R (2003). A self-sustaining, lightentrainable circadian oscillator in the *Drosophila* brain. *Curr Biol* 13:1758-1767.

Viskochil D, White R, Cawthon R (1993). The *neurofibromatosis type 1* gene. *Annu. Rev. Neurosci*. 16:183-205.

Wang T and Montell C (2007). Phototransduction and retinal degeneration in *Drosophila. Pflugers Arch.* 454(5):821-47.

Webel R, Haug-Collet K, Pearson B, Szerencsei RT, Winkfein RJ, Schnetkamp PP, Colley NJ (2002). Potassium-dependent sodium-calcium exchange through the eye of the fly. *Ann N Y Acad Sci.* 976:300-14.

Wertz A, Borst A, Haag J (2008). Nonlinear integration of binocular optic flow by DNOVS2, a descending neuron of the fly. *J. Neurosci.* 28:3131-40.

Wong AM, Wang JW, Axel R (2002). Spatial representation of the glomerular map in the *Drosophila* protocerebrum. *Cell* 109:229-241.

Wright GJ (2009). Signal initiation in biological systems: the properties and detection of transient extracellular protein interactions. *Mol Biosyst.* 5(12):1405-12.

Wülbeck C and Helfrich-Förster C (2007). RNA *in situ* hybridizations on *Drosophila* whole mounts. *Methods Mol. Biol.* 362:495-511.

Yasuyama K, Meinertzhagen IA, Schurmann FW (2002). Synaptic organization of the mushroom body calyx in *Drosophila melanogaster*. *J Comp Neurol.* 445:211-226.

Yasuyama K, Meinertzhagen IA, Schuermann FW (2003). Synaptic connections of cholinergic antennal lobe relay neurons in the brain of *Drosophila melanogaster*. *J Comp Neurol.* 466:299-315.

Yoshii T, Heshiki Y, Ibuki-Ishibashi T, Matsumoto A, Tanimura T, Tomioka K (2005). Temperature cycles drive *Drosophila* circadian oscillation in constant light that otherwise induces behavioural arrhythmicity. *Eur J Neurosci* 22:1176-1184.

Yu P, Ma D, Xu M (2005). Nested genes in the human genome. *Genomics* 86**:**414-422.

Yu W, Zheng H, Houl JH, Dauwalder B, Hardin PE (2006). PER dependent rhythms in CLK phosphorylation and E-box binding regulate circadian transcription. *Genes Dev* 20:723-733.

Zachar Z and Bingham PM (1982). Regulation of *white* locus expression: the structure of mutant alleles at the *white* locus of *Drosophila melanogaster*. *Cell* 30(2):529-41.

Zars T (2000). Behavioral functions of the insect mushroom bodies. *Curr Opin Neurobiol.* 10(6):790-5.

Zars T, Fischer M, Schulz R, Heisenberg M (2000). Localization of a short-term memory in *Drosophila*. *Science* 288(5466):672-5.

Zars T (2010). Short-term memories in *Drosophila* are governed by general and specific genetic systems. *Learn Mem.* 17(5):246-51.

Zordan MA, Benna C, Mazzotta G (2007). Monitoring and analyzing *Drosophila* circadian locomotor activity. *Methods Mol. Biol.* 362:67-81

Zweifel E, Smith J, Romero D, Giddings TH Jr, Winey M, Honts J, Dahlseid J, Schneider B, Cole ES (2009). Nested genes CDA12 and CDA13 encode proteins associated with membrane trafficking in the ciliate *Tetrahymena thermophila*. *Eukaryot Cell.* 8(6):899-912.

Acknowledgments

I would like to thank my Supervisor Prof. Federica Sandrelli, who gave me the opportunity to attend my PhD in her lab, who guided me in these three years with useful adivised and comments, teaching me how to improve in the scientific field.
I thank Prof. Aram Megighian for ERG analyses.
I would like to acknowledge Dr. Clara Benna, who taught me different techniques and helped me to familiarize with the project at the beginning of my PhD.
I would like to thank Dr. Moyra Mason, for her support regarding the screening of the Two-Yeast Hybrid library and for her useful suggestions.
I thank Dr. Andrea Bozzato, who did the phylogenetic analyses concerning 2MIT conservation in other organisms.
I also thank Moira Cognolato, for her support regarding the experiments related to the memory phenotype.
I am grateful also to all the present and former members of my lab, for their useful advises: Prof. Rodolfo Costa, Prof. Mauro A. Zordan, Dr. Cristiano de Pittà, Dr. Gabriella Mazzotta, Cinzia Curto, Paola Cusumano, Caterina Da Re, Elena Carbognin, Pamela Menegazzi, Paola Cisotto, Laura Caccin, Stefano Vanin, Damiano Zanini, Stefano Montelli, Luca Schiesari, Gabriele Andreatta and Antonia Piazzesi.